KU LEUVEN

ARENBERG DOCTORAL SCHOOL
Faculty of Engineering Science

Spectrum-based methods and algorithms for the Robustness Stability Analysis of Delay Systems

Francesco Borgioli

Supervisor:
Prof. dr. ir. Wim Michiels

Dissertation presented in partial fulfillment of the requirements for the degree of Doctor of Engineering Science (PhD): Computer Science

January 2020

Spectrum-based methods and algorithms for the Robustness Stability Analysis of Delay Systems

Francesco BORGIOLI

Examination committee:
Prof. dr. ir. Paul Sas, chair
Prof. dr. ir. Wim Michiels, supervisor
Prof. dr. ir. Karl Meerbergen
Prof. dr. ir. Panagiotis Patrinos
Prof. dr. Emre Mengi
(Koç University)
Prof. dr. ir. Silviu Iulian Niculescu
(Centrale Supélec-CNRS-Université Paris Sud)

Dissertation presented in partial fulfillment of the requirements for the degree of Doctor of Engineering Science (PhD): Computer Science

January 2020

© 2016 KU Leuven – Faculty of Engineering Science
Uitgegeven in eigen beheer, Francesco Borgioli, Celestijnenlaan 200A box 2402, B-3001 Leuven (Belgium)

Alle rechten voorbehouden. Niets uit deze uitgave mag worden vermenigvuldigd en/of openbaar gemaakt worden door middel van druk, fotokopie, microfilm, elektronisch of op welke andere wijze ook zonder voorafgaande schriftelijke toestemming van de uitgever.

All rights reserved. No part of the publication may be reproduced in any form by print, photoprint, microfilm, electronic or any other means without written permission from the publisher.

Preface

When I decided to move to Belgium four years ago, I probably made the biggest step in the dark in my life, despite the several perplexities of many family members and friends, who were reasonably concerned about long winters and frequent rainfalls. After this long time, I can look back and consider myself extremely grateful and lucky for the long journey I have been through. I had the chance to work and live with so many people I would like to thank, and this preface will never be enough to express my gratefulness.

First of all, I would like to thank my supervisor, Wim. I feel extremely lucky to have been guided by you during my PhD, and I have really admired your broad knowledge and enthusiasm for research. Since my first day at the department, the door of your office was always open for me whichever problem I had, and I am also grateful for the many weekends you spent proofreading my papers. I am particularly thankful for the never-ending support you gave me during the hard moments of the PhD, you always made me think positive and your encouragement helped me to remain confident about the best outcome of our works.

Thanks to all jury members for taking part in the examination committee and for carefully proofreading my manuscript. I thank Prof. P. Sas for chairing the committee, Prof. K. Meerbergen and Prof. P. Patrinos for their assistance during my PhD, and Prof. E. Mengi and Prof. S.I. Niculescu for the extensive discussion and the precious comments that I have received during the preliminary defense.

During my PhD, I had the chance to visit and collaborate with the Department of Applied Mechanics of the Budapest University of Technology and Economics. I would like to thank Prof. G. Stépán, Prof. T. Insperger and D. Hajdu for introducing me in their group, and for the enthusiasm they showed in our collaboration.

I would also like to thank my research group, I could have not asked for a more collaborative and welcoming group of people: Dan, Libo, Deesh, Yanling, Alexey, Koen, Pieter, Haik, Kirill, Marco and Luca, thank to all of you! A

special acknowledge to Deesh, with whom I shared a wonderful stay in Cyprus and who helped me to clarify all my doubts about control theory whenever I needed. Thanks to Pieter, who contributed to this thesis in his (probably) most difficult part :) Thanks to Luca, we shared so much since the first day, and I could have not asked for a better mate during this experience.

Of course, a special thank also goes to all the other colleagues of the NUMA group, with whom I enjoyed spending most of my coffee breaks and lunches. A special thank to Adrian, I hope you learned at least a bit of Italian during your PhD; to Julian, although we met pretty late in these four years, it was a real pleasure to share the office with you; finally, to Ward, Bert and Pieterjan, for the interesting project we worked on and the possibly even more interesting wine tastings.

But life in Leuven was not simply life at the department, so there are other people I would like to thank. Thanks to a huge (more or less) Italian community that made me feel at home in these years: Andreas, Nadia, Max, Emiliano, Giulio, Martina, Dario, Isa, Luca, Valentina, Luigi, Aggela, Edoardo, Francesca, Jacopo, Leone. Thanks also to Francesco, whose endurance in swimming trainings I learned to admire, and Marta, who introduced me to sbrisolona, probably one of the best things I discovered in Leuven. Thanks of course to Susa and Karel, my wonderful flatmates and friends.

I would also like to thank my friends from Florence, a second family for me. Every time I come back I feel so lucky and honoured to have you still there, no matter how far we are or how often we call each other. Thanks to my family, I think there is really no need to try to put in words how much I love you.

Finally, thanks to Lisa. I consider myself so lucky to have met such a wonderful person, with whom I share so much.

Abstract

Investigating the asymptotic stability of an equilibrium of a dynamical system is a very relevant topic in science and engineering. Considering linear autonomous systems, the frequency domain approach represents an effective strategy as it provides necessary and sufficient stability conditions: in a continuous-time framework, asymptotic stability is under mild conditions equivalent to a strictly negative spectral abscissa.

In real life applications, the uncertainties affecting the system unavoidably perturb its spectrum and potentially induce instability. The pseudospectral abscissa and the distance to instability are important spectrum-based measures for the analysis of the stability robustness; an advantage of using these measures compared to time-domain, Lyapunov-based methods is that they do not introduce any conservatism, in the sense that they are grounded in a necessary and sufficient condition. These quantities can be already efficiently computed for standard eigenvalue problems, which stem from ordinary differential equations. The goal of this thesis is to develop computational methods for the same measures for a broad class of nonlinear eigenvalue problems, with a particular emphasis on delay eigenvalue problems and on exploiting the structure of the classes of perturbations considered.

Firstly, we present a computational method for the pseudospectral abscissa of nonlinear eigenvalue problems affected by real-valued perturbations on the nominal matrices: the algorithm employs geometric optimization techniques and fully exploits the structure of the perturbed eigenvalue problem. The method is also instrumental in designing robust feedback controllers of uncertain systems.

Secondly, we introduce two distinct computational methods for the distance to instability of delay systems: the first one uses the connection with the pseudospectral abscissa, while the latter one is a criss-cross method exploiting the characterization of the distance to instability in terms of the global maximum of a structured singular value function.

Finally, we make the leap from autonomous to time-periodic delay systems, where the asymptotic stability is determined by the modulus of the Floquet multipliers, i.e. the eigenvalues of the monodromy operator. Here, we extend

the geometric optimization technique to compute the largest Floquet multiplier that the system can attain within a given class of real-valued perturbations. Several application case-studies complete the dissertation.

Beknopte samenvatting

De asymptotische stabiliteit onderzoeken van een evenwichtspunt van een dynamisch systeem is een belangrijk probleem in de (ingenieurs)wetenschappen. Voor lineaire autonome systemen is een frequentie-domein gebaseerde aanpak uitermate geschikt omdat deze zowel nodige als voldoende voorwaarden voor stabiliteit geeft: voor continue tijd systemen is asymptotische stabiliteit onder milde assumpties equivalent met een strikt negatieve spectrale abscis.

In de meeste concrete toepassingen zijn er echter onzekerheden die het systeem beïnvloeden. Deze onzekerheden verstoren ook het spectrum van het systeem en kunnen mogelijks instabiliteit veroorzaken. De *pseudospectrale abscissa* en *de afstand tot instabiliteit* zijn belangrijke spectrum-gebaseerde metrieken voor de analyse van de robuustheid van de stabiliteit van het systeem. Het voordeel van de frequentie gebaseerde aanpak is dat deze niet conservatief is in tegenstelling tot tijdsdomein-, Lyapunov-gebaseerde methodes, in de zin dat de gepresenteerde methode zowel nodige als voldoende voorwaarden geeft voor stabiliteit. De pseudospectrale abscissa en de afstand tot instabiliteit kunnen reeds efficiënt berekend worden voor lineaire eigenwaarden problemen, afkomstig van gewone differentiaal vergelijkingen. Het doel van deze thesis is om methodes te ontwikkelen die deze metrieken voor een brede klasse van niet-lineaire eigenwaarde problemen kan berekenen. Hierbij wordt er gefocust op eigenwaarden problemen met tijdsvertraging en op het uitbuiten van de structuur van de beschouwde klasse van verstoringen.

Eerst presenteren we een methode om de pseudospectrale abscissa van niet-lineaire eigenwaarden problemen met reële perturbaties op de nominale matrices te berekenen: het gepresenteerde algoritme gebruikt geometrische optimalisatie technieken en buit de structuur van het geperturbeerde eigenwaarden probleem maximaal uit. De methode kan vervolgens gebruikt worden om robuuste feedback regelaars te ontwerpen voor onzekere systemen.

Ten tweede introduceren we twee verschillende methodes om de afstand tot instabiliteit van een systeem met tijdsvertraging te berekenen: de eerste gebruikt de relatie met de pseudospectrale abscissa, terwijl de tweede een criss-cross methode is die de relatie van de afstand tot instabiliteit en het globale maximum

van een gestructureerde singular waarde functie uitbuit.

Tot slot gaan we over van autonome naar tijdsperiodische systemen. De asymptotische stabiliteit van zulke tijdsperiodische systemen wordt bepaald door de modulus van de *Floquet multipliers*, dit zijn de eigenwaarden van de *monodromy operator*. Dit werk presenteert een uitbreiding van de geometrische optimalisatie techniek om de grootste Floquet multiplier die het systeem binnen een bepaalde klasse van reële perturbaties kan bereiken, te berekenen. Verschillende case-studies besluiten deze thesis.

Contents

Abstract iii

Beknopte samenvatting v

Contents vii

Abbreviations xi

List of Symbols xiii

1 Introduction 1
- 1.1 Nonlinear eigenvalue problems . . . 1
- 1.2 The stability robustness problem . . . 6
- 1.3 Research aims and motivations . . . 21
- 1.4 Overview of the thesis . . . 21

2 Computing the real pseudospectral abscissa for nonlinear eigenvalue problems 25
- 2.1 Problem statement and main assumptions . . . 26
- 2.2 The Frobenius norm case . . . 27
  - 2.2.1 Implementation . . . 34
- 2.3 The spectral norm case . . . 34
  - 2.3.1 Implementation . . . 43
- 2.4 Numerical experiments . . . 44
  - 2.4.1 Experiments on the Frobenius norm . . . 45
  - 2.4.2 Experiments on the spectral norm . . . 47
  - 2.4.3 Application to large-scale problems . . . 48
- 2.5 Conclusions . . . 49

3 Robustness measures for delay differential algebraic equations 51
- 3.1 A general class of DDEs . . . 51
- 3.2 Problem statement and main assumptions . . . 55

3.3 Computing the real structured pseudospectral abscissa for DEPs 58
3.3.1 Implementation 66
3.4 A bisection-Newton's method for the distance to instability . . 67
3.5 Numerical experiments 69
3.6 Conclusions 72

4 Designing robust controllers for DDAEs 73
4.1 Smoothness properties and optimization of the pseudospectral abscissa 76
4.2 Numerical experiments 78
4.3 A scalable design method for stabilising decentralised controllers of delay-coupled networks 83
4.3.1 Interconnected systems 83
4.3.2 Decoupling for the stabilisation problem 86
4.3.3 Design of the controller 86
4.3.4 Numerical examples 88
4.4 Conclusions 91

5 A globally convergent method to compute the real stability radius for time-delay systems 93
5.1 Introduction and problem statement 94
5.2 Distance to instability: a criss-cross algorithm 95
5.2.1 The $\mu_{\mathbb{R}}$ function 96
5.2.2 The criss-cross algorithm 98
5.2.3 The rank one case 100
5.3 A new solver for DEPs with positive and negative delays 103
5.3.1 Spectral discretization of the eigenvalue problem 103
5.3.2 Determining the number of discretization points 105
5.3.3 Correcting the eigenvalues with block-Newton method . 107
5.4 Numerical experiments 109
5.5 Conclusions 111

6 Robustness measures for linear periodic systems of DDEs 113
6.1 Chebyshev-polynomial based solver for Floquet multipliers . . . 117
6.2 Worst case analysis for Floquet multipliers 123
6.2.1 Matrix uncertainties: from the time-periodic system to the GEP 123
6.2.2 Algorithm to compute the Floquet *pseudospectral radius* 126
6.3 Explicit construction of the GEP for $T > \tau_m$ 129
6.4 Models with periodically time-varying delays 133
6.4.1 Extension of the approach 133
6.4.2 Spindle speed variation in turning 134
6.5 Models with piecewise-smooth periodic functions 135

6.5.1 Extension of the approach 136
6.5.2 Robustness analysis of linear systems stabilized by act-and-wait controllers 138
6.6 Stability robustness of milling operations 139
6.6.1 Modelling of milling operations 140
6.6.2 Case study and experiment 143
6.7 Conclusions 147

7 Conclusions **149**
7.1 Future research 151

A **153**

Bibliography **157**

Curriculum Vitae **169**

List of publications **171**

Abbreviations

ODE	Ordinary differential equation
DDE	Delay differential equation
DDAE	Delay differential algebraic equation
PDE	Partial differential equation
IVP	Initial value problem
EP	Eigenvalue problem
GEP	Generalized eigenvalue problem
PEP	Polynomial eigenvalue problem
DEP	Delay eigenvalue problem
LTI	Linear time-invariant
TPDDE	Time-periodic delay differential equation
SVD	Singular value decomposition

List of Symbols

Sets

$\mathbb{N}$	Set of natural numbers
$\mathbb{R}$	Set of real numbers
$\mathbb{R}^+$	Set of positive real numbers including zero
$\mathbb{C}$	Set of complex numbers

Set operations

$\in$	Belongs to
$\notin$	Does not belong to
$\subset$	Is included
$\bigcap$	Intersection
$\bigcup$	Union
$\setminus$	Set difference

Scalars, vectors and matrices

λ	Complex number
$\overline{\lambda}$	Conjugate of a complex number
$\imath$	Imaginary unit
$\mathfrak{R}$	Real part
$\mathfrak{I}$	Imaginary part
$\lvert \cdot \rvert$	Absolute value
$A,\ y$	Matrix, column vector
$A^T,\ y^T$	Transpose of A, transpose of y

A^*, y^*	Conjugate transpose of A, conjugate transpose of y
A^{-1}	Inverse of A
$\det(A)$	Determinant of A
$\operatorname{rank}(A)$	Rank of A
I	Identity matrix
I_n	Identity matrix of dimension n
$\otimes$	Kronecker product
$\langle \cdot, \cdot \rangle$	Scalar product
$\|\cdot\|$	Norm
$\|\cdot\|_2$	Spectral norm
$\|\cdot\|_F$	Frobenius norm
$\|\cdot\|_\infty$	Infinity norm

Eigenvalues

$\Lambda(A)$	Spectrum of A
$\alpha(A)$	Spectral abscissa of A
$\Lambda_\varepsilon(A)$	ε-pseudospectrum of A
$\alpha_\varepsilon(A)$	ε-pseudospectral abscissa of A
$\sigma_i(A)$	i-th largest singular value of A

Chapter 1

Introduction

The stability analysis and the stabilization of linear autonomous dynamical systems are among the most relevant and investigated fields of study within control theory: a frequency domain approach to the stability analysis relies on the computation of the associated eigenvalues, and it is convenient as it represents a necessary and sufficient condition to investigate its asymptotic stability. Linear autonomous systems may be considered not just as the result of a modelization for some engineering applications; in addition, they may stem from the linearization of nonlinear autonomous dynamical systems *around some equilibirium point*: in this case, we might want to study the properties of the *equilibrium solution*, in particular whether it is a local attractor for small perturbations of such a solution or not . In this dissertation we will focus on *nonlinear eigenvalue problems*, which play a fundamental role in a wide variety of science and engineering applications, such as the dynamic analysis of mechanical systems (where the eigenvalues represent vibrational frequencies), the linear stability of flows in fluid mechanics, the analysis and design of control systems, where feedback and communication delays are ubiquitous. In the next section we introduce the general class of nonlinear eigenvalue problems adopted in this dissertation and illustrate how this shows up in the frequency domain analysis of different classes of linear autonomous dynamical systems.

1.1 Nonlinear eigenvalue problems

A general description for a wide class of nonlinear eigenvalue problems is given by

$$P(\lambda)y = \left(\sum_{i=1}^{m} A_i p_i(\lambda)\right) y = 0, \tag{1.1}$$

where $\lambda \in \mathbb{C}$ is an eigenvalue, $y \in \mathbb{C}^n,\ y \neq 0$ is the right eigenvector, while $A_i \in \mathbb{R}^{n\times n}$ with $n \geq 2$, and the function p_i is assumed to be entire for $i = 1, \ldots, m$. Besides the right eigenvector, each eigenvalue λ is also associated with a left eigenvector $x \in \mathbb{C}^n,\ x \neq 0$ such that

$$x^* P(\lambda) = 0,$$

where x^* denotes the conjugate transpose of x.

In the following, we show how the most popular classes of eigenvalue problems (EPs), such as the linear, the polynomial or the delay eigenvalue problem appear as a special case of (1.1); for each class, a short list of the most popular solvers is given and the connection with specific dynamical systems is highlighted.

For nonlinear EPs in the general form (1.1) and their connections with differential equations, we refer to [5] and the references therein, while eigenvalue solvers for general problems of form (1.1) are proposed in [70, 126, 86, 127].

Linear eigenvalue problem and first-order ODEs

We consider a dynamical system of first-order homogeneous ordinary differential equations (ODEs) as

$$\dot{\mathbf{x}}(t) = A_1 \mathbf{x}(t), \tag{1.2}$$

where t indicates time, and $\mathbf{x}$ is the vector of state variables. Observe that a system of this form can also be generated by an n-th order scalar homogeneous ODE as

$$a_0 x^{(n)}(t) + a_1 x^{(n-1)}(t) + \cdots + a_{n-1} x^{(1)}(t) + a_n x(t) = 0, \tag{1.3}$$

where $a_0 \neq 0$ and $x^{(i)}$ denotes the i-th order derivative of the scalar function x. The equation (1.3) can be reformulated in the form (1.2) with

$$\mathbf{x}(t) = \left(x(t), \ldots, x^{(n-1)}(t)\right)^T,\ A_1 = \begin{bmatrix} 0 & 1 & \ldots & 0 \\ \vdots & \ddots & \ddots & \\ 0 & \ldots & 0 & 1 \\ \frac{-a_n}{a_0} & \ldots & \ldots & \frac{-a_1}{a_0} \end{bmatrix}.$$

For any $t_0 \in \mathbb{R},\ \mathbf{x}_0 \in \mathbb{R}^n$, the initial value problem (IVP) associated with (1.2) is defined as

$$\begin{cases} \dot{\mathbf{x}}(t) = A_1 \mathbf{x}(t), \\ \mathbf{x}(t_0) = \mathbf{x}_0, \end{cases} \tag{1.4}$$

and always admits a unique solution, whose value at time t will be indicated by $\mathbf{x}(t; t_0, x_0)$.

Definition 1.1. *Given $t_0 \in \mathbb{R}$, $x_0 \in \mathbb{R}^n$, the null solution of (1.2) is asymptotically stable if*

$$\lim_{t \to +\infty} \mathbf{x}(t; t_0, x_0) = 0.$$

When adopting a frequency domain approach for the analysis of the (asymptotic) stability, we need to solve the *standard eigenvalue problem*

$$(\lambda I_n - A_1)y = 0, \tag{1.5}$$

with I_n the identity matrix of dimension n; this problem is also obtained from (1.1) by setting $p_1(\lambda) \equiv -1,\ p_2(\lambda) = \lambda,\ A_2 = I_n$. Then, a well-known result states that the null solution of (1.2) is asymptotically stable *if and only if* all the characteristic roots of (1.5) lie in the open left-half of the complex plane; equivalently, we can say that it is asymptotically stable if the spectral abscissa, i.e. the real part of the rightmost eigenvalue of (1.5), is negative. In this case, matrix A_1 is said to be *stable* or a *Hurwitz matrix*.

Another common linear EP is the *generalized eigenvalue problem* (GEP)

$$(\lambda A_2 - A_1)y = 0,$$

where a matrix A_2 replaces the identity matrix used in the standard EP. There exists a large amount of numerical methods to compute *all* the eigenpairs (λ, y) of a standard EP. To mention a few, we recall the QR algorithm ([77, 35, 36]), which extends to the QZ algorithm for GEPs, and the Cholesky factorization for Hermitian (symmetric) problems. In the context of the analysis of stability of continuous-time systems for large-scale problems, it is common to compute only a small subset of the eigenvalues, namely the rightmost ones. A widely used method for this purpose is the restarted Arnoldi method, which was first introduced in [3]. Popular surveys on the solution of linear EPs are [122, 23].

Polynomial eigenvalue problem and higher order ODEs

We now consider a linear system of higher order homogeneous ODEs

$$\sum_{i=1}^{m} A_i \mathbf{x}^{(i-1)}(t) = 0,$$

where $\mathbf{x}$ and $\mathbf{x}^{(i)}$ still represent the vector of state functions and its i-th derivative, respectively. It is easy to see that by augmenting the dimension of the system, it is always possible to rewrite it as a system of first order ODEs. Then, the definitions of IVP and of asymptotic stability are analogous to what we have seen before.

Using a frequency domain approach, we obtain the polynomial eigenvalue problem (PEP)

$$\left(\sum_{i=1}^{m} A_i \lambda^{i-1}\right) y = 0, \tag{1.6}$$

which is obtained from (1.1) by setting $p_i(\lambda) = \lambda^{i-1}$ for $i = 1, \ldots, m$, and which reduces to the well-known *quadratic eigenvalue problem* (QEP) when $m = 3$. A standard way to solve PEP is to rewrite it in the form of a (larger) linear EP [2, 45, 83]. For QEPs, the QUADEIG algorithm [58] can be used for computing all $2n$ eigenvalues, while a survey is available in [118].

Delay eigenvalue problem and DDEs

We consider a system of linear autonomous delay differential equations (DDEs) of retarded type such as

$$\dot{\mathbf{x}}(t) = B_0 \mathbf{x}(t) + \sum_{i=1}^{l} B_i \mathbf{x}(t - \tau_i) \tag{1.7}$$

where $\mathbf{x}$ is the vector of state variables, $B_0, \ldots, B_l \in \mathbb{R}^{n \times n}$, and $(\tau_1, \ldots, \tau_l)^T \in \mathbb{R}^l$ is a set of delays such that $0 < \tau_1 < \cdots < \tau_l$. For any given time $t_0 \in \mathbb{R}$, in order to define an IVP we must consider a function segment

$$\varphi \in \mathcal{G} := \mathcal{C}([t_0 - \tau_m, t_0], \mathbb{R}^n),$$

where $\mathcal{G}$ is the Banach space of continuous functions mapping the interval $[t_0 - \tau_m, t_0]$ into $\mathbb{R}^n$ and equipped with the supremum norm $\|\cdot\|_s$ defined by

$$\|\varphi\|_s := \sup_{\theta \in [t_0 - \tau_m, t_0]} \|\varphi(\theta)\|_2 .$$

Then, under mild conditions, we can define

$$\mathbf{x}(\cdot; t_0, \varphi) : \ t \in [t_0 - \tau_m, +\infty) \to \mathbf{x}(t; t_0, \varphi)$$

as the unique forward solution of (1.7) with initial condition $\varphi \in \mathcal{G}$, and the state of the solution at time $t \geq t_0$ is defined by the function segment $\mathbf{x_t}(t_0, \varphi) \in \mathcal{G}$ which reads

$$\mathbf{x_t}(t_0, \varphi)(\theta) = \mathbf{x}(t + \theta; t_0, \varphi), \ \theta \in [t_0 - \tau_m, t_0].$$

The definition of asymptotic stability of the null solution is then analogous to what is seen before in Definition 1.1.

Definition 1.2. *Given $t_0 \in \mathbb{R}$, the null solution of system (1.7) is asymptotically stable if*

$$\lim_{t \to +\infty} \mathbf{x}(t; t_0, \varphi) = 0$$

for any $t_0 \in \mathbb{R}$ and $\varphi \in \mathcal{G}$.

In the specific case of systems of DDEs of retarded type, the asymptotic stability is equivalent to another type of stability, the so-called *exponential stability*.

Definition 1.3. *The null solution of system (1.7) is exponentially stable if there exist constants $C > 0$ and $\gamma > 0$ such that for any $t_0 \in \mathbb{R},\ \varphi \in \mathcal{G},\ t > 0$, it holds that*

$$\|\mathbf{x_t}(t_0, \varphi)\|_s \leq Ce^{-\gamma t} \|\varphi\|_s .$$

Adopting a frequency domain approach, we obtain a *delay eigenvalue problem* (DEP) defined as follows

$$\left(\lambda I_n - B_0 - \sum_{i=1}^{l} B_i e^{-\lambda \tau_i}\right) y = 0, \tag{1.8}$$

which is still retrieved from the general form (1.1) by setting $m = l + 2$, $p_1(\lambda) = \lambda, p_2(\lambda) = 1, A_1 = I, A_2 = B_0$ and $p_i(\lambda) = -e^{-\lambda \tau_{i-1}}, A_i = B_{i-1}$, for $2 \leq i \leq l + 2$.

As for the dynamical systems introduced before, the asymptotic stability of the null solution of (1.7) is guaranteed *if and only if* the spectral abscissa of the DEP (1.8) is negative. However, contrary to the previous two classes of EPs, the DEP has infinitely many eigenvalues. Therefore, as in the case of large-scale linear EPs, in the context of stability analysis of continuous time systems we are interested in the computation of the rightmost eigenvalues. Many methods and packages are available in the literature to compute a subset of eigenpairs. Among these, in this thesis we use the spectral discretization method described in [89] (which relies on an automatic procedure to compute the number of discretization points proposed in [132]). Among the many other softwares we recall the DDE-BIFTOOL ([33, 32]), the TRACE-DDE ([15, 14]) and the QpMR ([128, 129]), while another popular method for the computation of the eigenvalues is reported in [69]. Popular surveys on stability and stabilization of time-delay systems are [96, 48]. As we will introduce more in detail in Chapter 3, another common type of delay systems is the class of *neutral type*. However, in this dissertation we focus on the class of retarded type, as its spectrum has more favourable properties in the context of stability analysis.

1.2 The stability robustness problem

As mentioned in the previous section, under mild conditions the asymptotic stability of the null solution of an LTI system[1] is guaranteed when all eigenvalues lie in the left open half of the complex plane and, for the purpose of determining stability, many algorithms to compute the rightmost eigenvalues have been developed. However, when we switch to practical applications, verifying that the rightmost point of the spectrum lies in the left half of the complex plane might not result in the stability of the examined system: a common reason for this discrepancy is represented by the potential model mismatch. As a matter of fact, the coefficients of the matrices A_i in (1.1) may be subject to perturbations, as well as the delays in the DEP (1.8): this naturally results in a variation of the spectrum, and potentially pushes one or more eigenvalues in the closed right-half of the complex plane, thus observing instability of the system. As we will explain more in detail in the following chapters, each eigenvalue generally moves continuously under continuous variations of the coefficients of the system matrices.

An intuitive approach to check whether asymptotic stability is preserved under the mentioned uncertainties (i.e. how *robust* is the stability of the system) is to investigate the shift of the eigenvalues in the complex plane. This concept is formally tackled by introducing the notion of pseudospectrum, that is the set in the complex plane to which eigenvalues can be moved when the original system is subject to perturbations whose norms are bounded by a specified upper bound. The pseudospectral abscissa, the supremum of the real parts of the pseudospectrum, constitutes a bound on the asymptotic growth rate of the solutions of the perturbed system, which is uniform over all possible perturbations under consideration: therefore, the pseudospectral abscissa allows to assess the degree of robustness of the stability.

Let us formally introduce the uncertainties on the nonlinear EP (1.1) as follows

$$P(\lambda;\Delta)y = \left(\sum_{i=1}^{m}(A_i + \delta A_i)p_i(\lambda)\right)y = 0, \tag{1.9}$$

where uncertainties δA_i are called *unstructured perturbations* as no additional structure is imposed. Denoting with Δ the set of uncertainties $\Delta = (\delta A_1, \ldots, \delta A_m)$, suppose we define on each Δ an overall norm $\|\Delta\|_{\text{glob}}$. Then, a formal definition of ε-pseudospectrum is

$$\Lambda_\varepsilon := \left\{\lambda \in \mathbb{C} :\ \det(P(\lambda;\Delta)) = 0 \text{ for some } \Delta \text{ with } \|\Delta\|_{\text{glob}} \leq \varepsilon\right\}, \tag{1.10}$$

[1] For reasons of conciseness we will often use the less precise formulation "The system is asymptotically stable".

while the ε-pseudospectral abscissa α_ε can be defined as

$$\alpha_\varepsilon := \sup\{\Re(\lambda) : \ \lambda \in \Lambda_\varepsilon\}, \tag{1.11}$$

and each λ in the ε-pseudospectrum is called a *pseudoeigenvalue*. From this definition, we formally define a stable dynamical system affected by a class of ε-bounded perturbations *robustly stable* if and only if $\alpha_\varepsilon < 0$.

The concept of *distance to instability* of a nonlinear EP (also called *stability radius*) is strictly connected with the ε-pseudospectral abscissa. Intuitively, given a stable system associated with the matrix-valued function $P(\lambda)$, the distance to instability is the minimum norm a perturbation must attain to make the system unstable. Assuming the continuity of the spectral abscissa w.r.t. the considered perturbation, the distance to instability is then the norm of the smallest perturbation pushing one (or more) eigenvalues on the imaginary axis, which can be formally written as

$$d_{\text{INS}} := \inf_{\lambda=\imath\omega} \inf_{\Delta} \left\{ \|\Delta\|_{\text{glob}} : \ \det(P(\lambda;\Delta)) = 0 \right\}. \tag{1.12}$$

Intuitively, the distance to instability is then equal to the smallest ε such that the associated ε-pseudospectral abscissa is equal to zero.

Of course, the nature of the uncertainties affecting the system can be further defined and it can be chosen depending on the problem of interest: for example, one might want to perturb only single coefficients or specific submatrices, in which case we talk about *structured perturbations*. Moreover, the considered perturbations δA_i may be either real-valued or complex-valued, and the former kind is usually preferable in the context of practical applications. Observe that for any fixed $\varepsilon > 0$ the following relation holds

$$\{\Delta \in (\mathbb{R}^{n\times n})^m : \|\Delta\|_{\text{glob}} \leq \varepsilon\} \subset \{\Delta \in (\mathbb{C}^{n\times n})^m : \|\Delta\|_{\text{glob}} \leq \varepsilon\},$$

and it trivially implies that the *real* ε-pseudospectrum $\Lambda_\varepsilon^{\mathbb{R}}$ is contained in the *complex* ε-pseudospectrum $\Lambda_\varepsilon^{\mathbb{C}}$, and thus that the *real* ε-pseudospectral abscissa $\alpha_\varepsilon^{\mathbb{R}}$ is smaller than the *complex* ε-pseudospectral abscissa $\alpha_\varepsilon^{\mathbb{C}}$. In the literature, there is a large number of methods to draw the complex ε-pseudospectrum and to compute the complex ε-pseudospectral abscissa of EPs compared to the number of methods available for the real-valued case. On the other hand, as we have just seen the real-valued case is more important from an application point of view, and considering $\alpha_\varepsilon^{\mathbb{C}}$ instead of $\alpha_\varepsilon^{\mathbb{R}}$ can lead to an overestimation of the effect of the uncertainties. The first part of this dissertation focuses on a novel method to compute the real ε-pseudospectral abscissa for *nonlinear EPs*. Below, we summarize some of the most popular methods in the literature to compute $\alpha_\varepsilon^{\mathbb{C}}$ and $\alpha_\varepsilon^{\mathbb{R}}$ for the standard EP and $\alpha_\varepsilon^{\mathbb{C}}$ for the nonlinear EP, together with the related algorithms to compute the distance to instability.

Complex-valued perturbation of a standard EP

We consider the standard EP (1.5), where for simplicity we now denote A_1 with A, and assume a complex-valued uncertainty $\delta A \in \mathbb{C}^{n\times n}$ affecting A. We then adopt the spectral norm $\|\cdot\|_2$ as a measure of the uncertainty, in which case the complex ε-pseudospectrum reads as follows:

$$\begin{aligned}\Lambda_\varepsilon^{\mathbb{C}}(A) &= \left\{\lambda \in \mathbb{C} : \exists\ \delta A \in \mathbb{C}^{n\times n},\ 0 < \|\delta A\|_2 \le \varepsilon,\ \text{s.t. } \det(\lambda I_n - A - \delta A) = 0\ \right\} \\ &= \left\{\lambda \in \mathbb{C} : \exists\ \delta A \in \mathbb{C}^{n\times n},\ 0 < \|\delta A\|_2 \le \varepsilon,\ \text{s.t. } \det(I_n - (\lambda I_n - A)^{-1}\delta A) = 0\right\} \\ &= \left\{\lambda \in \mathbb{C} : \frac{1}{\sigma_1((\lambda I_n - A)^{-1})} \le \varepsilon\right\}, \\ &= \{\lambda \in \mathbb{C} : \sigma_n(\lambda I_n - A) \le \varepsilon\}, \end{aligned} \tag{1.13}$$

where we have employed the characterization of the largest singular value of a matrix illustrated in the appendix. Then, thanks to this description the complex ε-pseudospectrum $\Lambda_\varepsilon^{\mathbb{C}}$ of a standard EP can simply be drawn by using a contour plotter on a grid of a region of the complex plane where the function $f(\lambda) = \sigma_{\min}(\lambda I_n - A)$ has been evaluated.
However, this technique can be very expensive and inaccurate at the same time, for instance when the region to examine is too large or the chosen grid too rough. Moreover, as we have seen, for the simple purpose of assessing the stability robustness of a continuous-time system it is sufficient to compute the pseudospectral abscissa. Here we briefly introduce four among the most popular methods to compute $\alpha_\varepsilon^{\mathbb{C}}$ for a standard EP.

(i) A criss-cross algorithm introduced in [17] relies on the characterization of the singular values of a matrix as the purely imaginary eigenvalues of an Hamiltonian EP of double dimension. In particular, it exploits the following two results.

Proposition 1.4 (Vertical search)**.** *Let $\alpha,\ \beta \in \mathbb{R}$, then $\varepsilon > 0$ is a singular value of $(\alpha+\imath\beta)I_n - A$ if and only if $\imath\beta$ is an eigenvalue of the Hamiltonian matrix*

$$H(\alpha) = \begin{bmatrix} \alpha I_n - A^* & \varepsilon I_n \\ -\varepsilon I_n & A - \alpha I_n \end{bmatrix}.$$

Proposition 1.5 (Horizontal search)**.** *Let $\alpha,\ \beta \in \mathbb{R}$, then $\varepsilon > 0$ is a singular value of $(\alpha + \imath\beta)I_n - A$ if and only if $\imath\alpha$ is an eigenvalue of the Hamiltonian matrix*

$$\widetilde{H}(\beta) = \begin{bmatrix} \imath A^* - \beta I_n & \varepsilon I_n \\ -\varepsilon I_n & \imath A + \beta I_n \end{bmatrix}.$$

The criss-cross algorithm exploits these two results and the description (1.13) of the ε-pseudospectrum, performing the following operations at each iteration i (where $\alpha^{(0)}$ is initialized as the spectral abscissa of the matrix at hand):

1 Find all the values

$$\ell_1^{(i)} < u_1^{(i)} < \cdots < \ell_k^{(i)} < u_k^{(i)}$$

such that $\imath\beta = \imath\ell_j^{(i)}$, $\imath\beta = \imath u_j^{(i)}$ for $j = 1, \ldots, k$, are eigenvalues of $H(\alpha^{(i)})$, and discard the values such that

$$\sigma_{\min}\left((\alpha^{(i-1)} + \imath\beta)I_n - A\right) < \varepsilon;$$

2 For each $j = 1, \ldots, k$, define

$$\beta_j^{(i)} := \frac{\ell_j^{(i)} + u_j^{(i)}}{2},$$

and find the largest $\alpha_j^{(i)}$ such that $\imath\alpha_j^{(i)}$ is an eigenvalue of $\widetilde{H}(\beta_j^{(i)})$;

3 Set

$$\alpha^{(i)} := \max_{j=1,\ldots,k}\{\alpha_j^{(i)}\},$$

and increase i by one.

This algorithm is proven to globally converge with quadratic rate to the ε-pseudospectral abscissa $\alpha_\varepsilon^{\mathbb{C}}$; on the other hand, it is not suitable for large-scale problems as constructing and solving the Hamiltonian EPs becomes a very expensive operation.

(*ii*) A fixed point iteration presented in [52] is based on the computation of the spectral abscissa of a sequence of matrices B_i defined as follows

$$B_{i+1} = A + L_{i+1} = A + \varepsilon y_i x_i^*,$$

where x_i, y_i are the left and right eigenvectors corresponding to the rightmost eigenvalue λ_i of B_i and normalized such that $\|x_i\| = \|y_i\| = 1$ and $x_i^* y_i \in (0, 1]$. It is worth to remark that each perturbation matrix L_i is a rank-one matrix: in particular, the authors demonstrate that each pseudoeigenvalue in the ε-pseudospectrum can be generated as an eigenvalue of a rank-one ε-bounded perturbation of A. As a consequence, the ε-pseudospectrum can be equally generated by restricting to rank-one perturbations of A. Therefore, as a result of (A.4) and (A.5), using the

Frobenius norm to measure the magnitude of the uncertainty (instead of the spectral norm) would generate exactly the same pseudospectrum.

From a numerical point of view, the authors observe that the sequence of eigenvalues $\{\lambda_i\}_{i\geq 1}$ almost always converge to the globally rightmost point of the ε-pseudospectrum; on the other hand, the convergence analysis turns out to be very complicated, and the method has only been proven to converge to *locally rightmost points* with a linear rate and for sufficiently small ε. Nevertheless, the method represents an effective tool for the computation of ε-pseudospectral abscissa, as its basic iteration only requires the computation of the rightmost eigenvalue of a matrix. An alternative version where the monotonicity of the sequence $\{\mathfrak{R}(\lambda_i)\}_{i\geq 1}$ is guaranteed is also proposed.

(*iii*) A continuous counterpart of the previous method was proposed in [50]: the idea underlying this new method is to construct a continuous path in the manifold

$$\mathcal{M} := \left\{E \in \mathbb{C}^{n\times n} : \|E\|_2 = 1,\ \text{rank}(E) = 1\right\}$$

leading to an *optimal perturbation* of the matrix A, i.e. to a perturbed matrix whose rightmost eigenvalue is a local maximum of the ε-pseudospectrum. In particular, the path is defined by rank-one matrices $E = E(s),\ s \geq 0$, solving the following differential equation

$$\dot{E} = P_E(xy^*), \tag{1.14}$$

where $x(s)$, $y(s)$ are the left and right eigenvectors of the rightmost eigenvalue $\lambda(s)$ of $A + \varepsilon E(s)$, with $\|x(s)\| = \|y(s)\| = 1$ and $x(s)^* y(s) \in (0, 1]$, while $P_E(M)$ indicates the projection of a generic matrix M onto the space tangent to the manifold $\mathcal{M}$ at $E(s)$. It can be easily proven that for $E(s)$ satisfying the differential equation (1.14) it holds that

$$\mathfrak{R}(\dot{\lambda}(s)) \geq 0.$$

In particular, the derivative is maximized in the direction defined by $E(s)$, so that the path identified by (1.14) defines the direction of steepest ascent for $\mathfrak{R}(\lambda(s))$ w.r.t. the variations of A. Thanks to this property, the proposed iterative algorithm is defined by a basic iteration where the differential equation (1.14) is numerically solved via a projected exponential Euler method ([60]) with adaptive stepsize. The method presents two main benefits with respect to the one proposed in [52]: first, given his nature of (projected) gradient-ascent method, the convergence analysis is very simple; second, it allows to track the boundary contour of the ε-pseudospectrum in a neighborhood of the locally rightmost points.

(*iv*) In [75] a subspace acceleration method is proposed, which is proven to converge *superlinearly* to locally rightmost points of the ε-pseudospectrum; numerically, even a quadratic rate of convergence is observed. The method relies on the definition of ε-pseudospectrum for a (rectangular) matrix pencil $\widehat{A} - z\widehat{B} := AV - zV$, where the columns of $V \in \mathbb{C}^{n\times k}$ form an orthonormal basis for some subspace $\mathcal{V}$ of $\mathbb{C}^{n\times n}$. This definition reads as

$$\Lambda_\varepsilon(\widehat{A}, \widehat{B}) := \left\{ z \in \mathbb{C} : \ \sigma_{\min}(\widehat{A} - z\widehat{B}) \leq \varepsilon \right\}. \tag{1.15}$$

Then, the following two propositions proven in [75] pave the way to the proposed algorithm.

Proposition 1.6. *Let U and V be orthonormal bases of subspaces $\mathcal{U}$ and $\mathcal{V}$ in $\mathbb{C}^{n\times n}$ with $\mathcal{U} \subset \mathcal{V}$, then*

$$\Lambda_\varepsilon(AU, U) \subset \Lambda_\varepsilon(AV, V) \subset \Lambda_\varepsilon(A),$$

which trivially implies that

$$\alpha_\varepsilon^{\mathbb{C}}(AU, U) \leq \alpha_\varepsilon^{\mathbb{C}}(AV, V) \leq \alpha_\varepsilon^{\mathbb{C}}(A).$$

Proposition 1.7. *Let $A \in \mathbb{C}^{n\times n}$ and the columns of V form an orthonormal basis for a subspace $\mathcal{V}$ of $\mathbb{C}^{n\times n}$. Then $\alpha_\varepsilon^{\mathbb{C}}(AV, V) = \alpha_\varepsilon^{\mathbb{C}}(A)$ if and only if $\mathcal{V}$ contains a vector v_α such that v_α is a right singular vector corresponding to $\sigma_{min}(A - \mu_\alpha I_n)$ for some $\mu_\alpha \in \Lambda_\varepsilon^{\mathbb{C}}(A)$ with $\Re(\mu_\alpha) = \alpha_\varepsilon^{\mathbb{C}}(A)$.*

Therefore, the algorithm tries to construct a subspace $\mathcal{V}$ containing a good approximation of the vector v_α. At each iteration i, the following operations are performed:

1 Compute the globally rightmost point μ_i of $\Lambda_\varepsilon(AV_i, V_i)$: this is accomplished by applying a modified version of criss-cross algorithm ([17]) on matrices with dimension $2i \times i$;
2 Compute the right singular vector v_i corresponding to $\sigma_{\min}(A - \mu_i I_n)$;
3 Compute $V_{i+1} = \mathrm{orth}([V_i, \ v_i])$.

In the appendix (Equation (A.7)) we show that the smallest singular value $\sigma_{\min}(A)$ of a stable matrix A is equal to the norm of a minimal perturbation making A unstable; as an immediate consequence, the distance to instability of a matrix A subject to a complex-valued perturbation can be characterized as

$$d_{\mathrm{INS}}^{\mathbb{C}} := \inf_{\omega\in\mathbb{R}} \sigma_{\min}(A - \imath\omega I_n).$$

The bisection algorithm proposed in [19] exploits this characterization to compute the distance to instability and its convergence was later speeded up in [37], while in [59] a method for the computation of the structured complex distance to instability of a matrix is proposed.

Real-valued perturbation of a standard EP

We now consider real-valued perturbations $\delta A \in \mathbb{R}^{n\times n}$ of a matrix A. As we will see more in detail in the following, each pseudoeigenvalue in the real ε-pseudospectrum of a matrix A can be generated by a perturbation with rank smaller than or equal to two. In addition, the pseudospectra generated considering in terms of the 2-norm or the Frobenius norm are generally different (unless each pseudoeigenvalue is generated by a rank-one perturbation). The definition for the real ε-pseudospectrum reads as

$$\Lambda_\varepsilon^{\mathbb{R}}(A) = \left\{\lambda \in \mathbb{C} :\ \exists\ \delta A \in \mathbb{R}^{n\times n},\ \|\delta A\| \le \varepsilon \text{ s.t. } \det(\lambda I_n - A - \delta A) = 0\right\}, \tag{1.16}$$

and in the following we will indicate it with $\Lambda_{\varepsilon,2}^{\mathbb{R}}$, respectively $\Lambda_{\varepsilon,F}^{\mathbb{R}}$, when the spectral norm, respectively the Frobenius norm, is used to measure the norm of the uncertainty.

Let us introduce a novel notion, the so-called *real structured singular value*.

Definition 1.8. *Given a class of perturbations $\Delta \in \mathbb{R}^{n\times n}$, the real structured singular value of a matrix $M \in \mathbb{R}^{n\times n}$ is defined as*

$$\mu_{\mathbb{R}}(M) := \left(\inf_{\Delta\in\mathbb{R}^{n\times n}} \{\|\Delta\|_2 : \det(I_n - \Delta M) = 0\}\right)^{-1}. \tag{1.17}$$

A popular formula to compute $\mu_{\mathbb{R}}$ is derived in [107], to which we refer the reader for a detailed proof. This formula is stated in the next result.

Proposition 1.9. *For a given stable matrix $M \in \mathbb{R}^{n\times n}$, the real structured singular value can be computed as follows*

$$\mu_{\mathbb{R}}(M) = \inf_{\gamma\in(0,1]} \underbrace{\sigma_2\left(\begin{bmatrix} \Re(M) & -\gamma\Im(M) \\ \gamma^{-1}\Im(M) & \Re(M) \end{bmatrix}\right)}_{=:\, g_2(M,\gamma)} \tag{1.18}$$

This formula can be exploited to draw the pseudospectrum $\Lambda_{\varepsilon,2}^{\mathbb{R}}$: as a matter of fact, we write

$$\begin{aligned}
\Lambda_{\varepsilon,2}^{\mathbb{R}}(A) &= \left\{\lambda \in \mathbb{C} :\ \exists\ \delta A \in \mathbb{R}^{n\times n},\ \|\delta A\|_2 \le \varepsilon \text{ s.t.} \det(\lambda I_n - A - \delta A) = 0\right\} \\
&= \left\{\lambda \in \mathbb{C} :\ \exists\ \delta A \in \mathbb{R}^{n\times n},\ \|\delta A\|_2 \le \varepsilon \text{ s.t.} \det(I_n - \delta A(\lambda I_n - A)^{-1}) = 0\right\} \\
&= \left\{\lambda \in \mathbb{C} :\ \mu_{\mathbb{R}}((\lambda I_n - A)^{-1}) \ge \frac{1}{\varepsilon}\right\} \\
&= \left\{\lambda \in \mathbb{C} :\ \inf_{\gamma\in(0,1]} g_2((\lambda I_n - A)^{-1}, \gamma) \ge \frac{1}{\varepsilon}\right\},
\end{aligned}$$

$$= \left\{ \lambda \in \mathbb{C} : \sup_{\gamma \in (0,1]} g_{-2}((\lambda I_n - A), \gamma) \leq \varepsilon \right\}, \tag{1.19}$$

where the last equality was proven for the first time in [4], with

$$g_{-2}(M, \gamma) := \sigma_{-2} \left(\begin{bmatrix} \Re(M) & -\gamma \Im(M) \\ \gamma^{-1} \Im(M) & \Re(M) \end{bmatrix} \right), \tag{1.20}$$

and $\sigma_{-2}(M)$ indicating the second smallest singular value of a matrix. Therefore, the pseudospectrum $\Lambda^{\mathbb{R}}_{\varepsilon,2}$ can be drawn by using again a contour plotter on a grid of a region in the complex plane where the function $f(\lambda) = \sup_{\gamma \in (0,1]} g_{-2}(\lambda I_n - A, \gamma)$ has been evaluated. On the other hand, there are no methods available to draw the pseudospectrum $\Lambda^{\mathbb{R}}_{\varepsilon,F}$. As before, drawing the pseudospectrum is anyway expensive and possibly useless, as computing the ε-pseudospectral abscissa is sufficient to evaluate the degree of robustness of the stability of a system. In the following we describe two main methods from the literature.

(i) In [51] two alternative methods are proposed to compute the ε-pseudospectral abscissae $\alpha^{\mathbb{R}}_{\varepsilon,2}$, $\alpha^{\mathbb{R}}_{\varepsilon,F}$: the methods are inspired by the one proposed in [50] and thus rely on the construction of continuous paths of perturbations along which the spectral abscissa of the perturbed matrix is monotonically increasing. As in [50], only convergence to local maxima can be proven, but in practice the methods almost always converge to the global maximum.

We first consider the one employing the Frobenius norm, which relies on the following fundamental result.

Theorem 1.10. *For $A \in \mathbb{R}^{n \times n}$, let λ_* be a locally rightmost point of the ε-pseudospectrum $\Lambda^{\mathbb{R}}_{\varepsilon,F}(A)$, and a simple pseudoeigenvalue for some perturbation E. Then, there exists an $E_* \in \mathbb{R}^{n \times n}$, $\|E_*\|_F = 1$ such that λ_* is a (simple) eigenvalue of $A + \varepsilon E_*$, and such that*

- *If λ_* is real, then E_* has rank 1;*
- *If $\Im(\lambda_*) \neq 0$, then E_* has rank 2.*

From the first point, it follows trivially that if the globally rightmost point is real, then the ε-pseudospectral abscissa $\alpha^{\mathbb{R}}_{\varepsilon,F}$ coincides with $\alpha^{\mathbb{C}}_{\varepsilon}$ and thus can be computed using any of the methods described in the previous subsection. Then, [51] concentrates on a method to compute $\alpha^{\mathbb{R}}_{\varepsilon,F}$ when the associated eigenvalue is non-real. In order to exploit the low-rank property of the optimal perturbation, the authors consider the manifold

$$\mathcal{M}_F := \left\{ E \in \mathbb{R}^{n \times n} : \ \mathrm{rank}(E) = 2 \right\},$$

where they identify a path $E(s),\ s \geq 0$, such that $\|E(0)\|_F = 1$ and

$$\dot{E} = P_E\left(\Re(xy^*) - \langle E, \Re(xy^*)\rangle E\right), \tag{1.21}$$

where $x(s)$ and $y(s)$ are the left and right eigenvectors of the rightmost eigenvalue $\lambda(s)$ of the perturbed matrix $A + \varepsilon E(s)$, and are such that $\|x(s)\| = \|y(s)\| = 1$ and $x^*(s)y(s) \in (0, 1]$, while $\langle A, B\rangle = \text{Trace}(A^T B)$ indicates the inner product associated with the Frobenius norm, and $P_E(M)$ still indicates the projection of a generic matrix M onto the space tangent to the manifold $\mathcal{M}_F$ at $E(s)$. In order to exploit the low-rank property, a continuous and differentiable path of matrices $E(s)$ with rank *exactly* equal to two and solving a differential equation like (1.21) can be equivalently expressed via a decomposition.

Proposition 1.11. *Let $s \to E(s)$ be a matrix-valued function defined by the differential equation*

$$\dot{E}(s) = P_E(Z(s)) \tag{1.22}$$

with $s \to Z(s)$ a generic matrix-valued function and such that rank$(E(s)) = 2$ for all s. Let assume for $E(s)$ a decomposition as follows

$$E(s) = U(s)Q(s)V(s)^T,$$

where $U(s),\ V(s) \in \mathbb{R}^{n\times 2}$ have orthonormal columns and are such that $U^T(s)\dot{U}(s) = V^T(s)\dot{V}(s) = 0$, and $Q(s) \in \mathbb{R}^{2\times 2}$ is non-singular. Then, the differential equation (1.22) can be equivalently written as

$$\dot{E} = \dot{U}QV^T + U\dot{Q}V^T + UQ\dot{V}^T,$$

where

$$\begin{cases} \dot{Q} = U^T Z V, \\ \dot{U} = (I_n - UU^T)ZVQ^{-1}, \\ \dot{V} = (I_n - VV^T)Z^T UQ^{-T}. \end{cases} \tag{1.23}$$

The result of this proposition can be applied to (1.21) where $Z = \Re(xy^*) - \langle E, \Re(xy^*)\rangle E$. Then, similarly to [50], a forward Euler method with adaptive stepsize is applied to (1.23) to generate at each iteration a novel perturbation of the original matrix A with a larger spectral abscissa.

We now consider the method to compute the pseudospectral abscissa $\alpha^{\mathbb{R}}_{\varepsilon,2}$, for which a counterpart of Theorem 1.10 is given below.

Theorem 1.12. *For $A \in \mathbb{R}^{n\times n}$, let λ_* be a locally rightmost point of the ε-pseudospectrum $\Lambda^{\mathbb{R}}_{\varepsilon,2}(A)$ and a simple pseudoeigenvalue for some perturbation E. Then there exists $E_* \in \mathbb{R}^{n\times n}$, $\|E_*\|_2 = 1$ such that λ_* is a (simple) eigenvalue of $A + \varepsilon E_*$, and such that*

- *If λ_* is real, then E_* has rank 1;*
- *If $\Im(\lambda_*) \neq 0$, then E_* has rank 2, and $\sigma_1(E_*) = \sigma_2(E_*) = 1$.*

Following the practice used for the Frobenius norm, in order to compute $\alpha^{\mathbb{R}}_{\varepsilon,2}$ when it is associated with a complex pseudoeigenvalue, the authors identify a path in the Riemannian manifold

$$\mathcal{M}_2 := \big\{E \in \mathbb{R}^{n\times n} : E \text{ has rank 2 and both nonzero singular values of } E \text{ are equal to } 1\big\},$$

along which the spectral abscissa of the perturbed matrix $A + \varepsilon E(s)$ is monotonically increasing. Again, in order to exploit the low-rank property of matrices $E(s)$, they prove that a path in $\mathcal{M}_2$ can be equivalently expressed via the decomposition

$$E(s) = U(s)Q(s)V(s)^T,$$

where $U(s),\ V(s) \in \mathbb{R}^{n\times 2}$ have orthonormal columns and are such that $U^T(s)\dot{U}(s) = V^T(s)\dot{V}(s) = 0$, while $Q(s) \in \mathbb{R}^{2\times 2}$ is orthogonal and is such that $Q(s)^T\dot{Q}(s)$ is skew-symmetric. Then, a path guaranteeing the increasing monotonicity of the spectral abscissa of the perturbed matrix $A+\varepsilon E(s)$ is defined by the matrix-valued solutions of the following system of differential equations:

$$\begin{cases} \dot{U} = (I_n - UU^T)XY^TVQ^T, \\ \dot{V} = (I_n - VV^T)YX^TUQ, \\ \dot{Q} = Q\ \mathrm{skew}(Q^TU^TXY^TV), \end{cases} \tag{1.24}$$

where $\mathrm{skew}(A)$ indicates the anti-symmetric part of a matrix A, i.e. $\mathrm{skew}(A) = \frac{1}{2}(A - A^T)$, while $X,\ Y$ are defined as follows

$$X = \begin{bmatrix}\Re(x) & \Im(x)\end{bmatrix}, \quad Y = \begin{bmatrix}\Re(y) & \Im(y)\end{bmatrix}. \tag{1.25}$$

A discrete counterpart of this method, using a fixed-point iteration like in [52], is presented in [108].

(*ii*) In [29] a criss-cross type algorithm for the computation of the real ε-pseudospectral abscissa $\alpha^{\mathbb{R}}_{\varepsilon,2}$ is introduced. The algorithm relies on the characterization of the ε-pseudospectrum given in (1.19) and on the property that

$$\Lambda^{\mathbb{R}}_{\varepsilon,2} = \bigcap_{\gamma\in(0,1]} \Lambda^{\mathbb{R},\gamma}_{\varepsilon,2} := \bigcap_{\gamma\in(0,1]} \{\lambda \in \mathbb{C} : g_{-2}(\lambda I_n - A, \gamma) \leq \varepsilon\},$$

and, likewise [17], exploits the characterizations of intersections of horizontal and vertical lines with the boundary of superset $\Lambda_{\varepsilon,2}^{\mathbb{R},\gamma}$ in terms of the eigenvalues of an Hamiltonian standard EP of dimension $4n \times 4n$. This method is proven to converge to the globally rightmost point of the ε-pseudospectrum with a linear convergence rate. Moreover, in order to cope with large-scale problems and inspired by [75], a subspace acceleration of the method is proposed and proved to converge superlinearly.

Using the definition of real structured singular value and the formula (1.18) provided in [107], the real distance to instability of a stable matrix A can be characterised as

$$\begin{aligned} d_{\mathrm{INS}}^{\mathbb{R}} &= \inf_{\omega\in\mathbb{R}} \inf_{\Delta\in\mathbb{R}^{n\times n}} \{\|\Delta\|_2 : \det(\imath\omega I_n - A - \Delta) = 0\} \\ &= \inf_{\omega\in\mathbb{R}} \inf_{\Delta\in\mathbb{R}^{n\times n}} \{\|\Delta\|_2 : \det(I_n - \Delta(\imath\omega I_n - A)^{-1}) = 0\} \\ &= \inf_{\omega\in\mathbb{R}} \left[\mu_{\mathbb{R}}\left((\imath\omega I_n - A)^{-1}\right)\right]^{-1}, \end{aligned}$$

which implies

$$\begin{aligned} (d_{\mathrm{INS}}^{\mathbb{R}})^{-1} &= \sup_{\omega\in\mathbb{R}} \mu_{\mathbb{R}}\left((\imath\omega I_n - A)^{-1}\right) \\ &= \sup_{\omega\in\mathbb{R}} \inf_{\gamma\in(0,1]} g_2((\imath\omega I_n - A)^{-1}, \gamma). \end{aligned} \tag{1.26}$$

A fast method to compute the real structured distance to instability, which inspired the criss-cross algorithm in [29], is proposed in [114].

Complex-valued perturbation of a nonlinear EP

We now consider again the general nonlinear EP (1.1) and its perturbation (1.9). As already indicated the expression in (1.1) includes many different types of EPs, and there are plenty of works in the literature addressing the problem of plotting the pseudospectrum for some specific nonlinear EPs; among the others, [117] and [47] propose methods for the polynomial and the delay EP, respectively. Here, we describe a generalization of these two methods which holds for the same formulation of nonlinear EP here adopted, and which was proposed in [93]. Since the uncertainty on the EP can be defined by one or more perturbations affecting the matrices A_i, it is necessary to formally introduce an overall measure of the uncertainties. For given weights $w_i \in \overline{\mathbb{R}}_0^+ := \mathbb{R}^+ \setminus \{0\} \cup \{+\infty\}$ for $i = 1, \ldots, m$,

we consider the norm of $\Delta := (\delta A_1, \dots, \delta A_m)$ defined by

$$\|\Delta\|_{\text{glob}} := \left\| \begin{bmatrix} w_1 \|\delta A_1\|_{q_1} \\ \vdots \\ w_m \|\delta A_m\|_{q_1} \end{bmatrix} \right\|_{q_2}, \tag{1.27}$$

where $q_1,\ q_2 \in \overline{\mathbb{N}}_0^+$.

Let us consider $f:\ \mathbb{C} \to \overline{\mathbb{R}}^+$ associated with the inverse of the norm of the minimal perturbation that makes a given $\lambda \in \mathbb{C}$ an eigenvalue, formally defined as

$$f(\lambda) = \begin{cases} 0, & \text{if } \det(P(\lambda;\Delta)) \neq 0 \ \forall\ \Delta \\ +\infty, & \text{if } \det(P(\lambda)) = 0, \\ \left(\inf\{\|\Delta\|_{\text{glob}} : \det(P(\lambda;\Delta)) = 0\}\right)^{-1}, & \text{otherwise.} \end{cases} \tag{1.28}$$

Now, the ε-pseudospectrum Λ_ε can alternatively be defined as

$$\Lambda_\varepsilon = \left\{\lambda \in \mathbb{C} : f(\lambda) > \varepsilon^{-1}\right\}. \tag{1.29}$$

For a set of *complex-valued* uncertainties $\delta A_1, \dots, \delta A_m$, the following result from [93] gives an explicit formula for the function f.

Theorem 1.13. *For the perturbation measure (1.27), the function f defined in (1.28) can alternatively be defined as*

$$f(\lambda) = \begin{cases} +\infty, & \text{if } \det\left(\sum_{i=1}^m A_i p_i(\lambda)\right) = 0, \\ \left\| \left(\sum_{i=1}^m A_i p_i(\lambda)\right)^{-1} \right\|_\alpha \cdot \|w(\lambda)\|_\beta, & \text{if } \det\left(\sum_{i=1}^m A_i p_i(\lambda)\right) \neq 0, \end{cases} \tag{1.30}$$

where $\alpha = q_1$, β is such that $1/q_2 + 1/\beta = 1$ and

$$w(\lambda) = \begin{bmatrix} \frac{p_0(\lambda)}{w_0} \\ \vdots \\ \frac{p_m(\lambda)}{w_m} \end{bmatrix}.$$

Therefore, thanks to this theorem and to the equivalent definition (1.29), it is possible to draw the boundary of the ε-pseudospectrum by using a contour plotter. An example, also reported in [93], is given below.

Example 1.14. *We consider the first-order delay system*

$$\dot{x}(t) = A_0 x(t) + A_1 x(t-1), \tag{1.31}$$

where

$$A_0 = \begin{bmatrix} -5 & 1 \\ 2 & -6 \end{bmatrix}, \quad A_1 = \begin{bmatrix} -2 & 1 \\ 4 & -1 \end{bmatrix}$$

and the global norm on the uncertainty is measured as

$$\|\Delta\|_{\text{glob}} := \left\| \begin{bmatrix} w_0 \|\delta A_0\|_2 \\ w_1 \|\delta A_1\|_2 \end{bmatrix} \right\|_\infty,$$

i.e. we set $q_1 = 2,\ q_2 = +\infty$. *Therefore, by setting* $\beta = 1$, *we can exploit Theorem 1.13 and characterize the* ε*-pseudospectrum by means of*

$$f(\lambda) = \| \left(\lambda I - A_0 - A_1 e^{-\lambda\tau}\right)^{-1} \|_2 \left(\frac{1}{w_0} + \frac{|e^{-\lambda\tau}|}{w_1}\right), \tag{1.32}$$

where $\lambda \in \mathbb{C},\ \lambda \notin \Lambda$, *with* Λ *being the spectrum of the nominal system (1.31). In Figure 1.1* (a), *we plot the eigenvalues of the original system, while in Figure 1.1* (b),(c),(d), *we have represented the* ε*-pseudospectrum* Λ_ε *with weights* $[w_0,\ w_1] = [+\infty,\ 1]$, $[w_0,\ w_1] = [2,\ 2]$, $[w_0,\ w_1] = [1,\ +\infty]$, *respectively. The* ε*-pseudospectra are drawn by means of a contour plotter for* $\varepsilon = 1,\ 10^{0.5},\ 10$.

In the following we describe the two methods available in the literature for the computation of the complex ε-pseudospectral abscissa of nonlinear EPs.

(i) In [94], a fixed point iteration is proposed: considering again the global norm introduced in (1.27) with $q_1 = 2,\ q_2 = \infty$, it is demonstrated that each pseudoeigenvalue can be generated by a set of rank-one perturbations δA_i of the nominal matrices A_i for $i = 1, \ldots, m$. In particular, an explicit formulation of the perturbations generating the locally rightmost points of the ε-pseudospectrum is provided.

Proposition 1.15. *Let* λ_ε *be a locally rightmost point of the* ε*-pseudospectrum and let assume that* λ_ε *is simple. Then* λ_ε *is the rightmost eigenvalue of the perturbed eigenvalue problem*

$$\left(\sum_{i=1}^{m} \left(A_i - \frac{\overline{p_i(\lambda_\varepsilon)}}{w_i |p_i(\lambda_\varepsilon)|} uv^* \varepsilon\right) p_i(\lambda)\right) y = 0,$$

where $(u, v) \in \mathbb{C}^n \times \mathbb{C}^n$ *is a pair of (normalized) left and right singular vectors corresponding to* $\sigma_{\min}(\sum_{i=1}^m A_i p_i(\lambda_\varepsilon))$, *and such that they satisfy the conditions*

$$\begin{cases} \Im\left(u^* \left(\sum_{i=1}^m A_i p_i'(\lambda_\varepsilon)\right) v\right) - \varepsilon \sum_{i=1}^m \frac{\Im\left(\overline{p_i(\lambda_\varepsilon)} p_i'(\lambda_\varepsilon)\right)}{w_i |p_i(\lambda_\varepsilon)|} = 0, \\ \Re\left(u^* \left(\sum_{i=1}^m A_i p_i'(\lambda_\varepsilon)\right) v\right) - \varepsilon \sum_{i=1}^m \frac{\Re\left(\overline{p_i(\lambda_\varepsilon)} p_i'(\lambda_\varepsilon)\right)}{w_i |p_i(\lambda_\varepsilon)|} > 0. \end{cases}$$

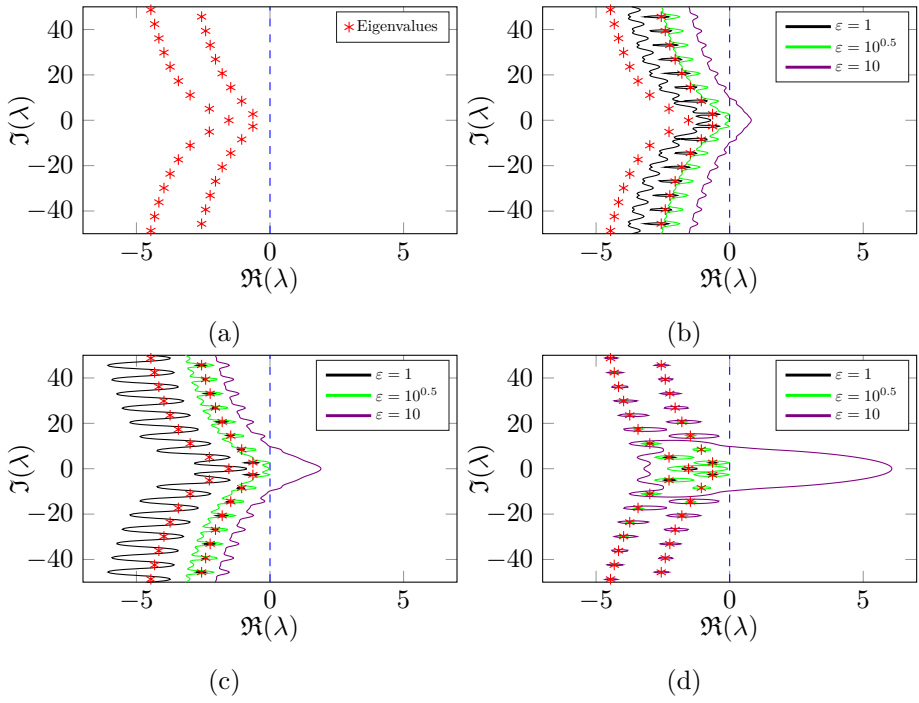

Figure 1.1: Complex ε-pseudospectra associated to system (1.31) for different choices of the weights w_i.

This result is the basis for the fixed-point iteration. Since the optimality conditions are satisfied by the globally rightmost point of the ε-pseudospectrum, as well as by the locally rightmost ones, the fixed point iteration is restarted several times from different rightmost eigenvalues of the original spectrum. Although no guarantee of convergence to the globally rightmost point can be proposed, the method has proved to work very well in practice.

(*ii*) In [85] another algorithm to compute the ε-pseudospectral abscissa is proposed, which is proven to converge to the globally rightmost point of the ε-pseudospectrum. The method relies on the characterization (1.29) of the ε-pseudospectrum, with $f(\lambda)$ defined in (1.30) for $\alpha = 2,\ \beta = 1$ (i.e. using the same global norm as in the previous method). In this case, it is easy to see that the ε-pseudospectrum can be rewritten as

$$\Lambda_\varepsilon^{\mathbb{C}} = \left\{ \lambda \in \mathbb{C} :\ \sigma_{\min}\left(\sum_{i=1}^{m} A_i p_i(\lambda) \right) \leq \varepsilon \left\| w(\lambda) \right\|_1 \right\}. \tag{1.33}$$

The authors exploit the fact that the nonzero singular values of a generic matrix M are the square roots of the nonzero eigenvalues of M^*M. Then the ε-pseudospectral abscissa $\alpha_\varepsilon^{\mathbb{C}}$ can be obtained as the solution of the following optimization problem:

$$\begin{array}{ll} \max_{\lambda\in\mathbb{C}} & \Re(\lambda) \\ \text{s. t.} & z_{min}\left[(\sum_{i=1}^m A_i p_i(\lambda))^*(\sum_{i=1}^m A_i p_i(\lambda))\right] - \varepsilon^2 \left\|w(\lambda)\right\|_1^2 \leq 0, \end{array} \tag{1.34}$$

where $z_{min}[A]$ indicates the eigenvalue of A with *smallest modulus*. Two main ingredients are used in the basic iteration of this algorithm. The first is a method ([87]) to solve an optimization problem where the cost function is a linear function, and the constraint is a smallest eigenvalue function: this is used to solve the optimization problem (1.34) and returns a *locally* rightmost point $\widetilde{\lambda} = \widetilde{\alpha} + \imath\widetilde{\beta}$ of the ε-pseudospectrum. In this phase, the authors also employ the subspace acceleration ([75]), making the method suitable for large-scale problems.

Then, $\widetilde{\lambda}$ is such that

$$g(\widetilde{\alpha},\widetilde{\beta}) := \frac{\sigma_{\min}\left(\sum_{i=1}^m A_i p_i(\widetilde{\alpha}+\imath\widetilde{\beta})\right)}{\left\|w(\widetilde{\alpha}+\imath\widetilde{\beta})\right\|_1} = \varepsilon.$$

The second ingredient is employed in order to check whether $\widetilde{\lambda}$ is also a globally rightmost point: to this end, a minimization of $g(\widetilde{\alpha},\beta)$ over β is performed using the algorithm in [88] for the global optimization of an eigenvalue of an Hermitian and analytic matrix-valued function. This step is intended to look for inner points of the ε-pseudospectrum lying on the same vertical line where $\widetilde{\lambda}$ lies, or equivalently to look for points $\lambda = \widetilde{\alpha} + \imath\beta$ such that

$$g(\widetilde{\alpha},\beta) < g(\widetilde{\alpha},\widetilde{\beta}) = \varepsilon.$$

If such points exist, then $\widetilde{\lambda}$ is just a locally but not globally rightmost point of the ε-pseudospectrum, and (at least) another iteration must be repeated.

Depending on the norm adopted to measure the uncertainty magnitude, several numerical methods for the computation of the distance to instability exist. Some approaches for the PEP are proposed for instance in [105] and [44]. For the general formulation of nonlinear EPs here adopted, a Newton-type method exploiting the ideas in [94] was described in [125].

1.3 Research aims and motivations

Although the effect of real-valued perturbations affecting a nonlinear EP is a topic of major impact for practical applications, there is a lack of techniques to sketch the real ε-pseudospectrum of a nonlinear EP, because a characterization of the ε-pseudospectrum boundary in terms of the singular values is not known to this date. In addition, there does not exist methods to compute the real ε-pseudospectral abscissa either.

The first motivation of this dissertation is to solve the latter problem by defining an algorithm which maximally exploits the structure of the EP and of the perturbations. As a matter of fact, a possible approach to handle nonlinearity in the frequency domain consists of applying a linearization of the nonlinear EP resulting in a standard EP, followed by the pseudospectral abscissa computation using standard techniques. However, this approach does not necessarily simplify the problem: for example, a linearization of the delay eigenvalue problem gives rise to an infinite-dimensional EP of a differentiation operator with non-local boundary conditions [96]. In addition, an analysis based on the unstructured pseudospectra of the linearization does not respect the structure of equation (1.9), leading to an eventual over-bounding of the actual uncertainty and to a conservative robust stability criterion. In this thesis, we describe a method to compute the real ε-pseudospectral abscissa of perturbed nonlinear EPs like (1.9). The methodology proposed fully exploits the nonlinear structure of the EP and does not require any linearization. At the same time, it allows to incorporate structured perturbations of A_i. In addition, the method is computationally very efficient and it is applicable for large-scale problems.

Secondly, this method is applied in the context of robust stabilisation of dynamical systems. As a matter of fact, by minimising the ε-pseudospectral abscissa w.r.t. some controller parameters, it is possible to design a stabilising controller which by definition guarantees the robust stability of the system as well. From an application point of view, this approach is more convenient than other methods aimed at minimizing the spectral abscissa or at assigning the rightmost eigenvalues of the spectrum (such as pole placement).

Finally, the thesis extends the adopted approach to the analysis of the stability robustness of time-periodic linear delay systems. These models are applicable in a large number of mechanical engineering applications, such as the turning and the milling model, but the literature about the analysis of the robust stability is still very poor.

1.4 Overview of the thesis

We here give a brief description of the structure of this thesis and of the contents of each chapter.

Chapter 1 introduced the motivations for the new research here described and placed this work within the state of the art, by giving an overview particularly on the available methods for the computation of the ε-pseudospectral abscissa and of the distance to instability for linear and nonlinear EPs.

Chapter 2 presents a method for the computation of the real ε-pseudospectral abscissa of nonlinear EPs, considering both the Frobenius and the spectral norms as measures of the uncertainty. To the best of the authors' knowledge, this is the first method addressing such a problem. *This chapter is based on [11].*

Chapter 3 focuses on the stability robustness of DEPs. The method introduced in Chapter 2 is extended to compute the real ε-pseudospectral abscissa when matrices A_i are affected by *structured* uncertainties, and, simultaneously delay terms are also subject to perturbations. In addition, the close connection between the concepts of pseudospectral abscissa and distance to instability is illustrated, and a bisection-Newton's method to compute the distance to instability for the same class of systems is presented. *This chapter is based on [7] and [10].*

Chapter 4 proposes the design of a robust controller for uncertain delay systems, which is achieved by minimizing the ε-pseudospectral abscissa w.r.t. some control parameters. An application of this method is provided in the design of stabilising decentralised controllers for networks of delay-coupled systems. *This chapter is based on [8], [9] and [27].*

Chapter 5 describes another method for the computation of the distance to instability for delay systems affected by real-valued structured perturbations on the coefficient matrices. The method totally differs from the one presented in Chapter 3 in the following sense: a characterization of the distance to instability analogous to (1.26) is exploited; moreover a different definition of the class of perturbations (and of the corresponding norm) is considered. In addition, the implemented method is guaranteed to globally converge to the global maximum of the $\mu_{\mathbb{R}}$ function. *This chapter is based on [12].*

Chapter 6 deals with time-periodic delay systems. An introduction to the stability analysis of these systems is given here, and a novel solver for the computation of the Floquet multipliers is presented. By means of this solver, we also introduce a new methodology for the assessment of the stability robustness of this kind of systems, which is a problem that to the best of the author's knowledge is addressed here for the first time. In addition, the chapter

includes an analysis of the stability robustness of a large number of application case-studies in mechanical engineering; in particular, the stability robustness of a milling operation is investigated, and the numerical results are validated against experimental tests. *This chapter is based on [6] and [56].*

Chapter 7 summarizes the main achievements of the thesis and presents conclusions and possible developments for future research.

Chapter 2

Computing the real pseudospectral abscissa for nonlinear eigenvalue problems

In this chapter we present two methods to compute the real ε-pseudospectral abscissa of the perturbed nonlinear EP (1.9): the first method employs the Frobenius norm as a measure of each uncertainty δA_i, while the second adopts the spectral norm. In both cases, it is proven that the pseudoeigenvalue associated with the pseudospectral abscissa $\alpha_\varepsilon^{\mathbb{R}}$ is generated by a set of perturbations with rank smaller than or equal to two and such that they share their column and row spaces. This is a surprising property, given that the combined additive perturbation matrix on the characteristic equation is highly structured.

The proposed methods are basically equivalent to a projected gradient method aimed at maximizing the spectral abscissa of the perturbed problems: the methods rely on the identification of a steepest ascent direction in a manifold of coefficient matrices perturbations, where the global maximizer of the spectral abscissa is proven to be contained. Methods based on a gradient flow discretization are more advantageous than methods based on a fixed-point iteration induced by a characterization of rightmost points ([17, 94]): as a matter of fact, the monotonicity property of the real part of the rightmost eigenvalue along the flow favours the local convergence, therefore is preferable in terms of a globalization strategy.

The chapter is structured as follows: Section 2.1 presents the problem and states the main assumptions. Sections 2.2 and 2.3 present the algorithms and the theoretical results on which they are grounded: the two sections consider the Frobenius and the spectral norm, respectively. Section 2.4 describes the results

obtained in several numerical experiments, and also addresses the application to large-scale problems. Finally we give our conclusions in Section 2.5.

2.1 Problem statement and main assumptions

We consider the nonlinear EP as defined in the introduction, that is

$$P(\lambda)y = \left(\sum_{i=1}^{m} A_i p_i(\lambda)\right) y = 0,\ \lambda \in \mathbb{C},\ y \in \mathbb{C}^n, \tag{2.1}$$

with $A_i \in \mathbb{R}^{n\times n},\ n \geq 2$, and the perturbed nonlinear EP

$$P(\lambda;\Delta)y = \left(\sum_{i=1}^{m} (A_i + \delta A_i) p_i(\lambda)\right) y = 0, \tag{2.2}$$

where the overall measure on the set of perturbations $\Delta = (\delta A_1, \ldots, \delta A_m) \in (\mathbb{R}^{n\times n})^m := \underbrace{\mathbb{R}^{n\times n} \times \cdots \times \mathbb{R}^{n\times n}}_{m \text{ times}}$ is defined as

$$\|\Delta\|_{\text{glob}} := \left\| \begin{bmatrix} w_1 \|\delta A_1\| \\ \vdots \\ w_m \|\delta A_m\| \end{bmatrix} \right\|_{\infty}, \tag{2.3}$$

where each weight $w_i \in \overline{\mathbb{R}}_0^+$, and we will adopt $\|\cdot\| = \|\cdot\|_F$ in Section 2.2 and $\|\cdot\| = \|\cdot\|_2$ in Section 2.3. In the following, we will refer by a (weighted) ε-bounded set of perturbations to a set Δ such that

$$\|\delta A_i\| \leq \frac{\varepsilon}{w_i},\ i = 1, \ldots, m.$$

By choosing some of the weights equal to infinity, we can impose that some coefficient matrices are not perturbed.

Throughout the chapter we make the following assumption on the shape of the real ε-pseudospectrum.

Assumption 2.1. *The set $\Lambda_\varepsilon^{\mathbb{R}} \cap \{\lambda \in \mathbb{C} : \Re(\lambda) \geq r\}$ is bounded for all $r \in \mathbb{R}$.*

Assumption 2.1 guarantees that a globally rightmost point of the ε-pseudospectrum exists, hence, the supremum defining the real ε-pseudospectral abscissa (1.11) can be replaced by a maximum. Thus, the real ε-pseudospectral abscissa is *exactly* the real part of the globally rightmost point of the ε-pseudospectrum. We refer to [94, Section 2] for an elaborate discussion on this assumption. We remark that this assumption is always satisfied by EPs inferred

by delay systems of retarded type, and by PEPs such that A_m is invertible and $\varepsilon < w_m \sigma_n(A_m)$. It is trivial to see then that Assumption 2.1 holds for standard EPs.

Secondly, an assumption is made that plays an important role in the characterization of the rank of optimal perturbations.

Assumption 2.2. *Let λ_{RM} be a rightmost eigenvalue of the ε-pseudospectrum of (2.2), and let x, y be the corresponding left and right eigenvectors respectively. If $\mathfrak{I}(\lambda_{\mathrm{RM}}) \neq 0$, then vectors $\mathfrak{R}(x)$ and $\mathfrak{I}(x)$ are independent, as well as vectors $\mathfrak{R}(y)$ and $\mathfrak{I}(y)$. Equivalently, matrices*

$$X = [\mathfrak{R}(x)\ \mathfrak{I}(x)],\ Y = [\mathfrak{R}(y)\ \mathfrak{I}(y)]$$

in $\mathbb{R}^{n\times 2}$ have rank 2.

Even though Assumption 2.2 always holds for the standard EP (recall that $n \geq 2$) and it sounds very natural, it is not satisfied for all nonlinear EPs under consideration. As a counter example, consider the QEP

$$\left(\lambda^2 I + \begin{bmatrix} 1 & 0 \\ 0 & 3 \end{bmatrix}\right) y = 0,$$

for which the rightmost complex eigenvalues admit a purely real eigenvector. However, we can consider this assumption as not very restrictive.

Finally, we make the following technical assumption.

Assumption 2.3. *Let λ_{RM} be a rightmost point of the ε-pseudospectrum. Then we have $p_i(\lambda_{\mathrm{RM}}) \neq 0$ whenever w_i is finite, for $i = 1, \ldots, m$.*

In [94] this assumption is motivated by showing that the violation corresponds to a degenerate case (the conclusions of Proposition 3.3 in [94] carry over from the complex pseudospectrum to the real one since they share intersections with the real axis). For the special case of the PEP, a violation would imply that $\lambda_{\mathrm{RM}} = 0$ and that this eigenvalue is invariant under perturbations.

2.2 The Frobenius norm case

In this section, we adopt the Frobenius norm in the definition of the global norm (2.3). Before we introduce the main theoretical results on which our algorithm is grounded, we recall the formula to compute the derivative of a simple eigenvalue of a general EP w.r.t. any parameter of the characteristic matrix, which is a simple consequence of the implicit function theorem. A proof for this formula is available in [109, Lemma 2.7].

Lemma 2.4. *Let $M : \mathbb{C} \to \mathbb{C}^{n\times n}$, $\lambda \to M(\lambda;\theta)$ be an analytic function depending smoothly on parameters $\theta \in \mathbb{R}^d$. Let λ be a simple root of* $\det M(\cdot;\theta) = 0$ *such that $M(\lambda;\theta)y = 0$ and $x^*M(\lambda;\theta) = 0$, with $x,\ y \in \mathbb{C}^n$ with unit norm, and x^* the complex conjugate transpose of x, then*

$$\frac{\partial\lambda}{\partial\theta_i} = -\frac{x^*\frac{\partial M(\lambda;\theta)}{\partial\theta_i}y}{x^*\frac{\partial M(\lambda;\theta)}{\partial\lambda}y}, \qquad i = 1,\dots,d. \tag{2.4}$$

From this lemma, we easily retrieve the derivative of a simple eigenvalue of (2.2) w.r.t. the variations in the coefficient matrices δA_i. In particular, if we see each perturbation δA_i as depending on n^2 independent variables in the form

$$\delta A_i = \begin{pmatrix} v_{1,1}^{(i)} & \dots & v_{1,n}^{(i)} \\ \vdots & \ddots & \vdots \\ v_{n,1}^{(i)} & \dots & v_{n,n}^{(i)} \end{pmatrix}, \tag{2.5}$$

then the derivative is

$$\frac{\partial\lambda}{\partial v_{s,t}^{(i)}} = -\frac{\bar{x}_s p_i(\lambda) y_t}{x^*\Big(\sum_{i=1}^m (A_i+\delta A_i)p_i'(\lambda)\Big)y},\ i = 1,\dots,m,\ s,t = 1,\dots,n, \tag{2.6}$$

where we indicate with $p_i'(\lambda)$ the derivative of the entire function p_i w.r.t. the complex variable λ.

The main idea of the proposed algorithm is to solve the following optimization problem

$$\begin{array}{ll} \max & \Re\lambda(\Delta) \\ \text{s.t.} & \Delta \in (\mathbb{R}^{n\times n})^m,\ \|\Delta\|_{\text{glob}} \le \varepsilon, \end{array} \tag{2.7}$$

where $\lambda(\Delta)$ is the rightmost eigenvalue of the perturbed problem $P(\lambda;\Delta)$. In practice, we look for a set Δ of *optimal perturbations*, i.e. a set of perturbations generating the globally rightmost point of the ε-pseudospectrum. The next theorem is the fundamental result of this section and it provides an explicit expression for a set of optimal perturbations.

Theorem 2.5. *Let λ_{RM} be a globally rightmost point in the real ε-pseudospectrum and assume it is a simple eigenvalue of the problem perturbed by the ε-bounded set of perturbations $(\delta A_1,\dots,\delta A_m)$. Let x and y be the corresponding left and right eigenvectors with unit norms and uniquely determined by the condition*

$$\xi := x^*\left(\sum_{i=1}^m (A_i+\delta A_i)p_i'(\lambda_{\text{RM}})\right)y > 0. \tag{2.8}$$

Defining

$$X = [\Re(x)\ \Im(x)],\ Y = [\Re(y)\ \Im(y)],\ \Gamma_i = \begin{bmatrix} \Re(p_i(\lambda_{\mathrm{RM}})) & -\Im(p_i(\lambda_{\mathrm{RM}})) \\ \Im(p_i(\lambda_{\mathrm{RM}})) & \Re(p_i(\lambda_{\mathrm{RM}})) \end{bmatrix},$$

for $i = 1, \ldots, m$, we have $X\Gamma_i Y^T \neq 0$; then, we can express a particular set of optimal perturbations as

$$\delta A_i = -\frac{\varepsilon}{w_i} \frac{X\Gamma_i Y^T}{\|X\Gamma_i Y^T\|_F}. \tag{2.9}$$

Proof. Let us consider the perturbed nonlinear EP (2.2) and let us define every perturbation matrix $\delta A_i \in \mathbb{R}^{n\times n}$ as depending on n^2 independent variables as in (2.5). We then write the gradient of $\Re(\lambda_{\mathrm{RM}})$ w.r.t. δA_i as a matrix whose (s,t)-th component is the derivative w.r.t. $v_{s,t}^{(i)}$ as expressed in (2.6), then

$$\begin{aligned} \frac{\partial \Re(\lambda_{\mathrm{RM}})}{\partial \delta A_i} := \left(\frac{\partial \Re(\lambda_{\mathrm{RM}})}{\partial v_{s,t}^{(i)}} \right)_{s,t=1,\ldots,n} &= -\frac{1}{\xi} \Re\left(\bar{x}_s p_i(\lambda_{\mathrm{RM}}) y_t \right)_{s,t=1,\ldots,n} \\ &= -\frac{1}{\xi} X\Gamma_i Y^T \neq 0, \end{aligned}$$

where $X\Gamma_i Y^T$ is a nonzero matrix as a result of Assumptions 2.2 and 2.3 and of the Sylvester's rank inequality. We want the set of perturbations $\Delta = (\delta A_1, \ldots, \delta A_m)$ to be ε-bounded w.r.t. the global norm defined in (2.3), thus we impose on each of them the following constraint

$$g_i := \sum_{s,t=1,\ldots,n} \left(v_{s,t}^{(i)} \right)^2 - \frac{\varepsilon^2}{w_i^2} \leq 0,\ i = 1, \ldots, m. \tag{2.10}$$

Since λ_{RM} is a globally rightmost point, the following optimality conditions are satisfied,

$$\frac{\partial \Re(\lambda_{\mathrm{RM}})}{\partial v_{s,t}^{(i)}} - 2\mu_i v_{s,t}^{(i)} = 0,\ i = 1, \ldots, m,\ s,t = 1, \ldots, n,$$

and they can be reshaped in a more compact form, namely

$$\frac{\partial \Re(\lambda_{\mathrm{RM}})}{\partial \delta A_i} - 2\mu_i \delta A_i = 0,\ i = 1, \ldots, m,$$

where $\mu_i \geq 0,\ i = 1, \ldots, m$, are the Lagrange multipliers corresponding to the set of constraints (2.10). Since $\frac{\partial \Re(\lambda_{\mathrm{RM}})}{\partial \delta A_i} \neq 0$, we must have $\mu_i > 0,\ i = 1, \ldots, m$. Therefore, the constraints on the norm are all active and each optimal perturbation δA_i must lie on the boundary of the weighted ε-radius ball. Since δA_i is also a positive multiple of $\frac{\partial \Re(\lambda_{\mathrm{RM}})}{\partial \delta A_i}$, by imposing $\|\delta A_i\|_F = \dfrac{\varepsilon}{w_i},\ i = 1, \ldots, m$, we get the assertion of the theorem. □

In the previous theorem we have provided a characterization of the set of optimal perturbations, from which we derive two main properties which will be lately exploited by our algorithm. Firstly, each optimal perturbation δA_i has maximal norm and has rank equal to two if the globally rightmost eigenvalue λ_{RM} is complex, or equal to one when λ_{RM} is real. Secondly, all the optimal perturbations δA_i share the same column space with the matrix X and the same row space with the matrix Y^T. In practice, we know now that the global maximum of the optimization problem (2.7) is also the global maximum of a new optimization problem with a restricted search space, namely

$$\begin{array}{ll} \max & \Re\lambda(\Delta) \\ \text{s.t.} & \Delta \in \mathcal{S}_F, \end{array} \tag{2.11}$$

where $\mathcal{S}_F$ is a manifold of matrices defined as follows

$$\mathcal{S}_F := \left\{ (\delta A_1, \ldots, \delta A_m) \in \left(\mathbb{R}^{n\times n}\right)^m : \ \mathrm{rank}(\delta A_i) \le 2, \ w_i \left\|\delta A_i\right\|_F = \varepsilon, \right.$$
$$\left. \delta A_i \text{ share the same space of columns and rows}, \ i = 1, \ldots, m \right\}.$$

In order to find the pseudospectral abscissa $\alpha^{\mathbb{R}}_{\varepsilon,F}$, we want to construct a path of perturbations Δ in $\mathcal{S}_F$ along which the spectral abscissa of the corresponding perturbed problem $P(\lambda;\Delta)$ is monotonically increasing; in particular, we would like to identify the direction of steepest ascent. Let us assume that the set of perturbations Δ depends in a continuous and a.e. differentiable manner on a real parameter $s \ge 0$. From now on, we use "dot-quantities" $(\dot{\delta A_i}, \dot{\widehat{U}}_i, \ldots)$ to refer to the derivatives w.r.t. the parameter s. To build our iterative method we make use of the following result.

Proposition 2.6. *Let the function $\mathbb{R}^+ \ni s \mapsto \delta A_i(s) \in \mathcal{S}_F$ s.t. $w_i \left\|\delta A_i\right\|_F = \varepsilon$ be continuous for all s and differentiable a.e. Then we can always decompose $\delta A_i(s)$ as follows*

$$\delta A_i(s) = -\frac{\varepsilon}{w_i} U(s) Q_i(s) V(s)^T, \tag{2.12}$$

where $U(s) \in \mathbb{R}^{n\times 2}$, $V(s) \in \mathbb{R}^{n\times 2}$ have orthonormal columns and are such that $U(s)^T\dot{U}(s) = V(s)^T\dot{V}(s) = 0$ a.e., and $Q_i(s) \in \mathbb{R}^{2\times 2}$ is s.t. $\left\|Q_i(s)\right\|_F = 1$ for all $i = 1, \ldots, m$.

Proof. Let us first consider the compact SVD for each $\delta A_i(s)$, that is

$$\delta A_i(s) = -\frac{\varepsilon}{w_i} \widehat{U}(s) \widehat{\Sigma}_i(s) \widehat{V}(s)^T, \ s \in \mathbb{R}^+,$$

where $\widehat{U}(s), \widehat{V}(s) \in \mathbb{R}^{n\times 2}$ have orthonormal columns and $\widehat{\Sigma_i}(s) \in \mathbb{R}^{2\times 2}$ is a diagonal matrix such that $\left\|\widehat{\Sigma_i}(s)\right\|_F = 1$. Observe that since the SVD is not

unique and $(\delta A_1(s), \dots, \delta A_n(s)) \in \mathcal{S}_F$, we can assume the same $\widehat{U}(s)$, $\widehat{V}(s)$ for all $\delta A_i(s)$, for $i = 1, \dots, m$. As a consequence of [25, Theorem 4.3], the factors of the compact singular value decomposition of each δA_i also depend on s in a continuous and a.e. differentiable way. Then, by the orthonormality of the columns of $\widehat{U}(s)$, we have that

$$\dot{\widehat{U}}(s)^T \widehat{U}(s) + \widehat{U}(s)^T \dot{\widehat{U}}(s) = 0, \ \forall\ s \geq 0,$$

thus $\widehat{U}(s)^T \dot{\widehat{U}}(s)$ is a 2×2 skew-symmetric matrix, as well as $\widehat{V}(s)^T \dot{\widehat{V}}(s)$.

Let $Q_1(s)$ be a solution of the Cauchy problem

$$\dot{Q}_1(s) = -Q_1(s)^{-T} [\widehat{U}(s)^T \dot{\widehat{U}}(s)]^T, \ Q_1(0) = I_2, \tag{2.13}$$

defined in each interval where $\delta A_i(s)$ is continuous and differentiable for $i = 1, \dots, m$. From (2.13) we can conclude the following: $Q_1^T(s)\dot{Q}_1(s)$ is skew-symmetric, from which we derive that

$$\frac{d}{ds}\left(Q_1^T(s)Q_1(s)\right) = 0 \Longrightarrow Q_1^T(s)Q_1(s) = \text{constant}.$$

As for $s = 0$ we have $Q_1(0) = I_2$, then $Q_1(s)$ is orthogonal for all $s \geq 0$. If we now define $U(s) := \widehat{U}(s)Q_1(s)^T$ (and below we omit s for simplicity), we have

$$\begin{aligned} U^T\dot{U} &= Q_1\widehat{U}^T\dot{U} = Q_1\dot{Q}_1^T + Q_1\widehat{U}^T\dot{\widehat{U}}Q_1^T \\ &= -Q_1[\widehat{U}^T\dot{\widehat{U}}]Q_1^{-1} + Q_1\widehat{U}^T\dot{\widehat{U}}Q_1^T = 0, \end{aligned}$$

where we use (2.13) for the third equality. Thus, we proved that the matrix $\widehat{U}(s) \in \mathbb{R}^{n\times 2}$ can be decomposed into the product of a matrix $U(s) \in \mathbb{R}^{n\times 2}$ such that $U(s)^T\dot{U}(s) = 0$ and of an orthogonal matrix $Q_1(s) \in \mathbb{R}^{2\times 2}$. By applying the same reasoning to matrix $\widehat{V}(s)$ (using factors $V(s)$ and $Q_2(s)$), we have that (omitting again the dependences s)

$$\delta A_i = -\frac{\varepsilon}{w_i}\widehat{U}\widehat{\Sigma}_i\widehat{V}^T = -\frac{\varepsilon}{w_i}UQ_1\widehat{\Sigma}_iQ_2V^T = -\frac{\varepsilon}{w_i}UQ_iV^T,$$

where $\|Q_i(s)\|_F = 1$ because Frobenius norm is invariant to orthogonal transformations. □

Thanks to the last result, we thus obtain a decomposition of the perturbations δA_i which exploits the low-rank property; as explicitly demonstrated in [73], without loss of generality the factors of the decomposition (2.12) can be equivalently expressed as the solutions of the following differential equations

$$\begin{cases} \dot{U}(s) = \left(I_n - U(s)U(s)^T\right)R(s), \\ \dot{V}(s) = \left(I_n - V(s)V(s)^T\right)S(s), \\ \dot{Q}_i(s) = M_i(s) - \langle M_i(s), Q_i(s)\rangle Q_i(s), \end{cases} \tag{2.14}$$

where $R(s),\ S(s) \in \mathbb{R}^{n\times 2}$, $M_i(s) \in \mathbb{R}^{2\times 2}$ for $i = 1, \ldots, m$, are arbitrary matrix-valued functions which will be explicitly defined to identify a direction of change within the manifold $\mathcal{S}_F$, and where $\langle \cdot, \cdot \rangle$ indicates the Frobenius inner product defined as $\langle A, B\rangle = \mathrm{trace}(A^T B)$.

Observe that the differential equation defined for $Q_i(s)$ is a consequence of the constraint on the Frobenius norm of $Q_i(s)$, which forces $Q_i(s)$ to be orthogonal to $\dot{Q}_i(s)$ w.r.t. the Frobenius inner product: in practice, the projection is necessary to avoid the violation on the norm constraint and defines a direction of change which is on the tangent space to the 1-radius ball at $Q_i(s)$.

In what follows we specify the matrix-valued functions $R(s),\ S(s),\ M_i(s)$ in order to individuate a continuous and a.e. differentiable path of perturbations $\Delta(s)$ in $\mathcal{S}_F$ along which the spectral abscissa $\mathfrak{R}(\lambda(s))$ is monotonically increasing. Since this direction is clearly not unique, we look for *the direction of steepest ascent*. Using again Lemma 2.4, the derivative w.r.t. s of a simple eigenvalue λ of (2.2) is given by

$$\frac{d\lambda(s)}{ds} = -\frac{x^*\Big(\sum_{i=1}^m \delta\dot{A}_i(s)p_i(\lambda)\Big)y}{x^*\Big(\sum_{i=1}^m \big(A_i + \delta A_i(s)\big)p_i'(\lambda)\Big)y}, \tag{2.15}$$

where $x,\ y$ are again the left and right eigenvectors, respectively, with unit norm and uniquely determined by the normalization constraint (2.8). Now, defining the matrices $X,\ Y,\ \Gamma_i$ for $i = 1, \ldots, m$ as in Theorem 2.5, and employing (2.14) in (2.15) as well as the decomposition (2.12) for δA_i, we have that

$$\begin{aligned}
\mathfrak{R}(\dot{\lambda}) &= \textstyle\sum_{i=1}^m \frac{\varepsilon}{\xi w_i}\mathfrak{R}\big(x^*(\dot{U}Q_iV^T + U\dot{Q}_iV^T + UQ_i\dot{V}^T)y\big)p_i(\lambda)\\
&= \textstyle\sum_{i=1}^m \frac{\varepsilon}{\xi w_i}\big\langle X, (I_n - UU^T)RQ_iV^TY\Gamma_i^T\big\rangle +\\
&\quad \textstyle\sum_{i=1}^m \frac{\varepsilon}{\xi w_i}\big\langle X, U(M_i - \langle M_i, Q_i\rangle Q_i)V^TY\Gamma_i^T\big\rangle +\\
&\quad \textstyle\sum_{i=1}^m \frac{\varepsilon}{\xi w_i}\big\langle X, UQ_iS^T(I_n - VV^T)Y\Gamma_i^T\big\rangle\\
&= \textstyle\sum_{i=1}^m \frac{\varepsilon}{\xi w_i}\big\langle X\Gamma_iY^TVQ_i^T, (I_n - UU^T)R\big\rangle +\\
&\quad \textstyle\sum_{i=1}^m \frac{\varepsilon}{\xi w_i}\big\langle U^TX\Gamma_iY^TV, M_i - \langle M_i, Q_i\rangle Q_i\big\rangle +\\
&\quad \textstyle\sum_{i=1}^m \frac{\varepsilon}{\xi w_i}\big\langle S, (I_n - VV^T)Y\Gamma_i^TX^TUQ_i\big\rangle\\
&= \textstyle\frac{\varepsilon}{\xi}\big\langle X\sum_{i=1}^m \frac{1}{w_i}\Gamma_iY^TVQ_i^T, (I_n - UU^T)R\big\rangle +\\
&\quad \textstyle\sum_{i=1}^m \frac{\varepsilon}{\xi w_i}\big\langle U^TX\Gamma_iY^TV, M_i - \langle M_i, Q_i\rangle Q_i\big\rangle +\\
&\quad \textstyle\frac{\varepsilon}{\xi}\big\langle S, (I_n - VV^T)Y\sum_{i=1}^m \frac{1}{w_i}\Gamma_i^TX^TUQ_i\big\rangle.
\end{aligned}$$

Since $(I_n - UU^T), (I_n - VV^T)$ are positive semi-definite, the *steepest ascent direction* for $\mathfrak{R}(\lambda)$ is obtained by the following choices:

$$R = X \sum_{i=1}^{m} \frac{1}{w_i} \Gamma_i Y^T V Q_i^T,$$

$$M_i = U^T X \Gamma_i Y^T V, \tag{2.16}$$

$$S = Y \sum_{i=1}^{m} \frac{1}{w_i} \Gamma_i^T X^T U Q_i.$$

Then, substituting these expressions in (2.14), we have

$$\begin{cases} \dot{U} = \left(I_n - UU^T\right) X \sum_{i=1}^{m} \frac{1}{w_i} \Gamma_i Y^T V Q_i^T, \\ \dot{V} = \left(I_n - VV^T\right) Y \sum_{i=1}^{m} \frac{1}{w_i} \Gamma_i^T X^T U Q_i, \\ \dot{Q}_i = U^T X \Gamma_i Y^T V - \langle U^T X \Gamma_i Y^T V, Q_i \rangle Q_i. \end{cases} \tag{2.17}$$

Finally, we have a set of differential equations whose solutions $U(s),\ V(s) \in \mathbb{R}^{n\times 2},\ Q_i(s) \in \mathbb{R}^{2\times 2}$ for $i = 1, \ldots, m$, define a path in the manifold $\mathcal{S}_F$ along which the spectral abscissa of the perturbed nonlinear EP $P(\lambda; \Delta(s))$ is monotonically increasing. The basic idea of our algorithm is to discretize this system of equations with a forward Euler step method, and thus to generate at each iteration a novel perturbed EP with a larger spectral abscissa: since the sequence of the spectral abscissae is bounded from above, it must at least converge to a locally rightmost point of the pseudospectrum. In the next subsection we give the details of our implementation.

Remark 2.7. *For the special case of the standard EP, the difference with [51] is as follows. For the case of a complex rightmost point a differential equation is proposed in [51] on the manifold of matrices of rank exactly equal to two, which is a Riemannian manifold, equipped with the natural geometry (see also [73]). In this way, geodesics can be infinitely extended on the manifold, and the induced distance to a rank-one matrix is infinite. Although geometrically very neat, the consequence is that a distinction needs to be made in the overall algorithm between the cases of a real valued and of a complex valued rightmost point in the pseudospectrum (rank-one or rank-two critical perturbations). In our setting we do not impose any rank constraints on Q_i, hence, we can address both cases simultaneously. In several examples, we have even observed switches, in the sense that starting from a complex eigenvalue, the real rightmost point of the pseudospectrum is found, and vice versa.*

2.2.1 Implementation

In Algorithm 1 we provide a detailed description of the projected gradient method to compute the pseudospectral abscissa $\alpha^{\mathbb{R}}_{\varepsilon,F}$, where the steepest ascent direction is identified by the solutions of the differential equations (2.17). In each iteration, a new perturbation Δ is defined by discretizing (2.17) with a forward Euler method with adaptive stepsize: this always requires a normalization of the perturbations to ensure that the iterate lies in $\mathcal{S}_F$. After the computation of the rightmost eigenvalue of the newly perturbed problem and of its corresponding left and right eigenvectors, a normalization of the eigenvectors is also needed in order to satisfy the condition (2.8).

The adaptive stepsize is used to guarantee increasing monotonicity: at each iteration the initial standard stepsize is reduced by a scaling factor h (that we set equal to 2) until monotonicity is guaranteed; on the other hand, if the initial stepsize already guarantees monotonicity, an extra computation with a double stepsize is carried out. The stepsize that guarantees the rightmost eigenvalue is then adopted.

The initialization is as follows. We consider a rightmost eigenvalue of the unperturbed problem, and the corresponding left and right eigenvectors. Then we initialize $X, Y, \Gamma_i,\ i = 1, \dots, m$ as in Theorem 2.5. We apply a compact QR decomposition of X, Y such that $X = Q_X R_X,\ Y = Q_Y R_Y$ and we define

$$U^{(1)} = Q_X,\ V^{(1)} = Q_Y,\ Q_i^{(1)} = \frac{R_X \Gamma_i R_Y^T}{\left\| R_X \Gamma_i R_Y^T \right\|_F},\ i = 1, \dots, m.$$

Finally we construct the perturbed system $\sum_{i=1}^{m} \big(A_i - \frac{\varepsilon}{w_i} U^{(1)} Q_i^{(1)} V^{(1)T}\big) p_i(\lambda)$ and, once again, we compute the rightmost eigenvalue and the corresponding eigenvectors. The algorithm terminates if the norm of the (projected) gradient of the spectral abscissa is below a given tolerance. Clearly this condition also holds on local maxima, and the algorithm cannot distinguish between locally and globally rightmost points. However, in practice, a convergence to a locally rightmost point is seldom observed. Moreover, we run the algorithm several times using different eigenvalues (located in the right part of the original spectrum) as initial points. This has already proved to be an effective strategy to converge to the globally rightmost point in [50], [51].

2.3 The spectral norm case

In this section we describe a method to compute the real pseudospectral abscissa $\alpha^{\mathbb{R}}_{\varepsilon,2}$ when the spectral norm is chosen in definition (2.3). Again, we use the low-rank and the maximum norm properties of the optimal perturbations, and we perform a discretization of the gradient flow in a manifold of perturbations. As we shall illustrate, there are two fundamental differences with the previous

Algorithm 1 Computing $\alpha^{\mathbb{R}}_{\varepsilon,F}$ via forward Euler discretization of (2.17).

Input: Problem data: A_i, p_i, ε, tolerance η, scaling factor $h > 1$.
Initialization data: $U^{(1)}, Q_i^{(1)}, V^{(1)}, \lambda_1, x_1, y_1, r_1$

Set $\gamma = +\infty$, $n = 1$.
while $\gamma > \eta$ **do**
  Compute
$$\begin{cases} X = [\Re(x_n)\ \Im(x_n)], \\ Y = [\Re(y_n)\ \Im(y_n)], \\ \Gamma_i = \begin{bmatrix} \Re(p_i(\lambda_n)) & -\Im(p_i(\lambda_n)) \\ \Im(p_i(\lambda_n)) & \Re(p_i(\lambda_n)) \end{bmatrix}, \ i = 1 \dots m. \end{cases}$$
  Compute the derivatives
$$\begin{cases} \dot{U}^{(n)} = \left(I_n - U^{(n)}U^{(n)T}\right) X \sum_{i=1}^m \frac{1}{w_i} \Gamma_i Y^T V^{(n)} Q_i^{(n)T} \\ \dot{V}^{(n)} = \left(I_n - V^{(n)}V^{(n)T}\right) Y \sum_{i=1}^m \frac{1}{w_i} \Gamma_i^T X^T U^{(n)} Q_i^{(n)} \\ \dot{Q}_i^{(n)} = U^{(n)T} X \Gamma_i Y^T V^{(n)} - \langle U^{(n)T} X \Gamma_i Y^T V^{(n)}, Q_i^{(n)} \rangle Q_i^{(n)}, \ i = 1, \dots, m. \end{cases}$$
  Compute
$$\begin{cases} \widehat{U}^{(n+1)} = U^{(n)} + r_n \dot{U}^{(n)}, \\ \widehat{V}^{(n+1)} = V^{(n)} + r_n \dot{V}^{(n)}, \\ \widehat{Q}_i^{(n+1)} = Q_i^{(n)} + r_n \dot{Q}_i^{(n)}, \ i = 1, \dots, m. \end{cases}$$
  Compute the compact QR decompositions s.t.
$$\begin{cases} \widehat{U}^{(n+1)} = Q_U R_U, \\ \widehat{V}^{(n+1)} = Q_V R_V. \end{cases}$$
  Set
$$\begin{cases} U^{(n+1)} = Q_U, \\ V^{(n+1)} = Q_V, \\ Q_i^{(n+1)} = \widehat{Q}_i^{(n+1)} / \left\| \widehat{Q}_i^{(n+1)} \right\|_F, \ i = 1, \dots, m. \end{cases}$$
  Define a new Δ such that $\delta A_i = -\frac{\varepsilon}{w_i} U^{(n+1)} Q_i^{(n+1)} V^{(n+1)T}, \ i = 1, \dots, m$.
  Compute the rightmost eigenvalue $\hat{\lambda}$ of the perturbed problem $P(\lambda; \Delta)$, and the corresponding normalized left and right eigenvectors $\hat{x}, \hat{y}$.
  Set $r = r_n$.
  while $\Re(\hat{\lambda}) \leq \Re(\lambda_n)$ **do**
    Set $r = r/h$ and repeat steps from 5 to 8 with step r.
    Compute the rightmost eigenvalue $\hat{\lambda}$ of the perturbed problem $P(\lambda; \Delta)$, and the corresponding normalized left and right eigenvectors $\hat{x}, \hat{y}$.
  end while
  if $r < r_n$ **then**
    Set $\lambda_{n+1} = \hat{\lambda}, x_{n+1} = \hat{x}, y_{n+1} = \hat{y}, r_{n+1} = r$
  else
    Set $\tilde{r} := h r_n$ and repeat steps from 5 to 8 with step $\tilde{r}$.
    Compute the rightmost eigenvalue $\hat{\lambda}$ of the perturbed problem $P(\lambda; \Delta)$, and the corresponding normalized left and right eigenvectors $\tilde{x}, \tilde{y}$.
    if $\Re(\hat{\lambda}) \leq \Re(\tilde{\lambda})$ **then**
      Set $\lambda_{n+1} = \tilde{\lambda}, x_{n+1} = \tilde{x}, y_{n+1} = \tilde{y}, r_{n+1} = \tilde{r}$
    else
      Set $\lambda_{n+1} = \hat{\lambda}, x_{n+1} = \hat{x}, y_{n+1} = \hat{y}, r_{n+1} = r_n$
    end if
  end if
  Set $\gamma = \Re(\dot{\lambda}_{n+1})$ and $n \to n + 1$.
end while
return $\alpha_\varepsilon = \Re(\lambda_{n+1})$.

case: firstly, the 2×2 matrix Q_i, obtained from the decomposition, has to be orthogonal; secondly, we define a path within a manifold of matrices with rank *exactly* equal to two.

In the following we present several theoretical results: Theorem 2.8 demonstrates that, as for the Frobenius norm case, there always exists a set of optimal perturbations with maximal norm and with rank equal to two, respectively equal to one, when the globally rightmost point λ_{RM} is complex, respectively real; in addition, when λ_{RM} is complex, the two nonzero singular values of each optimal perturbation δA_i are equal. Theorem 2.10 proposes a decomposition of the optimal perturbations δA_i which exploits the low rank property, and demonstrates that, also in this case, the optimal perturbations share the same column and row spaces. The algorithm presented here will ground on this latter property.

Although the proposed method still relies on the discretization of a gradient flow in the manifold of perturbations, with the purpose of making the description as complete as possible in Theorem 2.11 we provide an explicit characterization of the optimal perturbations: this potentially directly gives rise to a fixed-point iteration for computing the ε-pseudospectral abscissa, thereby generalizing the method of [94] from complex to real perturbations, and the method of [108] from linear to nonlinear EPs.

Theorem 2.8. *Let λ_{RM} be a globally rightmost point of the ε-pseudospectrum. Assume λ_{RM} is an eigenvalue for some ε-bounded set of perturbations $(\delta A_1, \dots, \delta A_m)$, with*

$$\delta A_i = -\frac{\varepsilon}{w_i}\widehat{E}_i, \quad \|\widehat{E}_i\|_2 \leq 1 \quad \text{for } i = 1, \dots, m,$$

and let x and y be the corresponding left and right eigenvectors normalized such that

$$x^* \left(\sum_{i=1}^{m} (A_i + \delta A_i) p_i'(\lambda_{\mathrm{RM}}) \right) y > 0. \tag{2.18}$$

Then $\|\widehat{E}_i\|_2 = 1$, $i = 1, \dots, m$. Moreover, if λ_{RM} is a simple eigenvalue, then there exist real-valued matrices $\widetilde{E}_i$, $i = 1, \dots, m$, with unit spectral norm, such that

$$\left(\sum_{i=1}^{m} \left(A_i + \widetilde{\delta A}_i \right) p_i(\lambda_{\mathrm{RM}}) \right) y = 0, \quad x^* \left(\sum_{i=1}^{m} \left(A_i + \widetilde{\delta A}_i \right) p_i(\lambda_{\mathrm{RM}}) \right) = 0,$$

where $\widetilde{\delta A}_i = -\dfrac{\varepsilon}{w_i}\widetilde{E}_i$ and $\widetilde{E}_i$ has the following property:

(i) if λ_{RM} is real, $\widetilde{E}_i$ has rank 1;

(ii) if λ_{RM} is not real, $\widetilde{E}_i$ has rank 2 and two singular values equal to 1.

Proof. On the real axis the real pseudospectrum $\Lambda_\varepsilon^{\mathbb{R}}$ and the complex pseudospectrum $\Lambda_\varepsilon^{\mathbb{C}}$ coincide, so we refer to [94] for case (i). Let us then consider the case (ii), where λ_{RM} is genuinely complex. For smooth matrix-valued functions $\widehat{E}_i(s)$, with $\widehat{E}_i(0) = \widehat{E}_i$ and $\|\widehat{E}_i(s)\|_2 \leq 1$, the classical derivative formula for a simple eigenvalue of the nonlinear EP with matrices $A_i - \frac{\varepsilon}{w_i}\widehat{E}_i(s)$ leads to

$$\left.\frac{d\lambda}{ds}\right|_{s=0} = c\, x^* \left(\sum_{i=1}^{m} \frac{\varepsilon}{w_i} p_i\left(\lambda_{\mathrm{RM}}\right) \dot{\widehat{E}}_i(0) \right) y \tag{2.19}$$

where c is a positive constant as a consequence of (2.18). Now let $\dot{\widehat{E}}_i(s) \equiv 0$ for all $i = 1, \ldots, m$ except i_*. Formula (2.19) gives

$$\left.\frac{d\lambda}{ds}\right|_{s=0} = c\, \frac{\varepsilon}{w_{i_*}} p_{i_*}\left(\lambda_{\mathrm{RM}}\right) x^* \dot{\widehat{E}}_{i_*}(0)\, y. \tag{2.20}$$

Recall that x and y are the left and right eigenvectors, respectively, both of unit norm and scaled according to (2.18). Let $p_{i_*}(\lambda_{\mathrm{RM}}) = re^{\imath\theta}$ (note that by Assumption 2.3 we have $r \neq 0$); set $z = e^{\imath\theta} y$ (a rotated eigenvector) and denote by $x = \Re(x) + \imath\Im(x)$, $y = \Re(y) + \imath\Im(y)$ and $z = \Re(z) + \imath\Im(z)$. Then we define the matrices X, Y (and Z coherently) as we did in Theorem 2.5.

By the rightmost property of λ_{RM}, (2.20) gives $0 \geq \Re\left(x^* \dot{\widehat{E}}_{i_*}(0)\, z\right)$, which implies

$$0 \geq \Re(x)^T \dot{\widehat{E}}_{i_*}(0) \Re(z) + \Im(x)^T \dot{\widehat{E}}_{i_*}(0) \Im(z) = \operatorname{trace}(X^T \dot{\widehat{E}}_{i_*}(0) Z). \tag{2.21}$$

Assume, by contradiction, that $\|\widehat{E}_{i_*}\|_2 = \|\widehat{E}_{i_*}(0)\|_2 < 1$. Then we can always set $\dot{\widehat{E}}_{i_*}(0)$ such that violates (2.21) and increase the real part of the rightmost eigenvalue λ_{RM}.

Now let $\widehat{U}, \widehat{V} \in \mathbb{R}^{n\times n}$ be orthogonal matrices whose first two columns $U, V \in \mathbb{R}^{n\times 2}$ span the range of X, and of Y and Z respectively, so that

$$X = \widehat{U} \begin{bmatrix} S \\ 0 \end{bmatrix} = US, \quad Z = \widehat{V} \begin{bmatrix} T \\ 0 \end{bmatrix} = VT \quad \text{for some } S, T \in \mathbb{R}^{2\times 2}.$$

Let $\widehat{E}_{i_*}(s)$, for small $s \geq 0$, be a continuously differentiable path, which we write as

$$\widehat{E}_{i_*}(s) = \widehat{U} \widehat{R}(s) \widehat{V}^T, \qquad \|\widehat{R}(s)\|_2 = 1,$$

where $\widehat{E}_{i_*}(0) = \widehat{E}_{i_*}$.

Let $R(s) \in \mathbb{R}^{2\times 2}$ denote the left upper 2×2 block of $\widehat{R}(s)$, and define

$$\widetilde{E}_{i_*}(0) = UR(0)V^T =: \widetilde{E}_{i_*} \qquad \text{with} \quad \|\widetilde{E}_{i_*}\|_2 \leq 1. \tag{2.22}$$

Observe that, as a consequence of (2.21),

$$0 \geq \operatorname{trace}(X^T \dot{\widehat{E}}_{i_*}(0) Z) \tag{2.23}$$

$$= \operatorname{trace}\left(\begin{bmatrix} S^T & 0 \end{bmatrix} \widehat{U}^T \widehat{U} \dot{\widehat{R}}(0) \widehat{V}^T \widehat{V} \begin{bmatrix} T \\ 0 \end{bmatrix} \right) \tag{2.24}$$

$$= \operatorname{trace}(S^T \dot{R}(0) T) \tag{2.25}$$

Again, this inequality holds for every path $\widehat{R}(s)$ of unit norm such that $\|R(0)\|_2 = 1$, otherwise we could choose $\dot{R}(0)$ arbitrarily, so that $\operatorname{trace}(S^T \dot{R}(0) T) > 0$, contradicting (2.23). Thus $\|\widetilde{E}_{i_*}\|_2 = 1$. Let us write

$$R(0) = P \Sigma Q^T, \qquad \Sigma = \begin{pmatrix} 1 & 0 \\ 0 & \sigma_2 \end{pmatrix},$$

with $P, Q \in \mathbb{R}^{2\times 2}$ orthogonal matrices and $0 \leq \sigma_2 \leq 1$. Defining

$$\widehat{R}(0) = \begin{pmatrix} R(0) & \widehat{R}_{12} \\ \widehat{R}_{21} & \widehat{R}_{22} \end{pmatrix}, \tag{2.26}$$

we will show below that $\sigma_2 = 1$, so that $\widetilde{E}_{i_*}$ has rank two and the submatrix $\widehat{R}_{21}(0) = 0$, since otherwise one of the first two columns of $\widehat{R}(0)$ has norm larger than one, in contradiction with $\|\widehat{R}(0)\|_2 = 1$. Hence

$$\widehat{R}(0) = \begin{pmatrix} R(0) & 0 \\ 0 & \widehat{R}_{22} \end{pmatrix},$$

with a matrix $\widehat{R}_{22}$ such that $\|\widehat{R}_{22}\|_2 \leq 1$. Given the structure of $\widehat{R}(0)$, it is easy to see that the perturbed problem where we substitute $\widehat{E}_{i_*}$ with $\widetilde{E}_{i_*}$ has the same eigenvalue λ_{RM} with the same eigenvectors x and y. Finally, since these arguments are independent of the choice of i_*, they hold for every $i = 1, \ldots, m$, which yields that

$$\left(\sum_{i=1}^{m} \left(A_i + \widetilde{\delta A_i} \right) p_i(\lambda_{\mathrm{RM}}) \right) y = 0, \quad x^* \left(\sum_{i=1}^{m} \left(A_i + \widetilde{\delta A_i} \right) p_i(\lambda_{\mathrm{RM}}) \right) = 0$$

with $\widetilde{\delta A_i} = -\dfrac{\varepsilon}{w_i} \widetilde{E}_i$ of rank-2 for all i. Hence the theorem is proven.

Now it is left to demonstrate that $\sigma_2 = 1$. We assume by contradiction that $\sigma_2 < 1$; choosing the matrices $R_k(s) = P \Sigma_k(s) Q$ with

$$\Sigma_1(s) = \begin{pmatrix} 1 & 0 \\ 0 & \sigma_2 \pm s \end{pmatrix}, \quad \Sigma_2(s) = \begin{pmatrix} 1 - as^2 & \pm s \\ 0 & \sigma_2 \end{pmatrix}, \quad \Sigma_3(s) = \begin{pmatrix} 1 - as^2 & 0 \\ \pm s & \sigma_2 \end{pmatrix},$$

it is easily verified that if $\sigma_2 < 1$ it is possible to find $a > 0$ such that both matrices $R_{2,3}(s)$ have spectral norm not larger than one in a sufficiently small neighborhood of $s = 0$.

Next we find that the inequality $0 \geq \mathrm{trace}(S^T \dot{R}(0) T)$ (see (2.25)) implies

$$0 = \mathrm{trace}(S^T P e_\ell e_j^T Q^T T) = e_j^T Q^T T S^T P e_\ell \quad \text{for } (\ell, j) \in \{(2,2),(1,2),(2,1)\},$$

where $e_1 = (1 \quad 0)^T$ and $e_2 = (0 \quad 1)^T$. As a consequence

$$Q^T T S^T P = \begin{pmatrix} \eta & 0 \\ 0 & 0 \end{pmatrix} \qquad \text{with real } \eta$$

and therefore S or T must be of rank 1. This yields that $\Re(x)$ and $\Im(x)$ are linearly dependent or $\Re(z)$ and $\Im(z)$ (and therefore $\Re(y)$ and $\Im(y)$) are linearly dependent. Let us first assume the latter. Then, there is a real φ such that $y = \cos(\varphi) w + \imath \sin(\varphi) w$ for some real vector w. Rotating both x and y does not change the normalization property (2.18), so we can state that y is a real eigenvector of the perturbed problem, thus implying that λ_{RM} is real, which is contradictory. The argument is analogous assuming that $\Re(x)$ and $\Im(x)$ are linearly dependent. Therefore it must hold that $\sigma_2 = 1$. □

In order to prove the next theorem, we first need to introduce the following lemma, whose prove can be found in [50].

Lemma 2.9. *(a) Let B be a real square matrix. Then we have* $\mathrm{trace}(BZ) = 0$ *for every skew-symmetric matrix Z if and only if B is symmetric.*

(b) Let B be a symmetric matrix. Then we have $\mathrm{trace}(BM) \geq 0$ *for every symmetric positive semi-definite matrix M if and only if B is positive semi-definite.*

Theorem 2.10. *Let λ_{RM} be a globally rightmost point of the ε-pseudospectrum with λ_{RM} a simple non-real eigenvalue generated by an ε-bounded set of perturbations Δ, and let x, y be the corresponding left and right normalized eigenvectors such that (2.18) holds. Let also the matrices X, Y, Γ_i, $i = 1, \ldots, m$ be defined as in Theorem 2.5.*

If $\delta A_i = -\dfrac{\varepsilon}{w_i} E_i$ has rank 2 for $i = 1, \ldots, m$, with

$$E_i = U Q_i V^T, \tag{2.27}$$

where $U, V \in \mathbb{R}^{n \times 2}$ have orthonormal columns and $Q_i \in \mathbb{R}^{2 \times 2}$, then

(i) Q_i is an orthogonal matrix;

(ii) X and U have the same range, Y and V have the same range;

(iii) the matrix $Q_i^T\, U^T\, X\, \Gamma_i^T\, Y^T V$ is symmetric and positive definite for $i = 1, \ldots, m$.

Proof of Theorem 2.10. Property (ii) has been obtained in the proof of Theorem 2.8. Property (i) is a consequence of the representation of a rank-2 matrix with both singular values equal to 1 and image given by span(U) and kernel span$(V^\perp)$. For the proof of (iii) we make use of Lemma 2.9 and similar arguments to those used in [50].

For a chosen $i_* \in \{1, \ldots, m\}$ consider the smooth matrix-valued function

$$E_{i_*}(s) = U Q_{i_*} e^{sW} V^T,$$

where W is a skew-symmetric matrix, and let all the other matrices be unchanged. Denote by $\lambda(s)$ the eigenvalues $\lambda(s)$ with $\lambda(0) = \lambda_{\mathrm{RM}}$.

By local optimality, we have (see (2.21))

$$\begin{aligned} 0 \;&\geq\; \Re\left(p_i(\lambda_{\mathrm{RM}})\, x^* \dot{E}_{i_*}(0)\, y\right) = \mathrm{trace}(X^T \dot{E}_{i_*}(0) Y \Gamma_{i_*}) \\ &=\; \left\langle X\, \Gamma_i^T\, Y^T, U Q_{i_*} W V^T \right\rangle = \left\langle Q_{i_*}^T\, U^T\, X\, \Gamma_{i_*}^T\, Y^T V, W \right\rangle, \end{aligned}$$

which holds for every skew-symmetric matrix W. By Lemma 2.9, $Q_{i_*}^T\, U^T\, X\, \Gamma_{i_*}^T\, Y^T V$ is symmetric.

We next consider the smooth matrix-valued function

$$E_{i_*}(s) = U Q_{i_*} e^{-sM} V^T$$

where M is a symmetric positive semi-definite matrix and the other matrices are left unchanged. Then we obtain

$$0 \geq \Re(p_i(\lambda_{\mathrm{RM}})\, x^* \dot{E}_{i_*}(0) y) = -\left\langle Q_{i_*}^T\, U^T\, X\, \Gamma_{i_*}^T\, Y^T V, M \right\rangle$$

for every symmetric positive semi-definite matrix M. By Lemma 2.9 and invertibility $Q_{i_*}^T\, U^T\, X\, \Gamma_{i_*}^T\, Y^T V$ is positive-definite. As this argument is independent of i_*, the proof is complete. □

Theorem 2.11. *Let λ_{RM} be a globally rightmost point of the ε-pseudospectrum.* Case 1: λ_{RM} is non-real. *Assume λ_{RM} is a simple eigenvalue for some ε-bounded set of perturbations Δ, where each δA_i has rank two and two singular values equal to ε/w_i, and let x and y be the corresponding normalized left and right eigenvectors such that (2.18) is satisfied. Let X, Y and Γ_i be defined as in Theorem 2.5. Let the decomposition*

$$X \Gamma_i Y^T = U_i \Sigma_i V_i^T, \quad i = 1, \ldots, m, \tag{2.28}$$

correspond to the compact SVD. Then a particular set of optimal perturbations can be expressed as

$$\delta A_i = -\frac{\varepsilon}{w_i} U_i V_i^T, \;\; i = 1, \ldots, m.$$

Case 2: λ_{RM} is real. *Assume λ_{RM} is a simple eigenvalue for some ε-bounded set of perturbations Δ, where each δA_i has rank one, and let $x \in \mathbb{R}^n$ and $y \in \mathbb{R}^n$ be the corresponding normalized left and right eigenvectors such that (2.18) is satisfied. Then a particular set of optimal perturbations can be expressed as*

$$\delta A_i = -\frac{\varepsilon}{w_i}\mathrm{sign}(p_i(\lambda_{\mathrm{RM}}))\ xy^T,\ i = 1, \ldots, m. \tag{2.29}$$

Proof. We restrict ourselves to the first case. For the case of a rightmost real eigenvalue the derivation is the same as for complex pseudospectra and we refer to [94]. By a property of the singular value decomposition and the fact that Γ_i is invertible, X and U_i have the same column space, and Y and V_i have the same column space. Based on the first two properties in Theorem 2.10 we can write

$$\delta A_i = -\frac{\varepsilon}{w_i}U_i Q_i V_i^T, \tag{2.30}$$

where Q_i is some 2-by-2 orthogonal matrix for $i = 1, \ldots, m$.

From the last property in Theorem 2.10 we have

$$Q_i^T U_i^T X \Gamma_i Y^T V_i > 0,\ i = 1, \ldots, m,$$

which, using (2.28), can be rewritten as

$$Q_i^T \Sigma_i > 0,\ i = 1, \ldots, m. \tag{2.31}$$

Assuming for the moment that Q_i corresponds to a rotation, i.e.

$$Q_i = \begin{bmatrix} \cos\theta & \sin\theta \\ -\sin\theta & \cos\theta \end{bmatrix},\ \theta \in (-\pi,\ \pi],$$

and letting $\Sigma = \mathrm{diag}(\sigma_1, \sigma_2)$, then the satisfaction of condition (2.31) requires $\theta = 0$. Using a similar argument one can show that Q_i cannot correspond to a reflection. In conclusion, the only possibility is to have $Q_i = I,\ i = 1, \ldots, m$, in (2.30). □

Thanks to the provided characterization of the set of optimal perturbations, we construct our algorithm in an analogous way to the one for the Frobenius norm case. We want to identify a continuous and a.e. differentiable path of perturbations $\Delta(s)$ within a manifold of matrices, which defines the direction of steepest ascent for the spectral abscissa $\mathfrak{R}(\lambda(s))$ of the perturbed EP $P(\lambda; \Delta(s))$.

Consider a path in the manifold

$$\mathcal{S}_S := \Big\{(\delta A_1, \ldots, \delta A_m) \in \left(\mathbb{R}^{n\times n}\right)^m :\ \mathrm{rank}(\delta A_i) = 2,\ w_i \left\|\delta A_i\right\|_F = \varepsilon,$$

$$\delta A_i \text{ share the same column and row spaces, and}$$

$$\sigma_1(\delta A_i) = \sigma_2(\delta A_i),\ i = 1, \ldots, m\Big\},$$

parametrized as

$$\delta A_i(s) = -\frac{\varepsilon}{w_i} U(s) Q_i(s) V(s)^T$$

with $U(s),\ V(s) \in \mathbb{R}^{n\times 2}$ s.t. $U(s)^T\dot{U}(s) = V(s)^T\dot{V}(s) = 0$ and $Q_i(s) \in \mathbb{R}^{2\times 2}$ orthogonal.

As seen in the Frobenius norm case, the conditions on $U(s)$ and $V(s)$ can be recast as

$$\begin{cases} \dot{U}(s) = \Big(I_n - U(s)U(s)^T\Big)R(s), \\ \dot{V}(t) = \Big(I_n - V(s)V(s)^T\Big)S(s), \end{cases}$$

for some $R(s), S(s) \in \mathbb{R}^{n\times 2}$. The condition that $Q_i(s)$ is orthogonal for all $s \geq 0$ (assuming Q_i is differentiable) is equivalent to the condition that $Q_i(0)$ is orthogonal, supplemented with

$$\begin{aligned} 0 &= \tfrac{d}{ds}\big(Q_i(s)^T Q_i(s)\big) \\ &= Q_i(s)^T\dot{Q}_i(s) + \big(Q_i(s)^T\dot{Q}_i(s)\big)^T, \quad \forall\ s \geq 0. \end{aligned}$$

The latter property, specifying that $Q_i(s)^T\dot{Q}_i(s)$ is skew-symmetric, can be recast in a parametrization of the form

$$\dot{Q}_i(s) = Q_i(s)\mathrm{skew}(P_i(s)),$$

where $\mathrm{skew}(P_i) = (P_i - P_i^T)/2$ is the skew-symmetric part of some matrix P_i.

Now, in order to guarantee monotonicity of the flow, we want to identify the steepest ascent direction for the derivative of the real part of the rightmost eigenvalue, which will ultimately lead to the specification of R, S and P_i. To this end, let us consider

$$\begin{aligned} \Re(\dot{\lambda}) &= \textstyle\sum_{i=1}^m \frac{\varepsilon}{\xi w_i}\Re\big(x^*(\dot{U}Q_iV^T + U\dot{Q}_iV^T + UQ_i\dot{V}^T)y\big)p_i(\lambda) \\ &= \textstyle\sum_{i=1}^m \frac{\varepsilon}{\xi w_i}\big\langle X, (I_n - UU^T)RQ_iV^TY\Gamma_i^T\big\rangle + \\ &\quad \textstyle\sum_{i=1}^m \frac{\varepsilon}{\xi w_i}\big\langle X, UQ_i\mathrm{skew}(P_i)V^TY\Gamma_i^T\big\rangle + \\ &\quad \textstyle\sum_{i=1}^m \frac{\varepsilon}{\xi w_i}\big\langle X, UQ_iS^T(I_n - VV^T)Y\Gamma_i^T\big\rangle \\ &= \tfrac{\varepsilon}{\xi}\big\langle X\textstyle\sum_{i=1}^m \frac{1}{w_i}\Gamma_iY^TVQ_i^T, (I_n - UU^T)R\big\rangle + \\ &\quad \textstyle\sum_{i=1}^m \frac{\varepsilon}{\xi w_i}\big\langle Q_i^TU^TX\Gamma_iY^TV, \mathrm{skew}(P_i)\big\rangle + \\ &\quad \tfrac{\varepsilon}{\xi}\big\langle S, (I_n - VV^T)Y\textstyle\sum_{i=1}^m \frac{1}{w_i}\Gamma_i^TX^TUQ_i\big\rangle. \end{aligned}$$

Thus, the steepest ascent direction is guaranteed by the choices

$$\begin{cases} \dot{U} = \Big(I_n - UU^T\Big)X\textstyle\sum_{i=1}^m \frac{1}{w_i}\Gamma_iY^TVQ_i^T, \\ \dot{V} = \Big(I_n - VV^T\Big)Y\textstyle\sum_{i=1}^m \frac{1}{w_i}\Gamma_i^TX^TUQ_i, \\ \dot{Q}_i = Q_i\ \mathrm{skew}(Q_i^TU^TX\Gamma_iY^TV), \end{cases} \tag{2.32}$$

where the formulas on $\dot{U}, \dot{V}$ are identical to the ones obtained in the Frobenius norm case. It is worth to point out that the formula on $\dot{Q}_i$ guarantees the orthogonality of $Q(s)$ for every s only if $Q(0)$ is orthogonal.

Remark 2.12. *As for the Frobenius norm case, this construction allows us to treat simultaneously the cases of either a real or complex globally rightmost point of the pseudospectrum. We have demonstrated that in case of a real rightmost point, the optimal perturbations can be expressed as rank-one matrices; however, thanks to the properties of the spectral norm, the same eigenvalue can be obtained through perturbation matrices with a higher rank and the same largest singular value. For this reason our algorithm is able to converge to a real rightmost point moving along a path of rank-two matrices, where the orthogonality of matrices Q_i is imposed. Indeed, in several simulations we could observe our algorithm converging to a rightmost real eigenvalue although it was started from a non-real value.*

2.3.1 Implementation

The algorithm is developed analogously to Algorithm 1, where the only main differences are given by the new differential equations for matrices Q_i and the re-orthogonalization after every step, as follows:

- on line 4, the formula for $\dot{Q}_i$ has to be replaced by the one in (2.32);
- on line 6, we compute the QR decomposition of $\widehat{Q}_i^{(n+1)}$ s.t. $\widehat{Q}_i^{(n+1)} = QR$ where all entries on the diagonal of R are nonnegative; then we set $Q_i^{(n+1)} = Q$. The additional condition on the diagonal of R is to avoid the possibility of a change in the direction of the vector during the re-orthogonalization.

The characterization of the optimal perturbations given in Theorem 2.11 is exploited in the initialization of the algorithm, as will be clarified next.

Let us first assume that the starting eigenvalue is complex. If XY^T has the compact singular value decomposition $XY^T = U\Sigma V^T$ and if

$$(U^T X)\Gamma_i(Y^T V) = \tilde{U}_i \Sigma_i \tilde{V}_i^T \in \mathbb{R}^{2\times 2}$$

also corresponds to an SVD, then the decomposition (2.28) holds, where

$$U_i = U\tilde{U}_i, \quad V_i = V\tilde{V}_i, \ i = 1, \ldots, m.$$

This has two consequences. First, in order to compute the singular value decomposition of $X\Gamma_i Y^T$, $i = 1, \ldots, m$ only one compact singular value

decomposition of a n-by-n matrix needs to be performed. Second, the optimal perturbations have the form

$$\delta A_i = -\frac{\varepsilon}{w_i} U \left(\tilde{U}_i \tilde{V}_i^T\right) V^T,\ i = 1, \ldots, m.$$

From the starting eigenvalue and corresponding eigenvectors we can compute $X,\ Y$ and $\Gamma_i,\ i = 1, \ldots, m$. Subsequently, the gradient flow discretization is initialized with U, V and $Q_i(0) := \tilde{U}_i \tilde{V}_i^T$. Note that this initialization can be interpreted as performing one iteration of the fixed-point iteration as in [108].

If the starting eigenvalue λ is real, we obtain U and V by extending eigenvectors x and y to $n \times 2$ matrices with orthogonal columns, and initialize Q_i with $\text{sign}(p_i(\lambda))I_2$.

2.4 Numerical experiments

In this section we show the results obtained from a MATLAB implementation of the algorithms previously described, illustrating applications to the DEP and to the PEP. For the DEP, the rightmost eigenvalues are computed with the method of [89] based on a spectral discretization. We start with an introductory example.

Example 2.13. *Consider the same DEP introduced in Example 1.14*

$$\left(\lambda I - (A_0 + \delta A_0) - A_1 e^{-\lambda\tau}\right) y = 0 \tag{2.33}$$

with

$$A_0 = \begin{bmatrix} -5 & 1 \\ 2 & -6 \end{bmatrix}, \qquad A_1 = \begin{bmatrix} -2 & 1 \\ 4 & -1 \end{bmatrix}, \qquad \tau = 1,$$

and the vector of weights $w = [1, +\infty]$ (where we have implicitly assumed that the identity matrix remains unperturbed); thus, we allow a perturbation only on matrix A_0. In Figure 2.1 the complex and real ε-pseudospectra are shown for $\varepsilon = 3.5$. The complex ε-pseudospectrum $\Lambda_\varepsilon^{\mathbb{C}}$ is computed using again the characterization (1.32). For the real ε-pseudospectrum $\Lambda_{\varepsilon,2}^{\mathbb{R}}$ (where the spectral norm is adopted as a measure of the perturbations), since only matrix A_0 is perturbed we can use the expression in (1.19) by adapting it to the case at hand giving rise to

$$\Lambda_{\varepsilon,2}^{\mathbb{R}} = \left\{ \lambda \in \mathbb{C} :\ \mu_{\mathbb{R}} \left((\lambda I - A_0 - A_1 e^{-\lambda\tau})^{-1} \right) \geq \frac{1}{\varepsilon} \right\}.$$

In this particular case the real ε-pseudospectral abscissa is equal to the complex ε-pseudospectral abscissa, since the globally rightmost pseudoeigenvalue is real. However, the pseudospectrum $\Lambda_\varepsilon^{\mathbb{C}}$ is much larger than $\Lambda_{\varepsilon,2}^{\mathbb{R}}$, which is indeed the

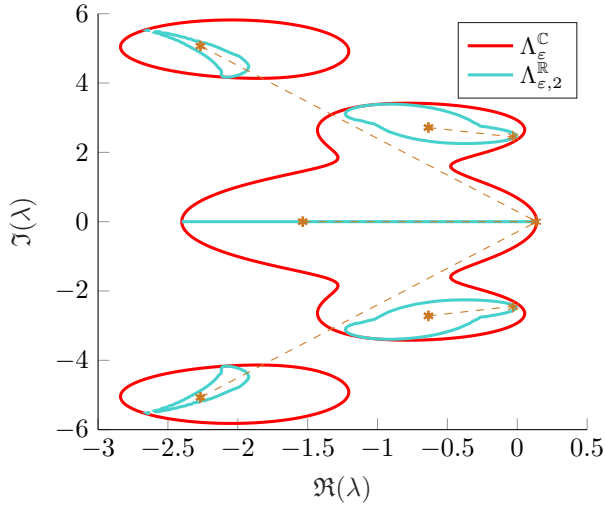

Figure 2.1: Comparison between the real and the complex ε-pseudospectra of the DEP (2.33) for $\varepsilon = 3.5$.

reason why we are interested in computing the real ε-pseudospectral abscissa. The importance of using several eigenvalues with large real part as starting values is also clarified from this figure, where the orange dashed lines connect each starting value to the locally rightmost eigenvalue to which the algorithm has converged. The algorithm was here run three times, and each time it was initialized by a different eigenvalue of the original spectrum. In this case, the iterations starting from the rightmost eigenvalue of the original problem converge to a locally but not globally rightmost point of the ε-pseudospectra, whereas the algorithm converges to the globally rightmost one when initialized on other eigenvalue of the original spectrum.

In addition, it is worth to highlight that in the latter case the algorithm is able to switch from a complex (starting) eigenvalue to the real eigenvalue to which it converges, as previously described in Remark 2.12.

2.4.1 Experiments on the Frobenius norm

We show here the results obtained by applying our algorithm to some nonlinear EPs. We first consider a DEP defined as

$$\left(\lambda I_n - A_0 - \sum_{i=1}^{m} A_i e^{-\lambda \tau_i}\right) y = 0. \tag{2.34}$$

Table 2.1: Computation of the ε-pseudospectral abscissa $\alpha^{\mathbb{R}}_{\varepsilon,F}$ for some DEPs contained in the collection[1].

Prob.	$(n,\, m)$	α	ε	$\alpha^{\mathbb{R}}_{\varepsilon,F}$	Iterations
1	$(3, 2)$	-2.866038e-02	1.e-1	7.242821e-02	15
			1.e-2	-1.463286e-02	10
			1.e-4	-2.851134e-02	5
6	$(10, 8)$	-3.775473e-01	1.e-1	1.506399+00	232
			1.e-2	-1.823559e-01	31
			1.e-4	-3.754178e-01	20
10	$(4, 4)$	-9.858488e-02	1.e-1	3.048429e-02	47
			1.e-2	-9.189037e-02	24
			1.e-4	-9.851861e-02	10

We assume that the weights are given by

$$w_i = \|A_i\|_F^{-1}\,,\ i = 0, \ldots, m,$$

in order to allow a maximal relative perturbation equal to ε on each matrix (while the identity matrix associated with the first derivative of the state vector remains as usual unperturbed). The algorithm is tested on some of the DEPs in the benchmark collection used in [94] and publicly available[1] ; in Algorithm 1 we adopt the tolerance $\eta = 10^{-4}$. In Table 2.1 we display the ε-pseudospectral abscissa found for these problems using different values for ε. The first column refers to the number of the problem in the collection[1]; in the second column n refers to the problem dimension, and m to the number of delays, while the last column shows the number of iterations needed before convergence.

We now illustrate an application of the algorithm to the a particular PEP used in [94]; we consider the problem introduced in (1.6) with

$$A_1 = \begin{bmatrix} 121 & 18.9 & 15.9 \\ 0 & 2.7 & 0.145 \\ 11.9 & 3.64 & 15.5 \end{bmatrix},\ A_2 = \begin{bmatrix} 7.66 & 2.45 & 2.1 \\ 0.23 & 1.04 & 0.223 \\ 0.6 & 0.756 & 0.658 \end{bmatrix},$$
$$A_3 = \begin{bmatrix} 17.6 & 1.28 & 2.89 \\ 1.28 & 0.824 & 0.412 \\ 2.89 & 0.413 & 0.725 \end{bmatrix}. \tag{2.35}$$

Table 2.2 shows the values obtained for the ε-pseudospectral abscissa $\alpha^{\mathbb{R}}_{\varepsilon,F}$ for several values of ε, where in this case all weights w_i are set equal to one. The tolerance η is again set equal to 10^{-4}.

[1]The collection is available on the webpage http://twr.cs.kuleuven.be/research/software/delay-control/benchmarks.

Table 2.2: Computation of the ε-pseudospectral abscissa $\alpha^{\mathbb{R}}_{\varepsilon,F}$ of the PEP defined by the matrices in (2.35), whose spectral abscissa α is equal to 9.462649e-02.

ε	$\alpha^{\mathbb{R}}_{\varepsilon,F}$	Iterations
10^{-1}	1.649534e-01	28
$10^{-1.5}$	1.160533e-01	16
10^{-2}	1.013171e-01	10
$10^{-2.5}$	9.673361e-02	7
10^{-3}	9.529195e-02	4
10^{-4}	9.469300e-02	2

Table 2.3: Computation of the ε-pseudospectral abscissa $\alpha^{\mathbb{R}}_{\varepsilon,2}$ for some DEPs contained in the collection[1].

Prob.	$(n,\, m)$	α	ε	$\alpha^{\mathbb{R}}_{\varepsilon,2}$	Iterations
1	$(3, 2)$	−2.866038e-02	1.e-1	5.607794e-02	7
			1.e-2	−1.716339e-02	7
			1.e-4	−2.853917e-02	3
6	$(10, 8)$	−3.775473e-01	1.e-1	1.019638+00	162
			1.e-2	−2.307810e-01	23
			1.e-4	−3.759759e-01	11
10	$(4, 4)$	−9.858488e-02	1.e-1	−2.026579e-02	29
			1.e-2	−9.402496e-02	13
			1.e-4	−9.853953e-02	5

2.4.2 Experiments on the spectral norm

We still consider the problems introduced in the previous subsection, and we now investigate their robust stability by means of the algorithm described in Section 2.3, thus evaluating the uncertainty measure by means of the spectral norm. Once again, the algorithm is run setting a tolerance $\eta = 10^{-4}$ for convergence.

We first consider the DEPs in the previous subsection, where this time the weights are defined in terms of the spectral norm of the nominal matrices A_i, i.e.,

$$w_i = \|A_i\|_2^{-1}, \ i = 0, \ldots, m.$$

The results are reported in Table 2.3.

Finally, the QEP introduced in the previous subsection is investigated by means of the spectral norm as the perturbation measure. The values of the ε-pseudospectral abscissa $\alpha^{\mathbb{R}}_{\varepsilon,2}$ for several values of ε are reported in Table 2.4.

Table 2.4: Computation of the ε-pseudospectral abscissa $\alpha^{\mathbb{R}}_{\varepsilon,2}$ of the PEP defined by the matrices in (2.35), whose spectral abscissa α is equal to 9.462649e-02.

ε	$\alpha^{\mathbb{R}}_{\varepsilon,2}$	Iterations
10^{-1}	1.749188e-01	34
$10^{-1.5}$	1.188936e-01	12
10^{-2}	1.021872e-01	8
$10^{-2.5}$	9.700605e-02	5
10^{-3}	9.537783e-02	4
10^{-4}	9.470157e-02	2

2.4.3 Application to large-scale problems

Given the low-rank property of the optimal perturbations, an application of the method to sparse and large-scale EPs is natural. In this section, we illustrate this by means of unstructured perturbations on the DEPs; we also exploit the property that the optimal perturbations share the same column and row spaces.

For large-scale problems, the method in [89] for computing the rightmost roots of dense systems of DDEs would not be feasible. However, various methods have been developed to solve sparse large-scale EPs, e.g. Krylov type methods. In our extension to large-scale systems, we have used the infinite Arnoldi method for DEPs described in [69]. Let us consider a DEP in the form

$$\left(\lambda I_n - \sum_{i=0}^{m} A_i e^{-\lambda \tau_i}\right) y = 0.$$

As evident from Theorem 3.1 in [69], for the computation of the rightmost roots of the DEP the infinite Arnoldi solver requires the solution of a system of linear equations with matrix $\left(\sum_{i=0}^{m} A_i\right)$. Since our algorithm repeatedly requires the computation of the rightmost eigenvalue of a newly perturbed problem, at each iteration we need to solve a new linear system with matrix $\left(\sum_{i=0}^{m}(A_i + \delta A_i)\right)$. In order to reduce the computational costs of this operation, and thanks to the property that the optimal perturbations share the same column and row spaces, we exploit the Sherman-Morrison-Woodbury formula which is generally written as

$$(A + UQV)^{-1} = A^{-1} - A^{-1}U(Q^{-1} + VA^{-1}U)^{-1}VA^{-1}.$$

In order to fit the matrix of our perturbed problem in this formula, we exploit the decomposition (2.27) of δA_i, that is we write

$$\left(\sum_{i=0}^{m} A_i + \delta A_i\right) = \left(\sum_{i=0}^{m} A_i - \frac{\varepsilon}{w_i} U Q_i V^T\right) = \left(\sum_{i=0}^{m} A_i\right) + U\left(\sum_{i=1}^{m} -\frac{\varepsilon}{w_i} Q_i\right) V^T, \tag{2.36}$$

Table 2.5: Computation of the ε-pseudospectral abscissa $\alpha^{\mathbb{R}}_{\varepsilon,2}$ for the sparse large-scale delay system (2.37).

α	ε	$\alpha^{\mathbb{R}}_{\varepsilon,2}$	Iterations
−3.312133336e-01	1	8.647127e-01	5
	1.e-1	−1.937166e-01	4
	1.e-2	−3.170982e-01	3
	1.e-4	−3.297978e-01	3

where $U,\ V \in \mathbb{R}^{n\times 2}$ and $Q_i \in \mathbb{R}^{2\times 2},\ i = 0, \ldots, m$. Our algorithm starts with a sparse LU factorization of $\left(\sum_{i=0}^{m} A_i\right)$. In each iteration, this factorization is reused to solve the current linear system by exploiting equation (2.36), where, in addition, we only need to perform the LU factorization of another 2×2 matrix: this is a major consequence of the low-rank property of the optimal perturbations.

Example 2.14. *A typical sparse large-scale DEP arises from the discretization of partial differential equations (PDEs) with delays. The matrices generated by this procedure are most likely large and sparse. Let us consider the following PDE with one delay:*

$$\frac{\partial v(x,t)}{\partial t} = \frac{\partial^2 v(x,t)}{\partial x^2} + a_0(x)v(x,t) + a_1(x)v(\pi - x, t-1),$$

where $a_0(x) = -2\sin(x),\ a_1(x) = 2\sin(x)$ *and* $v_x(0,t) = v_x(\pi,t) = 0$.

We discretize the PDE and construct a DDE by approximating the second derivative in space with central difference. We obtain a system of the type

$$\dot{x}(t) = A_0 x(t) + A_1 x(t-1), \tag{2.37}$$

with size $n = 5000$ *and we apply 40 iterations of the Krylov method to compute the rightmost eigenvalues accurately. We also employ weights* $w_i = 0.5,\ i = 0, 1$, *and again* $\eta = 10^{-4}$. *Since the ε-pseudospectral abscissa of this system lies on the real axis, in Table 2.5 we only report the results obtained with the algorithm for the spectral norm.*

2.5 Conclusions

In this chapter, we have introduced two novel methods to compute the ε-pseudospectral abscissa generated by unstructured real-valued perturbations on the coefficient matrices of a nonlinear EP, whose general definition encompasses linear EPs, DEPs and PEPs. The two methods differ in the norm adopted to measure the magnitude of the uncertainty. The first method considers the

Frobenius norm on each uncertainty matrix δA_i, while the second adopts the spectral norm. Both methods rely on the construction of a set of optimal perturbations (i.e. perturbation matrices generating the globally rightmost point of the ε-pseudospectrum) as the maximizer of the spectral abscissa over all allowed perturbed EPs. Some notable properties of these perturbations are demonstrated, i.e., they always have rank smaller than or equal to two, and they share the same column and row spaces. This allows us to search these perturbations inside manifolds of low-rank matrices; here, we construct continuous and a.e. differentiable paths of perturbations defining the steepest ascent direction for the spectral abscissa of the associated perturbed EPs. The proposed algorithms are indeed equivalent to a projected gradient method, where each iteration defines a newly perturbed EP with a larger spectral abscissa.

Even though the main contributions concern the nonlinear EP, the proposed methods also contribute to the special case of the standard EP in the following way. For the Frobenius norm case, we have provided differential equations generating a path in the space of perturbations of rank smaller than or equal to two (instead of rank exactly two in the literature), allowing us to treat the case of a complex or real globally rightmost pseudoeigenvalue simultaneously. For the spectral norm case, we have derived explicit optimality conditions in terms of the compact singular value decomposition; in addition, we exploit the fact that a real globally rightmost eigenvalue can be generated by a set of rank-two perturbations as well.

Finally, the afore-mentioned properties of the optimal perturbations allow to extend the methods to sparse large-scale systems: solving the DEP with the infinite Arnoldi method proposed in [69], we have described how to further exploit the property that the optimal perturbations share the same column and row spaces in order to minimize the number of operations on large-scale matrices and save a memory space.

Chapter 3

Robustness measures for delay differential algebraic equations

In this chapter we change our focus from the general class of nonlinear EPs defined in (1.1) and treated in Chapter 2 to the special class of DEPs. We will extend Algorithm 1 for the computation of the ε-pseudospectral abscissa $\alpha^{\mathbb{R}}_{\varepsilon,F}$ to systems of *delay differential algebraic equations* where the nominal matrices A_i are affected by real-valued, *structured* perturbations and the delay values τ_i are also subject to uncertainty. This algorithm will be the basis for a bisection-Newton's algorithm to compute the *distance to instability* of such systems. In the next section, we introduce the systems of delay differential algebraic equations and demonstrate the connections with the systems of retarded and neutral type.

3.1 A general class of DDEs

As briefly mentioned in Section 1.1, there exists two main classes of delay systems: the delay systems of *retarded type* and the delay systems of *neutral type*. A system of DDEs of retarded type is usually written as

$$\dot{x}(t) = A_0 x(t) + \sum_{i=1}^{m} A_i x(t - \tau_i), \tag{3.1}$$

where $x(t) \in \mathbb{R}^n$ is the state variable at time t, $A_i \in \mathbb{R}^{n\times n}$ for $i = 0, \ldots, m$ and $0 < \tau_1 < \cdots < \tau_m$ are the time-delays. Although the spectrum of the associated

DEP contains infinitely many eigenvalues, it is demonstrated ([96, Chapter 1]) that each sequence of characteristic roots $\{\lambda_k\}_{k\geq 1}$ is such that

$$\lim_{k\to+\infty} |\lambda_k| = +\infty \Longrightarrow \lim_{k\to+\infty} \Re(\lambda_k) = -\infty.$$

This result trivially implies the following qualitative properties of the spectrum:

- There are only a finite number of charachteristic roots in any vertical strip of the complex plane defined as

  $$\{\lambda \in \mathbb{C} : \alpha < \Re(\lambda) < \beta\}$$

  for any $\alpha,\ \beta \in \mathbb{R}$;

- There exists a $\gamma \in \mathbb{R}$ such that all the characteristic roots are confined to the half plane

  $$\{\lambda \in \mathbb{C} :\ \Re(\lambda) < \gamma\}.$$

The DEP associated with a system of DDEs of retarded type thus clearly satisfy Assumption 2.1 made at the beginning of Chapter 2. In addition, it can be proven that in this case the spectral abscissa is continuous w.r.t. the coefficients of the matrices A_i and w.r.t. the delay values τ_i.

A system of DDEs of *neutral type* is usually defined as

$$\dot{x}(t) + \sum_{i=1}^{m} H_i \dot{x}(t-\tau_i) = A_0 x(t) + \sum_{i=1}^{m} A_i x(t-\tau_i), \tag{3.2}$$

where the newly introduced matrices $H_i \in \mathbb{R}^{n\times n}$ for $i = 1, \ldots, m$, and the equation

$$x(t) + \sum_{i=1}^{m} H_i x(t-\tau_i) = 0 \tag{3.3}$$

is defined as the associated *delay-difference equation*. The characteristic matrix of the neutral equation is given by

$$M_N(\lambda) = \underbrace{\lambda \left(I_n + \sum_{i=1}^{m} H_i e^{-\lambda\tau_i} \right)}_{:=M_D(\lambda)} - \sum_{i=0}^{m} A_i e^{-\lambda\tau_i}, \tag{3.4}$$

where $M_D(\lambda)$ indicates instead the characteristic matrix of the delay-difference equation. Also in this case the associated DEP admits infinitely many eigenvalues, and a fundamental property of the sequences of characteristic roots is described by the following result (proven in [96, Chapter 1]).

Proposition 3.1. *Let us define*

$$Z_D := \{\Re(\lambda) : \det M_D(\lambda) = 0\},$$

then for $\zeta \in \overline{Z}_D$*, there exists a sequence of characteristic roots* $\{\lambda_k\}_{k\geq 1}$ *of* $M_N(\lambda)$ *such that*

$$\lim_{k\to+\infty} \Re(\lambda_k) = \zeta, \quad \lim_{k\to+\infty} \Im(\lambda_k) = \pm\infty.$$

An immediate consequence of this result is that Assumption 2.1 is not satisfied for DEPs associated with systems of DDEs of neutral type. In addition, from the spectral properties of the delay-difference equations ([90, 99]) the spectral abscissa of $M_N(\lambda)$ may not be continuous w.r.t. infinitesimal perturbations of the delay values $\vec{\tau} = (\tau_1, \ldots, \tau_m)$, whereas it remains continuous w.r.t. the coefficients of the matrices A_i.

Systems of DDEs of both retarded and neutral type can be retrieved from a more general class of systems of DDEs, namely the systems of *delay differential algebraic equations* (DDAEs) of the form

$$E\dot{x}(t) = A_0 x(t) + \sum_{i=1}^{m} A_i x(t-\tau_i), \tag{3.5}$$

where the leading matrix $E \in \mathbb{R}^{n\times n}$ is allowed to be singular, while the other quantities are defined as usual. The characteristic matrix associated with (3.5) is then given by

$$M(\lambda) = \lambda E - A_0 - \sum_{i=1}^{m} A_i e^{-\lambda\tau_i}. \tag{3.6}$$

Observe that, when referring to system of DDAEs and to the related DEPs, in this and the following chapters, we will mainly use the compact summation for i running from 0 to m, where we implicitly consider $\tau_0 = 0$.

Setting $E = I_n$ in (3.5) a system of retarded type is immediately recovered, while the system of neutral type (3.2) can be rewritten as

$$\begin{cases} \dot{v}(t) = \sum_{i=0}^{m} A_i x(t-\tau_i), \\ 0 = -v(t) + x(t) + \sum_{i=1}^{m} H_i x(t-\tau_i), \end{cases}$$

where v is a slack variable, and the state variable of the latter system is $[v^T \ x^T]$.

Systems of DDAEs are widely used in practical applications and they typically arise as the feedback interconnection of a plant model with a controller with a fixed-order or structure: some examples and applications of DDAEs will be largely studied in the next chapter. In the rest of this section, we introduce two assumptions that guarantee retarded dynamics for a systems of DDAEs.

This is necessary to satisfy Assumption 2.1 and thus to extend the method to compute the ε-pseudospectral abscissa introduced in the previous chapter.

Let $\operatorname{rank}(E) = n - \nu$ and let $U,\ V \in \mathbb{R}^{n\times\nu}$ be respectively a (minimal) basis for the left and the right null space of E. Then, if we define

$$\mathbf{U} = [U^{\perp}\ U],\ \mathbf{V} = [V^{\perp}\ V] \text{ and } x = \mathbf{V}[x_1^T\ x_2^T]^T, \tag{3.7}$$

system (3.5) can be rewritten as follows

$$\begin{cases} E^{(11)}\dot{x_1}(t) = \sum_{i=0}^{m} A_i^{(11)} x_1(t-\tau_i) + \sum_{i=0}^{m} A_i^{(12)} x_2(t-\tau_i), \\ 0 = A_0^{(22)} x_2(t) + \sum_{i=1}^{m} A_i^{(22)} x_2(t-\tau_i) + \sum_{i=0}^{m} A_i^{(21)} x_1(t-\tau_i), \end{cases} \tag{3.8}$$

where $E^{(11)} = {U^{\perp}}^T E V^{\perp}$, and

$$\begin{aligned} A_i^{(11)} &= {U^{\perp}}^T A_i V^{\perp}, \quad A_i^{(12)} = {U^{\perp}}^T A_i V \\ A_i^{(21)} &= U^T A_i V^{\perp}, \quad\ A_i^{(22)} = U^T A_i V, \quad i = 0, \dots, m. \end{aligned}$$

Thus, we have separated system (3.5) into a set of DDEs (of retarded type) and a set of delay-difference equations: observe that $E^{(11)}$ is guaranteed to be invertible because

$$\operatorname{rank}(E^{(11)}) = \operatorname{rank}(\mathbf{U}^T E \mathbf{V}) = \operatorname{rank}(E) = n - \nu.$$

Equation (3.8) is semi-explicit DDAEs of index 1, because delay differential equations are obtained by differentiating the second equation, and it precludes the occurrence of impulsive solutions [41]. In the rest of the chapter we make the following assumption.

Assumption 3.2. *The matrix $U^T A_0 V$ is nonsingular.*

The previous assumption prevents the system from being of advanced-type, and hence non causal, i.e. a system where the present state is determined by a future one, as in the following example.

Example 3.3. *We consider a system*

$$\begin{cases} \dot{x}_1(t) = x_1(t) + x_2(t), \\ 0 = 0x_2(t) + x_2(t-\tau) + x_1(t). \end{cases}$$

If we substitute the second equation in the first one we obtain

$$\dot{x}_1(t) = x_1(t) + x_2(t) = x_1(t) + x_1(t+\tau),$$

which is clearly a system of advanced type.

Now, observing the system of DDAEs recasted in the form (3.8), it is easy to see that it has retarded dynamics if $A_i^{(22)} = 0$ for $i = 1, \dots, m$. Therefore we also make the following assumption.

Assumption 3.4. *Matrices* $U^T A_i V = 0$ *for* $i = 1, \dots, m$.

In the next section we give the last fundamental assumption for the proposed algorithm, and we formally define the uncertainties affecting system (3.5). We will compute the ε-pseudospectral abscissa and the distance to instability defined over these uncertainties.

3.2 Problem statement and main assumptions

In this section we define a class of perturbations affecting the system of DDAEs (3.5) significantly larger than the one considered in Chapter 2. First of all, we assume that the system is simultaneously affected by real-valued uncertainties on the matrices A_i and on the delays τ_i; in addition, any structure can be imposed on the coefficient matrices, independently of each other, in order to potentially perturb a submatrix, e.g. a single block or a single coefficient. Moreover, we consider the potential inter-dependencies between the uncertainties perturbing the nominal matrices A_i, which are relevant to those uncertain system parameters present in more than one matrix A_i. On the other hand, some properties of the optimal perturbations deduced in Section 2.2 do not hold anymore, e.g., the properties that the optimal perturbations all have maximum norm and that they share the same spaces of columns and rows.

Nevertheless, given the wide class of perturbations considered, and because of the adopted eigenvalue-based approach grounding on a necessary and sufficient criterion for stability, the proposed method to compute the distance to instability represents a substantial improvement w.r.t. to the existing techniques, of which we summarize the most popular ones below.

- Firstly, due to the nonlinear dependence of the characteristic equation on the delay parameters, a reformulation in the form $\det(I - M(\lambda)\Delta)) = 0$, with Δ denoting the combined uncertainty, is not possible, while the structured singular value (μ) framework precisely relies on such a reformulation. It should be remarked that when considering the delays as unperturbed but allowing the perturbations on different matrices to be structured, *independently* of each other, as we shall do, the characteristic equation can still be recast in the above form where Δ is block diagonal with real-valued diagonal blocks. Such a structure is however difficult to exploit when estimating the corresponding structured singular values. In [61], a formula for the real stability radius of either retarded or neutral system with multiple delays is provided; in that work, the spectral norm is used to measure the uncertainty magnitude.

- Secondly, since we aim at computing the exact value of the distance to instability, an over-bounding of the uncertainty on the delay or an embedding into a larger set of perturbations, followed by the application of the small gain theorem or other methods for robust control are not possible, as this will lead to possibly conservative lower bounds for the distance to instability. Using this approach, a lower-bound on the stability radius of a time-delay system subject to real-valued perturbations on the delay parameters and to complex-valued perturbations on the system matrices simultaneously is presented in [92]. For the same reason methods relying on the construction of Lyapunov functionals are not suitable.
- Thirdly, a direct parametric analysis and the explicit construction of stability charts (see, e.g., [113, 49]) are suitable for uncertain parameters, while they are not adopted for matrix-valued uncertainty.

Let us now consider the system of DDAEs (3.5), and assume that its zero solution is asymptotically stable. We consider the associated eigenvalue problem

$$M(\lambda)y = \left(\lambda E - \sum_{i=0}^{m} A_i e^{-\lambda\tau_i}\right) y = 0; \tag{3.9}$$

we then define the following perturbed EP

$$M(\lambda;\Delta)y = \left(\lambda E - \sum_{i=0}^{m}\left(A_i + \sum_{j=1}^{K} D_{i,j}\delta A_j E_{i,j}\right) e^{-\lambda(\tau_i+\delta\tau_i)}\right) y = 0. \tag{3.10}$$

In this perturbed DEP we assume the following: the perturbed characteristic matrix $M(\lambda;\Delta)$ can be affected by K independent uncertainties δA_j, and each nominal matrix A_i can be perturbed by one or more δA_j, whose structure (and weight) is defined by real-valued scaling matrices $D_{i,j}$ and $E_{i,j}$. The dimension of $D_{i,j}$ and $E_{i,j}$ thus depend on the dimension of the associated δA_j, i.e. for $\delta A_j \in \mathbb{R}^{p_j\times q_j}$, we have $D_{i,j} \in \mathbb{R}^{n\times p_j}$, $E_{i,j} \in \mathbb{R}^{q_j\times n}$ for $i = 0,\dots,m$. If the nominal matrix A_i is not affected by δA_j, then we set $D_{i,j} = 0$ and $E_{i,j} = 0$. The delay values τ_i are affected by real-valued (scalar) uncertainties $\delta\tau_i$ such that $|\delta\tau_i| < \tau_i$; as a consequence, $\tau_0 = 0$ implies $\delta\tau_0 = 0$. The combined set of perturbations is denoted by $\Delta = (\Delta A, \Delta\vec{\tau}) = (\delta A_1,\dots,\delta A_K,\delta\tau_1,\dots,\delta\tau_m) \in \mathbb{R}^*\times\mathbb{R}^m$, with $\mathbb{R}^* = \mathbb{R}^{p_1\times q_1}\times\cdots\times\mathbb{R}^{p_K\times q_K}$. To motivate the adopted model we present an example.

Example 3.5. *We consider a simple model for a turning process as presented in [64], specifically we consider*

$$\ddot{x}(t) + 2\xi\omega\dot{x}(t) + \omega^2 x(t) = \frac{k}{m}\left(x(t-\tau) - x(t)\right), \tag{3.11}$$

whose corresponding unperturbed DEP (after rewriting the system into a set of first order DDEs) reads

$$\left(\lambda I - A_0 - A_1 e^{-\lambda\tau}\right) y = 0,$$

where

$$A_0 = \begin{bmatrix} 0 & 1 \\ -\omega^2 - \frac{k}{m} & -2\xi\omega \end{bmatrix}, \; A_1 = \begin{bmatrix} 0 & 0 \\ \frac{k}{m} & 0 \end{bmatrix}, \tag{3.12}$$

with ω denoting the natural frequency, ξ the damping ratio, m the modal mass, k the cutting force coefficient and, considering the compact formulation (3.9), $\tau = \tau_1$. Let us now assume that parameters k and ξ are respectively affected by $\delta k = \delta A_1$ and $\delta\xi = \delta A_2$, and that the delay τ also admits a perturbation $\delta\tau$. Then, the perturbed DEP reads

$$\begin{aligned} M(\lambda;\Delta) = \lambda I - \Big(A_0 + D_{0,1}\delta k E_{0,1} + D_{0,2}\delta\xi E_{0,2}\Big) - \\ \Big(A_1 + D_{1,1}\delta k E_{1,1} e^{-\lambda(\tau+\delta\tau)}\Big), \end{aligned} \tag{3.13}$$

where

$$D_{1,1} = \begin{bmatrix} 0 \\ \frac{1}{m} \end{bmatrix}, E_{1,1} = \begin{bmatrix} 1 \\ 0 \end{bmatrix}^T, D_{0,2} = \begin{bmatrix} 0 \\ -2\omega \end{bmatrix}, E_{0,2} = \begin{bmatrix} 0 \\ 1 \end{bmatrix}^T$$

and $D_{0,1} = -D_{1,1}$, $E_{0,1} = E_{1,1}$.

Given the new class of perturbations specified above, and for a set of weights $v_i \in \mathbb{R}_0^+$, we now employ the global norm

$$\|\Delta\|_{\text{glob}} := \left\| \begin{bmatrix} \|\delta A_1\|_F \\ \vdots \\ \|\delta A_K\|_F \\ v_0|\delta\tau_1| \\ \vdots \\ v_m|\delta\tau_m| \end{bmatrix} \right\|_\infty \tag{3.14}$$

on Δ. Hence, an ε-bounded set of perturbations Δ is such that

$$\|\delta A_j\|_F \le \varepsilon, \; v_i|\delta\tau_i| \le \varepsilon, \quad j = 1,\dots,K, \; i = 1,\dots,m,$$

where with the choice $v_i = +\infty$, we consider a delay parameter τ_i not subject to uncertainty.

We still consider the definitions of the ε-pseudospectrum and ε-pseudospectral abscissa introduced in Chapter 1, but now by employing the global norm (3.14) to measure the perturbations, that is we consider

$$\Lambda^{\mathbb{R}}_{\varepsilon,F} := \bigcup_{\substack{\Delta \in \mathbb{R}^* \times \mathbb{R}^m \\ \|\Delta\|_{\text{glob}} \leq \varepsilon}} \left\{ \lambda \in \mathbb{C} : \det M(\lambda; \Delta) = 0 \right\}, \tag{3.15}$$

$$\alpha^{\mathbb{R}}_{\varepsilon,F} := \max\{\Re(\lambda) : \lambda \in \Lambda^{\mathbb{R}}_{\varepsilon,F}\}. \tag{3.16}$$

Observe that the definition of the ε-pseudospectral abscissa employs the maximum function because we are assuming that the system of DDAEs under consideration has retarded dynamics, and thus satisfies Assumption 2.1. To this purpose, we must guarantee that any perturbation of the considered nominal DEP still has retarded dynamics. Therefore, besides Assumptions 3.2 and 3.4, the following assumption is also necessary.

Assumption 3.6. *For each $i = 1, \ldots, m$ and $j = 1, \ldots, K$ it must hold that either $U^T D_{i,j} = 0$ or $E_{i,j} V = 0$, with U, V defined in* (3.7).

3.3 Computing the real structured pseudospectral abscissa for DEPs

In this section, we describe the algorithm to compute the ε-pseudospectral abscissa $\alpha^{\mathbb{R}}_{\varepsilon,F}$. The proposed method extends the one in Section 2.2, thus is again grounded on the construction of a path in a prescribed subspace of perturbations that identifies the steepest ascent direction for the spectral abscissa of the perturbed DEP (3.10). The following theorem provides a characterization of the optimal perturbations, i.e. the matrices and the delays perturbations that generate the globally rightmost point in the ε-pseudospectrum. Observe that in the following, we denote with k_j the number of matrices A_i affected by the uncertainty δA_j.

Theorem 3.7. *Let λ_{RM} be the globally rightmost point of the ε-pseudospectrum (3.15) for a set of optimal ε-bounded perturbations $\Delta = (\Delta A, \Delta\vec{\tau})$ and assume λ_{RM} is a simple eigenvalue. Then the following holds:*

(i) There always exists a set of ε-bounded perturbations $\widetilde{\Delta A} = (\widetilde{\delta A_1}, \ldots, \widetilde{\delta A_K})$, such that for each $j = 1, \ldots, K$

$$\operatorname{rank}(\widetilde{\delta A_j}) \leq \rho_j^* := \min(2k_j, p_j, q_j)$$

and for which the rightmost eigenvalue is λ_{RM};

(ii) Let x, y be respectively the left and the right eigenvectors (with unit norms) of λ_{RM} and such that

$$\xi := -x^* \left(E + \sum_{i=0}^{m} \left(A_i + \sum_{j=1}^{K} D_{i,j} \delta A_j E_{i,j} \right) (\tau_i + \delta\tau_i) e^{-\lambda_{\mathrm{RM}}(\tau_i+\delta\tau_i)} \right) y > 0, \tag{3.17}$$

and let us define again

$$X = [\Re(x)\ \Im(x)], \quad Y = [\Re(y)\ \Im(y)],$$

$$\Gamma_i = \begin{bmatrix} \Re(e^{-(\tau_i+\delta\tau_i)\lambda_{\mathrm{RM}}}) & -\Im(e^{-(\tau_i+\delta\tau_i)\lambda_{\mathrm{RM}}}) \\ \Im(e^{-(\tau_i+\delta\tau_i)\lambda_{\mathrm{RM}}}) & \Re(e^{-(\tau_i+\delta\tau_i)\lambda_{\mathrm{RM}}}) \end{bmatrix}, \quad \text{for } i = 0, \dots m.$$

Now, for each $j = 1, \dots, K$, the matrix $\sum_{i=0}^{m} D_{i,j}^T X \Gamma_i Y^T E_{i,j}^T$ can be either zero or nonzero. In the latter case we can express a particular optimal perturbation as

$$\delta A_j = -\varepsilon \frac{\sum_{i=0}^{m} D_{i,j}^T X \Gamma_i Y^T E_{i,j}^T}{\left\| \sum_{i=0}^{m} D_{i,j}^T X \Gamma_i Y^T E_{i,j}^T \right\|_F}. \tag{3.18}$$

(iii) Let x, y be defined as before, then

$$\frac{\partial \Re(\lambda_{\mathrm{RM}})}{\partial \delta\tau_i} = \frac{1}{\xi} \Re\Big(x^* \big(A_i + \sum_{j=1}^{K} D_{i,j} \delta A_j E_{i,j} \big) \lambda_{\mathrm{RM}} e^{-\lambda_{\mathrm{RM}}(\tau_i+\delta\tau_i)} y \Big) \tag{3.19}$$

can also be either zero or nonzero. If it is nonzero, then the optimal time-delay perturbation $\delta\tau_i$ is such that $v_i|\delta\tau_i| = \varepsilon$.

Proof. (*i*) Suppose without loss of generality that the delay terms are free from uncertainties. Moreover, in order to simplify the notation, let us also suppose, without loss of generality, that each uncertainty δA_j perturbs the first k_j nominal matrices.

It is trivial to see that the relation $\operatorname{rank}(\delta A_j) \le \min\{p_j, q_j\}$ always holds. Let us now also assume that $2k_j < \min\{p_j, q_j\}$, and thus that $\rho_j^* = 2k_j$. For each $j = 1, \dots, K$, we let $r_j^* \le \rho_j^*$ be the rank of the space spanned by vectors in $Z := \big\{\Re(E_{1,j}y), \Im(E_{1,j}y), \dots, \Re(E_{k_j,j}y), \Im(E_{k_j,j}y)\big\}$; then we define a matrix H_j such that the span of its first r_j^* columns includes the space spanned by vectors in Z, and the other columns complete a basis for $\mathbb{R}^{q_j}$, in a way such that H_j is orthogonal. Then, let us introduce $\widehat{\delta A_j}$ such that $\delta A_j = \widehat{\delta A_j} H_j^T$, $j = 1, \dots, K$. With this factorization,

$$0 = \left(\lambda_{\mathrm{RM}} E - \sum_{i=0}^{m} \left(A_i + \sum_{j=1}^{K} D_{i,j} \delta A_j E_{i,j} \right) e^{-\lambda_{\mathrm{RM}}\tau_i} \right) y$$

$$=M(\lambda)y-\sum_{i=0}^{m}\sum_{j=1}^{K}D_{i,j}\widehat{\delta A_j}H_j^T e^{-\lambda_{\mathrm{RM}}\tau_i}\left(\Re(E_{i,j}y)+\imath\Im(E_{i,j}y)\right)$$

$$=M(\lambda)y-\sum_{i=0}^{m}\sum_{j=1}^{K}D_{i,j}\widehat{\delta A_j}e^{-\lambda_{\mathrm{RM}}\tau_i}\begin{pmatrix}\langle H_j^{(1)},\Re(E_{i,j}y)+\imath\Im(E_{i,j}y)\rangle\\ \vdots\\ \langle H_i^{(r_j^*)},\Re(E_{i,j}y)+\imath\Im(E_{i,j}y)\rangle\\ 0\\ \vdots\\ 0\end{pmatrix},$$

where $H_l^{(k)}$ denotes the k-th column of H_j. From the last expression it is easy to see that we can discard the last $q_j - r_j^*$ columns of H_j. Thus, for every $j = 1, \ldots, K$ we define a new matrix $H_j^\star$ by resetting all elements in H_j to zero except for the elements in the first r_j^* columns. Therefore, defining $\widetilde{\delta A_j} = \widehat{\delta A_j}{H_j^\star}^T$ we obtain matrices with rank r_j^* that preserve the eigenvalue λ_{RM} and its right eigenvector y.

We still have to prove that $\left\|\widetilde{\delta A_j}\right\|_F \leq \|\delta A_j\|_F$; this is equivalent to proving that the Euclidean norm of each row of δA_j is larger than that of the same row in $\widetilde{\delta A_j}$. Without loss of generality, let us investigate the Euclidean norm of the first row in each matrix. Let

$$\left(\widehat{\delta A_j}\right)_{(1)} = \begin{bmatrix}\beta_1 & \ldots & \beta_{q_j}\end{bmatrix}$$

be the first row of $\widehat{\delta A_j}$, and the matrices H_j^T and ${H_j^\star}^T$ be defined as

$$H_j^T = \begin{bmatrix}p_1^T & p_2^T & p_3^T & \ldots & p_{q_j}^T\end{bmatrix}^T, \qquad {H_j^\star}^T = \begin{bmatrix}p_1^T & \ldots & p_{r_j^*}^T & 0 & \ldots & 0\end{bmatrix}^T,$$

with orthonormal columns $p_i \in \mathbb{R}^{q_j},\ i = 1, \ldots, q_j$.

Thus

$$\begin{array}{rcl}\left(\delta A_j\right)_{(1)} = & \left(\widehat{\delta A_j}\right)_{(1)}H_j^T & = \beta_1 p_1^T + \cdots + \beta_{q_j}p_{q_j}^T,\\ \left(\widetilde{\delta A_j}\right)_{(1)} = & \left(\widehat{\delta A_j}\right)_{(1)}{H_j^\star}^T & = \beta_1 p_1^T + \cdots + \beta_{r_j^*}p_{r_j^*}^T.\end{array}$$

Since $p_1, \ldots, p_{q_j}$ are orthonormal, it follows that

$$\left\|\left(\widetilde{\delta A_j}\right)_{(1)}\right\|_2 \leq \left\|\left(\delta A_j\right)_{(1)}\right\|_2.$$

(*ii*) For each $j = 1, \ldots, m$, let us indicate with $(\delta A_j)_{s,t}$ the coefficient in position (s,t) of δA_j, and with $D_{i,j}^{(s)}, E_{i,j(t)}$ respectively the s-*th* column

of $D_{i,j}$ and the t-*th* row of $E_{i,j}$, for $s = 1, \dots, p_j,\ t = 1, \dots, q_j$. From Lemma 2.4, using some algebraic manipulations, we obtain

$$\begin{aligned}
\frac{\partial \Re(\lambda_{\mathrm{RM}})}{\partial \delta A_j} &= \left(\frac{\partial \Re(\lambda_{\mathrm{RM}})}{\partial (\delta A_j)_{s,t}} \right)_{\substack{s=1,\dots,p_j \\ t=1,\dots,q_j}} \\
&= -\frac{1}{\xi} \sum_{i=0}^{m} \Re \left(x^* D_{i,j}^{(s)} E_{i,j(t)} y e^{-\lambda_{\mathrm{RM}}(\tau_i + \delta\tau_i)} \right)_{\substack{s=1,\dots,p_j \\ t=1,\dots,q_j}} \\
&= -\frac{1}{\xi} \sum_{i=0}^{m} \left(D_{i,j}^{(s)T} \Re \left(x y^* e^{-\lambda_{\mathrm{RM}}(\tau_i + \delta\tau_i)} \right) E_{i,j(t)}^T \right)_{\substack{s=1,\dots,p_j \\ t=1,\dots,q_j}} \\
&= -\frac{1}{\xi} \sum_{i=0}^{m} D_{i,j}^T X \Gamma_i Y^T E_{i,j}^T \neq 0,
\end{aligned}$$

where the last step stems from the hypothesis. The assertion is then derived following the same procedure adopted in the proof of Theorem 2.5.

(*iii*) The same reasoning used in (*ii*) can be applied here; by hypothesis we have that

$$\frac{\partial \Re(\lambda_{\mathrm{RM}})}{\partial \delta \tau_i} \neq 0,$$

thus the constraint on the size of $\delta\tau_i$ must be active. As a consequence, the optimal $\delta\tau_i$ is such that $v_i |\delta\tau_i| = \varepsilon$.

□

Assertion (*i*) of the theorem thus proves that the ε-pseudospectral abscissa is always generated by a set of matrix perturbations whose ranks are independent of n. Hence for high-dimensional systems ($n \gg \rho_j^*$) we can still restrict ourselves to low rank perturbations; as a consequence, in analogy to what we did in Section 2.2, we can reduce the search space for the optimal perturbations and solve the following simplified optimization problem

$$\begin{aligned}
\max \quad & \Re\lambda(\Delta) \\
\text{s.t.} \quad & \Delta \in \mathcal{S} := \mathcal{S}_F \times \mathcal{S}_\tau
\end{aligned} \tag{3.20}$$

where

$$\begin{aligned}\mathcal{S}_F :=& \{\Delta A \in \mathbb{R}^* : \operatorname{rank}(\delta A_j) \leq \rho_j^* := \min(2k_j, p_j, q_j),\\ & \|\delta A_j\|_F \leq \varepsilon,\ j = 1, \ldots, K\},\\ \mathcal{S}_\tau :=& \prod_{i=1}^{m} \left[-\frac{\varepsilon}{v_i}, +\frac{\varepsilon}{v_i}\right].\end{aligned} \tag{3.21}$$

Theorem 3.7 also demonstrates that, surprisingly, the optimal perturbations can also correspond to a stationary point of the spectral abscissa in the space of perturbations. In the following, we provide an example where the optimal matrix perturbation does not have the maximal norm.

Example 3.8. *Let us consider the following perturbed delay system*

$$\dot{x}(t) = A_1 x(t) + (A_2 + D\delta a E)\, x(t - \tau), \tag{3.22}$$

where δa is a scalar, the delay τ is set equal to 0.1*, $A_1 = 0.0123\ I_4$ and*

$$A_2 = \frac{0.998}{100} \begin{bmatrix} 0 & 4 & 0 & 0 \\ -301 & -56 & 301 & 224 \\ 0 & 0 & 0 & 16 \\ 1.9531 & 109.375 & -3.9063 & -437.5 \end{bmatrix}.$$

The structured perturbation on matrix A_2 is defined by

$$D = \begin{bmatrix} 0 & 3.1102 & 0 & 0 \end{bmatrix}^T, \quad E = \begin{bmatrix} 1.6 & 0 & -1.6 & 0 \end{bmatrix}.$$

We also assume that the delay τ is unperturbed. In Figure 3.1 we represent the root locus of the rightmost eigenvalue of system (3.22) with the uncertain scalar parameter δa varying in modulus between 0 *and* 0.6*. It is easy to observe that the rightmost point of the locus (whose real part is approximately zero) is generated by a perturbation δa whose modulus is between* 0.1 *and* 0.4*, while a perturbation such that $\delta a = \pm 0.6$ generates a rightmost eigenvalue with a smaller real part. Hence, for $\varepsilon = 0.6$ the ε-pseudospectral abscissa $\alpha^{\mathbb{R}}_{\varepsilon,F}$ is not generated by a perturbation of size ε.*

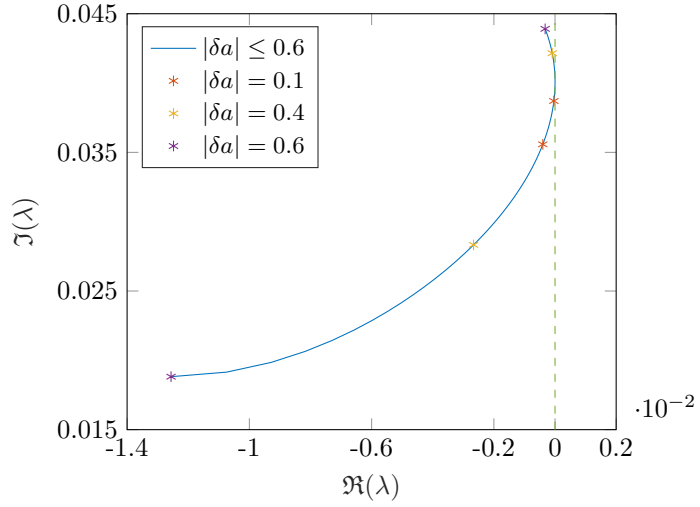

Figure 3.1: The root locus represents the rightmost eigenvalue of system (3.22) under different values for the scalar perturbation δa.

We now aim to construct within $\mathcal{S}$ the path of steepest ascent for the spectral abscissa of the perturbed DEP (3.10). By definition, each point in $\mathcal{S}$ defines a perturbation of the nominal DEP. Again, we consider perturbations $(\Delta A, \Delta\vec{\tau}) \in \mathcal{S}$ as continuously depending on a parameter s (as well as the corresponding rightmost eigenvalue $\lambda(s)$) and, exploiting Proposition 2.6, we use the decomposition

$$\begin{cases} \delta A_j(s) &= -\varepsilon U_j(s) Q_j(s) V_j(s)^T, & s \in \mathbb{R}^+,\ j = 1, \dots, K, \\ \delta\tau_i(s) &= \frac{\varepsilon}{v_i} q_i(s), & s \in \mathbb{R}^+,\ i = 1, \dots, m, \end{cases} \tag{3.23}$$

with $U_j(s) \in \mathbb{R}^{p_j \times \rho_j^*}$, $V_j(s) \in \mathbb{R}^{q_j \times \rho_j^*}$, $Q_j(s) \in \mathbb{R}^{\rho_j^* \times \rho_j^*}$ for $j = 1, \dots, K$, and $q_i(s) \in \mathbb{R}$ for $i = 1, \dots, m$ are such that the following properties are satisfied

$$\begin{cases} U_j(s)^T \dot{U}_j(s) = 0, & \forall\ s \geq 0, \\ V_j(s)^T \dot{V}_j(s) = 0, & \forall\ s \geq 0, \\ \|Q_j(s)\|_F \leq 1, & \forall\ s \geq 0, \\ |q_i(s)| \leq 1, & \forall\ s \geq 0. \end{cases} \tag{3.24}$$

Observe that we now consider distinct matrices U_j, V_j for each perturbation δA_j, as the property of sharing the same column and row space does not hold anymore. In addition, the norm of the matrix Q_j is not constrained to be equal to one.

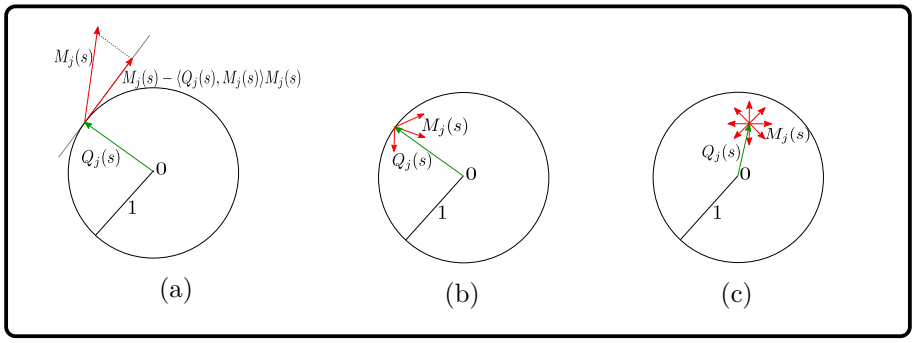

Figure 3.2: Three possible configurations for the choice of $\dot{Q}_j(s)$ in (3.25).

The matrices U_j, V_j, Q_j and the functions q_i can be also defined in an equivalent way. Following the approach in the previous chapter, and using the technique proposed in [73], we introduce some arbitrary matrix-valued functions R_j, S_j, Q_j such that $R_j(s) \in \mathbb{R}^{p_j \times \rho_j^*}$, $S_j(s) \in \mathbb{R}^{q_j \times \rho_j^*}$, $M_j(s) \in \mathbb{R}^{\rho_j^* \times \rho_j^*}$ for each s and $j = 1, \dots, K$, as well scalar functions r_i for $i = 1, \dots, m$. Then, conditions in (3.24) imply that (where s is omitted)

$$\begin{cases} \dot{U}_j = & \left(I_n - U_j U_j^T\right) R_j, \\ \dot{V}_j = & \left(I_n - V_j V_j^T\right) S_j, \\ \dot{Q}_j = & \begin{cases} M_j - \langle M_j, Q_j\rangle Q_j, & \text{if } \|Q_j\|_F = 1,\ \langle M_j, Q_j\rangle > 0 \\ M_j, & \text{otherwise,} \end{cases} \\ \dot{q}_i = & \begin{cases} 0, & \text{if } |q_i| = 1,\ r_i q_i > 0 \\ r_i, & \text{otherwise.} \end{cases} \end{cases} \tag{3.25}$$

The reason why we now have two separate cases in the equations defined for $\dot{Q}_j(s)$ (and for $\dot{q}_i(s)$) is the novel constraint imposed on its norm. If $\|Q_j(s)\|_F = 1$ and the intended direction of change, $M_j(s)$, points outwards the ball, then following this direction would lead to a solution $Q_j(s)$ such that $\|Q_j(s+\eta)\|_F > 1$ for $\eta > 0$ sufficiently small, violating the constraint. This can be overcome by projecting $M_j(s)$ on the tangent space to the ball, as shown in Figure 3.2a. If the direction $M(s)$ points inwards the ball, it is an allowed direction (Figure 3.2b). Finally, if $\|Q_j(s)\|_F < 1$ (Figure 3.2c) there is no constraint on the direction of change $M_j(s)$.

In what follows we determine the functions R_j, S_j, M_j, q_i in order to individuate a continuous and a.e. differentiable path of perturbations $\Delta(s)$ defining the steepest ascent direction in $\mathcal{S}$ for the spectral abscissa $\Re(\lambda(s))$. We exploit Lemma 2.4 to compute the derivative w.r.t. s of an eigenvalue whose

left and right eigenvectors (with unit norms) $x,\ y$ are such that $\xi > 0$ as in (3.17). Now the derivative is given by

$$\frac{d\lambda(s)}{ds} = \frac{1}{\xi}\Bigg\{ x^*\Bigg(-\sum_{i=0}^{m}\sum_{j=1}^{K} D_{i,j}\delta\dot{A}_j(s)E_{i,j}e^{-\lambda(\tau_i+\delta\tau_i(s))} + \\ + \sum_{i=0}^{m}\left(A_i + \sum_{j=1}^{K} D_{i,j}\delta A_j(s)E_{i,j}\right)\lambda\delta\dot{\tau}_i(s)e^{-\lambda(\tau_i+\delta\tau_i(s))}\Bigg)y\Bigg\}.$$

Substituting in the last formula the expressions in (3.25) and considering the case when $\dot{Q}_j(s) = M_j(s)$ and $\dot{q}_i(s) = r_i(s)$, we obtain (omitting, once again, the dependence on the variable s to make the notation less heavy)

$$\begin{aligned}
\mathfrak{R}(\dot{\lambda}) =& \sum_{i=0}^{m}\sum_{j=1}^{K}\frac{\varepsilon}{\xi}\mathfrak{R}\left(x^*D_{i,j}\dot{U}_jQ_jV_j^TE_{i,j}e^{-\lambda(\tau_i+\delta\tau_i)}y\right) \\
&+ \sum_{i=0}^{m}\sum_{j=1}^{K}\frac{\varepsilon}{\xi}\mathfrak{R}\left(x^*D_{i,j}U_j\dot{Q}_jV_j^TE_{i,j}e^{-\lambda(\tau_i+\delta\tau_i)}y\right) \\
&+ \sum_{i=0}^{m}\sum_{j=1}^{K}\frac{\varepsilon}{\xi}\mathfrak{R}\left(x^*D_{i,j}U_jQ_j\dot{V}_j^TE_{i,j}e^{-\lambda(\tau_i+\delta\tau_i)}y\right) \\
&+ \sum_{i=0}^{m}\frac{\varepsilon}{\xi v_i}\underbrace{\mathfrak{R}\left(x^*\left(A_i + \sum_{j=1}^{K}D_{i,j}\delta A_jE_{i,j}\right)\lambda e^{-\lambda(\tau_i+\delta\tau_i)}y\right)}_{=:\beta_i}\dot{q}_i \\
=& \sum_{i=0}^{m}\sum_{j=1}^{K}\frac{\varepsilon}{\xi}\left\langle X, D_{i,j}(I_n - U_jU_j^T)R_jQ_jV_j^TE_{i,j}Y\Gamma_i^T\right\rangle \\
&+ \sum_{i=0}^{m}\sum_{j=1}^{K}\frac{\varepsilon}{\xi}\left\langle X, D_{i,j}U_jM_jV_j^TE_{i,j}Y\Gamma_i^T\right\rangle \\
&+ \sum_{i=0}^{m}\sum_{j=1}^{K}\frac{\varepsilon}{\xi}\left\langle X, D_{i,j}U_jQ_jS_j^T(I_n - V_jV_j^T)E_{i,j}Y\Gamma_i^T\right\rangle + \sum_{i=0}^{m}\frac{\varepsilon}{\xi v_i}\beta_i\dot{q}_i \\
=& \sum_{j=1}^{K}\frac{\varepsilon}{\xi}\left\langle \sum_{i=0}^{m}D_{i,j}^TX\Gamma_iY^TE_{i,j}^TV_jQ_j^T, (I_n - U_jU_j^T)R_j\right\rangle
\end{aligned}$$

$$+\sum_{j=1}^{K}\frac{\varepsilon}{\xi}\Big\langle\sum_{i=0}^{m}U_j^TD_{i,j}^TX\Gamma_iY^TE_{i,j}^TV_j,M_j\Big\rangle$$

$$+\sum_{j=1}^{K}\frac{\varepsilon}{\xi}\Big\langle S_i,(I_n-V_jV_j^T)\sum_{i=0}^{m}E_{i,j}Y\Gamma_i^TX^TD_{i,j}U_jQ_j\Big\rangle+\sum_{i=0}^{m}\frac{\varepsilon}{\xi v_i}\beta_i\dot{q}_i,$$

Therefore, since $(I_n-U_jU_j^T)$, $(I_n-V_jV_j^T)$ are positive semi-definite, the steepest ascent direction for $\Re(\lambda)$ is guaranteed by the following choices

$$\begin{aligned}R_j&=\sum_{i=0}^{m}D_{i,j}^TX\Gamma_iY^TE_{i,j}^TV_jQ_j^T,\quad S_j=\sum_{i=0}^{m}E_{i,j}Y\Gamma_i^TX^TD_{i,j}U_jQ_j,\\M_j&=U_j^T\sum_{i=0}^{m}D_{i,j}^TX\Gamma_iY^TE_{i,j}^TV_j,\quad r_i=\beta_i.\end{aligned}\tag{3.26}$$

It can be verified that the other cases for the differential equations (3.25) give rise to the same expressions.

3.3.1 Implementation

The implementation of the algorithm is analogous to the one seen of Algorithm 1 in Section 2.2, so we will not illustrate the details here. The main differences are listed below.

- In line 4 of the new algorithm, the derivatives are computed using the differential equations (3.25) with the choices made in (3.26).
- In line 5, we now need to define a novel perturbed delay value as follows

$$\widehat{\tau}_i^{(n+1)}=\tau_i^{(n)}+r_n\dot{q}_i^{(n)},\ i=1,\dots,m.$$

- In line 7, the update of $Q_j^{(n+1)}$ is modified as follows

$$Q_j^{(n+1)}=\begin{cases}\widehat{Q}_j^{(n+1)}, & \text{if } \left\|\widehat{Q}_j^{(n+1)}\right\|_F\le 1,\\ \dfrac{\widehat{Q}_j^{(n+1)}}{\left\|\widehat{Q}_j^{(n+1)}\right\|_F}, & \text{otherwise.}\end{cases}$$

  In addition, for $i=1,\dots,m$, we possibly rescale $\widehat{\tau}_i^{(n+1)}$ to an ε-bounded perturbation of delay values:

$$\begin{cases}\tau_i^{(n+1)}=\min\Big(\tau_i+\frac{\varepsilon}{v_i},\widehat{\tau}_i^{(n+1)}\Big),\ \text{if } \dot{q}_i^{(n)}\ge 0\\ \tau_i^{(n+1)}=\max\Big(0,\tau_i-\frac{\varepsilon}{v_i},\widehat{\tau}_i^{(n+1)}\Big),\ \text{if } \dot{q}_i^{(n)}<0\end{cases}$$

The initialization of the algorithm is also different, and it works as follows: we compute the rightmost eigenvalue of the original problem, and its corresponding left and right eigenvectors (with unit norms and such that (3.17) holds). Then we initialize the matrices X, Y, Γ_i, for $i = 0, \ldots, m$ as in Theorem 3.7 and compute δA_j using formula (3.18). We apply a SVD decomposition such that $\delta A_j = W_j \Sigma_j Z_j$ and compute ρ_j^*. Then we set $U_j^{(1)}$, $V_j^{(1)}$ respectively equal to the first ρ_j^* columns of W_j and Z_j, and $Q_j^{(1)}$ equal to Σ_j (eventually normalized). The delays $\tau_i^{(1)}$ are simply initialized by employing the derivative in (3.19). Finally we construct the perturbed DEP (3.10) and, once again, we compute the rightmost eigenvalue λ_1 and the corresponding normalized eigenvectors x_1, y_1.

Observe that in the statement of Theorem 3.7 we have required the globally rightmost point of the ε-pseudospectrum to be simple. However, this hypothesis is exploited in the proofs of items (ii) and (iii), but not in item (i). Since items (ii) and (iii) are uniquely used for the initialization of the algorithm, while its main part relies on the characterization proven in item (i), we conclude that the proposed method is able to cope with the (degenerate) case where λ_{RM} is an eigenvalue with multiplicity larger than one.

3.4 A bisection-Newton's method for the distance to instability

In Chapter 1 we have introduced the notion of distance to instability (also known as stability radius) for a stable system, which corresponds to the norm of a minimal perturbation that makes a system unstable, and which can be formally defined as

$$d_{\mathrm{INS}} := \inf_{\lambda = \imath\omega} \inf_{\Delta} \{\|\Delta\| : \ \det(M(\lambda; \Delta)) = 0\}. \tag{3.27}$$

For any class of perturbations considered, and whatever is the norm used to measure its magnitude, the distance to instability can be alternatively computed using the notion of ε-pseudospectral abscissa (assuming of course the continuity of the eigenvalues w.r.t. the perturbations). As a matter of fact, we can define it as

$$d_{\mathrm{INS}} := \inf\{\varepsilon : \alpha_\varepsilon \geq 0\}. \tag{3.28}$$

In what follows, we show that the method proposed in the previous section can be used to compute the distance to instability with respect to perturbations of the DEP (3.10), thus considering the class of perturbations introduced in Section 3.2.

First, the equivalent definition (3.28) exploits the continuity of the ε-pseudospectral abscissa w.r.t. ε. Moreover, it is easy to verify that $\alpha_{\varepsilon,F}^{\mathbb{R}}$

is a monotone function w.r.t. ε: if $\varepsilon_1 < \varepsilon_2$, then $\Lambda^{\mathbb{R}}_{\varepsilon_1,F} \subseteq \Lambda^{\mathbb{R}}_{\varepsilon_2}$ must hold (i.e., the set of permissible perturbations is enlarged). Hence the function $\alpha^{\mathbb{R}}_{\varepsilon,F}$ is nondecreasing w.r.t. ε. This implies that the distance to instability is the (unique) root ε^* of the equation

$$\alpha^{\mathbb{R}}_{\varepsilon,F} = 0.$$

We want to use a combination of the bisection and Newton's method to find the unique root of this nonlinear equation. However, in order to use Newton's method, at least almost differentiability of the function is required. The ε-pseudospectral abscissa function is bounded on any interval $[\varepsilon_L, \varepsilon_R]$, thus it is a function of bounded variation. From the monotonicity property and from the Lebesgue's differentiation theorem of functions of bounded variation (see for instance [115, Theorem 3.4]), we can conclude that $\alpha^{\mathbb{R}}_{\varepsilon,F}$ is almost everywhere differentiable w.r.t. ε. In practice, it is differentiable whenever there exists one and one only globally rightmost point (and this eigenvalue is simple). Employing again Lemma 2.4, the next theorem provides the derivative.

Theorem 3.9. *Let $\big(\lambda_{\mathrm{RM}}(\varepsilon), x(\varepsilon), y(\varepsilon)\big)$ be respectively the globally rightmost point of $\Lambda^{\mathbb{R}}_{\varepsilon,F}$ and its left and right normalized eigenvectors; let also $\widetilde{\Delta}(\varepsilon) = \big(\widetilde{\Delta A}(\varepsilon), \widetilde{\Delta \tau}(\varepsilon)\big)$ be functions such that $\lambda_{\mathrm{RM}}(\varepsilon)$ is simple for all ε with*

$$\begin{aligned} \delta A_j = \quad & \widetilde{\delta A_j}(\varepsilon) = \quad -\varepsilon \widetilde{U_j}(\varepsilon)\widetilde{Q_j}(\varepsilon)\widetilde{V_j}(\varepsilon)^T, \quad j = 1, \dots, K \\ \delta \tau_j = \quad & \widetilde{\delta \tau_j}(\varepsilon) = \quad \tfrac{\varepsilon}{v_j}\widetilde{q_j}(\varepsilon), \qquad\qquad\qquad\quad i = 1, \dots, m. \end{aligned}$$

Then considering the constant of normalization ξ defined in (3.17) we can express the derivative of $\alpha^{\mathbb{R}}_{\varepsilon,F}$ w.r.t ε as follows:

$$\begin{aligned} \frac{\partial \alpha^{\mathbb{R}}_{\varepsilon,F}}{\partial \varepsilon} =& + \frac{1}{\xi}\Re\Bigg[x^*\Bigg(-\sum_{i=0}^{m}\sum_{j=1}^{K} D_{i,j}\frac{\partial \widetilde{\delta A_j}}{\partial \varepsilon}E_{i,j}e^{\left(-\lambda_{\mathrm{RM}}(\tau_i+\widetilde{\delta\tau_i})\right)} \\ & + \sum_{i=0}^{m}\Bigg(A_i + \sum_{j=1}^{K} D_{i,j}\widetilde{\delta A_j}E_{i,j}\Bigg)e^{\left(-\lambda_{\mathrm{RM}}(\tau_i+\widetilde{\delta\tau_i})\right)}\lambda_{\mathrm{RM}}\frac{\partial \widetilde{\delta\tau_i}}{\partial\varepsilon}\Bigg)y\Bigg] \\ =& \frac{1}{\xi}\Re\Bigg[x^*\Bigg(\sum_{i=0}^{m}\sum_{j=1}^{K} D_{i,j}\widetilde{U_j}\widetilde{Q_j}\widetilde{V_j}^T E_{i,j}e^{\left(-\lambda_{\mathrm{RM}}(\tau_i+\frac{\varepsilon}{v_i}\widetilde{q_i})\right)} \\ & + \sum_{i=0}^{m}\Bigg(A_i - \sum_{j=1}^{K}\varepsilon D_{i,j}\widetilde{U_j}\widetilde{Q_j}\widetilde{V_j}^T E_{i,j}\Bigg)e^{\left(-\lambda_{\mathrm{RM}}(\tau_i+\frac{\varepsilon}{v_i}\widetilde{q_i})\right)}\lambda_{\mathrm{RM}}\frac{\widetilde{q_i}}{v_i}\Bigg)y\Bigg], \end{aligned} \tag{3.29}$$

where we omit the dependence on ε. Note that we obtain the last expression because we are dealing with sets of optimal perturbations at every fixed ε.

As the Newton's method is a locally convergent method, we first look for a good starting value which possibly guarantees its convergence. Then, we first perform some iterations of the bisection method until we find an ε_1 whose associated ε-pseudospectral abscissa is close enough to 0 (for instance, ε_1 is s.t. $|\alpha^{\mathbb{R}}_{\varepsilon_1,F}| \leq 10^{-1}$). Then, we apply the Newton's method with the update rule

$$\varepsilon_{k+1} = \varepsilon_k - \alpha^{\mathbb{R}}_{\varepsilon_k,F} \Big/ \left.\frac{\partial \alpha^{\mathbb{R}}_{\varepsilon,F}}{\partial \varepsilon}\right|_{\varepsilon=\varepsilon_k},$$

where we employ the derivative defined in Theorem 3.9. Thus, if the ε-pseudospectral abscissa is correctly calculated, then our method returns, up to a tolerance induced by finite precision arithmetic, the exact distance to instability (instead of a conservative bound), as the approach is grounded on a necessary and sufficient robust stability condition.

Observe that iterations of the bisection method can also be employed to solve some degenerate cases. Firstly, when the ε-pseudospectrum has two (or more) distinct globally rightmost points or the globally rightmost point is a multiple eigenvalue, so that the derivative (3.29) does not exist. Secondly, it may happen that the derivative (3.29) is zero, for instance when the globally rightmost point is generated by a stationary point for the spectral abscissa (see Example 3.8).

3.5 Numerical experiments

Example 3.10. *Let us consider again the cutting machine system in Example 3.5. This time, we only assume an uncertainty δk on the cutting coefficient and an uncertainty $\delta\tau$ on the delay. We want to bound the uncertainties $|\delta k| \leq 1.5 * 10^6, |\delta\tau| \leq 1.5 * 10^{-3}$, thus we consider the characteristic equation*

$$\det\left(\lambda I - A_0 - D_{1,1}\delta k E_{1,1} - (A_1 + D_{2,1}\delta k E_{2,1})\, e^{-\lambda(\tau+\delta\tau)}\right) = 0$$

where

$$D_{1,1} = -D_{2,1} = \begin{bmatrix} 0 \\ -\frac{1}{m} \end{bmatrix}, \quad E_{1,1} = E_{2,1} = 1.5 * 10^6 \begin{bmatrix} 1 & 0 \end{bmatrix},$$

and we set $\varepsilon = 1,\ v = 0.0015^{-1}$, with v the weight associated with perturbation $\delta\tau$. In Figure 3.3, we represent the stability region of the system in the k-τ space: for any couple (k,τ) below the blue line the system is stable. The red line represents the 0 level set of the ε-pseudospectral abscissa (or, equivalently, the ε level set of the distance to instability). By definition, for each point whose $\alpha_\varepsilon = 0$ there exists a $\Delta = (\delta k, \delta\tau)$ with $\|\Delta\| = \varepsilon$ such that the perturbed system

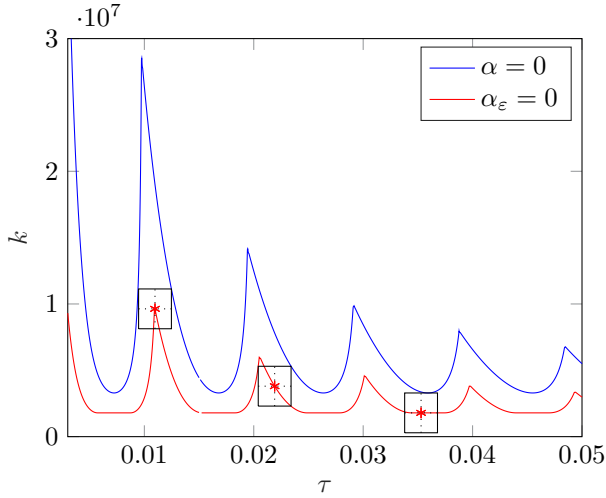

Figure 3.3: Stability and robust stability diagram of system (3.11) with uncertainties on the cutting coefficient k and on the delay τ.

is unstable. The rectangular blocks represent the space of all the ε-bounded perturbations $(\delta k, \delta\tau)$ of the point marked with a red asterisk. If we consider the rightmost rectangular block in Figure 3.3, we see that the ε-pseudospectral abscissa is not generated by a maximal-norm perturbation on the delay value. This behavior is equivalent to the one observed in Example 3.8 w.r.t. the structured perturbations on a system matrix, and it results in a flat profile for the level set.

Example 3.11. *In this example we consider the system from [92]*

$$\dot{x}(t) = A_0 x(t) + A_1 x(t-\tau_1) + A_2 x(t-\tau_2),$$

with

$$A_0 = \begin{bmatrix} -1 & 13.5 & -1 \\ -3 & -1 & -2 \\ -2 & -1 & -4 \end{bmatrix}, A_1 = \begin{bmatrix} -5.9 & 0 & 0 \\ 2 & 0 & 0 \\ 2 & 0 & 0 \end{bmatrix}, A_2 = \begin{bmatrix} 0 & 7.1 & -70.3 \\ 0 & -1 & 5 \\ 0 & 0 & 6 \end{bmatrix},$$

and $(\tau_1,\ \tau_2) = (0.05,\ 0.2)$. In [92], the delays are assumed uncertain with weights $v_1 = 1,\ v_2 = 0.5$. We want to compute the stability radius when also an uncertainty δA_0 affects A_0, and δA_1 affects the first column of A_1. We thus define

$$D_{0,0} = \|A_0\|_F\, I_3,\ E_{0,0} = I_3,\ D_{1,1} = \|A_1\|_F\, I_3,\ E_{1,1} = \begin{bmatrix} 1 & 0 & 0 \end{bmatrix}.$$

Table 3.1: Computation of the distance to instability d_{INS} for problems in the benchmark[1].

Problem	(n, m)	d_{INS}	$\alpha^{\mathbb{R}}_{d_{\text{INS}},F}$	# it
1	(3,2)	1.112792276e-02	-2.663325696e-17	6
2	(3,2)	5.600882011e-01	2.753544234e-15	4
3	(5,6)	1.589930029e+00	3.312381570e-16	7
4	(5,6)	1.459273837e-01	4.107825191e-16	6
5	(10,3)	2.352096503e-03	-5.969697629e-16	4
6	(10,3)	9.139676624e-02	-5.520865458e-16	5
7	(20,3)	1.041499774e-01	1.000000000e-15	5
8	(30,3)	1.013715072e-01	-9.059148660e-16	5

Choosing matrices $D_{0,0}$, $D_{1,1}$ as depending on the Frobenius norm of the perturbed matrices A_0 and A_1, we allow a maximal relative perturbation equal to ε. Our method returns the distance to instability $d_{\text{INS}} = 9.27826 * 10^{-3}$. Furthermore, if we only consider the uncertainties on the delays, we find $d_{\text{INS}} = 2.45684 * 10^{-2}$, which is consistent with the result in [92] ($d_{\text{INS}} = 2.45769 * 10^{-2}$).

Further results of the bisection-Newton's method to compute the distance to instability are reported in Table 3.1. We created a collection of problems from the literature where we have perturbed physical parameters appearing in the system matrices and in the delay terms[1]. On all of these problems we run the algorithm multiple times considering different perturbations, so they are listed more than once in Table 3.1; problems 1 and 2 are taken from [131], problems 3 and 4 are from [130]. Problems 5-8 are obtained from [71] as a discretization of a partial delay-differential equation, for which we adopt different refinements of the discretization. The details about the uncertainties considered in each problem are included in the benchmark[1]. In Table 3.1, the first column refers to the numbering of the problems in the benchmark, the second column displays the dimension of the problem and the number of delays, the third and fourth columns show, respectively, the distance to instability d_{INS} and the corresponding pseudospectral abscissa $\alpha^{\mathbb{R}}_{d_{\text{INS}},F}$, while the last column shows the number of iterations required by Newton's method to converge. The Newton's method is initialized after with an ε_1 such that $|\alpha^{\mathbb{R}}_{\varepsilon_1,F}| \leq 0.1$. The bisection method is initially used to find such an ε_1 in the interval $[10^{-3}, 1]$.

[1] The collection is available at the webpage http://twr.cs.kuleuven.be/research/software/delay-control/benchmarks-distance-instability.zip

3.6 Conclusions

In this chapter we have focused on DEPs associated to systems of DDAEs with retarded dynamics. By an adaptation of the algorithm presented in Section 2.2, we have proposed a method to compute the ε-pseudospectral abscissa of a DEP on which an extremely broad class of uncertainties can be defined. In particular, we can cope with DEPs that can be simultaneously affected by real-valued structured uncertainties on the matrices A_i, as well as uncertainties on the delay values τ_i. In addition, we take into account the possible interdependency among the matrix coefficients uncertainties, which is mainly relevant in practical applications, e.g. when an uncertain physical parameter is present in more than one nominal matrix A_i.

This method is also exploited in the computation of the distance to instability of the zero solution of a system of DDAEs. The proposed method aims at computing the (unique) ε such that the associated ε-pseudospectral abscissa $\alpha^{\mathbb{R}}_{\varepsilon,F}$ is equal to zero, and is grounded on the property that $\alpha^{\mathbb{R}}_{\varepsilon,F}$ is continuous, a.e. differentiable and non-decreasing w.r.t. ε.

By adopting the systems of DDAEs, the proposed method allows to consider a much larger class of systems, for instance modeling interconnections of (sub)systems and controllers, without the need for elimination of variables (this kind of systems will be largely treated in the next chapter). Another possible use of systems of DDAEs is the following. Let us we reconsider system (3.11), where we now assume that ξ and ω are uncertain. The nonlinear dependence on these parameters (i.e., the product $\xi\omega$) can be overcome by rewriting the equations as (with $x_1 = x$, $x_2 = \dot{x}$ and x_3 a slack variable),

$$\begin{cases} \dot{x}_1(t) &= x_2(t), \\ \dot{x}_2(t) &= \omega x_3(t) + \frac{k}{m}\left(x_1(t-\tau) - x_1(t)\right), \\ 0 &= x_3(t) + 2\xi x_2(t) + \omega x_1(t). \end{cases}$$

In a similar fashion, any multiplicative dependence on the uncertainty can be handled.

Chapter 4

Designing robust controllers for DDAEs

In the previous chapter we have seen that the use of DDAEs allows to represent a very broad class of delay systems, including systems of retarded and neutral type. In addition, systems of DDAEs allow to systematically model interconnections of systems, including interconnection between systems and controllers without the need for elimination of variables. In the next example, we illustrate how the description of an uncertain system with a static (or dynamic) feedback controller fits into the formulation of an uncertain system of DDAEs as introduced in Section 3.2 of the previous chapter.

Example 4.1. *Consider the system with uncertainties*

$$\begin{cases} \dot{x}(t) = (A + \delta A)x(t) + (B + \delta B)u(t - (\tau + \delta\tau)) \\ y(t) = (C + \delta C)x(t), \end{cases} \tag{4.1}$$

with static controller

$$u(t) = Ky(t). \tag{4.2}$$

Defining the new state variable $\boldsymbol{\xi} := (x^T, y^T, u^T)^T$*, the closed-loop system takes the form*

$$\begin{aligned}\underbrace{\begin{bmatrix} I & 0 & 0 \\ 0 & 0 & 0 \\ 0 & 0 & 0 \end{bmatrix}}_{:=\boldsymbol{E}} \dot{\boldsymbol{\xi}}(t) = &\left(\underbrace{\begin{bmatrix} A & 0 & 0 \\ C & -I & 0 \\ 0 & K & -I \end{bmatrix}}_{:=\boldsymbol{A_0}} + \underbrace{\begin{bmatrix} I \\ 0 \\ 0 \end{bmatrix} \delta A \begin{bmatrix} I \\ 0 \\ 0 \end{bmatrix}^T}_{:=\boldsymbol{D_{0,1}\delta A_1 E_{0,1}}} + \underbrace{\begin{bmatrix} 0 \\ I \\ 0 \end{bmatrix} \delta C \begin{bmatrix} I \\ 0 \\ 0 \end{bmatrix}^T}_{:=\boldsymbol{D_{0,2}\delta A_2 E_{0,2}}} \right) \boldsymbol{\xi}(t) \\ &+ \left(\underbrace{\begin{bmatrix} 0 & 0 & B \\ 0 & 0 & 0 \\ 0 & 0 & 0 \end{bmatrix}}_{:=\boldsymbol{A_1}} + \underbrace{\begin{bmatrix} I \\ 0 \\ 0 \end{bmatrix} \delta B \begin{bmatrix} 0 \\ 0 \\ I \end{bmatrix}^T}_{:=\boldsymbol{D_{1,3}\delta A_3 E_{1,3}}} \right) \boldsymbol{\xi}(t - (\tau + \delta\tau)).\end{aligned} \tag{4.3}$$

In the last equation we reformulated the original problem in form of an uncertain system of DDAEs as defined in Section 3.2. Note that the elimination of the input u would lead to a nonlinear dependence of the system matrices on the uncertainty. As a matter of fact, if one substitutes the control law (4.2) in the system of DDAE (4.1), then the uncertainty δB *could not be decoupled from the controller parameters in* K*. On the other hand, the adopted reformulation* (4.3) *in a DDAE framework then makes decoupling possible. More generally, thanks to the introduction of a slack variable, we are able to handle any polynomial dependence on the uncertainties within a DDAE framework. Therefore, the original perturbations* δA*,* δC *are treated as two independent perturbations (renamed* δA_1 *and* δA_2 *respectively) affecting the matrix* A_0 *of the new system of DDAE; the original* δB *is another independent perturbation affecting* A_1 *in the new system.*

Let us now consider instead the dynamic controller

$$\begin{cases} \dot{x}_c(t) &= A_c x_c(t) + B_c y(t), \\ u(t) &= C_c x_c(t) + D_c y(t), \end{cases} \tag{4.4}$$

then, renaming the new state variable $\boldsymbol{\xi} := (x^T, y^T, x_c^T, u^T)^T$*, the closed-loop system (4.1) is given by*

$$\underbrace{\begin{bmatrix} I & 0 & 0 & 0 \\ 0 & 0 & 0 & 0 \\ 0 & 0 & I & 0 \\ 0 & 0 & 0 & 0 \end{bmatrix}}_{:=\boldsymbol{E}} \dot{\boldsymbol{\xi}}(t) = \left(\underbrace{\begin{bmatrix} A & 0 & 0 & 0 \\ C & -I & 0 & 0 \\ 0 & B_c & A_c & 0 \\ 0 & D_c & C_c & -I \end{bmatrix}}_{:=\boldsymbol{A_0}} + \underbrace{\begin{bmatrix} I \\ 0 \\ 0 \\ 0 \end{bmatrix} \delta A \begin{bmatrix} I \\ 0 \\ 0 \\ 0 \end{bmatrix}^T}_{:=\boldsymbol{D_{0,1}\delta A_1 E_{0,1}}} + \underbrace{\begin{bmatrix} 0 \\ I \\ 0 \\ 0 \end{bmatrix} \delta C \begin{bmatrix} I \\ 0 \\ 0 \\ 0 \end{bmatrix}^T}_{:=\boldsymbol{D_{0,1}\delta A_1 E_{0,1}}} \right) \boldsymbol{\xi}(t)$$
$$+ \left(\underbrace{\begin{bmatrix} 0 & 0 & 0 & B \\ 0 & 0 & 0 & 0 \\ 0 & 0 & 0 & 0 \\ 0 & 0 & 0 & 0 \end{bmatrix}}_{:=\boldsymbol{A_1}} + \underbrace{\begin{bmatrix} I \\ 0 \\ 0 \\ 0 \end{bmatrix} \delta B \begin{bmatrix} 0 \\ 0 \\ 0 \\ I \end{bmatrix}^T}_{:=\boldsymbol{D_{1,3}\delta A_3 E_{1,3}}} \right) \boldsymbol{\xi}(t - (\tau + \delta\tau)) = 0. \tag{4.5}$$

The implementation of any kind of controller usually aims at asymptotically stabilizing a system, i.e., pushing all of its characteristic roots to the left-half of the complex plane. The stabilisation of linear time-delay systems is a topic of major relevance in control systems theory and a substantial amount of results have contributed to develop and partially solve this problem; without being exhaustive, possible approaches for stability analysis and stabilization are the use of Lyapunov-Krasovskii functionals and LMI conditions (see for instance [41, 106, 110]), the direct eigenvalue optimization approach ([124]), the minimization of the smoothed spectral abscissa ([46]), the continuous pole placement method ([91]) and the use of prediction based controllers (see [76] and references therein, [104, 95]). We refer the reader interested in a general overview on the various stabilisation methods to the monographs [101], [48] and [96].

In this chapter, we present a novel method to stabilize a system of DDAEs which is grounded on the minimization of the ε-pseudospectral abscissa: contrary to the strategy proposed in [124], where the spectral abscissa is minimized, the proposed method naturally guarantees the robust stability of the system for a prescribed class of uncertainties, and thus represents an effective tool for the design of *robust controllers*. It is preferable to many approaches grounded in Lyapunov's second method ([38]), which result in potentially very conservative criteria, e.g. LMI based ones (see [42] and [40] for a tutorial).

In this chapter, we then take into account systems affected by uncertainties whose closed-loop form can be expressed as

$$E\dot{x}(t) = \sum_{i=0}^{m} \left(A_i(p) + \sum_{j=1}^{K} D_{ij}\delta A_j E_{ij} \right) x(t - (\tau_i(p) + \delta\tau_i)), \tag{4.6}$$

where the matrices $A_i(p) \in \mathbb{R}^{n\times n}$ and the delay terms $\tau_0(p), \ldots, \tau_m(p)$ now depend on a vector of design or controller parameters $p \in \mathbb{R}^{n_p}$. Observe that the set of uncertainties $\Delta = (\Delta A, \Delta\vec{\tau})$ (and thus its maximum size) does not depend on the vector of controller parameters p, although these parameters may admit some uncertainty as well. Considering again the systems introduced in Example 4.1, for the closed-loop system (4.3) with static controller we have $p = K^T$, while for (4.5) with dynamic controller, we have $p = \mathrm{vec}(A_c, B_c, C_c, D_c)$.

In the next section, we provide formulas for the derivative of the ε-pseudospectral abscissa w.r.t. controller parameters, and we briefly describe the optimization method adopted to tackle the non-smooth nature of the objective function.

4.1 Smoothness properties and optimization of the pseudospectral abscissa

We recall here that in Chapter 3 we have imposed some assumptions in order to guarantee that the perturbed system of DDAEs maintains the retarded dynamics for any possible perturbation. This naturally results in a continuous and a.e. differentiable dependence of the ε-pseudospectral abscissa on the set of design or controller parameters p. In order to stress the dependence on p, let us write the eigenvalue problem associated with (4.6) as

$$M(\lambda;\Delta,p)y = \left(\lambda E - \sum_{i=0}^{m} \left(A_i(p) + \sum_{j=1}^{K} D_{ij}\delta A_j E_{ij} \right) e^{-\lambda(\tau_i(p)+\delta\tau_i)} \right) y = 0. \tag{4.7}$$

Then, we aim to minimize the function

$$\begin{array}{lcl} \mathbb{R}^{n_p} & \longrightarrow & \mathbb{R} \\ p & \longrightarrow & \alpha^{\mathbb{R}}_{\varepsilon,F}(M(\lambda;\Delta,p)). \end{array}$$

In practice, we want to solve a min-max problem, where we first maximize the rightmost eigenvalue of (4.7), and we then minimize it to design a robust controller for system (4.6). Observe that the objective function of the minimization is only a.e. differentiable, and that points of non-smoothness are in most cases characterized by the switch among the components of the

ε-pseudospectrum containing the globally rightmost eigenvalue. For this reason, local minima of the function are often points of non-differentiability and therefore they cannot be characterized by a zero gradient. Furthermore, the ε-pseudospectral abscissa is in general non-convex and possibly non-Lipschitz. In order to tackle these unfavourable properties we perform the minimization using the HANSO (Hybrid Algorithm for Nonsmooth Optimization) algorithm introduced in [81] (see also the website indicated in [102] for a detailed description): the method combines the BFGS method when the objective function is smooth with a bundle gradient method which is able to capture local minima characterized by non-differentiability. The effectiveness of the method to minimize eigenvalue-related functions has already been proven in works like [89] and [54], where respectively the spectral abscissa and the robust H_∞ norm of a system of DDAEs are optimized.

The next theorem provides a formula for the derivative of $\alpha^{\mathbb{R}}_{\varepsilon,F}$ w.r.t. to the design or controller parameters p, whenever this derivative exists.

Theorem 4.2. *Let $\big(\lambda_{\mathrm{RM}}(p), x(p), y(p)\big)$ be respectively the globally rightmost point of the ε-pseudospectrum and its left and right normalized eigenvectors. For each set of parameter $p \in \mathbb{R}^{n_p}$, let us also define $\widetilde{\Delta A}(p) = \big(\widetilde{\delta A_1}(p), \dots, \widetilde{\delta A_K}(p)\big)$ and $\widetilde{\Delta\vec{\tau}}(p) = \big(\widetilde{\delta\tau_0}(p), \dots, \widetilde{\delta\tau_m}(p)\big)$ as the optimal matrix perturbations and optimal delay perturbations functions such that $\lambda_{\mathrm{RM}}(p)$ is simple. Then setting*

$$\xi := -x^* \left(E + \sum_{i=0}^{m} \left(A_i + \sum_{j=1}^{K} D_{i,j} \widetilde{\delta A_j} E_{i,j} \right) (\tau_i + \widetilde{\delta\tau_i}) e^{-\lambda_{\mathrm{RM}}(\tau_i + \widetilde{\delta\tau_i})} \right) y$$

we can express the derivative of the ε-pseudospectral abscissa w.r.t each parameter p_j as

$$\frac{\partial \alpha^{\mathbb{R}}_{\varepsilon,F}}{\partial p_j} = \frac{\partial \Re(\lambda_{\mathrm{RM}})}{\partial p_j} = \frac{1}{\xi} \Re \left[x^* \left(- \sum_{i=0}^{m} \frac{\partial A_i}{\partial p_j} e^{-\lambda_{\mathrm{RM}}(\tau_i + \widetilde{\delta\tau_i})} + \sum_{i=0}^{m} \left(A_i + \sum_{j=1}^{K} D_{i,j} \widetilde{\delta A_j} E_{i,j} \right) e^{-\lambda_{\mathrm{RM}}(\tau_i + \widetilde{\delta\tau_i})} \lambda_{\mathrm{RM}} \frac{\partial \tau_i}{\partial p_j} \right) y \right],$$

where we omit the dependence on p to simplify the notation.

Observe that the values of the optimal perturbations $\widetilde{\delta A_i}$, $\widetilde{\delta\tau_i}$ does depend on the set of design or controller parameters p: indeed, although the maximal size of the optimal perturbations is prescribed, the optimal perturbations might assume different values in the parameter space. However, due to the optimality conditions, their derivative w.r.t. p does not affect the derivative of the ε-pseudospectral abscissa.

The main scope of our work is to tune parameters in order to have a negative ε-pseudospectral abscissa. For this reason, convergence to a local but not global minimum does not represent an issue. Even more, from a practical point of view, any negative value obtained for the ε-pseudospectral abscissa ensures the robust stability of our system, regardless of the convergence of the algorithm to a minimum. The HANSO algorithm is intended for unconstrained optimization; however, we might need to force our controller to stay in some region of the parameter space, e.g., we constrain the delay terms to have positive values. For this reason, we also include some penalties in our cost function, as we will explain case by case in the following section. In general, the penalties we introduce are continuous but non differentiable functions. It is worth to remind that HANSO method can cope with non-differentiability. Moreover, the ε-pseudospectral abscissa function is already likely to be non-differentiable in its minima, so we do not add any non-smoothness to the cost function.

4.2 Numerical experiments

Example 4.3. *We consider system (4.1) introduced in Example 4.1, where*

$$A = \begin{bmatrix} -0.08 & -0.03 & 0.2 \\ 0.2 & -0.04 & -0.005 \\ -0.06 & 0.2 & -0.07 \end{bmatrix}, \quad B = \begin{bmatrix} -0.1 \\ -0.2 \\ 0.1 \end{bmatrix}, \quad C = I_3. \tag{4.8}$$

This system is unstable, therefore we consider a delayed static feedback controller $u(t) = Ky(t)$ with $\tau = 5$. As in Example 4.1, we include the uncertainties δA, δB on the matrix coefficients and $\delta\tau$ on the time delay τ; we also include an uncertainty δC on the measure of the state variable. We thus set

$$\varepsilon = 0.05,\ D_{0,1} = \|A\|_F \begin{bmatrix} I \\ 0 \\ 0 \end{bmatrix},\ D_{0,2} = \|C\|_F \begin{bmatrix} 0 \\ I \\ 0 \end{bmatrix},\ D_{1,3} = \|B\|_F \begin{bmatrix} I \\ 0 \\ 0 \end{bmatrix},$$

$$v_1 = \frac{\varepsilon}{0.5},\ E_{0,1} = \begin{bmatrix} I \\ 0 \\ 0 \end{bmatrix}^T,\ E_{0,2} = \begin{bmatrix} I \\ 0 \\ 0 \end{bmatrix}^T,\ E_{1,3} = \begin{bmatrix} 0 \\ 0 \\ I \end{bmatrix}^T,$$

in order to allow a maximal relative error of 5% on matrices A, B and C, and to impose $|\delta\tau| \leq 0.5$. In Table 4.1 we report the values of the spectral abscissa α and of the ε-pseudospectral abscissa $\alpha^{\mathbb{R}}_{\varepsilon,F}$ in five different cases: in the first case the system is uncontrolled ($K = 0$); in the second case we assume the minimizer for the spectral abscissa $K^s = [0.472\ 0.505\ 0.603]$ (see [124]); in the third case the optimal controller $K^s_\varepsilon = [0.944\ 1.171\ 0.543]$ minimizes the ε-pseudospectral abscissa $\alpha^{\mathbb{R}}_{\varepsilon,F}$; in the last two cases, the controllers

Table 4.1: Computed spectral abscissa α and ε-pseudospectral abscissa $\alpha^{\mathbb{R}}_{\varepsilon,F}$ of system (4.1) with the matrices defined in (4.8) for five different controllers: $K = 0$ (uncontrolled), $K^s,\ K^s_\varepsilon,\ K^d$ and K^d_ε.

	α	$\alpha^{\mathbb{R}}_{\varepsilon,F}$
Uncontrolled	+1.081e-01	+1.266e-01
K^s	-1.492e-01	+5.550e-02
K^s_ε	-5.663e-02	-3.909e-03
K^d	-2.146e-01	+4.553e-02
K^d_ε	-7.867e-02	-1.490e-02

K^d, respectively K^d_ε, are minimizers for the spectral abscissa, respectively ε-pseudospectral abscissa, of system (4.1) coupled with the dynamic controller (4.4), where $K^d,\ K^d_\varepsilon$ are the vectorizations of the controller parameters included in $A_c,\ B_c,\ C_c,\ D_c$, assuming x_c and u as scalar functions. It is worth remarking that $\alpha^{\mathbb{R}}_{\varepsilon,F}(M(\lambda;\Delta,K^s_\varepsilon)) < 0$ and $\alpha^{\mathbb{R}}_{\varepsilon,F}(M(\lambda;\Delta,K^d_\varepsilon)) < 0$: this means that our optimization process provides an optimal controller that guarantees the robust stability. We also observe that $\alpha^{\mathbb{R}}_{\varepsilon,F}(M(\lambda;\Delta,K^s_\varepsilon)) < \alpha^{\mathbb{R}}_{\varepsilon,F}(M(\lambda;\Delta,K^s))$ and that $\alpha(M(\lambda;\Delta,K^s_\varepsilon)) > \alpha(M(\lambda;\Delta,K^s))$: this demonstrates the considerably different behaviours of functions α and $\alpha^{\mathbb{R}}_{\varepsilon,F}$ and justifies our optimization approach for robust stabilization: same considerations apply for $K^d,\ K^d_\varepsilon$. Finally, in Figure 4.1, we compare the rightmost eigenvalues in the unperturbed uncontrolled system, in the unperturbed system controlled with $K = K^s_\varepsilon$ and in the worst-case scenario for the system controlled with $K = K^s_\varepsilon$, for which the real part of the globally rightmost eigenvalue is the ε-pseudospectral abscissa.

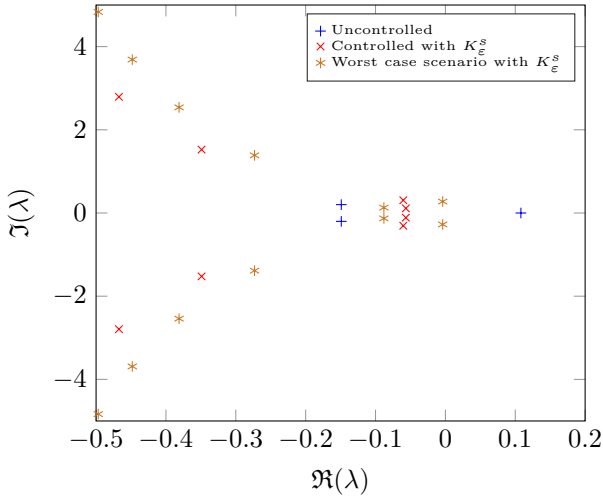

Figure 4.1: Rightmost eigenvalues of system (4.1) with the matrices defined in (4.8) when $K = 0$, when $K = K_\varepsilon^s$, and in the worst-case scenario for $K = K_\varepsilon^s$.

Let us now assume that matrix C is not affected by uncertainty, and let us consider the delay τ as a controller parameter in addition to the static feedback controller K, so that $p = [K^T;\ \tau]$. Note that a penalty function is needed to prevent the delay τ from taking negative values; since we are considering an uncertainty $\delta\tau$ such that $|\delta\tau| \leq 0.5$, we constrain the nominal value τ to be larger than 0.5 adding a continuous penalty to our cost function as follows:

$$f: \quad \begin{array}{ccc} \mathbb{R}^4 & \longrightarrow & \mathbb{R} \\ (K,\tau) & \longrightarrow & \begin{cases} \alpha^{\mathbb{R}}_{\varepsilon,F}(M(\lambda;\Delta,K,\tau)), & \text{if } \tau \geq 0.5, \\ \alpha^{\mathbb{R}}_{\varepsilon,F}(M(\lambda;\Delta,K,0.5)) + 10(0.5-\tau), & \text{if } \tau < 0.5. \end{cases} \end{array}$$

In Table 4.2 we report the values of the spectral abscissa α and of the ε-pseudospectral abscissa $\alpha^{\mathbb{R}}_{\varepsilon,F}$ in three different cases: in the first case the system is uncontrolled ($p_0 = [0;\ 0;\ 0;\ 5]$); in the second case the controller $p^* = [1.4709;\ 2.7602;\ 2.3328;\ 1.0029]$ is a minimizer for the spectral abscissa α; in the third case the controller $p^*_\varepsilon = [2.2354;\ 3.5256;\ 3.8240;\ 1.0516]$ is a minimizer for the objective function f. Again, it is easy to observe that our approach provides an optimal controller that guarantees stability against system's uncertainties and that the spectral abscissa and the ε-pseudospectral abscissa have distinct minimizers. Finally, in Figure 4.2, we compare the rightmost eigenvalues of the uncontrolled system, of the system controlled with $p = p^*_\varepsilon$ and of the system corresponding to the worst-case scenario for $p = p^*_\varepsilon$, for which the real part of the globally rightmost eigenvalue is the ε-pseudospectral abscissa.

Table 4.2: Computed spectral abscissa α and ε-pseudospectral abscissa $\alpha^{\mathbb{R}}_{\varepsilon,F}$ of system (4.1) with the matrices defined in (4.8) for three different controllers: $p = 0$ (uncontrolled), p^* and p^*_ε.

	α	$\alpha^{\mathbb{R}}_{\varepsilon,F}$
Uncontrolled	+1.0806e-01	+1.2659e-01
p^*	-4.8130e-01	-1.2531e-01
p^*_ε	-3.3006e-01	-2.0099e-01

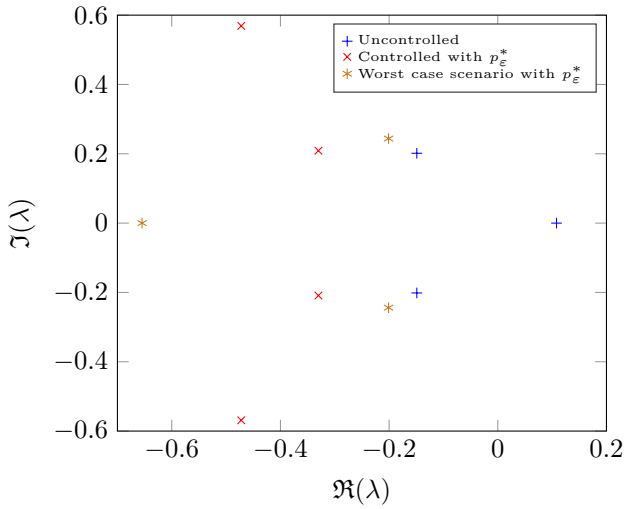

Figure 4.2: Rightmost eigenvalues of system (4.1) with the matrices defined in (4.8) when $p = 0$, when $p = p^*_\varepsilon$, and in the worst-case scenario for $p = p^*_\varepsilon$.

Example 4.4. *In this example, we consider again the system from Example 3.11, that is the system*

$$\dot{x}(t) = A_0x(t) + A_1x(t-\tau_1) + A_2x(t-\tau_2), \tag{4.9}$$

with

$$A_0 = \begin{bmatrix} -1 & 13.5 & -1 \\ -3 & -1 & -2 \\ -2 & -1 & -4 \end{bmatrix}, \; A_1 = \begin{bmatrix} -5.9 & 0 & 0 \\ 2 & 0 & 0 \\ 2 & 0 & 0 \end{bmatrix}, \; A_2 = \begin{bmatrix} 0 & 7.1 & -70.3 \\ 0 & -1 & 5 \\ 0 & 0 & 6 \end{bmatrix},$$

whose stability w.r.t. the delay parameters τ_1 and τ_2 is examined in [41]. In this example, time delays are considered unperturbed, and we assume an uncertainty δA_1 on the matrix A_0 and an uncertainty δA_2 affecting the nonzero part of A_1.

Thus, we define

$$D_{0,1} = \|A_0\|_F\, I_3, \quad E_{0,1} = I_3, \quad D_{1,2} = \|A_1\|_F\, I_3, \quad E_{1,2} = \begin{bmatrix} 1 & 0 & 0 \end{bmatrix},$$

and we set $\varepsilon = 0.005$*. We now consider the minimization of the pseudospectral abscissa, where the delays* τ_1 *and* τ_2 *are assumed as controller parameters. Again, we include some continuous penalties in our cost function* f *in order to prevent the delay terms from being negative*

$$f: \quad \mathbb{R}^2 \longrightarrow \mathbb{R}$$

$$(\tau_1, \tau_2) \longrightarrow \begin{cases} \alpha^{\mathbb{R}}_{\varepsilon,F}(M(\lambda;\Delta,\tau_1,\tau_2)), & \text{if } \tau_1 \geq 0,\ \tau_2 \geq 0, \\ \alpha^{\mathbb{R}}_{\varepsilon,F}(M(\lambda;\Delta,0,\tau_2)) - 100\tau_1, & \text{if } \tau_1 < 0,\ \tau_2 \geq 0, \\ \alpha^{\mathbb{R}}_{\varepsilon,F}(M(\lambda;\Delta,\tau_1,0)) - 100\tau_2, & \text{if } \tau_1 \geq 0,\ \tau_2 < 0, \\ \alpha^{\mathbb{R}}_{\varepsilon,F}(M(\lambda;\Delta,0,0)) - 100\tau_1 - 100\tau_2, & \text{if } \tau_1 < 0,\ \tau_2 < 0. \end{cases}$$

Optimizing the function f*, a minimizer is found in* $p^*_\varepsilon = [1.8955e{-}02;\ \ 1.5599e{-}02]$*, whereas the minimization of the spectral abscissa* α *converged to a point* $p^* = [3.5490e-05;\ \ 1.3920e-02]$*. The controllers are close to the negative half-planes for both variables* $\tau_1,\ \tau_2$*, however the configuration* $(\tau_1, \tau_2) = (0, 0)$ *is never a minimizer. In Figure 4.3 we compare the spectral abscissae and the worst-case scenarios for both controllers* p^* *and* p^*_ε*: the observations made for the previous example still hold, as* $\alpha(p^*) < \alpha(p^*_\varepsilon)$ *and* $\alpha^{\mathbb{R}}_{\varepsilon,F}(p^*_\varepsilon) < \alpha^{\mathbb{R}}_{\varepsilon,F}(p^*)$*.*

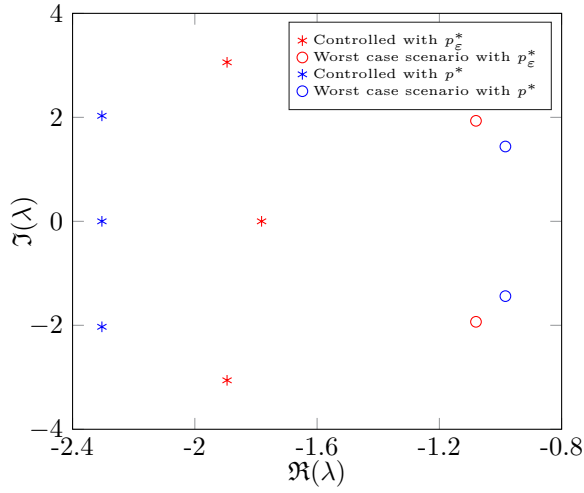

Figure 4.3: Rightmost eigenvalues of system (4.9) obtained for the controllers p^* and p^*_ε, and the rightmost eigenvalues of the corresponding worst-case scenarios.

4.3 A scalable design method for stabilising decentralised controllers of delay-coupled networks

In this section we present a scalable design method for stabilising fixed-order decentralised controllers for large scale LTI systems with time-delays. The application of centralised controllers for large scale systems is often impractical or costly (see [82], [111], and [84]). Generally, decentralised, distributed or other structurally constrained controllers are preferred for application to large scale systems. Traditional design methods for stabilising and $\mathcal{H}_\infty$ optimal controllers for LTI Multiple Input Multiple Output systems are grounded in the Riccati equation and linear matrix inequality framework (see [43], [39], and references therein). In most cases, controllers designed by these methods are not structured and their dimension is equal to or larger than the order of the plant.

We here consider the decentralized fixed-order stabilisation problem of a class of interconnected time-delay systems with a network structure, whose nodes host identical dynamical systems, using identical local controllers. We show that it is possible to exploit the systems' network structure in the controller synthesis procedure, in order to improve computational efficiency and scalability with respect to the number of subsystems. More precisely, we show how to perform a decoupling transformation of the network of interconnected systems, resulting in a simultaneous controller design problem for *one parameterised (sub)system*, where the allowable values of the parameter correspond to the spectrum of the network adjacency matrix.

For some network topologies, the values of the (eigenvalue) parameter related to the network structure are confined to a specific subset Ω of the complex plane (e.g. an interval on the real axis, a circle,...), which can be chosen independently of the number of nodes. In such a case, sufficient conditions for stability can be obtained by taking a robust control point of view and handling the network related parameter as an uncertain parameter confined to the full set Ω. Note that if the (Hausdorff) distance between the spectrum of the adjacency matrix and Ω goes to zero when the number of systems goes to infinity, the conservatism of the sufficient conditions disappears in the limit. In this section, we illustrate this approach by means of the decentralized stabilization problem for network topologies for which the set Ω is an interval on the real axis.

4.3.1 Interconnected systems

In this subsection, we describe the decomposition approach for designing a decentralised controller for an interconnected system which has by itself a network structure consisting of identical subsystems to be controlled by identical local controllers.

We consider a network described by a directed graph $\mathcal{G} = \{\mathcal{V}, \mathcal{E}, A_M\}$ with a set of nodes $\mathcal{V} = \{1, 2, 3, ..., n\}$ and a set of edges $\mathcal{E} \subset \mathcal{V} \times \mathcal{V}$. The edge $(i, j) \in \mathcal{E}$ connects node $j \in \mathcal{V}$ to node $i \in \mathcal{V}$. The graph $\mathcal{G}$ need not be strongly connected (which is the definition of a graph where each vertex is reachable from every other vertex). In addition, we assume that the graph is simple, which means that there is no self coupling. We denote by

$$A_M = [a_{Mij}]_{i,j=1}^{n}$$

the weighted adjacency matrix with zero diagonal entries and non-negative off-diagonal entries such that $a_{Mij} > 0$ if and only if the corresponding edge $(i, j) \in \mathcal{E}$.

Each of the n nodes hosts a dynamical system with time-delays described by the following equations,

$$\begin{cases} \dot{x}_{pi}(t) & = A_{p0}x_{pi}(t) + A_{p1}x_{pi}(t-\tau_1) \\ & \quad +B_{p1}u_i(t-\tau_2) + B_{p2}u_{ci}(t-\tau_3), \\ y_i(t) & = C_{p1}x_{pi}(t) + D_{p1}u_i(t-\tau_2), \\ y_{ci}(t) & = C_{p2}x_{pi}(t) \qquad \forall\ i = 1, \ldots, n. \end{cases} \tag{4.10}$$

The instantaneous state vector is denoted by $x_{pi}(t) \in \mathbb{R}^{n_p}$ at time t. Similarly, $u_i(t) \in \mathbb{R}^{n_u}$ and $y_i(t) \in \mathbb{R}^{n_y}$ are instantaneous controlled input and measured output vectors at time t. The additional input u_{ci} and output y_{ci} are related to the coupling with other nodes/subsystems in the network, which can be described by

$$u_{ci}(t) = \sum_{j=1}^{n} a_{Mij}y_{cj}(t), \quad i = 1, \ldots, n. \tag{4.11}$$

Hence, we consider the case where the interconnected system is composed of subsystems (4.10) and has a structure imposed by (4.11). We also consider each subsystem to be controlled by a fixed-order LTI feedback controller (order = n_c) of the form

$$\begin{cases} \dot{x}_{ci}(t) = A_c x_{ci}(t) + B_c y_i(t), \\ u_i(t) = C_c x_{ci}(t) + D_c y_i(t). \end{cases} \tag{4.12}$$

Here a static controller ($n_c = 0$) would have only the D_c component. We assume either $D_c = 0$ or $D_{p1} = 0$ to ensure that the closed-loop system is a delay system of retarded type.

Defining

$$x_i(t) = [x_{pi}^{\mathrm{T}}(t)\ u_i^{\mathrm{T}}(t)\ x_{ci}^{\mathrm{T}}(t)\ y_i^{\mathrm{T}}(t)\ u_{ci}^{\mathrm{T}}(t)]^{\mathrm{T}},$$

the closed-loop system including subsystems, controllers and interconnections, can be written using the new state $x_i \in \mathbb{R}^{n_{cl}}$ in the form of DDAEs

$$E\dot{x}_i(t) = A_0 x_i(t) + \sum_{k=1}^{3} A_k x_i(t-\tau_k) + \sum_{j=1}^{n} a_{Mij} BCx_j(t),\ i = 1, \ldots, n, \quad (4.13)$$

where

$$E = \begin{bmatrix} I & 0 & 0 & 0 & 0 \\ 0 & 0 & 0 & 0 & 0 \\ 0 & 0 & I & 0 & 0 \\ 0 & 0 & 0 & 0 & 0 \\ 0 & 0 & 0 & 0 & 0 \end{bmatrix}, A_0 = \begin{bmatrix} A_{p0} & 0 & 0 & 0 & 0 \\ C_{p1} & 0 & 0 & -I & 0 \\ 0 & 0 & \bar{A}_c & \bar{B}_c & 0 \\ 0 & -I & \bar{C}_c & \bar{D}_c & 0 \\ 0 & 0 & 0 & 0 & -I \end{bmatrix} \quad (4.14)$$

and

$$A_1 = \begin{bmatrix} A_{p1} & 0 & 0 & 0 & 0 \\ 0 & 0 & 0 & 0 & 0 \\ 0 & 0 & 0 & 0 & 0 \\ 0 & 0 & 0 & 0 & 0 \\ 0 & 0 & 0 & 0 & 0 \end{bmatrix}, A_2 = \begin{bmatrix} 0 & B_{p1} & 0 & 0 & 0 \\ 0 & D_{p1} & 0 & 0 & 0 \\ 0 & 0 & 0 & 0 & 0 \\ 0 & 0 & 0 & 0 & 0 \\ 0 & 0 & 0 & 0 & 0 \end{bmatrix}, B = \begin{bmatrix} 0 \\ 0 \\ 0 \\ 0 \\ I \end{bmatrix},$$

$$A_3 = \begin{bmatrix} 0 & 0 & 0 & 0 & B_{p2} \\ 0 & 0 & 0 & 0 & 0 \\ 0 & 0 & 0 & 0 & 0 \\ 0 & 0 & 0 & 0 & 0 \\ 0 & 0 & 0 & 0 & 0 \end{bmatrix}, C^{\mathrm{T}} = \begin{bmatrix} C_{p2} \\ 0 \\ 0 \\ 0 \\ 0 \end{bmatrix}.$$

Note that DDAEs are amenable for modelling interconnected systems with time-delays at any part of the system. Therefore the methodology proposed in this section is not restricted to time-delay systems (4.10) with three time-delays, which we have chosen for the sake of simplicity.

The state-space representation for the overall structured system takes the form

$$(I \otimes E)\,\dot{x}(t) = (I \otimes A_0)\,x(t) + \sum_{k=1}^{3} (I \otimes A_k)\,x(t-\tau_k) + (A_M \otimes BC)\,x(t), \quad (4.15)$$

where $x = [x_1\ \ldots\ x_n]^{\mathrm{T}}$ and the Kronecker product is denoted by "$\otimes$".

It is important to point out that all controller parameters are contained in matrix A_0 in (4.14), as indicated with the dashed box. In what follows we denote the controller parameters by vector

$$\boldsymbol{p} = \mathrm{vec}\begin{bmatrix} A_c & B_c \\ C_c & D_c \end{bmatrix}, \quad (4.16)$$

and, whenever appropriate, stress the dependence of A_0 and of the spectral abscissa α of (4.15) on these parameters with the notations $A_0(\boldsymbol{p})$, $\alpha(\boldsymbol{p})$, respectively.

4.3.2 Decoupling for the stabilisation problem

There always exists a transformation matrix $T \in \mathbb{C}^{n\times n}$ and an upper-triangular matrix $Z \in \mathbb{C}^{n\times n}$ such that

$$TA_MT^{-1} = Z. \tag{4.17}$$

Note that spectrum of A_M appears on the diagonal of Z. If we apply the transformation $x(t) = \hat{T}^{-1}\bar{x}(t)$ to (4.15), with $\hat{T} = T \otimes I$, we obtain equation

$$(I \otimes E)\,\dot{\bar{x}}(t) = (I \otimes A_0)\,\bar{x}(t) + \sum_{k=1}^{3} (I \otimes A_k)\,\bar{x}(t-\tau_k) + (Z \otimes BC)\,\bar{x}(t). \tag{4.18}$$

As the system in (4.18) has a cascaded structure, the following theorems holds true.

Theorem 4.5. *Let the spectrum of A_M be denoted by $\boldsymbol{\lambda_a} = \{\lambda_{a1}, \ldots, \lambda_{an}\}$. Let us consider the group of subsystems given by*

$$E\dot{\bar{x}}_i(t) = (A_0 + \lambda_{ai}BC)\,\bar{x}_i(t) + \sum_{k=1}^{3} A_k\bar{x}_i(t-\tau_k),\ i = 1, \ldots, n. \tag{4.19}$$

Then the system (4.18) is exponentially stable if and only if the system (4.19) for all $i = 1, ..., n$ is exponentially stable. Moreover, the spectral abscissa $\alpha(\boldsymbol{p})$ of (4.18) satisfies

$$\alpha(\boldsymbol{p}) = \max_{1\le i\le n} \sup_{\lambda\in\mathbb{C}} \{\Re(\lambda) : \det M(\lambda; \boldsymbol{p}, \lambda_{ai}) = 0\},$$

where

$$M(\lambda; \boldsymbol{p}, \lambda_{ai}) = \lambda E - A_0(\boldsymbol{p}) - \lambda_{ai}BC - \sum_{k=1}^{3} A_k \mathrm{e}^{-\lambda\tau_k}. \tag{4.20}$$

Proof. The assertions directly follow from the block-triangular structure of (4.18), with (4.19) appearing as a diagonal block, and from the structure of the associated eigenvalue problem. □

4.3.3 Design of the controller

From Theorem 4.5, the design of stabilizing decentralized controllers can be recast as the simultaneous stabilization problem of finding controller parameters such that (4.19) is exponentially stable for all $i = 1, \ldots, n$.

For some topologies, the eigenvalues corresponding to their network adjacency matrices (λ_{ai}) for any number of nodes (n) are confined to a real interval, i.e.,$\lambda_{ai} \in \Omega := [p, q]$ where $p,\ q \in \mathbb{R}$ and $p < q$. Since the only difference

between the systems' equations in (4.19) lies in parameters λ_{ai}, a sufficient condition for stability is given by the *robust stability* of "uncertain" system

$$E\dot{\eta}(t) = (A_0 + \lambda_a BC)\,\eta(t) + \sum_{k=1}^{3} A_k \eta(t-\tau_k), \tag{4.21}$$

subject to interval uncertainty $\lambda_a \in [p, q]$. The associated characteristic matrix of (4.21) can be written as

$$M(\lambda;\Delta) = \lambda E - (A_0 + B\lambda_{av}C + B\Delta C) - \sum_{k=1}^{3} A_k \mathrm{e}^{-\lambda\tau_k}, \tag{4.22}$$

with $\lambda_{av} = \frac{p+q}{2}$ and Δ a scalar uncertainty such that $|\Delta| \leq \varepsilon = \frac{|q-p|}{2}$. Thus, we have a formulation that falls into the scope of (3.10).

Hence, a *necessary and sufficient* condition for exponential stability of (4.21) for all $\lambda_a \in [p, q]$ is that the ε-pseudospectral abscissa of (4.22) is negative. In particular, this condition guarantees the stability of the network structure *whatever* the number of subsystems n is.

In order to find a robustly stabilizing controller, we thus minimize the pseudospectral abscissa by tuning controller parameters, i.e., we solve

$$\min_{\boldsymbol{p}} \alpha_\varepsilon. \tag{4.23}$$

Recall that vector $\boldsymbol{p}$ contains all the tunable controller parameters, which are contained in the closed-loop system matrix A_0 (see (4.14) and (4.16)).

In the next subsection, we show two examples for which $\lambda_{ai} \in \mathbb{R}$ for all $i = 1, ..., n$. However, there are other network topologies for which the adjacency matrix has non-real eigenvalues (e.g., a ring topology with unidirectional coupling), and this would translate to a problem with complex valued perturbations ($B\lambda_a C$) to system matrix A_0.

The ε-pseudospectral abscissa optimization approach for designing decentralised controller has many advantages. First, the size n of A_M increases with the number of subsystems in the structured system, leading to more eigenvalues λ_{ai}. The number of operations to compute the spectral abscissa of a DEP using the algorithm proposed in [89, 132] scales with the cube of the dimension of DEP. Therefore, the computational complexity of optimizing the spectral abscissa of the overall system depends on the number of subsystems $O(n \cdot (n_{cl})^3)$ (and even $O((nn_{cl})^3)$ if the decomposition is not employed). However, the computational complexity of the pseudospectral abscissa optimisation does not depend on the number of subsystems and thus reduces to $O(n_{cl}^3)$. Second, a controller designed to stabilise n subsystems might not be stabilizing for a different value of n, as will be demonstrated using a numerical example in the next subsection.

4.3.4 Numerical examples

Let us consider a simple numerical example for which a stabilising controller has to be designed such that it can control a group of identical subsystems arranged in a network topology (with adjacency matrix A_M whose eigenvalues satisfy $\lambda_{ai} \in [-1, 1]\ \forall\ i \in \{1, ..., n\}$). The sub-systems can be described by

$$\begin{cases} \dot{x}_{pi}(t) = & \begin{bmatrix} 1 & 3 \\ 2 & -0.5 \end{bmatrix} x_{pi}(t) + \begin{bmatrix} 0 \\ 1 \end{bmatrix} u_i(t-0.1) \\ & + \begin{bmatrix} 4 & 0 \\ 0 & 0 \end{bmatrix} \overbrace{u_{ci}(t-0.2)}^{\lambda_{ai} y_{ci}(t-0.2)}, \\ y_i(t) = & \begin{bmatrix} 1 & 1 \\ 0 & 1 \end{bmatrix} x_{pi}(t), \\ y_{ci}(t) = & I x_{pi}(t), \quad u_{ci}(t) = \sum_{j=1}^{n} a_{Mij} x_{pj}, \end{cases} \tag{4.24}$$

for all $i = 1, ..., n$. In the following subsections, we will consider systems (4.24), arranged in two network topologies.

Let us consider a ***linear network topology*** with bidirectional coupling, for which matrix A_M is of the form

$$A_M = \begin{bmatrix} 0 & 0.5 & 0 & \dots & 0 & 0 \\ 0.5 & 0 & 0.5 & \dots & 0 & 0 \\ 0 & 0.5 & 0 & \dots & 0 & 0 \\ \vdots & \vdots & \vdots & \ddots & \vdots & \vdots \\ 0 & 0 & 0 & \dots & 0 & 0.5 \\ 0 & 0 & 0 & \dots & 0.5 & 0 \end{bmatrix}_{n \times n}, \tag{4.25}$$

whose eigenvalues consist of

$$\lambda_{ai} = \cos(i \frac{\pi}{n+1}) :\ i = 1, ..., n. \tag{4.26}$$

For $n = 3$, the adjacency matrix has a spectrum given by $\hat{\boldsymbol{\lambda}}_{\boldsymbol{a}} = \{-0.7071, 0, 0.7071\}$. Choosing the controller order equal to one and minimizing the spectral abscissa $\alpha(\boldsymbol{p})$ of the coupled system lead us to the controller K_1 given by

$$\begin{cases} \dot{x}_{ci}(t) & = -9.5309 x_{ci}(t) + [-15.3689\ \ -3.5134] y_i(t), \\ u_i(t) & = -2.9752 x_{ci}(t) + [-19.3607\ 5.8863] y_i(t) \end{cases} \tag{4.27}$$

for $1 \leq i \leq 3$, for which we calculate the corresponding pseudospectral abscissa as $\alpha_\varepsilon = 0.3478$, where $\varepsilon = 1$.

The optimization of the pseudospectral abscissa of (4.22), constraining λ_{ai} to the interval $[-1, 1]$, leads us to controller K_α given by

$$\begin{cases} \dot{x}_{ci}(t) &= -4.3275 x_{ci}(t) + [-4.3547\ 6.2463] y_i(t) \\ u_i(t) &= 6.9677 x_{ci}(t) + [-13.8842\ 0.8332] y_i(t) \end{cases} \tag{4.28}$$

for $1 \leq i \leq n$, which is in fact stabilizing for any $n \in [1, \infty]$.

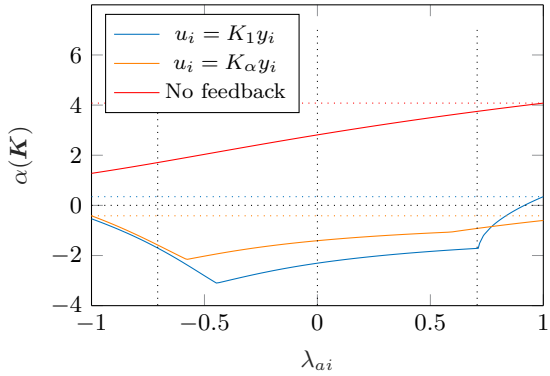

Figure 4.4: The spectral abscissa of (4.24) with (according to the decomposition) $u_{ci}(t) = \lambda_{ai} y_{ci}(t)$, for varying $\lambda_{ai} \in [-1, 1]$. We consider i) local controller K_1, ii) local controller K_α, and iii) the absence of feedback control.

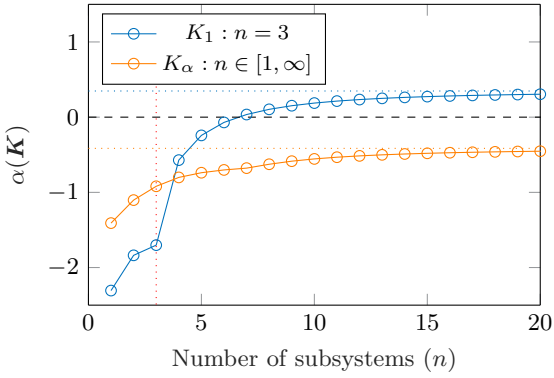

Figure 4.5: The local controller K_1 obtained by optimizing the spectral abscissa of three ($n = 3$) subsystems in a bidirectionally coupled linear network, with the spectrum of the adjacency matrix given by $\hat{\boldsymbol{\lambda}}_{\boldsymbol{a}} = \{-0.7071, 0, 0.7071\}$, results in an unstable network system for more than six subsystems.

In Fig. 4.4 and Fig. 4.5 we compare the performance of both controllers. The pseudospectral abscissa (when $\lambda_{ai} \in [-1, 1]$) for the system reduced from $\alpha_\varepsilon = 4.0793$ for the case of no feedback control to $\alpha_\varepsilon = -0.4151$ when controlled using K_α (see Fig. 4.4). Therefore, the structured closed loop system is stable as long as the adjacency matrix of the network structure A_M has all its eigenvalues in the interval $[-1, 1]$. This means that the closed loop system is guaranteed to be stable (with spectral abscissa ≤ -0.4151) for any number of nodes in the linear, ring, star and fully connected network topologies with bidirectional coupling, since, under mild conditions on the coupling weights, the eigenvalues of their adjacency matrices are contained in the interval $[-1, 1]$.

We also observe that controller K_1 achieves better for $\hat{\boldsymbol{\lambda}}_{\boldsymbol{a}}$, but it results in an unstable network for seven (or more) subsystems, as the corresponding ε-pseudospectral abscissa is positive.

Let us consider the sub-systems in (4.24) to be arranged in a ***ring topology*** with bidirectional coupling. We have a circulant A_M matrix of the form

$$A_M = \begin{bmatrix} 0 & 0.5 & 0 & \dots & 0 & 0.5 \\ 0.5 & 0 & 0.5 & \dots & 0 & 0 \\ 0 & 0.5 & 0 & \dots & 0 & 0 \\ \vdots & \vdots & \vdots & \ddots & \vdots & \vdots \\ 0 & 0 & 0 & \dots & 0 & 0.5 \\ 0.5 & 0 & 0 & \dots & 0.5 & 0 \end{bmatrix}_{n \times n}, \tag{4.29}$$

with the spectrum given in [97] as

$$\lambda_{ai} = \cos\left(\frac{2\pi}{n}(i-1)\right) : \ i = 1, ..., q \text{ and } n \in \mathbb{Z}^+ \setminus \{1\}, \tag{4.30}$$

where $q = \frac{n+2}{2}$ or $\frac{n+1}{2}$ for even or odd values of n respectively. All the eigenvalues given by (4.30) have a multiplicity of two, except for '± 1' which have multiplicity one.

Optimizing the spectral abscissa of the closed-loop system for $n = 3$ (for which the adjacency matrix has spectrum $\tilde{\boldsymbol{\lambda}}_{\boldsymbol{a}} = \{-0.5, -0.5, 1\}$) results in the controller K_2 given by

$$\begin{cases} \dot{x}_{ci}(t) &= -10.1209 x_{ci}(t) + [3.0604 \ 12.1140] y_i(t), \\ u_i(t) &= 3.5645 x_{ci}(t) + [-19.3998 \ 6.0459] y_i(t), \end{cases} \tag{4.31}$$

for $1 \leq i \leq 3$ ($n = 3$). Note that we can control the subsystems in this network also using controller K_α in (4.28), as the eigenvalues of the network adjacency matrix satisfy $\lambda_{ai} \in [-1, 1]$ $\forall i \in \{1, \dots, n\}$, $\forall\ n \in [1, \infty]$. We observe in Fig. 4.6 that the stability of this network is affected adversely by small change in n for the closed-loop system with controller K_2. This is due to the presence of the eigenvalue "-1" in the spectrum of A_M for even numbers of subsystems (n).

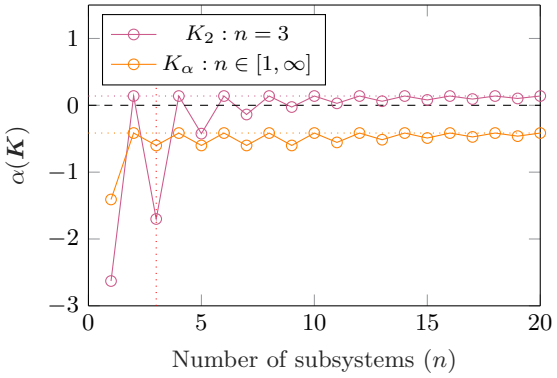

Figure 4.6: The local controller K_2 results in an unstable network system for two or four subsystems. On the contrary, the local controller K_α stabilises the system for any number of subsystems n.

4.4 Conclusions

In this chapter we illustrated a method to design a robust controller for a class of linear DDAEs affected by uncertainty on the system matrices and on the delay values. The method is based on the minimization of the ε-pseudospectral abscissa w.r.t. some controller or design parameters, that appear in the matrix coefficients or the delay values. The advantage of this method is evident: a very broad class of perturbations is allowed on the system of DDAEs and the nonlinear structure of the associated delay eigenvalue problem is taken into account. As a consequence, the ε-pseudospectral abscissa minimization allows to synthesize controllers for real-life applications, as it guarantees an asymptotically stable behavior of the solution despite the uncertainties affecting the system.

In the last section of the chapter, we presented a methodology to design dynamic LTI fixed-order controllers for large-scale interconnected systems, which was first introduced in [27]. We conclude that, using a direct optimization approach and a decomposition, it might be possible to design a stabilising decentralised controller independently of the number of nodes, where the network related eigenvalue parameter is handled by considering the pseudospectral abscissa as objective function. This approach ensures a computational complexity which is independent of the number of nodes. As already mentioned in [28], the decomposition approach can be easily extended to classes of distributed or overlapping controllers, including the case of interacting controllers communicating their state with neighbours.

Chapter 5

A globally convergent method to compute the real stability radius for time-delay systems

In this chapter we present another algorithm to compute the real structured distance to instability for LTI delay systems of retarded type. This time, we base our method on the characterization of the distance to instability as the reciprocal of the global maximum of the real structured singular value function $\mu_{\mathbb{R}}$, as already sketched in the introduction. We develop a criss-cross type algorithm that *globally* converges to this maximum, and whose convergence rate seems to be quadratic in numerical experiments. The algorithm proposed in this chapter is preferable to the one proposed in Chapter 3 in terms of convergence properties. As already explained, a potential drawback of the latter is represented by the underlying gradient method for the computation of the ε-pseudospectral abscissa, which potentially converges to a locally, but not a globally, rightmost point of the ε-pseudospectrum and thus yields an upper-bound estimate for the distance to instability. As we will see later, the price to pay to use this new method is a set of more restrictive hypotheses, and thus a smaller class of perturbations that can be taken into consideration.

The algorithm exploits that the intersections of these singular value functions with constant functions can be characterized as purely imaginary eigenvalues of certain Hamiltonian DEPs with positive and negative delays, and is inspired by the linear delay-free case considered in [114]. In addition, a novel numerical solver to compute all the imaginary eigenvalues of these DEPs is also developed. It combines an approximation using spectral discretizations and an automatic procedure to determine the required number of discretization points. Finally, due

to the presence of multiple eigenvalues at the maximum, these approximations are corrected with a block-Newton algorithm for nonlinear eigenvalue problems.

5.1 Introduction and problem statement

We propose a novel technique to compute the distance to instability for (asymptotically stable) LTI delay systems of retarded type affected by *structured, real-valued* uncertainties defined as

$$\dot{x}(t) = \sum_{i=1}^{m} \left(A_i + D\delta A_i E_i\right) x(t-\tau_i), \tag{5.1}$$

where $x(t) \in \mathbb{R}^n$ is the state variable at time t, $A_i \in \mathbb{R}^{n\times n}$ are the nominal matrices, $0 \le \tau_1 < \cdots < \tau_m$ are the time delays. For each nominal matrix A_i, we consider an uncertainty $\delta A_i \in \mathbb{R}^{p\times q_i}$ for $p, q_i \in \mathbb{N}$ whose structure is defined by the real-valued scaling matrices $D \in \mathbb{R}^{n\times p}$ and $E_i \in \mathbb{R}^{q_i\times n}$. Thus, the set of perturbations δA_i can be concatenated in a matrix Δ as

$$\Delta := [\delta A_1, \ldots, \delta A_m] \in \mathbb{R}^{p\times q}, \quad \text{with } q = \sum_{i=1}^{m} q_i. \tag{5.2}$$

Observe that the uncertainties δA_i may vary from one matrix A_i to another but the matrix D is the same.[1] Note also that, unlike the other chapters in the dissertation, we here set the index of the summation in (5.1) starting from 1 instead of 0. This turns out to be necessary to adopt a simpler notation in the rest of the chapter, as will become clearer in the next section.

The most evident differences between the problem considered here and the one proposed in Chapter 3 are the constraint on matrix D and the absence of uncertainties on the delay values. As a matter of fact, with the present hypotheses the characteristic equation of the eigenvalue problem associated with the system (5.1) can be rewritten in the form $\det(I - M(\lambda)\Delta) = 0$, with Δ as in (5.2): this allows us to compute the distance to instability as the reciprocal of the global maximum of the $\mu_{\mathbb{R}}$ function. Neglecting for a moment the uncertainties on the delay values, the same approach could not be used in Chapter 3 because in that case Δ is a real-valued block diagonal matrix. In addition, the hypotheses adopted here do not allow for an uncertainty δA to perturb more than one nominal matrix A_i.

In [61], the real structured distance to instability is computed for retarded delay systems, where the same hypothesis on matrix D, as in (5.1), is also adopted. Closely related to the problem treated in this chapter, the method

[1] The results in this chapter can be easily modified to treat the case of different D_i but common E.

described in [61] is based on computing the maximum of the real structured singular value function $\mu_{\mathbb{R}}$ by sampling the interval $[0, \omega^*]$ on a grid, where ω^* is a user-supplied upper bound on the frequencies ω such that $\lambda = \imath\omega$ solves the equation $\det(I - M(\lambda)\Delta) = 0$ for some Δ. One of the downsides of this method is that the interval and the grid size are hard to determine in an automated way. When the $\mu_{\mathbb{R}}$ function is very steep around its global maximum, a very fine grid is needed for accurate approximations, which will require many evaluations of the $\mu_{\mathbb{R}}$ function using the formula in [107]. As a remedy for this difficulty, and with the purpose of speeding up the computation, in this chapter we extend to delay-systems the criss-cross algorithm introduced in [114] for the real distance to instability of a delay-free system, which is itself an extension of the method [13] for the complex distance to instability. As we will show in detail in Section 5.2, our method exploits the existence of a set of functions $g_2(\imath\omega, \gamma)$, $\gamma \in (0, 1]$, whose point-wise infimum over all $\gamma \in (0, 1]$ is the desired $\mu_{\mathbb{R}}$ function. Moreover, the global convergence to the global maximum of $\mu_{\mathbb{R}}$ is guaranteed, using only a few evaluations of the $\mu_{\mathbb{R}}$ function per iteration.

5.2 Distance to instability: a criss-cross algorithm

We now consider the DEP associated with (5.1)

$$M(\lambda; \Delta)y := \left(\lambda I_n - \sum_{i=1}^{m} A_i e^{-\tau_i \lambda} - \sum_{i=1}^{m} D\delta A_i E_i e^{-\tau_i \lambda} \right) y = 0, \tag{5.3}$$

where $(\lambda, y) \in \mathbb{C} \times \mathbb{C}^n$ with nonzero y is an eigenpair. In this chapter, we will adopt the spectral norm of the matrix $\Delta = [\delta A_1, \ldots, \delta A_m]$ as a measure of the uncertainty magnitude. Therefore, the distance to instability considered in this chapter can be formally written as

$$\begin{aligned} d_{\text{INS}} &:= \inf_{\substack{\lambda = \imath\omega \\ \omega \geq 0}} \inf_{\Delta \in \mathbb{R}^{p \times q}} \{ \|\Delta\|_2 \colon \det(M(\lambda; \Delta)) = 0 \} \\ &= \inf_{\substack{\lambda = \imath\omega \\ \omega \geq 0}} \inf_{\Delta \in \mathbb{R}^{p \times q}} \left\{ \|\Delta\|_2 \colon \det\big(I - G(\lambda)\Delta\big) = 0 \right\}, \end{aligned} \tag{5.4}$$

where

$$G(\lambda) = \mathbf{E}(\lambda) F(\lambda)^{-1} D \in \mathbb{C}^{q \times p}, \tag{5.5}$$

with

$$F(\lambda) = \lambda I - \sum_{i=1}^{m} A_i e^{-\tau_i \lambda} \qquad \text{and} \qquad \mathbf{E}(\lambda) = \begin{bmatrix} E_1 e^{-\tau_1 \lambda} \\ \vdots \\ E_m e^{-\tau_m \lambda} \end{bmatrix}.$$

5.2.1 The $\mu_{\mathbb{R}}$ function

In accordance with the definition given in (1.18), we define the singular value functions

$$g_\ell(\lambda,\gamma) = \sigma_\ell\left(\begin{bmatrix} \Re(G(\lambda)) & -\gamma\Im(G(\lambda)) \\ \gamma^{-1}\Im(G(\lambda)) & \Re(G(\lambda)) \end{bmatrix}\right),\ \lambda = \imath\omega,\ \omega\in\mathbb{R}^+, \tag{5.6}$$

for $\gamma \in (0,1]$ and $\ell = 1,\ldots,N^*$ with $N^* = \min(q,p)$. We assume throughout that $\operatorname{rank}(\Im(G(\imath\omega))) \geq 2$ for all $\omega\in\mathbb{R}^+$ and treat the case where $\operatorname{rank}(\Im G(\imath\omega)) = 1$ later in Section 5.2.3. Thanks to the manipulation in (5.4–5.5) and the rank condition, we can apply the results from [107] (already introduced in (1.26)) to obtain

$$(d_{\text{INS}})^{-1} = \sup_{\omega\geq 0}\mu_{\mathbb{R}}(G(\imath\omega)) \quad \text{with } \mu_{\mathbb{R}}(G(\imath\omega)) = \min_{\gamma\in(0,1]} g_2(\imath\omega,\gamma), \tag{5.7}$$

where $g_2(\imath\omega,\gamma)$ is proven a unimodal function in $\gamma\in(0,1]$. Then we can define

$$\gamma_{\min}(\omega)\in(0,1] \quad \text{s.t.} \quad \mu_{\mathbb{R}}(G(\imath\omega)) = g_2(\imath\omega,\gamma_{\min}(\omega)). \tag{5.8}$$

For our criss-cross algorithm, we need the following theorem:

Theorem 5.1. *For a fixed $\gamma\neq 0$ and a level set parameter ξ, we have that*

$$g_\ell(\imath\omega,\gamma) = \xi \quad \textit{for some } \ell = 1,\ldots,N^*, \tag{5.9}$$

if and only if $\lambda = \imath\omega$ is a solution of

$$\mathcal{D}_{\xi\gamma}(\lambda)\cdot y = 0, \qquad y\neq 0, \tag{5.10}$$

with

$$\mathcal{D}_{\xi\gamma}(\lambda) = \lambda I + M_0 + \sum_{i\neq 0,\, i=-m}^{m}\left(M_i e^{-\tau_i\lambda} + N_i e^{-2\tau_i\lambda}\right), \tag{5.11}$$

where

$$M_0 = \begin{bmatrix} 0 & 0 & -\alpha\Phi & 0 \\ 0 & 0 & 0 & -\alpha\Phi \\ \alpha\Psi & \beta\Psi & 0 & 0 \\ \beta\Psi & \alpha\Psi & 0 & 0 \end{bmatrix},$$

and, for $i = 1,\ldots,m$, we define $\tau_{-i} = -\tau_i$,

$$M_i = \begin{bmatrix} 0 & 0 & 0 & 0 \\ 0 & -A_i^\top & 0 & 0 \\ 0 & 0 & -A_i & 0 \\ 0 & 0 & 0 & 0 \end{bmatrix}, \quad M_{-i} = \begin{bmatrix} A_i^\top & 0 & 0 & 0 \\ 0 & 0 & 0 & 0 \\ 0 & 0 & 0 & 0 \\ 0 & 0 & 0 & A_i \end{bmatrix},$$

and

$$N_i = \begin{bmatrix} 0 & 0 & 0 & 0 \\ 0 & 0 & -\beta\Phi_i & 0 \\ 0 & 0 & 0 & 0 \\ 0 & 0 & 0 & 0 \end{bmatrix}, \quad N_{-i} = \begin{bmatrix} 0 & 0 & 0 & -\beta\Phi_i \\ 0 & 0 & 0 & 0 \\ 0 & 0 & 0 & 0 \\ 0 & 0 & 0 & 0 \end{bmatrix},$$

with $\alpha = \frac{1+\gamma^2}{2\gamma}$, $\beta = \frac{1-\gamma^2}{2\gamma}$, $\Psi = \xi^{-1}DD^\top$, $\Phi_i = \xi^{-1}E_i^\top E_i$ *and* $\Phi = \sum_{i=1}^m \Phi_i$.

Proof. For any $\lambda \in \mathbb{C}$ we have by direct verification that

$$\begin{aligned} & 2\begin{bmatrix} \Re(G(\lambda)) & \imath\gamma\Im(G(\lambda)) \\ \imath\gamma^{-1}\Im(G(\lambda)) & \Re(G(\lambda)) \end{bmatrix} \\ &= \begin{bmatrix} I_p & \gamma I_p \\ \gamma^{-1}I_p & -I_p \end{bmatrix} \begin{bmatrix} G(\lambda) & \\ & \overline{G(\lambda)} \end{bmatrix} \begin{bmatrix} I_q & \gamma I_q \\ \gamma^{-1}I_q & -I_q \end{bmatrix} \\ &= \underbrace{\begin{bmatrix} \mathbf{E}(\lambda) & \gamma\overline{\mathbf{E}(\lambda)} \\ \gamma^{-1}\mathbf{E}(\lambda) & -\overline{\mathbf{E}(\lambda)} \end{bmatrix}}_{\mathbf{E}_\gamma(\lambda)} \underbrace{\begin{bmatrix} F(\lambda) & \\ & \overline{F(\lambda)} \end{bmatrix}^{-1}}_{F_{[2]}(\lambda)} \underbrace{\begin{bmatrix} D & \gamma D \\ \gamma^{-1}D & -D \end{bmatrix}}_{D_\gamma}, \end{aligned}$$

where we do not indicate the conjugate of D since D is real-valued. The augmented eigenvalue characterization of the singular value (5.9) then implies

$$\begin{aligned} 0 &= \det\left(\frac{1}{2}\begin{bmatrix} 0 & D_\gamma^\top F_{[2]}^{-H}(\lambda)\mathbf{E}_\gamma^H(\lambda) \\ \mathbf{E}_\gamma(\lambda)F_{[2]}^{-1}(\lambda)D_\gamma & 0 \end{bmatrix} - \xi I\right) \\ &= \det\left(\frac{1}{2}\begin{bmatrix} 0 & \mathbf{E}_\gamma^H(\lambda)\mathbf{E}_\gamma(\lambda)F_{[2]}^{-1}(\lambda) \\ D_\gamma D_\gamma^\top F_{[2]}^{-H}(\lambda) & 0 \end{bmatrix} - \xi I\right) \qquad (5.12) \\ &= \det\left(\frac{1}{2}\begin{bmatrix} 0 & \mathbf{E}_\gamma^H(\lambda)\mathbf{E}_\gamma(\lambda) \\ D_\gamma D_\gamma^\top & 0 \end{bmatrix} - \xi\begin{bmatrix} F_{[2]}^H(\lambda) & \\ & F_{[2]}(\lambda) \end{bmatrix}\right) \end{aligned}$$

where we exploited in the second equality the identity $\det(XY - \xi I) = \det(YX - \xi I)$ with

$$X = \begin{bmatrix} D_\gamma^\top F_{[2]}^{-H}(\lambda) & 0 \\ 0 & \mathbf{E}_\gamma(\lambda)F_{[2]}^{-1}(\lambda) \end{bmatrix}, \quad Y = \begin{bmatrix} 0 & \mathbf{E}_\gamma^H(\lambda) \\ D_\gamma & 0 \end{bmatrix},$$

and in the third equality we right multiplied with matrix Z

$$Z = \begin{bmatrix} F_{[2]}^H(\lambda) & 0 \\ 0 & F_{[2]}(\lambda) \end{bmatrix}.$$

Now we left multiply the last term of equation (5.12) with ξ^{-1} and plug into equation (5.12) the following

$$\frac{\mathbf{E}_\gamma^H(\lambda)\mathbf{E}_\gamma(\lambda)}{2} = \sum_{i=1}^{m} \begin{bmatrix} \alpha/\gamma E_i^\top E_i e^{-2\tau_i \Re(\lambda)} & -\beta E_i^\top E_i e^{-2\tau_i \overline{\lambda}} \\ -\beta E_i^\top E_i e^{-2\tau_i \lambda} & \alpha\gamma E_i^\top E_i e^{-2\tau_i \Re(\lambda)} \end{bmatrix}$$

and

$$\frac{D_\gamma D_\gamma^\top}{2} = \begin{bmatrix} \alpha\gamma DD^\top & \beta DD^\top \\ \beta DD^\top & \alpha/\gamma DD^\top \end{bmatrix},$$

so that we obtain

$$\det\left(\begin{bmatrix} -F^H(\lambda) & 0 & \alpha/\gamma\Phi(\Re(\lambda)) & -\beta\Phi(\overline{\lambda}) \\ 0 & -F^H(\overline{\lambda}) & -\beta\Phi(\lambda) & \alpha\gamma\Phi(\Re(\lambda)) \\ \alpha\gamma\Psi & \beta\Psi & -F(\lambda) & 0 \\ \beta\Psi & \alpha/\gamma\Psi & 0 & -F(\overline{\lambda}) \end{bmatrix}\right) = 0,$$

where $\Phi(\lambda) = \sum_{i=1}^m \Phi_i e^{-2\tau_i\lambda}$. Now, since parameter γ and the sign change operated on the blocks associated with $\Phi(\Re(\lambda))$ do not affect the determinant, this is equivalent to

$$\det\left(\underbrace{\begin{bmatrix} -F^H(\lambda) & 0 & -\alpha\Phi(\Re(\lambda)) & -\beta\Phi(\overline{\lambda}) \\ 0 & F^H(\overline{\lambda}) & -\beta\Phi(\lambda) & -\alpha\Phi(\Re(\lambda)) \\ \alpha\Psi & \beta\Psi & F(\lambda) & 0 \\ \beta\Psi & \alpha\Psi & 0 & -F(\overline{\lambda}) \end{bmatrix}}_{=:H(\lambda,\gamma)}\right) = 0. \tag{5.13}$$

Finally, recalling that the singular value equation (5.9) is defined for $\lambda = \imath\omega$, $\omega \in \mathbb{R}^+$, we consider a purely complex root of equation (5.13), hence such that $\overline{\lambda} = -\lambda$; it is easy to observe that such λ is also a solution of (5.11). □

Hence, we demonstrated that, for a fixed γ and ξ, we can obtain the intersections between the graph of $g_\ell(\cdot,\gamma)$ and the level set ξ by simply solving DEP (5.11) containing both positive and negative delay values: this is a natural extension to delay systems of the result demonstrated in [114].

5.2.2 The criss-cross algorithm

We now explain our algorithm to compute $d_{\text{INS}} = \left(\sup_{\omega\geq 0} \mu_{\mathbb{R}}(G(\imath\omega))\right)^{-1}$, which is an extension of that in [13, 78] to the delay case. The main idea of [13] to compute the maximum of a function $\mu(G(\imath\omega))$ is by iteratively improving a horizontal level ξ that represents the maximum. Starting with an initial

level ξ, it constructs the superlevel sets of $\mu(G(\imath\omega))$ at ξ, that is it constructs the intervals $\{\omega \in \mathbb{R}\colon \mu(G(\imath\omega)) \geq \xi\}$. Then it updates ξ as the largest value of $\mu(G(\imath\omega))$ attained among the mid points of each of these intervals. This procedure is guaranteed to converge globally; see [13].

To apply these ideas to $\mu_{\mathbb{R}}(G(\imath\omega))$, we start with (5.7) to observe that

$$g_2(\imath\omega, \gamma) \geq \mu_{\mathbb{R}}(G(\imath\omega)), \qquad \forall\ \gamma \in (0, 1],\ \omega \in \mathbb{R}^+,$$

and the equality is attained when $\gamma = \gamma_{\min}(\omega)$ is a global minimizer of $g_2(\imath\omega, \gamma)$, see (5.8). This means that for a fixed γ, the function $g_2(\imath\omega, \gamma)$ is a super function (that is, an overestimator) of $\mu_{\mathbb{R}}(G(\imath\omega))$, with the equality attained only in one point.

The main idea of our criss-cross algorithm is now as follows: given an approximate maximizer $\widetilde{\omega} \in \mathbb{R}^+$ and a searching interval Ω containing it, we evaluate $\xi = \mu_{\mathbb{R}}(G(\imath\widetilde{\omega}))$ by applying golden section searching on γ to (5.7). This also gives us $\widetilde{\gamma} = \gamma_{\min}(\widetilde{\omega})$. We then compute all the intersections between the horizontal line at ξ and the super function $g_2(\imath\omega, \widetilde{\gamma})$. Theorem 5.1 shows that this can be achieved by simply computing the purely imaginary eigenvalues of the DEP (5.10) and choosing only those that correspond to the second singular value that defines $g_2(\imath\omega, \widetilde{\gamma})$. With these points we can define, after intersection with Ω, the K intervals $[\ell_j, u_j]$ such that

$$\bigcup_{j=1}^{K} [\ell_j, u_j] \ = \ \{\omega\colon g_2(\imath\omega, \widetilde{\gamma}) \geq \xi\} \cap \Omega.$$

Then, we compute the $\mu_{\mathbb{R}}$ function in the midpoints $c_j = (\ell_j + u_j)/2$, and update $\widetilde{\omega}$ as

$$\widetilde{\omega}_{\text{new}} = \text{argmax}_{\omega = c_1, \ldots, c_K}\ \mu_{\mathbb{R}}(G(\imath\omega)).$$

Usually $\mu_{\mathbb{R}}(G(\imath\widetilde{\omega}_{\text{new}})) \geq \xi$, which means we can update the searching level and the super function as follows:

$$\xi_{\text{new}} = \mu_{\mathbb{R}}(G(\imath\widetilde{\omega}_{\text{new}})), \quad \gamma_{\text{new}} = \gamma_{\min}(\widetilde{\omega}_{\text{new}}).$$

Otherwise, we define $\widetilde{\omega}_{\text{new}} = c_{\max}$ as the midpoint of the largest interval and update as follows:

$$\xi_{\text{new}} = \xi, \quad \gamma_{\text{new}} = \gamma_{\min}(c_{\max}).$$

This situation is called *break down*. In this case, we keep the old searching level ξ and choose the new super function that intersects the largest searching interval in its midpoint, thus ensuring that the largest interval is at least halved. This whole procedure is repeated with the updated values $\widetilde{\omega}_{\text{new}}, \xi_{\text{new}}$, and the searching intervals

$$\Omega_{\text{new}} = \bigcup_{j=1}^{K} \Big([\ell_j, c_j] \cup [c_j, u_j] \Big).$$

The resulting scheme is illustrated in Figure 5.1. In particular, panel (a) shows the usual behavior without breakdown where the algorithm finds a strictly higher searching level ξ at each iteration and eventually converges to the global maximum. The break down case is illustrated in panel (b), where the midpoint in the first (red) iteration does not not produce a higher searching level of the $\mu_{\mathbb{R}}$ function. In the figure, $g_2(\imath\omega, \gamma_{\text{new}})$ is indicated with the blue dashed line.

The algorithm is initialized with the level set $\xi = \mu_{\mathbb{R}}(0)$ as $\lambda = 0$ is, in case the uncertainty is not confined to a single parameter, the only point where the function $\mu_{\mathbb{R}}$ may exhibit a discontinuity (we refer the reader interested in a proof to [107]). Since function $g_2(0, \gamma)$ does not actually depend on γ, the value γ is randomly initialized in the set $(0, 1]$. Since $\mu_{\mathbb{R}}$ is discontinuous in 0, given γ_0 and $\xi_0 = \mu_{\mathbb{R}}(0)$, we might not find any intersection of $g_2(\cdot, \gamma_0)$ with the level set ξ_0 other than $\omega = 0$: in this case, we can already conclude that the function $\mu_{\mathbb{R}}$ has its maximum in 0.

The algorithm stops when the length of the largest interval in Ω is smaller than a user supplied tolerance. However this condition may not be trivially satisfied. For instance, let us assume that $\imath\widetilde{\omega}$ is a global maximizer for $\mu_{\mathbb{R}}$, with $\widetilde{\omega} \neq 0$, and that there exists an interval $[\ell, u] \not\ni \widetilde{\omega}$ such that $g_2(\imath\omega, \gamma) \geq \widetilde{\mu} := \mu_{\mathbb{R}}(\imath\widetilde{\omega})$ for all $\omega \in [\ell, u]$; then, the length of the interval $[\ell, u]$ will hardly be smaller than our tolerance and the algorithm cannot converge. For this reason, we also stop the algorithm when the difference between two consecutive level sets is positive but smaller than another user supplied tolerance (typically smaller than the other one). In Figure 5.1c we illustrate the typical case of a convergence with a non-connected Ω (a zoom on the maxima is provided in Figure 5.1d), i.e. when the $\mu_{\mathbb{R}}$ function has a local and a global maximum with very close values.

A pseudo-code of the criss-cross algorithm is given in Algorithm 2. The search strategy based on horizontally intersecting superfunctions is also used in [78]. Whereas we apply this to the $\mu_{\mathbb{R}}$ function of a delay system, in [78] it is used for structured perturbations of LTI delay-free systems. The convergence analysis in both cases remains however the same, provided the intersections are computed exactly. In particular, Theorems 1 and 2 in [78] stating global convergence of the level set value and of the maximizing frequency also apply here.

5.2.3 The rank one case

Let us now examine the case of $\operatorname{rank}(\Im(G(\imath\omega))) = 1$ for all $\omega \in \mathbb{R}^+$. From (5.5), we see that this holds, for example, when $p = 1$ since then D and thus G are vectors. From [107] and with $X = \Re(G(\imath\omega))$, we know that in this case

$$\mu_{\mathbb{R}}(G(\imath\omega)) = \lim_{\gamma \to 0} g_2(\imath\omega, \gamma) = \max\{\sigma_1(U_2^\top X), \sigma_1(X V_2^\top)\}, \tag{5.14}$$

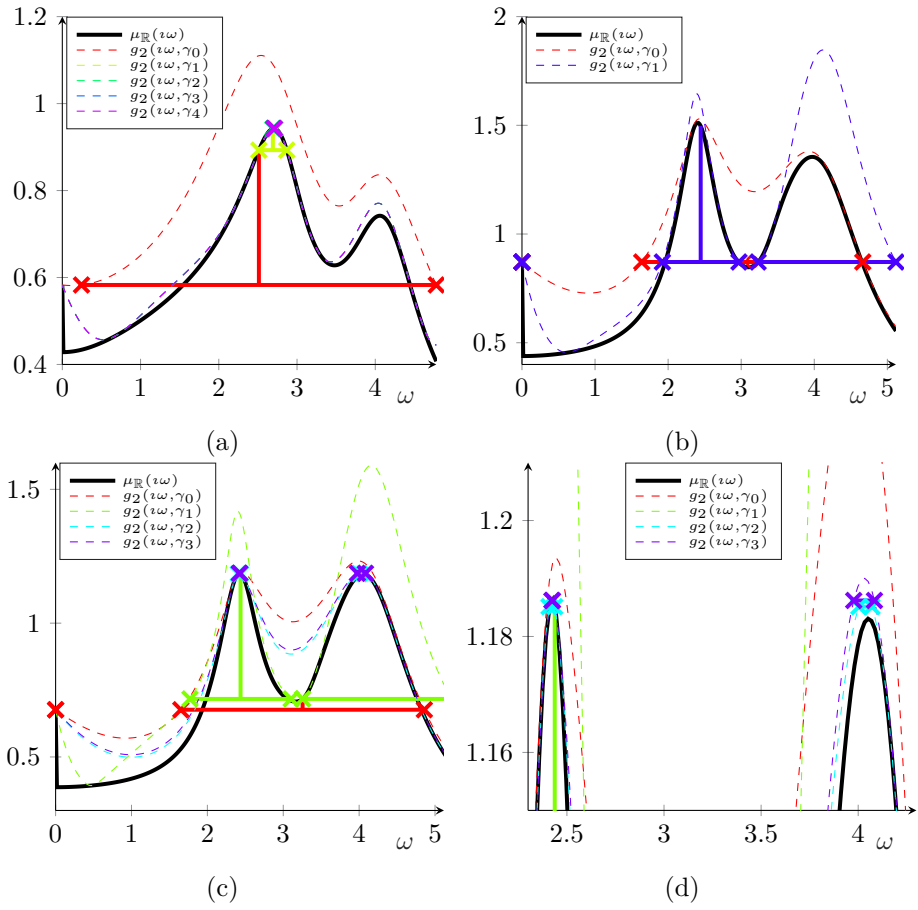

Figure 5.1: Different behaviors of Algorithm 2 applied to Example 1 in Section 5.4 are represented: the standard convergence in panel (a), the breakdown case in panel (b), and the convergence with two intervals in Ω in panel (c), whose zoom on the local maxima is shown in panel (d).

Algorithm 2 Criss-cross search by touching functions $g_2(\jmath\omega, \gamma)$ ($\operatorname{rank}(\Im G(\jmath\omega)) \geq 2$)

Input: System matrices $A_i \in \mathbb{R}^{n\times n}$, $B \in \mathbb{R}^{n\times p}$, $C_i \in \mathbb{R}^{q_i\times n}$, and delays $\tau_i \geq 0$, for $i = 1, \ldots, m$. Tolerances $\mathrm{tol}_1, \mathrm{tol}_2 > 0$, $\mathrm{tol}_1 > \mathrm{tol}_2$.

Output: Real distance to instability radius d_{INS}.

1: *Quick return:* if an eigenvalue of the DEP $F(s)$ has positive real part (i.e., delay system is unstable), return $d_{\mathrm{INS}} = 0$.
2: *Initialize*: $\omega_0 = 0$, random $\gamma_0 \in (0, 1]$, search level $\xi_0 = \mu_{\mathbb{R}}(G(\omega_0))$, search interval $\Omega_0 = [0, \infty]$.
3: **for** $i = 0, 1, \ldots$ until convergence **do**
4: Solve the DEP (5.10) with γ_i and ξ_i, and define the searching intervals $\{[\ell_j, u_j]\}_{j=1}^{K_i} = \{\omega \colon g_2(\jmath\omega, \gamma_i) \geq \xi_i\} \bigcap \Omega_i$.
5: **if** $\max_{j=1}^{K_i} |u_j - \ell_j| < \mathrm{tol}_1$, **then break**
6: **if** $0 < \xi_i - \xi_{i-1} < \mathrm{tol}_2$, **then break**
7: **for** $j = 1, \ldots, K_i$ **do**
8: Set midpoint $c_j = (\ell_j + u_j)/2$.
9: Evaluate $\mu'_j = \mu_{\mathbb{R}}(G(\jmath c_j))$ which also gives γ'_j.
10: **end for**
11: **if** $\mu_{\max} := \max_{j=1}^{K_i}\{\mu'_j\} > \xi_i$ **then**
12: Higher level found, set $\nu = \operatorname{argmax}_{j=1}^{K_i}\{\mu'_j\}$.
13: **else**
14: Breakdown detected, set $\nu = \arg\max_{j=1}^{K_i} |u_j - \ell_j|$.
15: **end if**
16: $\xi_{i+1} = \max\{\mu_{\max}, \xi_i\}$, $\gamma_{i+1} = \gamma'_\nu$, $\Omega_{i+1} = \cup_{j=1}^{K_i} \big([\ell_j, c_j] \cup [c_j, u_j] \big)$.
17: **end for**
18: Return $d_{\mathrm{INS}} = \xi_i^{-1}$.

where U_2, V_2 come from the singular value decomposition

$$\Im(G(\imath\omega)) = [U_1\ U_2] \begin{bmatrix} \sigma_1(\Im(G(\imath\omega))) & 0 \\ 0 & 0 \end{bmatrix} \begin{bmatrix} V_1 \\ V_2 \end{bmatrix}. \tag{5.15}$$

Due to this limit, Theorem 5.1 does not apply and therefore for each $\omega \in \mathbb{R}^+$ we cannot individuate

$$\gamma_{\min}(\omega) \quad \text{s.t. } \sigma_2(\imath\omega, \gamma_{\min}(\omega)) = \mu_{\mathbb{R}}(G(\imath\omega)).$$

We therefore set γ to some small value, say, $\gamma = 10^{-6}$, and consider function $g_2(\imath\omega, 10^{-6})$, which by continuity is close to $\mu_{\mathbb{R}}(G(\imath\omega))$ for each $\omega \in \mathbb{R}^+$. Since γ is now constant, we can directly apply the criss-cross algorithm to $g_2(\imath\omega, 10^{-6})$ (i.e., an adaptation of the Boyd-Balakrishnan method [13]) and accept the global maximum of $g_2(\imath\omega, 10^{-6})$ as an approximation of the global maximum of $\mu_{\mathbb{R}}(G(\imath\omega))$.

5.3 A new solver for DEPs with positive and negative delays

In this section, we provide the mathematical details of the DEP solver for (5.10) used in step 4 of Algorithm 2. A first observation is that the DEP (5.10) is Hamiltonian: this is easily seen thanks to the Hamiltonian structure of matrix H in (5.13)

$$\Big(J \cdot H(\gamma,\lambda)\Big)^H = J \cdot H(\gamma,\lambda) \qquad \text{with} \qquad J = \begin{bmatrix} 0 & I_{2n} \\ -I_{2n} & 0 \end{bmatrix}.$$

An immediate consequence is that for each λ solving (5.10), the values $-\lambda, \overline{\lambda}, -\overline{\lambda}$ are also eigenvalues of (5.10).

However, for the purpose of implementing Algorithm 2, it suffices to compute only the purely imaginary eigenvalues of the DEP (5.10). Taking $\lambda = \imath\omega$, we obtain immediately that these eigenvalues are bounded, more specifically

$$|\lambda| \le \|M_0\| + \sum_{i\neq 0,\, i=-m}^{m} \left(\|M_i\| + \|N_i\|\right). \tag{5.16}$$

Therefore, as isolated roots of an analytic function, there can be only finitely many imaginary eigenvalues of $\mathcal{D}_{\xi\gamma}(\lambda)$.

The overall solver has three components: an approximation of the DEP as a standard EP using a spectral discretization, an automated procedure to determine the resolution of this discretization, and a block-Newton correction to eliminate the approximation error.

Throughout this section we make the following assumption, which can always be achieved by solving for $\tilde{\lambda} = s\lambda$ in $\mathcal{D}_{\xi\gamma}(s^{-1}\tilde{\lambda})$ with a proper scaling s.

Assumption 5.2. *The maximum delay satisfies* $2\tau_m = 1$.

5.3.1 Spectral discretization of the eigenvalue problem

The DEP (5.10) can be formulated as a linear eigenvalue problem for a differential operator. Indeed, if (λ, y) is an eigenpair of (5.10), then $F(t) = e^{\lambda t}y$ is easily seen to be a solution of the ODE

$$\dot{F}(t) = \lambda F(t), \quad t \in [-1,\ 1], \tag{5.17}$$

with initial value $F(0)$ satisfying

$$(\lambda I + M_0)F(0) + \sum_{i\neq 0,\, i=-m}^{m} M_i F(-\tau_i) + N_i F(-2\tau_i) = 0. \tag{5.18}$$

Vice-versa, given λ, any solution of (5.17) is of the form $F(t) = e^{\lambda t}y$ for some $y \in \mathbb{C}^{4n}$. Substituting this expression into (5.18) yields (5.10) so that (λ, y) has to be an eigenpair.

To numerically solve (5.17)–(5.18), we can use spectral discretization [123, 15]. To this end, let $N \in \mathbb{N}$ and consider a grid on $[-1,\ 1]$ with grid points

$$\theta_{N,i} = -\cos\frac{\pi i}{2N+1},\ i = 1, \ldots, 2N. \tag{5.19}$$

We approximate $F(t)$ by a polynomial of degree $2N$,

$$f(t) = \sum_{i=0}^{2N} c_i T_i(t), \quad c_i \in \mathbb{C}^{4n},$$

where T_i is the Chebyshev polynomial of the first kind and order i. The coefficients c_i are determined by collocating (5.18) and (5.17) at the points $\theta_{N,i}$:

$$\begin{cases} \lambda f(0) = M_0 f(0) + \sum_{i\neq 0,\, i=-m}^{m} M_i f(-\tau_i) + N_i f(-2\tau_i), \\ \dot{f}(\theta_{N,i}) = \lambda f(\theta_{N,i}), \quad i = 1, \ldots, 2N. \end{cases} \tag{5.20}$$

Computations similar to Section 2.3 of [69] allow us to turn conditions (5.20) into a generalized eigenvalue problem of order $4n(2N+1)$,

$$(\Sigma_N - \lambda\Pi_N)\mathbf{c}_N = 0, \tag{5.21}$$

where $\mathbf{c}_N = [c_0^\top\ c_1^\top\ \cdots\ c_{2N}^\top]^\top$,

$$\Pi_N = \begin{bmatrix} T_0(1) & T_1(1) & T_2(1) & \cdots & & \cdots & T_{2N}(1) \\ 1 & 0 & -\frac{1}{2} & & & & \\ & \frac{1}{4} & 0 & -\frac{1}{4} & & & \\ & & \frac{1}{6} & 0 & -\frac{1}{6} & & \\ & & & \ddots & \ddots & \ddots & \\ & & & & \frac{1}{2(2N-1)} & 0 & -\frac{1}{2(2N-1)} \\ & & & & & \frac{1}{4N} & 0 \end{bmatrix} \otimes I_{4n} \tag{5.22}$$

and

$$\Sigma_N = \begin{bmatrix} R_0 & R_1 & \cdots & R_{2N} \\ & I_{4n} & & \\ & & \ddots & \\ & & & I_{4n} \end{bmatrix}, \tag{5.23}$$

with

$$R_k = M_0 T_k(1) + \sum_{i\neq 0, i=-m}^{m} \left(M_i T_k\left(-\tau_i\right) + N_i T_k\left(-2\tau_i\right)\right).$$

Given an eigenpair $(\lambda, \mathbf{c}_N)$ of (5.21), we have thus obtained $(\lambda, f(0))$ as an approximate eigenpair of the DEP.

5.3.2 Determining the number of discretization points

The choice of N involves a trade-off. The parameter should be chosen large enough to assure all eigenvalues on or close to the imaginary axis are sufficiently well approximated (in the sense that Newton iterations with the approximations as initial values converge to the actual eigenvalues, see the following subsection), but not too large for reasons of computational efficiency. We present a heuristic inspired by [132], which is amenable for automation and integrated in our implementation.

By Proposition 1 in [132], the eigenvalue λ of the discretized eigenvalue problem (5.21) is also an eigenvalue of

$$\mathcal{D}^N_{\xi\gamma}(\lambda) = \lambda I + M_0 + \sum_{i\neq 0,\, i=-m}^{m} \left(M_i p_N(-\tau_i;\lambda) + N_i p_N(-2\tau_i;\lambda)\right), \tag{5.24}$$

where $p_N(t;\lambda)$ is a polynomial of degree $2N$ in t that satisfies

$$\begin{cases} \dot{p}_N(\theta_{N,i};\ \lambda) = \lambda p_N(\theta_{N,i};\ \lambda), \quad i = 1,\dots,2N, \\ p_N(0;\ \lambda) = 1. \end{cases} \tag{5.25}$$

Observe that (5.24) is obtained by replacing $e^{\lambda t}$ in the original eigenvalue problem (5.10) by $p_N(t;\lambda)$. Hence, $\mathcal{D}^N_{\xi\gamma}$ can be seen as the following perturbation of (5.10):

$$\mathcal{D}^N_{\xi\gamma}(\lambda) = \mathcal{D}_{\xi\gamma}(\lambda) + \mathcal{E}^N(\lambda)$$

with $e_N(t;\lambda) = p_N(t;\lambda) - e^{\lambda t}$ and

$$\mathcal{E}^N(\lambda) = \sum_{i\neq 0,\, i=-m}^{m} \left(M_i e_N(-\tau_i;\lambda) + N_i e_N(-2\tau_i;\lambda)\right).$$

Since $\det \mathcal{D}^N_{\xi\gamma}(\lambda) = \det \mathcal{D}_{\xi\gamma}(\lambda) + O(\|\mathcal{E}^N(\lambda)\|)$, the computed eigenvalue λ of (5.21) (as root of an analytic function) will be a good approximation to an eigenvalue of the DEP (5.10) if $|e_N(t;\lambda)|$ is small for $t \in [-1,1]$.

Given an accuracy $\varepsilon > 0$, we can therefore choose N as follows. Since we are interested only in the purely complex eigenvalues of the DEP, we define

$$N(\omega) = \min\left\{ n \in \mathbb{N} \colon |e_n(t;\imath\mu)| < \varepsilon,\ \forall \mu \in [0,\omega], t \in [-1,1] \right\}.$$

This number $N(\omega)$ is the smallest degree needed to accurately approximate any purely imaginary eigenvalue $\lambda \in [0,\imath\omega]$ since $\mathcal{E}^{N(\omega)}(\lambda) = O(\varepsilon)$.

As $N(\omega)$ is problem independent, we can compute it beforehand, for instance, by evaluating $e_n(t;\imath\mu) = p_n(t;\imath\mu) - e^{\imath\mu t}$ for $n = 0, 1, \dots$ on a sufficiently fine grid for $t \in [-1,1]$ and $\mu \in [0,\omega]$. In turn, for given μ, the polynomial $p_n(t;\imath\mu)$ can be computed in a Chebyshev expansion, as outlined in the proof of Proposition A.1

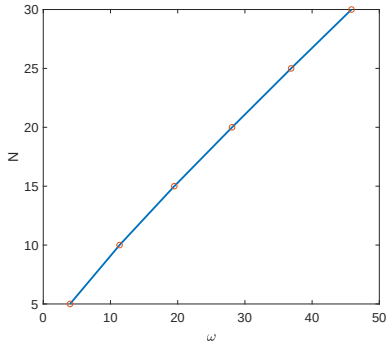

Figure 5.2: The function $N(\omega)$ for accuracy $\varepsilon = 10^{-4}$.

of [53]. An example for $\varepsilon = 10^{-4}$ is visible in Figure 5.2, which shows that $N(\omega)$ is approximately linear in ω.

It remains to determine an interval $[0, \imath\omega_c]$ that contains all the imaginary eigenvalues. A conservative choice is to estimate ω_c based on (5.16). However, it usually leads to unnecessarily large values of ω_c, and thus of N. Instead, we have adapted the approach from [132] that originally computes all the eigenvalues in right half plane of a DEP.

Let λ be an eigenvalue of the DEP (5.10), then from (5.11), we see that $-\lambda$ is also an eigenvalue of the matrix

$$M_0 + \sum_{i\neq 0, i=-m}^{m} \left(M_i e^{-\tau_i \lambda} + N_i e^{-2\tau_i \lambda}.\right)$$

For purely imaginary eigenvalue $\lambda = \imath\omega$, this matrix therefore belongs to the set

$$\mathcal{M} = \bigcup_{\theta\in[0,2\pi]^m} \left(M_0 + \sum_{i\neq 0, i=-m}^{m} M_i e^{-\imath\theta_i} + N_i e^{-\imath 2\theta_i} \right),$$

where $\theta_{-i} = -\theta_i$ for $i = 1, \ldots, m$. Hence, the original eigenvalue $-\lambda$ is also an eigenvalue of some matrix in $\mathcal{M}$. A bound for ω_c can then be determined by sampling the matrices in $\mathcal{M}$ on a grid for the parameters $\theta_i \in [0, 2\pi]$. We refer to [132] for the details on how to exploit commensurate delays.

In Algorithm 2 we can start with γ_0 and ξ_0 to obtain the initial estimate for ω_c. Since the searching intervals will be monotonically reducing (including also the corresponding eigenvalues), this ω_c can be reused for the following iterations as well. This is especially important in the rank one case. In particular, the strategy described above with $\gamma = 10^{-6}$ (see Section 5.2.3) would otherwise

lead to unnecessarily large values of ω_c since $M_0 = O(1/\gamma)$. We therefore use $\gamma_0 = 1$ in this case.

5.3.3 Correcting the eigenvalues with block-Newton method

In the previous subsections we described a method to find good approximations of the purely imaginary eigenvalues of the DEP (5.10); here we would like to improve this approximation by means of a Newton correction. It is easy to see that the maximum of $\mu_{\mathbb{R}}(G(\imath\omega))$ to which we converge in Algorithm 2 is always characterized by (at least) a double eigenvalue $\lambda = j\omega$. In cases like this, applying the single Newton correction is not safe; for this reason, we apply the block-Newton method for nonlinear eigenvalue problems as proposed in [74], which allows the *simultaneous correction* of a prescribed number of eigenvalues.

This method applies the standard Newton iteration to find a pair $(Y, S) \in \mathbb{C}^{n\times k} \times \mathbb{C}^{k\times k}$ that satisfies

$$YS + M_0 YS + \sum_{i\neq 0, i=-m}^{m} \left(M_i Y e^{-\tau_i S} + N_i Y e^{-2\tau_i S}\right) = 0 \tag{5.26}$$

and the normalization condition

$$\left[Y^\top \ (YS)^\top \ \dots \ (YS^{l-1})^\top\right] W - I_k = 0, \tag{5.27}$$

for some fixed integer l and matrix $W \in \mathbb{C}^{ln\times k}$ (we refer the reader interested in the implementation details to [74]).

A pair satisfying equations (5.26)–(5.27) is called a minimal invariant pair of the DEP (5.10): for such a pair it can be proven that the eigenvalues of S are also eigenvalues of the DEP (5.10). A common example for a minimal invariant pair is

$$(Y, S) = \left(\begin{bmatrix} y_1 & y_2 \end{bmatrix}, \begin{bmatrix} \lambda_1 & 0 \\ 0 & \lambda_2 \end{bmatrix} \right) \tag{5.28}$$

where $(\lambda_1, y_1), (\lambda_2, y_2)$ are two different eigenpairs of (5.10) such that $\lambda_1 \neq \lambda_2$. On the other hand, for a multiple eigenvalue $\lambda_1 = \lambda_2$ with geometric multiplicity one,

$$(Y, S) = \left(\begin{bmatrix} y & v \end{bmatrix}, \begin{bmatrix} \lambda_1 & 1 \\ 0 & \lambda_1 \end{bmatrix} \right) \tag{5.29}$$

is easily seen to be a minimal invariant pair. Here, y is the eigenvector and v is the first generalized eigenvector of problem (5.10), satisfying the Jordan chain condition

$$\mathcal{D}_{\xi,\gamma}(\lambda) \cdot v + \frac{\partial \mathcal{D}_{\xi,\gamma}(\lambda)}{\partial \lambda} \cdot y = 0. \tag{5.30}$$

The approximate eigenpairs computed by spectral discretization give approximate minimal invariant pairs that can be used as initial values for

the block-Newton method. Let $(\widehat{\lambda}_1, \widehat{y}_1)$ and $(\widehat{\lambda}_2, \widehat{y}_2)$ be two such pairs that correspond to an intersecting interval, then the values $\widehat{\lambda}_1$, $\widehat{\lambda}_2$ are sufficiently distant. Hence, we can use as initial guess

$$(Y_0, S_0) = \left(\begin{bmatrix} \widehat{y}_1 & \widehat{y}_2 \end{bmatrix}, \begin{bmatrix} \widehat{\lambda}_1 & 0 \\ 0 & \widehat{\lambda}_2 \end{bmatrix} \right).$$

However, as the horizontal level approaches its maximal value, the two intersections will converge, leading to multiple purely imaginary eigenvalue. As similarly observed in [53, Fig. 1], due to the Hamiltonian structure, the eigenvalue typically has geometric multiplicity one. In this case, the initial guess becomes

$$(Y_0, S_0) = \left(\begin{bmatrix} \widehat{y} & \widehat{v} \end{bmatrix}, \begin{bmatrix} \widehat{\lambda}_1 & 1 \\ 0 & \widehat{\lambda}_1 \end{bmatrix} \right),$$

with $\widehat{y}$ the approximate eigenvector of $\widehat{\lambda}_1 \approx \widehat{\lambda}_2$, and $\widehat{v}$ is defined analogously to (5.30) by solving the near-singular system

$$\mathcal{D}_{\xi,\gamma}(\widehat{\lambda}) \cdot \widehat{v} = -\frac{\partial}{\partial \lambda} \mathcal{D}_{\xi,\gamma}(\widehat{\lambda}) \cdot \widehat{y}. \tag{5.31}$$

Before we conclude, we here describe the details of the computation of an approximation of v if the eigenvalue $\widehat{\lambda}$ is (a perturbation of) a double eigenvalue with geometric multiplicity equal to one. While computing the approximate eigenvector $\widehat{y}$ is straightforward, obtaining the approximate generalized eigenvector $\widehat{v}$ is a bit more challenging. We want to retrieve $\widehat{v}$ from equation (5.31), thus we consider for the given value of $\widehat{\lambda}$ a QR decomposition of matrix $\mathcal{D}_{\xi,\gamma}(\widehat{\lambda})$ such that $QR = \mathcal{D}_{\xi,\gamma}(\widehat{\lambda})P$ where Q is orthogonal, R is upper-triangular and P is an orthogonal permutation matrix such that the diagonal elements of R are non-increasing. We then want to solve the system

$$RP^\top \widehat{v} = \underbrace{-Q^\top \frac{\partial \mathcal{D}_{\xi,\gamma}(\widehat{\lambda})}{\partial \lambda} \widehat{y}}_{=:x}, \tag{5.32}$$

where x is known. Since $\widehat{\lambda}$ is an eigenvalue, $\mathcal{D}_{\xi,\gamma}(\widehat{\lambda})$ is almost singular and the bottom-right element of R is approximately zero. Moreover, since $\widehat{\lambda}$ is close to a double eigenvalue, the last element of x must be almost zero. Therefore, we eliminate the last equation in (5.32). Denoting with $\widetilde{R}$ the matrix obtained by eliminating the last row and column of R and by $\widetilde{x}$ the vector obtained by eliminating the last element of x, one solution is given by

$$\widehat{v} = P \begin{bmatrix} \widetilde{R}^{-1}\widetilde{x} \\ 0 \end{bmatrix}.$$

5.4 Numerical experiments

The first example gives rise to the illustrations in Figure 5.1a which we used to graphically describe the scheme of Algorithm 2. Moreover, we observe that this algorithm exhibits a *quadratic* convergence. In the second example, we compute the distance to instability when matrix Δ of uncertainties has rank one.

Example 5.3. *We consider the following system*

$$\dot{x}(t) = \sum_{i=1}^{3} \left(A_i + D\delta A_i E_i\right) x(t - \tau_i), \tag{5.33}$$

where $(\tau_1,\ \tau_2,\ \tau_3) = (0,\ 0.1702,\ 0.5681)$, $D = I_3$

$$A_1 = \begin{bmatrix} -0.090 & -0.816 & -0.228 \\ 0.769 & -1.325 & -1.380 \\ 0.412 & 1.523 & -0.760 \end{bmatrix},\ A_2 = \begin{bmatrix} -0.869 & 0.136 & -1.077 \\ -0.149 & -0.939 & 0.445 \\ 0.476 & 1.862 & -0.191 \end{bmatrix},$$

$$A_3 = \begin{bmatrix} -0.462 & 0.389 & -0.752 \\ 0.517 & -0.042 & 1.058 \\ -0.270 & -1.106 & -2.480 \end{bmatrix},$$

and

$$E_1 = \begin{bmatrix} 0.057 \\ 0.204 \\ -0.063 \end{bmatrix}^\top,\quad E_2 = \begin{bmatrix} 0.157 \\ -0.921 \\ 0.221 \end{bmatrix}^\top,\quad E_3 = \begin{bmatrix} 0.816 \\ -0.639 \\ -0.418 \end{bmatrix}^\top.$$

In Figure 5.1a, we observe the convergence of Algorithm 2 to the global maximum of $\mu_{\mathbb{R}}$*, with the initialization* $\gamma_0 = 0.95$*. In Table 5.1, we report the iterations of the algorithm to illustrate its convergence. In the first column we show the iteration number* i*, in the second the level set* ξ_i*, in the third the distance between two consecutive level sets, in the forth the corresponding frequency* ω_i *and in the last the width of the interval* Ω_i*. From these results, the algorithm seems quadratically convergent.*

In Figure 5.1b the breakdown scheme is triggered with the initialization $\gamma_0 = 0.7$ *and by changing* E_3 *and* D *with* $\widetilde{E}_3 = 1.41E_3$ *and* $\widetilde{D}$*, with* $\widetilde{D}$ *given by*

$$\widetilde{D} = \begin{bmatrix} 0.932 & 0.104 & -0.780 \\ 0.635 & -1.077 & 0.057 \\ 0.170 & 0.433 & -1.725 \end{bmatrix}.$$

Finally, Figures 5.1c and 5.1d are obtained by adopting $\widetilde{D}$ *and* E_3*.*

Table 5.1: Results for the convergence of Algorithm 2.

k	ξ_i	$\lvert\xi_i - \xi_{i-1}\rvert$	ω_i	$\lvert\Omega_i\rvert$
1	0.5828159		2.490258410	4.6031×10^{0}
2	0.8832408	3.004×10^{-1}	2.688229335	3.960×10^{-1}
3	0.9420780	5.883×10^{-2}	2.704386454	3.232×10^{-2}
4	0.9425446	4.665×10^{-4}	2.704501012	2.292×10^{-4}
5	0.9425446	2.348×10^{-8}	2.704501012	3.836×10^{-8}

Example 5.4. *Let us consider the uncertain system*

$$\dot{x}(t) = (A_1 + D\delta A_1 E_1)x(t) + (A_2 + D\delta A_2 E_2)x(t-\tau),$$

where $D = [0 \;\; 1]^\top$, $E_1 = E_2 = [1 \;\; 1]$,

$$A_1 = \begin{bmatrix} 0 & 1 \\ -1 & -1 \end{bmatrix}, \quad A_2 = \begin{bmatrix} 0 & 0 \\ 0 & -1 \end{bmatrix}.$$

Observe that δA_0 *and* δA_1 *are both scalars; as a consequence its concatenation* Δ *and matrix* $G(\imath\omega)$ *as defined in (5.5) have rank one independently of* ω*. The nominal system is unstable for all the delay values* $\tau \geq \pi$ *(see [20] for a proof). In Figure 5.3a, we plot the distance to instability* d_{INS} *against the delay parameter* τ *varying in* $(0, \pi)$*. Note that* d_{INS} *is constant for delay values smaller than* $\tau^* \approx 1$*; the reason is that for* $\tau < \tau^*$ *the smallest perturbation generating instability shifts an eigenvalue to the origin. This eigenvalue is then solution of the characteristic equation* independently *of the delay value* τ*. In Figure 5.3b, we show the convergence of Boyd-Balakrishnan method [13] applied to* $g_2(\imath\omega, 10^{-6})$ *for* $\tau = 1$*; obviously dashed lines corresponding to different iterations are perfectly overlapping. From this figure, we also observe that* $g_2(\imath\omega, 10^{-6})$ *is a very good approximation of* $\mu_{\mathbb{R}}$*.*

Finally, in Table 5.2 we report the computation of the distance to instability for the benchmark problems[2] that were also used in [53] on computing the complex pseudospectral abscissa. In these problems, we consider *unstructured* matrix perturbations, so we set $B = C_i = I_n$ for each $i = 1, \ldots, m$. In the first column we show the plant number in the benchmark, the second the size n and the number of delays m, in the third the computed distance to instability, in the forth the frequency maximizing $\mu_{\mathbb{R}}$, and in the last one the computational time in seconds on a PC with an Intel Core i5 2.50 GHz processor with 8 GB RAM. We set the tolerance for the interval length equal to 10^{-5}. Note that plants 4 and 5 are not included as they define unstable problems.

[2] http://twr.cs.kuleuven.be/research/software/delay-control/psa/

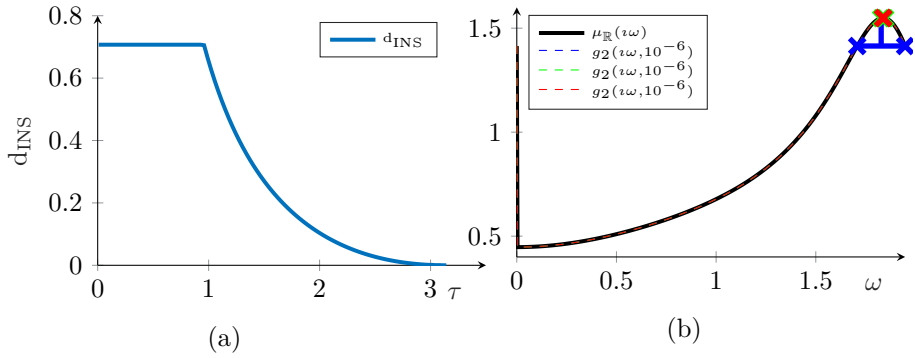

Figure 5.3: Left pane shows the distance to instability d_{INS} w.r.t. the delay τ; right pane shows the convergence of the algorithm for a fixed $\tau = 1$.

Table 5.2: Performance of Algorithm 2 on various delay systems.

Plants	(n, m)	d_{INS}	ω	time
1	$(3, 2)$	9.1595e-03	0	0.062
2	$(1, 2)$	1.0607e-00	0	0.100
3	$(3, 4)$	1.9917e-01	3.2287	0.910
6	$(10, 8)$	3.1091e-01	1.5447	6.670
7	$(20, 10)$	2.6094e-01	0	1.643
8	$(40, 3)$	8.4134e-02	0.1717	19.887
9	$(5, 2)$	3.2642e-01	1.2259	0.488
10	$(4, 4)$	7.1411e-01	0	0.082

5.5 Conclusions

We have presented a novel criss-cross type algorithm for computing the distance to instability for LTI delay systems of retarded type affected by real valued perturbations on the coefficient matrices. The method grounds on the well-known formula introduced in [107], which exploits the characterization of the distance to instability as the reciprocal of the global maximum of the structured singular value $\mu_{\mathbb{R}}$. The methodology proposed here is guaranteed to globally converge to the global maximum. From a convergence point of view, the method proposed in this chapter is thus preferable to the one proposed in Chapter 3 based on the computation of the pseudospectral abscissa. On the other hand, the algorithm proposed here is applicable for a smaller class of perturbations defined on the system, e.g. it cannot cope with uncertainties affecting the delay values. A solver for the computation of the purely imaginary roots of an Hamiltonian DEP with positive and negative delays is also introduced. This solver consists of

three main components: a spectral discretization approximating the DEP with a linear EP, an automated procedure to determine the number of discretization points, and a block-Newton correction method to improve the accuracy of the approximate eigenvalues obtained from the linear EP.

Chapter 6

Robustness measures for linear periodic systems of DDEs

For the realization of more accurate mathematical descriptions, many engineering applications are modeled by differential equations involving delays and periodic terms. Examples of applications modeled by time-periodic systems with delays can be found in different fields such as machine tools vibrations [63, 121], robotic systems [62], neural networks [55] and optimal control [24]. In this chapter, we consider systems of linear time-periodic delay differential equations (TPDDEs) of the form

$$\dot{x}(t) = \sum_{i=0}^{m} A_i(t)x(t-\tau_i), \qquad t \geq 0, \tag{6.1}$$

where $x(t) \in \mathbb{C}^n$ for each t, the delay values are such that $0 = \tau_0 < \tau_1 < \cdots < \tau_m$, and $A_i \in \mathcal{R}(T)^{n\times n}$, where $\mathcal{R}(T)$ is the set of smooth real-valued periodic functions with main period equal to $T > 0$ and formally defined by

$$\mathcal{R}(T) = \{f : \mathbb{R} \mapsto \mathbb{R} | f(t) = f(t+T) \ \forall \ t \in \mathbb{R} \ , f \text{ is smooth}\}.$$

As seen before, for LTI delay systems the asymptotic stability of the null solution can be assessed by checking the real part of the roots of the associated characteristic equation. In a different manner, asymptotic stability of null solutions of delay-free time-periodic systems [34], respectively TPDDEs [26, 57], is determined by the modulus of the eigenvalues of a linear operator with finite dimension, respectively infinite dimension, specifically the so-called *monodromy operator*.

In the following, we briefly summarize the basic notions of the Floquet theory for TPDDEs; for the more detailed introduction, we refer the reader to a monograph [16]. Let $X = \mathcal{C}([-\tau_m, 0],\ \mathbb{C}^n)$ be the space of smooth functions from interval $I = [-\tau_m, 0]$ to $\mathbb{C}^n$. We now introduce the Cauchy problem associated with equation (6.1), that is

$$\begin{cases} \dot{x}(t) = \sum_{i=0}^{m} A_i(t)x(t-\tau_i), & t \geq t_0, \\ x(t_0+t) = \varphi(t), & t \in [-\tau_m, 0], \end{cases} \tag{6.2}$$

with $\varphi \in X$. Under the above assumptions, the problem admits a unique solution in the interval $[t_0 - \tau_m, +\infty)$. In the following, we will indicate this solution as $x(t; t_0, \varphi)$ for $t \geq t_0$. The corresponding *state* at time t is denoted by $x_t(t_0, \varphi) \in X$, formally defined by

$$x_t := x(t+\theta), \qquad \theta \in [-\tau_m, 0]. \tag{6.3}$$

Given the well-posedness of the Cauchy problem, we can introduce the notion of *evolution operator*.

Definition 6.1. *The evolution operator is the operator $\mathcal{T}(t, t_0) : X \mapsto X$ associating the initial function $\varphi \in X$ with the state x_t at time $t \geq t_0$, i.e.*

$$\mathcal{T}(t, t_0)\varphi = x_t(t_0, \varphi).$$

This definition is suitable for any system of non-autonomous differential equations, thus the periodicity is not required. When we consider time-periodic systems, then we rather use the *monodromy operator* $U := \mathcal{T}(T, 0)$, where T is the main period of our system of interest. It can be proved that the spectrum $\Lambda(U)$ of the monodromy operator U is an at most countable compact set of $\mathbb{C}$ with the only possible accumulation point being zero. Moreover, it can be proved that if $\mu \in \Lambda(U)$, then μ belongs to the spectrum of the evolution operator $\mathcal{T}(t_0 + T, t_0)$ for all $t_0 \in \mathbb{R}$. Therefore, the spectrum of the evolution operator $\mathcal{T}(t_0 + T, t_0)$ is independent of the choice of t_0.

Definition 6.2. *Any element $\mu \in \Lambda(U) \setminus \{0\}$ is called a Floquet multiplier.*

Since all nonzero elements of the spectum of U correspond to eigenvalues, a Floquet multiplier can alternatively be defined as $\mu \in \mathbb{C},\ \mu \neq 0$, such that $\ker(\mu I - U) \neq \{0\}$. A graphical interpretation of the action of monodromy operator U is provided in Figure 6.1. The following two propositions characterize the importance of Floquet multipliers in the stability investigation of TPDDEs.

Proposition 6.3. *An element $\mu \in \mathbb{C},\ \mu \neq 0$, is a Floquet multiplier if and only if there exists an eigenfunction $\varphi \in X,\ \varphi \neq 0$ such that $\mathcal{T}(t+T, 0)\varphi = \mu\mathcal{T}(t, 0)\varphi$ for all $t \geq 0$.*

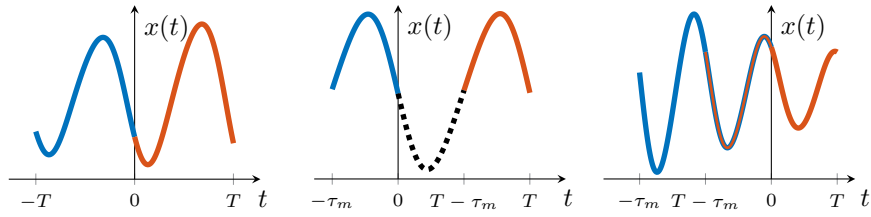

(a) $T = \tau_m$ (b) $T > \tau_m$ (c) $T < \tau_m$

Figure 6.1: The plots show the action of the monodromy operator U relating state x_0 in blue with state x_T in red for three different cases: in 6.1a $T = \tau_m$, in 6.1b $T > \tau_m$ and finally in 6.1c $T < \tau_m$ (notice that in this latter case the two states overlap). In particular, we here observe the effect of U on eigenstate x_0 such that $x_T = Ux_0 = \mu x_0$, with Floquet multiplier μ such that $|\mu| > 1$ (6.1a), $|\mu| = 1$ (6.1b) and $|\mu| < 1$ (6.1c).

Proposition 6.4. *The zero solution of (6.1) is uniformly asymptotically stable if and only if all the Floquet multipliers of the associated monodromy operator have modulus smaller than* 1.

In the literature, many different methods have been proposed for the computation of the Floquet multipliers of TPDDEs such as the semidiscretization method [68, 65], the spectral element method [72, 79], the pseudospectral method [15] or the truncation of the monodromy operator expanded in Chebyshev series [18]. However, when considering engineering applications, the stability condition on the modulus of the Floquet multipliers may not correspond to the system stability in practice. As a matter of fact, also for periodic systems the presence of uncertainties necessarily alters the spectrum of the monodromy operator and potentially generates instability. In this chapter, we address the robust stability problem by investigating the worst-case setting for a given class of uncertainties perturbing the nominal matrices. Analogous to the practice for LTI delay systems, we first introduce the class of perturbations and the maximal allowable perturbation, then we look for the largest Floquet multiplier that can be generated by any perturbation in the class under consideration. To the best of our knowledge, this is the first eigenvalue-based approach to the robust stability of TPDDEs with uncertainties in the coefficient matrices; intuitively, also the method proposed here grounds on a necessary and sufficient condition for the stability robustness. A Lyapunov-Krasovskii approach to the problem was previously proposed [80]. Similar problems to the one addressed here were considered in the literature, mainly in the context of discrete-time problems: for example, stability criterion [21] independent of the time-delay length were proposed for discrete TPDDEs, and a robust stabilization technique for such

problems was also suggested [22].

In this chapter, we examine the effect of real-valued time-periodic uncertainties affecting the nominal matrices $A_i \in \mathcal{R}(T)^{n\times n}$ on the Floquet multipliers: this is made possible by the introduction of a novel solver for the computation of Floquet multipliers. The solver is characterized by an approximation of the solution x of problem (6.1) with a truncated series of Chebyshev polynomials. The approach is a variant of the spectral discretization of the solution operator, which is accomplished with a collocation approach (different than the well-known spectral element method [72, 79], where Galerkin conditions are imposed and Lagrange base polynomials are used instead of Chebyshev base polynomials). The proposed solver results in the solution of a generalized eigenvalue problem (GEP) whose dimensions depend on the degree of the truncated series. The main benefit of the new solver is that it preserves linearity w.r.t. entries of nominal matrices A_i. As a consequence, *linear real-valued structured* perturbations on matrices A_i result in *linear real-valued structured* perturbations of the formulated GEP, where with the term *structured* we still mean that any specific structure can be considered for the uncertainty (thus a block or a single coefficient of the nominal matrix can be perturbed). Therefore, the largest Floquet multiplier is computed as the largest eigenvalue that the GEP can attain within a class of real-valued structured uncertainties. The algorithm used to find the largest Floquet multiplier is basically a projected gradient method: as we will see many of the favourable properties observed for the optimal perturbations in Chapters 2 and 3 do not hold here. Other main differences with the methods introduced in Chapters 2 and 3 are the objective function (in this chapter, we maximize the modulus of an eigenvalue, while for the spectral abscissa the real part of an eigenvalue is maximized), and the eigenvalue problem (GEP instead of DEPs).

The present chapter is structured as follows: in Section 6.1, we provide the details of the new Floquet multiplier solver; in Section 6.2, we formally introduce the uncertainties affecting the system and we illustrate the algorithm implemented to assess the robust stability; in Section 6.3, we provide an explicit construction of the GEP and its perturbations for the special case $T > \tau_m$; in Section 6.4, we extend the method to periodic systems with periodic delays: an analysis of the robust stability of a turning operation with spindle speed variation is presented; finally, in Section 6.5, we extend our algorithm also to TPDDEs with piecewise smooth periodic functions, and we provide numerical simulations for the robust stability of linear systems with act-and-wait controllers (used for instance in applications such as the inverted pendulum for balancing problems [116, 100]); Section 6.6 is dedicated to the robust stability of milling operations, for which our simulations are tested against experimental results.

6.1 Chebyshev-polynomial based solver for Floquet multipliers

In this section we propose a novel technique to compute the Floquet multipliers for linear systems of TPDDEs (6.1) as a generalization of previous approaches [16, 112]. First of all, we will illustrate the adopted discretization of the domain $[-\tau_m, T]$, which will be subdivided into a set of subintervals with length at the most equal to the period T: on each of these intervals, we will then define a mesh of Chebyshev-distributed points. Then, the solution x of (6.1) is approximated by a piecewise polynomial p; on each subinterval, the piecewise polynomial p is defined as a truncated series of Chebyshev polynomials. The conditions defining such an approximation give rise to a GEP whose nonzero eigenvalues approximate the Floquet multipliers of the monodromy operator U associated with (6.1). At the end of this section, we prove that solving the resulting GEP is equivalent to computing the eigenvalues of a matrix approximation of the monodromy operator.

In Figure 6.2, we illustrate the discretization of the domain of interest $[-\tau_m, T]$ in a collection of subintervals Ω_j whose length is at most T. On each Ω_j, we approximate the solution x by means of a polynomial $p_j(t)$ of degree M, therefore an overall approximation of x can be formally defined as

$$x(t) \approx p(t) = \sum_{j=1}^{N+2} p_j(t)\chi_{\Omega_j}(t), \quad \text{for } t \in [-\tau_m, T] \tag{6.4}$$

where $\chi_{\Omega_j}(t)$ is the indicator function of the subinterval Ω_j such that

$$\chi_{\Omega_j}(t) = \begin{cases} 1, & \text{if } t \in \Omega_j, \\ 0, & \text{elsewhere.} \end{cases}$$

In general, there always exists an integer $N \in \mathbb{N}$ such that $NT \leq \tau_m < (N+1)T$; as a consequence of the relation $NT \leq \tau_m$ and of the value of N, domain $[-\tau_m, T]$ can be discretized in different ways. In the following, we consider any possible ratio T/τ_m, and we describe the three discretizations that may occur.

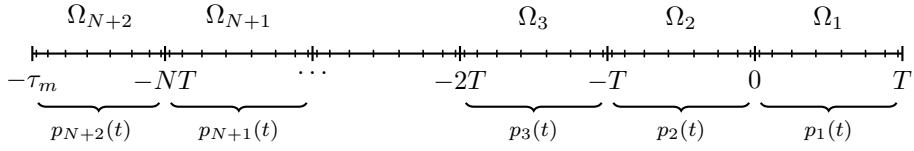

Figure 6.2: Discretization of the domain $[-\tau_m, T]$ when $T < \tau_m$.

- There exists $N \in \mathbb{N}$ such that $NT < \tau_m < (N+1)T$ (case in Figure 6.2): in this case we have $N+2$ subintervals defined as

$$\begin{array}{lcl} \Omega_1 & = & [0, T], \\ \Omega_j & = & [-(j-1)T, -(j-2)T], \text{ for } j = 2, \ldots, N+1, \\ \Omega_{N+2} & = & [-\tau_m, -NT]. \end{array}$$

- There exists $N \in \mathbb{N}, N \geq 1$, such that $\tau_m = NT$: in this case we have $N+1$ subintervals defined as

$$\begin{array}{lcl} \Omega_1 & = & [0, T], \\ \Omega_j & = & [-(j-1)T, -(j-2)T], \text{ for } j = 2, \ldots, N+1. \end{array}$$

- $\tau_m < T$: in this case we have 2 subintervals defined as

$$\begin{array}{lcl} \Omega_1 & = & [0, T], \\ \Omega_2 & = & [-\tau_m, 0]. \end{array}$$

In what follows, we consider the case represented in Figure 6.2 where $NT < \tau_m < (N+1)T$, and thus domain $(-\tau_m, +T)$ is subdivided into $N+2$ intervals; the developments for the other two cases are analogous.

We define a mesh of Chebyshev-distributed points on each subinterval Ω_j. Specifically, let us consider a general mesh of Chebyshev-distributed points $\{\alpha_\ell\}_{\ell=1,\ldots,M+1}$ defined on the interval $[-1, 1]$, where

$$\alpha_\ell = -\cos\left(\frac{\pi \ell}{M+1}\right), \quad \text{for } \ell = 1, \ldots, M+1. \tag{6.5}$$

Observe that this mesh includes only the right boundary point of the interval. If we write each interval $\Omega_j = [a_j, b_j]$ for $j = 1, \ldots, N+2$, then we can easily define a mesh of Chebyshev-distributed points on each Ω_j by applying the following transformation on mesh points α_ℓ

$$\theta_\ell^{(j)} = f_j(\alpha_\ell) := \frac{1}{2}(a_j + b_j) + \frac{\alpha_\ell}{2}(b_j - a_j), \quad \text{for } \ell = 1, \ldots, M+1, \tag{6.6}$$

and whose inverse transformation is given by

$$\alpha_\ell = g_j(\theta_\ell^{(j)}) = \left(\theta_\ell^{(j)} - \frac{1}{2}(a_j + b_j)\right)\frac{2}{b_j - a_j}, \quad \text{for } \theta_\ell^{(j)} \in \Omega_j,\ j = 1, \ldots, N+2. \tag{6.7}$$

Now, we describe at high level how the solution x of (6.1), corresponding to an eigenfunction, is approximated by the piecewise polynomial p, which coincides with polynomial p_j on each interval Ω_j. We define each p_j as a sum

of functions T_s, namely the Chebyshev polynomial of the first kind with degree s; in particular, we have

$$p_j(t) = \sum_{s=0}^{M} c_s^{(j)} T_s(g_j(t)), \text{ for } j = 1, \ldots, N+2, \tag{6.8}$$

where $c_s^{(j)} \in \mathbb{C}^n$ are coefficients to be determined.

From Proposition 6.3, we know that $\mu \neq 0$ is a Floquet multiplier if and only if there exists an eigenfunction φ such that

$$\mathcal{T}(t+T,0)\varphi = \mu \mathcal{T}(t,0)\varphi, \text{ for all } t \geq 0.$$

Then, setting $t = 0$, this implies that

$$x_T(0,\varphi) = \mathcal{T}(T,0)\varphi = \mu \mathcal{T}(0,0)\varphi = \mu\varphi, \tag{6.9}$$

which is equivalent to

$$x(\theta + T; 0, \varphi) = \mu\varphi(\theta), \text{ for all } \theta \in [-\tau_m, 0]. \tag{6.10}$$

Therefore, in order to calculate the Floquet multipliers, we approximate solutions x of equation (6.10), namely the solutions of the Cauchy problem (6.2) where the initial state φ is an (unknown) eigenfunction of the monodromy operator U associated with system (6.1).

We require that the piecewise polynomial p approximates x as follows. First, we express that it corresponds to a solution: this is done by imposing continuity at $t = 0$, and by imposing collocation requirements for the TPDDE (6.1) on interval $[0, T]$. Then, we also ensure that the solution corresponds to an eigenfunction of the monodromy operator U. This is done by imposing collocation conditions for equation (6.10) on the interval $[-\tau_m, 0]$. The imposition of these conditions generate a generalized eigenvalue problem of the kind

$$F(\mu)\vec{C} = (\mathcal{B} - \mu\mathcal{A})\vec{C} = 0 \tag{6.11}$$

whose nonzero eigenvalues μ are approximations of the Floquet multipliers of system (6.1) and where

$$\vec{C} = [c_0^{(N+2)\top} \ \ldots \ c_M^{(N+2)\top} \ \ldots \ c_0^{(1)\top} \ \ldots \ c_M^{(1)\top}]^\top, \tag{6.12}$$

i.e. $\vec{C} \in \mathbb{R}^{N_{eqn}}$, with $N_{eqn} = n(N+2)(M+1)$.

We now work out these conditions in detail:

- We impose the collocation constraints for equation (6.10), thus we want

$$\mu p(\theta) \approx p(T+\theta), \text{ for all } \theta \in [-\tau_m, 0]. \tag{6.13}$$

Observe now that in our discretization the interval $[-\tau_m, 0]$ corresponds to the union of subintervals $\Omega_2, \ldots, \Omega_{N+2}$. Since the width of each subinterval is less than or equal to T, it holds that $\theta_\ell^{(j)} + T \in \Omega_{j-1}$. Therefore we impose

$$\mu p_j(\theta_\ell^{(j)}) = p_{j-1}(\theta_\ell^{(j)} + T), \tag{6.14}$$

for $j = 2, \ldots, N+2,\ \ell = 1, \ldots, M+1$, which in its extended form reads (remember that $g_j(\theta_\ell^{(j)}) = \alpha_\ell$)

$$\mu \sum_{s=0}^{M} c_s^{(j)} T_s(\alpha_\ell) = \sum_{s=0}^{M} c_s^{(j-1)} T_s\left(g_{j-1}(\theta_\ell^{(j)} + T)\right) \tag{6.15}$$

for $j = 2, \ldots, N+2,\ \ell = 1, \ldots, M+1$. This system of equations can be rewritten into a compact matricial form as

$$\mu B\vec{C} = E\vec{C}, \tag{6.16}$$

where $B, E \in \mathbb{R}^{N_1 \times N_{eqn}}$, with $N_1 = n(N+1)(M+1)$. Observe then that the vector $B\vec{C}$, respectively $E\vec{C}$, contains the values of the piecewise polynomial p in the mesh points for the subdomain $[-\tau_m, 0]$, respectively $[T-\tau_m, T]$.

- We impose the continuity of p at 0, i.e. we require the following equation to be satisfied:

$$p_1(0) = p_2(0).$$

Substituting p_1 and p_2 with their expansion in Chebyshev polynomials, we get

$$\sum_{s=0}^{M} c_s^{(2)} T_s(1) - \sum_{s=0}^{M} c_s^{(1)} T_s(-1) = 0. \tag{6.17}$$

Observe now that the collocation conditions imposed in the previous point and the continuity of p in 0 automatically implies that p is also continuous in all the boundary points between subintervals Ω_j and Ω_{j+1}, for $j = 2, \ldots, N+1$.

- Finally, in Ω_1 we pointwise impose the collocation constraints for the TPDDE (6.1). Observe that we impose the collocation constraints only in the internal points of the mesh defined on Ω_1 in order to define p_1 as a polynomial of the same degree M as the other polynomials p_j for $j = 2, \ldots, N+2$.

Here, we must be careful when approximating the terms $x(t-\tau_i)$, as the point $t-\tau_i$ may fall in any subinterval Ω_j. As a consequence, $x(t-\tau_i)$ can be approximated by any $p_j(t-\tau_i)$ with $j=1,\dots,N+2$. In practice, (6.1) is approximated by

$$\dot{p}_1(\theta_\ell^{(1)}) = \sum_{i=0}^{m} A_i(\theta_\ell^{(1)}) \sum_{j=1}^{N+2} \chi_{\Omega_j}(\theta_\ell^{(1)}-\tau_i) p_j(\theta_\ell^{(1)}-\tau_i), \quad \text{for } \ell=1,\dots,M.$$

Let us recall that for the Chebyshev polynomial $U_s(t)$ of the second kind of degree s, we have $\dot{T}_s(t) = sU_{s-1}(t)$. Hence, for each $\theta_\ell^{(1)}$ with $\ell=1,\dots,M$ the previous equation reads

$$\begin{aligned} &\sum_{s=1}^{M} c_s^{(1)} g_1'(\theta_\ell^{(1)}) s U_{s-1}(\alpha_\ell) - \\ &\sum_{j=1}^{N+2} \chi_{\Omega_j}(\theta_\ell^{(1)}-\tau_i) \sum_{i=0}^{m} A_i(\theta_\ell^{(1)}) \sum_{s=0}^{M} c_s^{(j)} T_s\left(g_j(\theta_\ell^{(1)}-\tau_i)\right) = 0. \end{aligned} \tag{6.18}$$

Notice that these conditions and the constraint of continuity at 0 can be rewritten together using a compact matricial form as

$$M_1 \vec{C} = 0, \tag{6.19}$$

where this time $M_1 \in \mathbb{R}^{N_2 \times N_{eqn}}$ with $N_2 = n(M+1)$.

Now, our system in the coefficients $c_s^{(j)}$ has N_{eqn} equations, and thus it is square. Putting all the pieces together, equations (6.16) and (6.19) give rise to the GEP in (6.11), where $\mathcal{A},\ \mathcal{B} \in \mathbb{R}^{N_{eqn} \times N_{eqn}}$ and the nonzero eigenvalues μ are the Floquet multipliers we are looking for.

At this point, it is worth remarking that the GEP generated by our spectral discretization is linear w.r.t. (samples of) the original system matrices; as we will see in detail in the next section, an additive perturbation on the entries of nominal matrices A_i results in an additive perturbation of the GEP (6.11).

Before we conclude this section we demonstrate that the Floquet multiplier approximations solving (6.11) could alternatively be obtained by solving for the eigenvalues of a finite dimensional approximation (i.e. a matrix approximation) of the monodromy operator U which relates the discretized state functions in intervals $[-\tau_m, 0]$ and $[-\tau_m+T, T]$.

Let $x = B\vec{C}$ be the discretized state of the piecewise polynomial p in some mesh points $\{\theta_B^i\}_{i=1,\dots,K_1}$; let also the approximate solution p satisfy

the collocation constraints for the TPDDE (6.1) in some mesh points $\theta_T = \{\theta_T^i\}_{i=1,\dots,K_2}$ and continuity condition at 0, namely system $M_1\vec{C} = 0$ is satisfied. Therefore, an approximation of the solution with (discretized) initial condition x must satisfy the following

$$\begin{cases} M_1\vec{C} = 0 \\ B\vec{C} = x \end{cases} \iff \vec{C} = \begin{bmatrix} M_1 \\ B \end{bmatrix}^{-1} \begin{bmatrix} 0 \\ x \end{bmatrix}$$

Then, sampling the approximate solution in the interval $[T - \tau_m, T]$ gives

$$y = E\vec{C} = E \begin{bmatrix} M_1 \\ B \end{bmatrix}^{-1} \begin{bmatrix} 0 \\ x \end{bmatrix} = E \begin{bmatrix} M_1 \\ B \end{bmatrix}^{-1} \begin{bmatrix} 0 \\ I_{nK_1} \end{bmatrix} x := \widehat{U}x.$$

Therefore matrix $\widehat{U}$ is an approximation of monodromy operator U, and its eigenvalues $\mu \neq 0$ satisfy

$$\det\left(I_{nK_1} - \frac{1}{\mu} E \begin{bmatrix} M_1 \\ B \end{bmatrix}^{-1} \begin{bmatrix} 0 \\ I_{nk_1} \end{bmatrix} \right) = 0. \tag{6.20}$$

Some simple algebraic manipulations yields that (6.20) is equivalent to

$$\begin{cases} M_1\vec{C} = 0, \\ E\vec{C} = \mu B\vec{C} \end{cases} \tag{6.21}$$

for some vector $\vec{C} \neq 0$, which on its turn corresponds to (6.11).

As mentioned before, in a similar way a generalized eigenvalue problem of the form (6.11) can be obtained also in the cases $\tau_m = NT,\ N \geq 1$ and $\tau_m < T$. In Section 6.3, matrices $\mathcal{A},\ \mathcal{B}$ are explicitly constructed for the latter case.

Remark 6.5. *In this section we have considered TPDDEs with smooth periodic matrix-valued functions: this implies that the eigenfunctions, that we approximate with piecewise polynomials, are also smooth on the domain* $[-\tau_m, T]$. *The reader might then wonder why the domain was discretized into subintervals of width smaller than or equal to* T, *rather than defining a single polynomial on* $[-\tau_m, T]$. *The motivation is as follows: when using Chebyshev-distributed points, most of the information is "captured" in the extremities of the gridded interval; then, for cases where* $T \gg \tau_m$ *the collocation constraints for* (6.1) *will be concentrated on the right extremity of the interval only (equivalently, if* $\tau_m \gg T$ *the collocation constraints for* (6.13) *will be concentrated on the left extremity). The price to pay for a good approximation of the Floquet multipliers will then be a larger number of discretization points. In order to avoid this, we therefore adopt the previously described subdivision of the interval* $[-\tau_m, T]$*: this is the most natural choice as it allows to easily impose the collocation constraints in* (6.13). *In addition, the continuity imposed at* $t = 0$ *is automatically backpropagated to all the points of the kind* $t = -NT$ *for* $N \geq 1$.

6.2 Worst case analysis for Floquet multipliers

In this section we make the leap from unperturbed systems of TPDDEs to perturbed systems affected by matrix uncertainties. We want to perform a worst-case analysis on the stability of the system (6.1), namely we aim to compute the largest modulus a Floquet multiplier can attain under a class of uncertainties with prescribed maximal norms. In the first subsection, we formally introduce the space of uncertainties affecting the system (6.1), and we show how matrix perturbations on the system (6.1) are propagated on the GEP (6.11). As we will see, linear uncertainties on matrices A_i result in linear perturbations of the GEP (6.11). The worst-case analysis is then performed by adapting the strategy introduced in the previous chapters to the current problem. In the second subsection, we present the algorithm, highlighting main differences and similarities.

6.2.1 Matrix uncertainties: from the time-periodic system to the GEP

We consider a set of K independent real-valued matrix perturbations δA_k such that $\|\delta A_k\|_F \leq \varepsilon$. These uncertainties are included in our system (6.1) as follows

$$\dot{x}(t) = \sum_{i=0}^{m} \left(A_i(t) + \sum_{k=1}^{K} D_{i,k}(t) \delta A_k E_{i,k}(t) \right) x(t - \tau_i), \qquad t \geq 0, \tag{6.22}$$

where $D_{i,k}$, $E_{i,k}$ are time-dependent scaling matrices with time-periodic coefficients with period T. Their dimensions depend on the dimension of the associated uncertainty δA_k; for $\delta A_k \in \mathbb{R}^{p_k \times q_k}$, we have $D_{i,k} \in \mathcal{R}(T)^{n \times p_k}$, $E_{i,k} \in \mathcal{R}(T)^{q_k \times n}$. The introduction of $D_{i,k}$, $E_{i,k}$ allows us to define a (potentially) time-periodic uncertainty that affects only a submatrix of the nominal A_i, e.g. a single parameter or a block. As a consequence, various structured perturbations of the original system fall into the scope of (6.22). In addition, multiple uncertainties δA_k may affect a matrix A_i simultaneously and, at the same time, each uncertainty δA_k may affect multiple coefficient matrices A_i. Note that if δA_k does not affect A_i, then we set $D_{i,k}(t) \equiv 0$ and $E_{i,k}(t) \equiv 0$ for each t.

To illustrate the definition of auxiliary matrices $D_{i,k}(t)$ and $E_{i,k}(t)$, we provide an example based on a well-known system from the literature.

Example 6.6. *We consider the delayed Mathieu equation of second order [68, 66], which we recast in a system of first order TPDDEs as*

$$\begin{bmatrix} 1 & 0 \\ 0 & 1 \end{bmatrix} \dot{x}(t) = \underbrace{\begin{bmatrix} 0 & 1 \\ -(\eta + \beta\cos(\omega t)) & 0 \end{bmatrix}}_{:=A_0(t)} x(t) + \underbrace{\begin{bmatrix} 0 & 0 \\ b_0 & 0 \end{bmatrix}}_{:=A_1(t)} x(t-\tau), \tag{6.23}$$

where ω is such that $T = 2\pi/\omega$ and the ratio τ/T is arbitrary. We here mention three different possibilities for the perturbations:

- *Suppose we want to impose two uncertainties $\delta A_1 = \delta\eta$ and $\delta A_2 = \delta b_0$ s.t. $|\delta A_1| \le 0.5$ and $|\delta A_2| \le 0.1$. Then, we set $\varepsilon = 1$, and*

$$D_{0,1}(t) = \begin{bmatrix} 0 \\ 0.5 \end{bmatrix},\ E_{0,1}(t) = \begin{bmatrix} 1 \\ 0 \end{bmatrix}^\top,\ D_{1,2}(t) = \begin{bmatrix} 0 \\ 0.1 \end{bmatrix},\ E_{1,2}(t) = \begin{bmatrix} 1 \\ 0 \end{bmatrix}^\top,$$

  while $D_{0,2}(t) = D_{1,1}(t) = [0\ 0]^\top$ and $E_{0,2}(t) = E_{1,1}(t) = [0\ 0]$.

- *Suppose now that we want to impose two uncertainties $\delta A_1 = \delta\beta$ and $\delta A_2 = \delta b_0$ s.t. $|\delta A_1| \le 0.3$ and $|\delta A_2| \le 0.1$. Then, we set $\varepsilon = 1$, and*

$$D_{0,1}(t) = \begin{bmatrix} 0 \\ 0.3 \end{bmatrix},\ E_{0,1}(t) = \begin{bmatrix} \cos(\omega t) \\ 0 \end{bmatrix}^\top,\ D_{1,2}(t) = \begin{bmatrix} 0 \\ 0.1 \end{bmatrix},\ E_{1,2}(t) = \begin{bmatrix} 1 \\ 0 \end{bmatrix}^\top,$$

  while $D_{0,2}(t) = D_{1,1}(t) = [0\ 0]^\top$ and $E_{0,2}(t) = E_{1,1}(t) = [0\ 0]$.

- *Finally, consider two uncertainties $\delta A_1 = \delta\eta$ and $\delta A_2 = \delta\beta$ s.t. $|\delta A_1| \le 0.5$ and $|\delta A_2| \le 0.3$. Then, we set $\varepsilon = 1$, and*

$$D_{0,1}(t) = \begin{bmatrix} 0 \\ 0.5 \end{bmatrix},\ E_{0,1}(t) = \begin{bmatrix} 1 \\ 0 \end{bmatrix}^\top,\ D_{0,2}(t) = \begin{bmatrix} 0 \\ 0.3 \end{bmatrix},\ E_{0,2}(t) = \begin{bmatrix} \cos(\omega t) \\ 0 \end{bmatrix}^\top,$$

  while $D_{1,1}(t) = D_{1,2}(t) = [0\ 0]^\top$ and $E_{1,1}(t) = E_{1,2}(t) = [0\ 0]$.

From the previous example we observe that by introducing weights in the auxiliary matrices $D_{i,k}(t)$, $E_{i,k}(t)$, it is possible to consider a set of uncertainties with different magnitudes as a set of ε-bounded uncertainties for some $\varepsilon > 0$. Then, collecting the set of uncertainties in $\Delta = (\delta A_1, \dots, \delta A_K) \in \mathbb{R}^* := \mathbb{R}^{p_1 \times q_1} \times \cdots \times \mathbb{R}^{p_K \times q_K}$, we formally define a global measure of the uncertainty by

$$\|\Delta\| := \left\| \begin{bmatrix} \|\delta A_1\|_F & \dots & \|\delta A_K\|_F \end{bmatrix}^\top \right\|_\infty. \tag{6.24}$$

Clearly, the condition $\|\Delta\| \le \varepsilon$ is equivalent to the condition $\|\delta A_k\|_F \le \varepsilon$ for all $k = 1, \dots, K$.

Now, borrowing a definition from the worst-case analysis of linear time-invariant systems, we can define the ε-pseudospectrum $\mathcal{M}_\varepsilon$ of (6.22) as the union set of the Floquet multipliers associated with any ε-bounded perturbation of the matrices, that is

$$\mathcal{M}_\varepsilon := \bigcup_{\substack{\Delta \in \mathbb{R}^* \\ \|\Delta\| \leq \varepsilon}} \left\{ \mu \in \mathbb{C} : \exists\ \Delta \text{ s.t. } \mu \text{ is a Floquet multiplier of (6.22)} \right\}. \tag{6.25}$$

The *pseudospectral radius* μ_ε of the monodromy operator U (or the Floquet *pseudospectral radius*) is then defined as

$$\mu_\varepsilon := \max\{|\mu| : \mu \in \mathcal{M}_\varepsilon\},$$

which corresponds to the modulus of the Floquet multiplier in the ε-pseudospectrum $\mathcal{M}_\varepsilon$ that is the furthest away from the origin.

In the next subsection, we investigate how the uncertainties δA_k propagate on the GEP defined in (6.11).

Defining the perturbed GEP

First of all, we observe that a potential uncertainty on the matrices A_i only affects the collocation constraints for the TPDDE (6.1), thus only matrix $\mathcal{B}$ of the GEP (6.11). Now, given an uncertainty δA_k we want to define appropriate auxiliary matrices that propagate this uncertainty on (6.11). Let us consider the nominal matrix $A_i(t)$ affected by a perturbation $D_{i,k}(t)\delta A_k E_{i,k}(t)$ for each $t \in [0, T]$. In our discretized version, we must consider the effect of this perturbation on each $\theta_\ell^{(1)}$ for $\ell = 1, \dots, M$. Therefore, for each uncertainty δA_k, $k = 1, \dots, K$, affecting the matrix A_i, $i = 0, \dots, m$, we define $2M$ matrices $\mathcal{D}_{i,k}^\ell \in \mathbb{R}^{N_{eqn} \times p_k}$, $\mathcal{E}_{i,k}^\ell \in \mathbb{R}^{q_k \times N_{eqn}}$ which propagate such uncertainty on (6.11) for $t = \theta_\ell^{(1)}$, $\ell = 1, \dots, M$. Then an uncertainty δA_k is propagated on the GEP (6.11) by perturbing matrix $\mathcal{B}$ with $\delta\mathcal{B}^{(k)} = -\sum_{i=0}^{m} \sum_{\ell=1}^{M} \mathcal{D}_{i,k}^\ell \delta A_k \mathcal{E}_{i,k}^\ell$, where the minus sign is inherited by the equation (6.18).

Finally, the GEP associated with a system of TPDDEs perturbed by a set $\Delta = (\delta A_1, \ldots, \delta A_K)$ corresponding to (6.22) is of the form

$$\begin{aligned} F(\mu;\Delta)\vec{C} &= \left[\left(\mathcal{B} - \sum_{k=1}^{K} \underbrace{\sum_{i=0}^{m} \sum_{\ell=1}^{M} \mathcal{D}_{i,k}^{\ell} \delta A_k \mathcal{E}_{i,k}^{\ell}}_{=-\delta\mathcal{B}^{(k)}} \right) - \mu\mathcal{A} \right] \vec{C} \\ &= \left[\left(\mathcal{B} + \sum_{k=1}^{K} \delta\mathcal{B}^{(k)} \right) - \mu\mathcal{A} \right] \vec{C} = 0. \end{aligned} \tag{6.26}$$

In Section 6.3 we give explicit forms for the matrices $\mathcal{D}_{i,k}^{\ell}, \mathcal{E}_{i,k}^{\ell}$ for the special case where $T > \tau_m$.

We have seen now that a set Δ of matrix uncertainties affecting a system of TPDDEs like in (6.22) defines a highly structured perturbation (6.26) of the GEP (6.11). Thus the Floquet multipliers of the perturbed system (6.22) correspond to the nonzero eigenvalues of the perturbed GEP (6.26). We thus approximate the pseudospectrum $\mathcal{M}_\varepsilon$ defined in (6.25) with the structured pseudospectrum of nominal GEP (6.11) defined as follows

$$M_\varepsilon := \bigcup_{\Delta \in \mathbb{R}^*, \|\Delta\| \leq \varepsilon} \left\{ \mu \in \mathbb{C} : \exists\ \Delta\ , \mu \neq 0 \text{ s.t. } \det F(\mu;\Delta) = 0 \right\}. \tag{6.27}$$

Therefore, we will estimate the pseudospectral radius μ_ε of the monodromy operator U with the modulus of the outermost eigenvalue in M_ε. In the next subsection, we present an algorithm to estimate μ_ε following such an approach.

6.2.2 Algorithm to compute the Floquet *pseudospectral radius*

In this section we illustrate how the method to compute the ε-pseudospectral abscissa of DEPs presented in Chapter 3 can be adapted to the present problem. In the current setting, we need to compute the pseudoeigenvalue with largest modulus of a GEP subject to highly structured real-valued perturbations. Although the underlying idea remains the same, besides the objective function also the eigenvalue problem considered here is different. In addition, as we will see later, the optimal perturbations generating the Floquet *pseudospectral radius*, i.e., the Floquet multiplier with largest modulus in the pseudospectrum (6.27), do not have favourable properties to exploit when solving the optimization problem. For this reason, the projected gradient method employed here has a

simpler implementation than the one presented in Chapter 3, as we will see in detail in the rest of this section.

In order to compute the Floquet *pseudospectral radius* we must solve the following optimization problem

$$\begin{array}{ll} \max & |\mu| \\ \text{s.t.} & F(\mu;\Delta)x = 0 \text{ for some } x \in \mathbb{C}^{N_{eqn}}, \\ & \Delta \in \mathbb{R}^*,\ \|\Delta\| \leq \varepsilon. \end{array} \tag{6.28}$$

The next theorem is analogous to Theorem 3.7, and characterizes the set of optimal perturbations: in particular, it gives an explicit formula for the optimal perturbations when the norm constraint is active.

Theorem 6.7. *Let μ_ε be the Floquet multiplier with largest modulus in the ε-pseudospectrum, and assume it is simple and generated by some set of perturbations Δ. Let also x, y be respectively the left and the right eigenvectors corresponding to μ_ε (with unit norms) uniquely defined by the condition*

$$\xi := x^* \mathcal{A} y > 0, \tag{6.29}$$

where $\mathcal{A}$ is as in (6.11)*, and let*

$$X = [\Re(x)\ \Im(x)], \quad Y = [\Re(y)\ \Im(y)], \quad \Gamma = \begin{bmatrix} \Re(\mu_\varepsilon) & \Im(\mu_\varepsilon) \\ -\Im(\mu_\varepsilon) & \Re(\mu_\varepsilon) \end{bmatrix}. \tag{6.30}$$

If for some $k \in \{1, \ldots, K\}$ the matrix $\sum_{i=0}^{m} \sum_{\ell=1}^{M} \mathcal{D}_{i,k}^{\ell^\top} X \Gamma Y^\top \mathcal{E}_{i,k}^{\ell^\top}$ is nonzero, then the optimal perturbation δA_k satisfies

$$\delta A_k = -\varepsilon \frac{\sum_{i=0}^{m} \sum_{\ell=1}^{M} \mathcal{D}_{i,k}^{\ell^\top} X \Gamma Y^\top \mathcal{E}_{i,k}^{\ell^\top}}{\left\| \sum_{i=0}^{m} \sum_{\ell=1}^{M} \mathcal{D}_{i,k}^{\ell^\top} X \Gamma Y^\top \mathcal{E}_{i,k}^{\ell^\top} \right\|_F}. \tag{6.31}$$

Proof. The proof employs the same reasoning used in Theorem 3.7. □

It is worth remarking that the *low-rank property* of the optimal matrices generating the pseudospectral abscissa does not hold for the maximizers of the modulus of Floquet multipliers. For this reason, the well-known decomposition of uncertainties δA_k into $U_k Q_k V_k^\top$ (which sensibly reduced the number of optimization variables as the matrix Q_k has small dimensions) will not be considered here. To be precise, using arguments similar to Theorem 3.7, it could be proven for an optimal δA_k that $\operatorname{rank}(\delta A_k) \leq \rho_k^* := \min(2M\eta_k, p_k, q_k)$, with M denoting the degree of the piecewise polynomial p approximating the solution, and η_k the number of matrices A_i perturbed by uncertainty δA_k. However, since M usually has to be quite large, the inequality in practice reduces to $\operatorname{rank}(\delta A_k) \leq \min(p_k, q_k)$.

Therefore, the optimization problem (6.28) can be solved by using a simpler implementation of the projected gradient method in the space of ε-bounded perturbations Δ. In order to construct the gradient of an eigenvalue μ of the perturbed GEP (6.26) w.r.t. δA_k, we consider again $x, y \in \mathbb{C}^{N_{\text{eqn}}}$ as the left and the right eigenvectors corresponding to μ with unit norms and normalized so that $\xi := x^* \mathcal{A} y > 0$, and we define X, Y, Γ as in (6.30). Then, let δA_k^{st} be the (s,t)-th entry of uncertainty δA_k, with $s = 1, \ldots, p_k$, $t = 1, \ldots, q_k$, and e_s, e_t be the column vectors of the canonical basis such that $e_s \in \mathbb{R}^{p_k}$, $e_t \in \mathbb{R}^{q_k}$. Then,

$$\begin{aligned}
\frac{\partial |\mu|^2}{\partial \delta A_k^{st}} &= 2\mathfrak{R}\left(\bar{\mu} \frac{\partial \mu}{\partial \delta A_k^{st}}\right) = \frac{2}{\xi}\mathfrak{R}\left(\bar{\mu} x^* \frac{\partial \mathfrak{B}^{(k)}}{\partial \delta A_k^{st}} y\right) = \\
&- \frac{2}{\xi}\mathfrak{R}\left(\sum_{i=0}^{m}\sum_{\ell=1}^{M} \bar{\mu} x^* \mathcal{D}_{i,k}^{\ell} e_s e_t^\top \mathcal{E}_{i,k}^{\ell} y\right) = \\
&- \frac{2}{\xi}\sum_{i=0}^{m}\sum_{\ell=1}^{M} \mathfrak{R}\left(\left(\overline{e_s^\top \mathcal{D}_{i,k}^{\ell^\top} x}\right)\left(\bar{\mu} y^* \mathcal{E}_{i,k}^{\ell^\top} e_t\right)\right) = \\
&- \frac{2}{\xi}\sum_{i=0}^{m}\sum_{\ell=1}^{M} e_s^\top \left(\mathcal{D}_{i,k}^{\ell^\top} X \Gamma Y^\top \mathcal{E}_{i,k}^{\ell^\top}\right) e_t,
\end{aligned}$$

where ξ is as in (6.29). The gradient of $|\mu|^2$ w.r.t. δA_k can be written in the form of a matrix whose (s,t)-th component is the derivative in the previous expression, which gives rise to

$$G_k := \frac{\partial |\mu|^2}{\partial \delta A_k} = -\frac{2}{\xi}\sum_{i=0}^{m}\sum_{\ell=1}^{M} \mathcal{D}_{i,k}^{\ell^\top} X \Gamma Y^\top \mathcal{E}_{i,k}^{\ell^\top}, \tag{6.32}$$

for $k = 1, \ldots, K$. We can now use a (projected) gradient method to solve the optimization problem (6.28) using the following fundamental step at each iteration n

$$\delta A_k^{(n+1)} = \delta A_k^{(n)} + r_n P_k^{(n)}, \quad k = 1, \ldots, K,$$

where r_n is the stepsize at iteration n and $P_k^{(n)}$ is the ascent direction defined as

$$P_k^{(n)} = \begin{cases} G_k^{(n)} - \langle G_k^{(n)}, \delta A_k^{(n)} \rangle \delta A_k^{(n)}, & \text{if } \left\|\delta A_k^{(n)}\right\|_F = 1,\ \langle G_k^{(n)}, \delta A_k^{(n)} \rangle > 0, \\ G_k^{(n)}, & \text{otherwise.} \end{cases} \tag{6.33}$$

Note that above $\langle \cdot, \cdot \rangle$ still stands for the Frobenius inner product, and $G_k^{(n)}$ is the gradient of the *largest eigenvalue* of the GEP (6.26) perturbed with uncertainties $\delta A_k^{(n)}$. Observe that $P_k^{(n)}$ is the projection of gradient $G_k^{(n)}$ on the feasible set, which is needed to avoid the violation of the norm constraint.

The algorithm is initialized using formulas (6.31). Also in this case we use an adaptive stepsize and the restarting strategy, thus we run the algorithm several times starting from several distinct eigenvalues with largest moduli of the nominal problem. A scheme of the algorithm is given in Algorithm 3.

6.3 Explicit construction of the GEP for $T > \tau_m$

In this section, we provide explicit expressions to generate the GEP (6.11) and its perturbations in the case $\tau_m < T$: in this case the construction of the matrices is easier as the domain $[-\tau_m, T]$ is discretized in only two subintervals Ω_1 and Ω_2. Nevertheless, this can be very instructive, as for the cases where $\tau_m \geq T$ the construction of the GEP is analogous.

Let us consider again the three different conditions imposed to generate the GEP:

Firstly, we consider collocation constraints for equation (6.10), thus we have

$$\mu p_2(\theta_\ell^{(2)}) = p_1(\theta_\ell^{(2)} + T), \text{ for } \ell = 1, \ldots, M+1,$$

which is recast as follows into matricial form

$$\mu \left[T_0(\alpha_\ell) \otimes I_n \quad \ldots \quad T_M(\alpha_\ell) \otimes I_n \quad \overbrace{0 \otimes I_n}^{\substack{n(M+1) \\ \text{columns}}} \right] \vec{C} =$$

$$\left[\overbrace{0 \otimes I_n}^{\substack{n(M+1) \\ \text{columns}}} \quad T_0\left(g_1(\theta_\ell^{(2)} + T)\right) \otimes I_n \quad \ldots \quad T_M\left(g_1(\theta_\ell^{(2)} + T)\right) \otimes I_n \right] \vec{C}.$$

Secondly, when imposing the continuity at 0, the condition $p_1(0) = p_2(0)$ has the following matricial form:

$$I_n \otimes \left[T_0(1) \quad \ldots \quad T_M(1) \quad -T_0(-1) \quad \ldots \quad -T_M(-1) \right] \vec{C} = 0.$$

Finally we consider the collocation constraints associated with TPDDE (6.1). As remarked before, the point $t - \tau_i$ may fall either in Ω_1 or in Ω_2. Then, for each $\theta_\ell^{(1)}$ we consider the index m_ℓ s.t. $\theta_\ell^{(1)} \geq \tau_i$ for $i = 0, \ldots, m_\ell$, and $\theta_\ell^{(1)} < \tau_i$ for $i = m_\ell + 1, \ldots, m$. Observing that $g_1'(t) = 2/T$, equation (6.18) can be

Algorithm 3 Computation of the Floquet *pseudospectral radius*.

Input: Problem data: $A_i, D_i, E_i, \tau_i, \varepsilon$, tolerance η, scaling factor $h > 1$, n_{start}.

For $\ell = 1, \dots, M$, for $i = 0, \dots, m$, and for $k = 1, \dots, K$ define matrices $\mathcal{D}_{i,k}^{\ell}$ and $\mathcal{E}_{i,k}^{\ell}$ (see Section 6.3).
Solve GEP (6.11) and for $i = 1, \dots, n_{\text{start}}$ store the i-th largest eigenvalue $\mu(i)$ and the corresponding eigenvectors $x(i)$ and $y(i)$ s.t. $x(i)^* \mathcal{A} y(i) > 0$.
for $i = 1 : n_{\text{start}}$ **do**
    Set $\mu_{i,1} = \mu(i)$, $x_{i,1} = x(i)$, $y_{i,1} = y(i)$.
    Initialize perturbations $\delta A_1^*, \dots, \delta A_K^*$ using equations (6.31).
    For $k = 1, \dots, K$ define $\delta \mathcal{B}^{(k)}$ and the perturbed GEP (6.26).
    Solve the GEP and set $\mu_{i,2}$ equal to the largest eigenvalue and $x_{i,2}$, $y_{i,2}$ equal to its left and right eigenvectors.
    Set $\zeta = +\infty$, $n = 2$, $r_n = 1$, $\delta A_k^{(n)} = \delta A_k^*$.
    while $\zeta > \eta$ **do**
        Compute the gradients $P_k^{(n)}$ for $k = 1, \dots, K$ using formulas (6.32) and (6.33).
        Compute

$$\delta \widehat{A}_k^{(n+1)} = \delta A_k^{(n)} + r_n P_k^{(n)}, \quad k = 1, \dots, K.$$

        For $k = 1, \dots, K$, normalize if necessary

$$\delta A_k^{(n+1)} = \begin{cases} \delta \widehat{A}_k^{(n+1)}, & \text{if } \left\| \delta \widehat{A}_k^{(n+1)} \right\|_F \le \varepsilon, \\ \dfrac{\varepsilon \delta \widehat{A}_k^{(n+1)}}{\left\| \delta \widehat{A}_k^{(n+1)} \right\|_F}, & \text{otherwise.} \end{cases}$$

        For $k = 1, \dots, K$ define $\delta \mathcal{B}^{(k)}$ and the perturbed GEP (6.26).
        Solve the GEP and set $\hat{\mu}$ equal to the largest eigenvalue and $\hat{x}$, $\hat{y}$ equal to its left and right eigenvectors.
        Set $r = r_n$.
        while $|\hat{\mu}| \le |\mu_{i,n}|$ **do**
            Set $r = r/h$ and repeat steps from 11 to 14 with step r.
            Solve the GEP and set $\hat{\mu}$ equal to the largest eigenvalue and $\hat{x}$, $\hat{y}$ equal to its left and right eigenvectors.
        end while
        if $r < r_n$ **then**
            Set $\mu_{i,n+1} = \hat{\mu}, x_{n+1} = \hat{x}, y_{n+1} = \hat{y}, r_{n+1} = r$
        else
            Set $\tilde{r} := h r_n$ and repeat steps from 11 to 14 with step $\tilde{r}$.
            Solve the GEP and set $\tilde{\mu}$ equal to the largest eigenvalue and $\tilde{x}$, $\tilde{y}$ equal to its left and right eigenvectors.
            if $|\hat{\mu}| \le |\tilde{\mu}|$ **then**
                Set $\mu_{i,n+1} = \tilde{\mu}, x_{i,n+1} = \tilde{x}, y_{i,n+1} = \tilde{y}, r_{n+1} = \tilde{r}$
            else
                Set $\mu_{i,n+1} = \hat{\mu}, x_{i,n+1} = \hat{x}, y_{i,n+1} = \hat{y}, r_{n+1} = r_n$
            end if
        end if
        Set $\zeta = \dot{\mu}_{i,n+1}$ and $n \to n + 1$.
    end while
    Set $\mu_i = \mu_{i,n+1}$.
end for
return $\mu_\varepsilon = \mu_{i^*}$ s.t. $|\mu_{i^*}| = \max_{i=1,\dots,n_{\text{start}}} |\mu_i|$.

recast in the following matricial form for $\ell = 1, \dots, M$:

$$\left[\overbrace{0 \otimes I_n}^{\substack{n(M+1)\\ \text{columns}}} \quad \tfrac{2}{T} U_0(\alpha_\ell) \otimes I_n \quad \dots \quad \tfrac{2}{T} M U_{M-1}(\alpha_\ell) \otimes I_n \right] \vec{C} -$$

$$\left[\overbrace{0 \otimes I_n}^{\substack{n(M+1)\\ \text{columns}}} \quad \sum_{i=0}^{m_\ell} A_i(\theta_\ell^{(1)}) T_0\left(g_1(\theta_\ell^{(1)} - \tau_i)\right) \quad \dots \quad \sum_{i=0}^{m_\ell} A_i(\theta_\ell^{(1)}) T_M\left(g_1(\theta_\ell^{(1)} - \tau_i)\right) \right] \vec{C} -$$

$$\left[\sum_{i=m_\ell+1}^{m} A_i(\theta_\ell^{(1)}) T_0\left(g_2(\theta_\ell^{(1)} - \tau_i)\right) \quad \dots \quad \sum_{i=m_\ell+1}^{m} A_i(\theta_\ell^{(1)}) T_M\left(g_2(\theta_\ell^{(1)} - \tau_i)\right) \quad \overbrace{0 \otimes I_n}^{\substack{n(M+1)\\ \text{columns}}} \right] \vec{C} = 0.$$

Of course, there exist two limit cases: if $\theta_\ell^{(1)} < \tau_i$ for all $i = 0, \dots, m$, then $m_\ell = 0$ and the second term on the left-hand side does not appear; on the other hand, if $\theta_\ell^{(1)} \geq \tau_i$ for all $i = 0, \dots, m$, then $m_\ell = m$ and the third term is not needed.

Putting all the equations together, we obtain the explicit forms for $\mathcal{A}$ and $\mathcal{B}$ as follows:

$$\mathcal{A} := \left(\begin{array}{c|c} A & 0 \\ \hline 0 & 0 \end{array}\right), \quad \text{with } A = \begin{bmatrix} T_0(\alpha_1) \otimes I_n & \dots & T_M(\alpha_1) \otimes I_n \\ \vdots & \vdots & \vdots \\ T_0(\alpha_{M+1}) \otimes I_n & \dots & T_M(\alpha_{M+1}) \otimes I_n \end{bmatrix},$$

$$\mathcal{B} := \mathcal{B}_1 - \mathcal{B}_2 = \left(\begin{array}{c|c} 0 & B_1^{(t)} \\ \hline 0 & B_1^{(b)} \end{array}\right) - \left(\begin{array}{c|c} 0 & 0 \\ \hline B_2^{(l)} & B_2^{(r)} \end{array}\right),$$

with

$$B_1^{(t)} = \begin{bmatrix} T_0\left(g_1(\theta_1^{(2)} + T)\right) \otimes I_n & \dots & T_M\left(g_1(\theta_1^{(2)} + T)\right) \otimes I_n \\ \vdots & \vdots & \vdots \\ T_0\left(g_1(\theta_{M+1}^{(2)} + T)\right) \otimes I_n & \dots & T_M\left(g_1(\theta_{M+1}^{(2)} + T)\right) \otimes I_n \end{bmatrix},$$

$$B_1^{(b)} = \begin{bmatrix} I_n \otimes 0 & I_n \otimes 0 & \dots & I_n \otimes 0 \\ \vdots & \frac{2}{T} U_0(\alpha_1) \otimes I_n & \dots & \frac{2}{T} M U_{M-1}(\alpha_1) \otimes I_n \\ \vdots & \vdots & \vdots & \vdots \\ I_n \otimes 0 & \frac{2}{T} U_0(\alpha_M) \otimes I_n & \dots & \frac{2}{T} M U_{M-1}(\alpha_M) \otimes I_n \end{bmatrix},$$

$$B_2^{(l)} = \begin{bmatrix} I_n \otimes T_0(1) & \dots & I_n \otimes T_M(1) \\ \sum_{i=m_1+1}^{m} A_i(\theta_1^{(1)}) T_0\left(g_2(\theta_1^{(1)} - \tau_i)\right) & \dots & \sum_{i=m_1+1}^{m} A_i(\theta_1^{(1)}) T_M\left(g_2(\theta_1^{(1)} - \tau_i)\right) \\ \vdots & \vdots & \vdots \\ \sum_{i=m_M+1}^{m} A_i(\theta_M^{(1)}) T_0\left(g_2(\theta_M^{(1)} - \tau_i)\right) & \dots & \sum_{i=m_M+1}^{m} A_i(\theta_M^{(1)}) T_M\left(g_2(\theta_M^{(1)} - \tau_i)\right) \end{bmatrix},$$

$$B_2^{(r)} = \begin{bmatrix} -I_n \otimes T_0(-1) & \dots & -I_n \otimes T_M(-1) \\ \sum_{i=0}^{m_1} A_i(\theta_1^{(1)}) T_0\left(g_1(\theta_1^{(1)} - \tau_i)\right) & \dots & \sum_{i=0}^{m_1} A_i(\theta_1^{(1)}) T_M\left(g_1(\theta_1^{(1)} - \tau_i)\right) \\ \vdots & \vdots & \vdots \\ \sum_{i=0}^{m_M} A_i(\theta_M^{(1)}) T_0\left(g_1(\theta_M^{(1)} - \tau_i)\right) & \dots & \sum_{i=0}^{m_M} A_i(\theta_M^{(1)}) T_M\left(g_1(\theta_M^{(1)} - \tau_i)\right) \end{bmatrix}.$$

In the following, we provide explicit expressions also for matrices $\mathcal{D}_{i,k}^{\ell}$, $\mathcal{E}_{i,k}^{\ell}$ introduced in subsection 6.2.1; these matrices propagate an uncertainty δA_k affecting the system onto the GEP (6.11). For a given uncertainty δA_k we must define matrices $\mathcal{D}_{i,k}^{\ell}$, $\mathcal{E}_{i,k}^{\ell}$ depending on whether value $(\theta_\ell^{(1)} - \tau_i)$ belongs to Ω_1 or Ω_2 for $\ell = 1, \dots, M$, $i = 0, \dots, m$: if $(\theta_\ell^{(1)} - \tau_i) \in \Omega_1$, then

$$\mathcal{D}_{i,k}^{\ell} = \begin{bmatrix} 0 & \dots & \overset{M+2+\ell}{\overset{\uparrow}{1}} & \dots & 0 \end{bmatrix}^{\top} \otimes D_{i,k}(\theta_\ell^{(1)}),$$

$$\mathcal{E}_{i,k}^{\ell} = \Big[\underbrace{0 \otimes I_n}_{\substack{n(M+1) \\ \text{columns}}} \quad E_{i,k}(\theta_\ell^{(1)}) T_0\left(g_1(\theta_\ell^{(1)} - \tau_i)\right) \quad \dots \quad E_{i,k}(\theta_\ell^{(1)}) T_M\left(g_1(\theta_\ell^{(1)} - \tau_i)\right)\Big].$$

On the other hand, if $(\theta_\ell^{(1)} - \tau_i) \in \Omega_2$, then

$$\mathcal{D}_{i,k}^{\ell} = \begin{bmatrix} 0 & \dots & \overset{M+2+\ell}{\overset{\uparrow}{1}} & \dots & 0 \end{bmatrix}^{\top} \otimes D_{i,k}(\theta_\ell^{(1)}),$$

$$\mathcal{E}_{i,k}^{\ell} = \Big[E_{i,k}(\theta_\ell^{(1)}) T_0\left(g_2(\theta_\ell^{(1)} - \tau_i)\right) \quad \dots \quad E_{i,k}(\theta_\ell^{(1)}) T_M\left(g_2(\theta_\ell^{(1)} - \tau_i)\right) \quad \underbrace{0 \otimes I_n}_{\substack{n \times (M+1) \\ \text{columns}}}\Big].$$

Observe that for the other cases ($NT \leq \tau_m < (N+1)T$, $N \geq 1$) the definition of $\mathcal{D}_{i,k}^{\ell}$ does not change, while the definition of $\mathcal{E}_{i,k}^{\ell}$ simply depends on the subinterval Ω_j to which value $(\theta_\ell^{(1)} - \tau_i)$ belongs.

6.4 Models with periodically time-varying delays

A straightforward extension of the method described in Sections 6.1 and 6.2 involves by the introduction of time-periodic delays in the TPDDE (6.1). This extension also has a large potential for engineering applications, for instance for turning models with spindle speed variation: numerical simulations for this model will be presented in subsection 6.4.2. In the next subsection, we describe the modifications needed to cope with time-periodic delays in our problem.

6.4.1 Extension of the approach

Let us consider

$$\dot{x}(t) = \sum_{i=1}^{m} A_i(t)x(t - \tau_i(t)), \qquad t \geq 0, \tag{6.34}$$

where $\tau_i \in \mathcal{R}(T)$ for $i = 0, \ldots, m$, i.e., they are periodic functions with main period T (that is they have the same main period as matrices A_i) and such that $0 \leq \tau_0(t) \leq \cdots \leq \tau_m(t)$ for each $t \in [0, T]$. For the well-posedness of the problem, we also assume that functions τ_i are differentiable and that $\dot{\tau}_i(t) < 1$ for every t. In [98], it is proven that violating this hypothesis is equivalent to denying the principle of causality: in practice, it is demonstrated that if $\dot{\tau}_i(t) > 1$ for some t, then the state function in t is determined by *future* states of the function.

Also in this case the Floquet theory can be used to investigate the system stability. However, some modifications need to be adopted in the solver described in Section 6.1 and in the algorithm for the worst-case analysis introduced in Section 6.2. In particular, in Section 6.1, a discretization of the interval $[-\tau_m, T]$ is performed, where $\tau_m > \tau_i$ for each $i = 0, \ldots, m-1$. For time-periodic delays, we must consider an interval such that it contains the value $t - \tau_i(t)$ for each $t \in [0, T]$ and for each $i = 1, \ldots, m$. Given the hypothesis that $\dot{\tau}_i(t) < 1$ for every t, then value $\tau_m(0)$ is such that $-\tau_m(0) \leq t - \tau_i(t)$ for each $i = 1, \ldots, m$, for all $t \in [0, T]$.

The solver described in Section 6.1 is then analogously adapted to the interval $[-\tau_m(0), T]$: as illustrated in Figure 6.2, it is divided into $N + 2$ subintervals Ω_k (where $NT < \tau_m(0) < (N+1)T$), and on each Ω_k, for $k = 1, \ldots, N+2$, we define a mesh of $M + 1$ Chebyshev-distributed points.

Let p still be the piecewise polynomial approximation of the solution x. Then, while the introduction of the time-periodic delays does not affect equations of the form (6.14), the collocation constraint for the TPDDE (6.34) now becomes

$$\dot{p}_1(\theta_\ell^{(1)}) = \sum_{i=0}^{m} A_i(\theta_\ell^{(1)}) \sum_{j=1}^{N+2} \chi_{\Omega_j}(t - \tau_i(\theta_\ell^{(1)}))p_j(t - \tau_i(\theta_\ell^{(1)})),$$

for each $\ell = 1, \ldots, M$, which implies

$$\sum_{s=1}^{M} c_s^{(1)} g_1'(\theta_\ell^{(1)}) s U_{s-1}(\alpha_\ell) -$$

$$\sum_{j=1}^{N+2} \chi_{\Omega_j}(\theta_\ell^{(1)} - \tau_i(\theta_\ell^{(1)})) \sum_{i=0}^{m} A_i(\theta_\ell^{(1)}) \sum_{s=0}^{M} c_s^{(j)} T_s \Big(g_j(t - \tau_i(\theta_\ell^{(1)})) \Big) = 0.$$

The presence of time-periodic delays does not alter the structure of Algorithm 3 introduced in Section 6.2 for the worst-case analysis. However, since a matrix uncertainty affects the collocation conditions for (6.34), auxiliary matrices $\mathcal{D}_{i,s}^{\ell}$ and $\mathcal{E}_{i,s}^{\ell}$ must be redefined. Suppose that matrix-valued uncertainties are defined on system (6.34) in an analogous way as in equation (6.22). Then, for a given perturbation $D_{i,k}(t)\delta A_k E_{i,k}(t)$, matrices $\mathcal{D}_{i,k}^{\ell}$ and $\mathcal{E}_{i,k}^{\ell}$ introduced in Section 6.3 are redefined by simply replacing τ_i with $\tau_i(\theta_\ell^{(1)})$ for $i = 0, \ldots, m,\ \ell = 1, \ldots, M$.

6.4.2 Spindle speed variation in turning

Machine tool chatter is a challenging problem in milling and turning operations. While the milling problem will be extensively considered in Section 6.6, we here focus our attention on the turning problem. A well-known method to suppress vibrations during turning processes is spindle speed variation. The main idea behind this concept is that spindle speed variation introduces a time-varying regenerative delay, which in some cases may stabilize the process. The dyn

amical model of a turning operation is presented in Fig. 6.3. The regenerative time delay in case of constant speed (Ω_0) is given as $\tau_0 = 60/\Omega_0$. Let us assume that the speed is modulated around the nominal value as

$$\Omega(t) = \Omega_0 + S(t)\Omega_1, \quad S(t+T) = S(t), \tag{6.35}$$

where Ω_1 is the amplitude of the harmonic variation $S(t) = \cos(2\pi t/T)$. For simplicity, the time delay is approximated by the relation

$$\tau(t) \approx \tau_0 - S(t)\tau_1, \quad \tau(t+T) = \tau(t), \tag{6.36}$$

where RVA $:= \tau_1/\tau_0 = \Omega_1/\Omega_0$ is the ratio of the variation and mean. Similarly, the ratio of the modulation frequency and the mean spindle speed can be defined as RVF $:= 60/(\Omega_0 T)$. The governing equation of the turning process is then given by

$$m\ddot{\eta}(t) + c\dot{\eta}(t) + k\eta(t) = G(t)\Big(\eta\big(t - \tau(t)\big) - \eta(t)\Big),$$

$$G(t) = wK_y q(v_{\mathrm{f}}\tau_0)^{q-1} \left(\frac{\tau(t)}{\tau_0}\right)^{q-1},$$

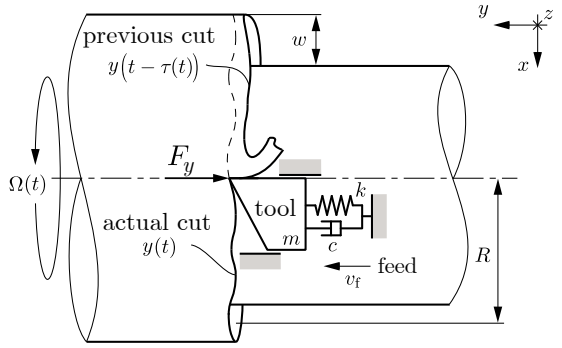

Figure 6.3: Dynamical model of spindle speed variation in turning.

where $G(t+T) = G(t)$ is a periodic function, moreover m, c and k are modal parameters, w is the depth of cut, $h_0 := v_f \tau_0$ is the theoretical prescribed chip thickness, q and K_y are cutting parameters. For more details on the model, see [68].

A stability diagram is visualized in the plane of nominal spindle speed Ω_0 and depth of cut w, while RVA and RVF are fixed. In Fig. 6.4 the nominal stability boundaries were calculated using the parameters $m = 1$ kg, $c = 40$ Ns/m, $k = 10^6$ N/m, $q = 3/4$, $K_y = 300$ N/m^{1+q}, $h_0 = 0.1$ mm. In panel a) RVA=0, i.e., spindle speed variation is off, therefore it gives the unmodulated constant speed turning model. In panel b) RVA=0.1 and RVF=0.5. In both cases we assume that modal damping c and modal stiffness k are uncertain, and we set $|\delta k| < 0.05k$ and $|\delta c| < 0.4c$.

As it is seen from Fig. 6.4 (a) and (b), the robustness of spindle speed variation at different speeds might significantly affect the selection of optimal machining parameters.

6.5 Models with piecewise-smooth periodic functions

In the previous sections, we have considered systems of TPDDEs with *smooth* time-periodic functions. However, many engineering applications modeled by TPDDEs require the use of *piecewise-smooth* time-periodic functions. Some classical examples in this sense are represented by linear systems with delayed act-and-wait controller and by the milling model [67, 63], for which numerical simulations will be presented in sections 6.5.2 and 6.6, respectively.

When the matrix-valued functions A_i in (6.1) are smooth, the eigenfunctions associated with (6.2) are also smooth on each subinterval Ω_j (in fact, as seen

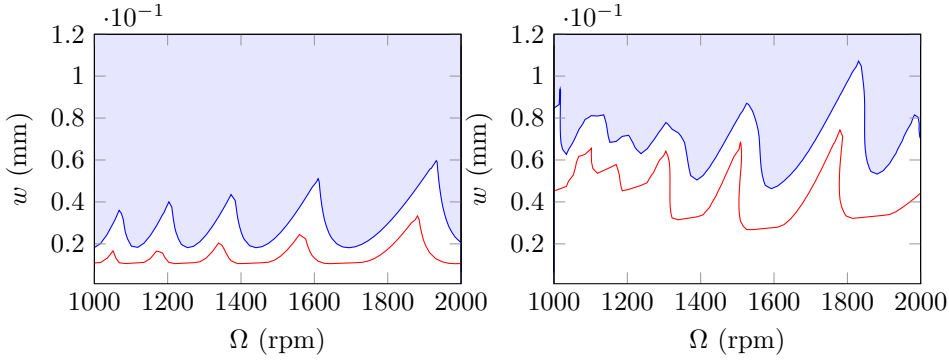

Figure 6.4: Robust stability diagram: the upper (blue) line is the stability boundary, the lower (red) line is the robust stability boundary for $|\delta k| < 0.05k$, $|\delta c| < 0.4c$. In panel (a) we set RVA=0, in panel (b) we set RVA=0.1 and RVF=0.5.

in the Remark 6.5, they are smooth on the whole domain $[-\tau_m, T]$). Hence, they can be well approximated by polynomials on each Ω_j, ensuring spectral convergence of the Floquet multipliers approximations as a function of the degree M. However, if A_i are only piecewise smooth, the discontinuities affect the smoothness of the solutions, and negatively affect the convergence rate of the polynomial approximation. Nevertheless, this problem can be overcome by the choice of a piecewise polynomial consistent with the location of the discontinuities, and thus by employing a novel discretization of the domain $[-\tau_m, T]$.

In order to investigate the stability (and its robustness) of TPDDEs with *piecewise-smooth* periodic functions, some important modifications then need to be introduced in the solver described in Section 6.1 and in the algorithm to compute μ_ε defined in Section 6.2. These changes are discussed in the next subsection.

6.5.1 Extension of the approach

Let us consider system

$$\dot{x}(t) = \sum_{i=0}^{m} A_i(t)x(t-\tau_i), \qquad t \geq 0, \tag{6.37}$$

where $A_i \in \mathcal{R}_{pws}(T)^{n\times n}$, and $\mathcal{R}_{pws}(T)$ denotes the set of *piecewise-smooth* real-valued periodic functions with main period equal to T. Therefore we assume that

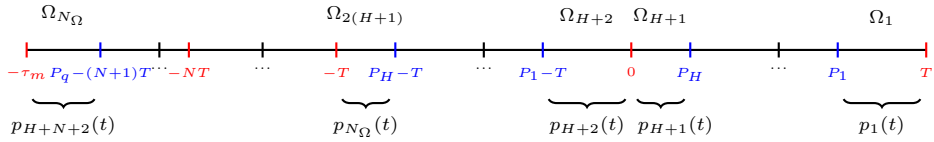

Figure 6.5: Discretization of the domain $[-\tau_m, T]$ for a system of TPDDE (6.37) with piecewise-smooth terms. Points colored in red are also present in the discretization of the domain adopted for TPDDEs with smooth terms. Points colored in blue are introduced in this discretization, in order to handle discontinuities. The solution x of (6.37) is non-differentiable in the blue points.

matrices A_i, $i = 0, \dots, m$ admit a finite set of discontinuity points $\{P_1, \dots, P_H\}$ disposed in decreasing order, i.e. $0 < P_H < \cdots < P_1 < T$. This peculiar choice about the order of points P_j is necessary in order to be consistent with the notation on subintervals Ω_j introduced in Section 6.1. Then, we subdivide the interval $[0, T]$ into a set of $H + 1$ subintervals Ω_j as follows

$$[0, T] = \bigcup_{j=0}^{H} \Omega_{H+1-j} = \bigcup_{j=0}^{H} [P_{H+1-j}, P_{H-j}], \quad \text{where } P_{H+1} = 0,\ P_0 = T.$$

The reason for the adopted discretization is that solution x of (6.37) is smooth but non-differentiable at points $P_1, \dots, P_H$. Moreover, as a consequence of the definition of eigenfunction for the monodromy operator and, in particular, of equation (6.10), this discretization must be propagated to the subdomain $[-\tau_m, 0]$ as well. In this description, we want to remain consistent with the discretization illustrated in Figure 6.2, thus we assume that there exists $N \in \mathbb{N}$ such that $NT < \tau_m < (N+1)T$; moreover, we assume that $P_{q+1} - (N+1)T < \tau_m < P_q - (N+1)T$ for some $q \in \{0, \dots, H\}$. Then the interval $[-\tau_m, T]$ is divided into $N_\Omega = (N+1)(H+1) + (q+1)$ subintervals as illustrated in Figure 6.5.

Also in this case we approximate the solution x with a piecewise polynomial defined as

$$x(t) \approx p(t) = \sum_{j=1}^{N_\Omega} p_j(t) \chi_{\Omega_j}(t), \quad \text{for } t \in [-\tau_m, T], \tag{6.38}$$

where $\chi_{\Omega_j}(t)$ is still the indicator function of the subinterval Ω_j. We define on each Ω_j a mesh of $M + 1$ Chebyshev-distributed points, and each polynomial is still expressed in terms of Chebyshev polynomials as

$$p_j(t) = \sum_{s=0}^{M} c_s^{(j)} T_s(g_j(t)), \ \text{for } j = 1, \dots, N_\Omega. \tag{6.39}$$

The construction of the GEP to find the Floquet multipliers is then similar to what is described in Section 6.1. The only difference is that we now impose the continuity of piecewise polynomial p not just at 0 but also at $P_1, \ldots, P_H$. The algorithm to compute the pseudospectral radius is also the same, provided that the matrices $\mathcal{D}^{\ell}_{i,k}$, $\mathcal{E}^{\ell}_{i,k}$ are modified according to the new subintervals.

6.5.2 Robustness analysis of linear systems stabilized by act-and-wait controllers

In this section, we analyse the robust stability of linear systems with delayed act-and-wait controller, which are characterized by the introduction of a piecewise constant function [67]. In our numerical examples, we will consider a second-order model which is often used to analyse the stabilization of an inverted pendulum [116] and in applications such as human balancing problems [100]. We consider the linear system

$$\begin{cases} \dot{x}(t) = Ax(t) + Bu(t) \\ y(t) = Cx(t) \end{cases} \tag{6.40}$$

where $x(t) \in \mathbb{R}^n$, $u(t) \in \mathbb{R}^m$, $y(t) \in \mathbb{R}^l$, denote the state, the input and the output, respectively, for each t, and $A \in \mathbb{R}^{n\times n}$, $B \in \mathbb{R}^{n\times m}$, $C \in \mathbb{R}^{l\times n}$. We consider a time-periodic controller

$$u(t) = Dg(t)y(t-\tau),$$

where $D \in \mathbb{R}^{m\times l}$ contains the control gains, τ is the time delay of the feedback loop, and g is a periodic function. The act-and-wait controller is a special case of time-periodic controllers, and we define the switching function g as

$$g(t) = \begin{cases} 0, & \text{if } \ 0 \le t \bmod T < t_w, \\ 1, & \text{if } \ t_w \le t \bmod T < t_w + t_a = T, \end{cases}$$

where t_w is the waiting period while the controller is not active, and $t_a = T - t_w$ is the acting period while the controller is active.

The mechanical model of an inverted pendulum of length L and mass m driven on a massless cart is shown in Figure 6.6a. The system is governed by the second-order TPDDE

$$\ddot{x}(t) + ax(t) = -g(t)\left(px(t-1) + d\dot{x}(t-1)\right), \tag{6.41}$$

where $a = -3g/(6L)$ is the system parameter and p and d are the proportional and the derivative control gains. This system can be written in the form of (6.40) with

$$A = \begin{bmatrix} 0 & 1 \\ -a & 0 \end{bmatrix}, \ B = \begin{bmatrix} 0 \\ 1 \end{bmatrix}, \ C = \begin{bmatrix} 1 & 0 \\ 0 & 1 \end{bmatrix}, \ D = \begin{bmatrix} -p & -d \end{bmatrix}, \tag{6.42}$$

and the feedback delay is set $\tau = 1$. In Figures 6.6b, 6.6c we analyse the robust stability for settings already introduced in the literature [67]. In panel (b) we consider $a = -2.5$, $t_w = 1.2$, $t_a = 0.8$ and in panel (c) $t_w = 0.8$, while a and t_a are the same. In both plots, we represent the stability boundary (outer line), the robust stability boundary for $|\delta a| \leq 0.02$, $|\delta p| \leq 0.05$, $|\delta d| \leq 0.05$ (middle line) and the robust stability boundary for $|\delta a| \leq 0.04$, $|\delta p| \leq 0.1$, $|\delta d| \leq 0.1$ (inner line).

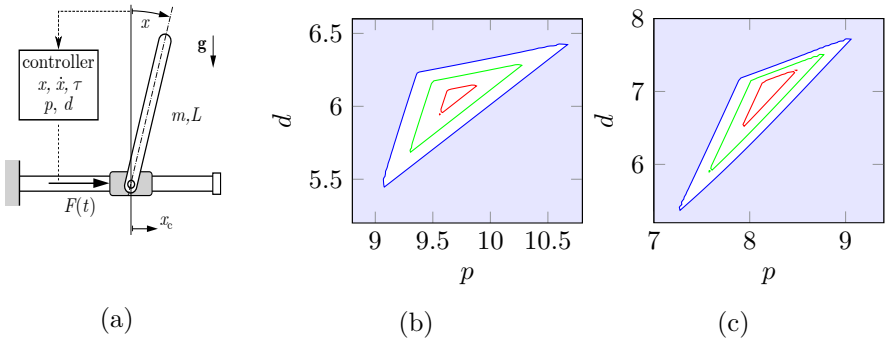

Figure 6.6: Panel (a) represents the mechanical model of an inverted pendulum (x_c is a cyclic coordinate that can be eliminated from the essential motion of the pendulum). Panels (b), (c) show the stability boundaries and the robust stability boundaries for system (6.41): in (b) we consider $a = -2.5, t_w = 1.2$, $t_a = 0.8$, in (c) $a = -2.5, t_w = 0.8$, $t_a = 0.8$. The shaded area represents the unstable region.

6.6 Stability robustness of milling operations

Manufacturing industry faces significant challenges in high speed cutting, because self-excited vibrations often arise during machining operations, such as milling and turning. These vibrations spoil the surface quality, increase the wear and reduce the productivity. The evolution of the unstable vibrations are described by TPDDEs, which originates from the so-called surface regeneration effect [120, 119]: the geometry of the chip is modified by the relative motion between the tool and workpiece, which induces variation in the cutting force. The vibrations in the past are preserved by the surface of the workpiece, which affects every subsequent cut by the modified geometry of the chip that depends on present and past states, too. When the stationary solution of the TPDDE loses stability, the amplitude of vibration increases until the tool loses contact with the workpiece. This large-amplitude self-excited vibration is called chatter. The domain of chatter free machining parameters is visualized by the so-called

stability lobe diagrams, but deterministic models considered during calculations often fail to accurately predict dynamical behavior and therefore experimental cutting tests do not always match the expectations. One of the reasons is the uncertainties in the dynamical model that affect the prediction of chatter-free machining parameters. As a result of a collaboration with the Department of Applied Mathematics of the Budapest University of Technology and Economics (BME), we have investigated the robust stability of milling operations using the method described in this chapter. In the next subsection, we describe the modelization of a *general* milling operation using modal coordinates; the definition of the modes values and of the modal parameters is then grounded on *two sets of preliminary experiments* which must be conducted on the *specific* machine whose stability properties we are investigating. Later, additional chatter tests are executed on the machine; these are used to validate the construction of the model and, at the same time, the results of our numerical simulations. All of the performed tests, which were conducted in the laboratories of the BME, are described in subsection 6.6.2: for major details, we refer the interested reader to [56].

6.6.1 Modelling of milling operations

A regular cutting tool with uniform helix angle is presented in Figure 6.7(a). The equation of motion of the tool-tip subjected to time-dependent forcing can be described in the modal space by introducing the vector of the modal coordinates $q(t) \in \mathbb{R}^d$. In case of proportional damping models, the eigenmodes of the system are real and the equation can be written as

$$\ddot{q}(t) + [2\zeta_l \omega_{\mathrm{n},l}]\dot{q}(t) + [\omega_{\mathrm{n},l}^2]q(t) = U^\top F\big(t, r(t), r(t-\tau)\big), \tag{6.43}$$

where $F(t,\cdot) \in \mathbb{R}^2$ is the forcing vector at the tool-tip in the (x,y)-plane, d is the modeled number of degrees of freedom, $[\cdot] = \mathrm{diag}(\cdot) \in \mathbb{R}^{d\times d}$ are diagonal matrices, $\omega_{\mathrm{n},l}$ is the l-th natural angular frequency for $l = 1,\dots,d$, ζ_l is the corresponding relative damping ratio, $r(t) = [x(t), y(t)]^\top$ denotes the displacement of the tool-tip in the (x,y)-plane and $U \in \mathbb{R}^{2\times d}$ is the modal transformation matrix that connects the modal space and the tool-tip's motion as $r(t) = Uq(t)$ [31].

The cutting force acting at the tool-tip is described by *empirical force models*, that highly depend on the tool geometry and material properties. Next, we consider regular cutting tools with Z number of equally distributed cutting edges and with uniform helix angle β. Thus, the angular position of the j-th cutting edge ($j = 1,\dots,Z$) along the axial direction reads

$$\varphi_j(t,z) = \Omega\frac{2\pi}{60}t + \frac{2\pi}{Z}j - \frac{2\tan\beta}{D}z, \tag{6.44}$$

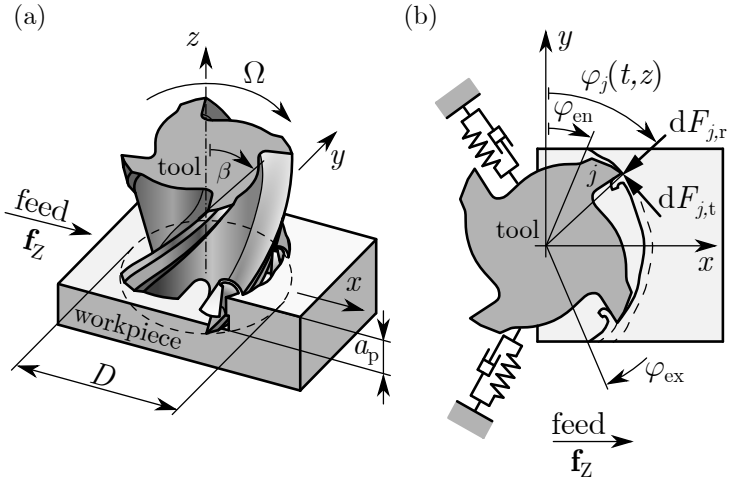

Figure 6.7: Dynamical model of milling in case of regular cutting tools with diameter D, helix angle $\beta = 45°$, $Z = 4$ cutting edges and depth of cut a_p. (a) Three-dimensional model; (b) Cutting forces acting on an elementary disk of width dz.

where z is the coordinate along the axial immersion and Ω is the spindle speed given in rpm (revolutions per minute). The cross-section of the cutter is presented in Fig. 6.7(b). The elementary cutting-force components in tangential and radial directions acting on tooth j at a disk element of width dz are given as

$$dF_{j,t}(t,z) = g_j(t,z) f_t\big(h_j(t,z)\big) dz, \tag{6.45}$$

$$dF_{j,r}(t,z) = g_j(t,z) f_r\big(h_j(t,z)\big) dz, \tag{6.46}$$

where $h_j(t,z)$ is the theoretical chip thickness cut by tooth j at axial immersion z; moreover $f_t(h)$ and $f_r(h)$ are the *empirical* cutting force characteristics assumed in the linear form

$$\begin{aligned} f_t(h) &= K_{t,e} + K_{t,c} h, \\ f_t(h) &= K_{r,e} + K_{r,c} h, \end{aligned} \tag{6.47}$$

where $K_{t,e}$ and $K_{r,e}$ are edge coefficients, and $K_{t,c}$ and $K_{r,c}$ are cutting coefficients in tangential and radial directions, respectively [1]. The indicator function $g_j(t,z)$ is a piecewise constant function which gives whether the cutting

edge is in contact with the material or not, and reads

$$g_j(t,z) = \begin{cases} 1, & \text{if } \varphi_{\text{en}} < \big(\varphi_j(t,z) \bmod 2\pi\big) < \varphi_{\text{ex}}, \\ 0, & \text{otherwise}, \end{cases} \tag{6.48}$$

where φ_{en} is the angle where the elementary disk starts cutting and φ_{ex} is the angular position where it leaves the workpiece, see Fig. 6.7(b). The actual chip thickness cut by tooth j at axial immersion z then can be calculated approximately as

$$h_j(t,z) \approx \begin{bmatrix} \sin\varphi_j(t,z) \\ \cos\varphi_j(t,z) \end{bmatrix}^{\top} \big(f_{\text{Z}} + r(t) - r(t-\tau)\big), \tag{6.49}$$

where $f_{\text{Z}} = [f_{\text{Z}}, 0]^{\top}$ is the feed per tooth in direction x, and the time-delay (now equal to the tooth-passing period) in case of equally distributed cutting edges is $\tau = 60/(Z\Omega)$. The resultant cutting force vector in the (x,y)-plane concentrated theoretically at the tool-tip is calculated as

$$F(t,\cdot) = -\sum_{j=1}^{Z} \int_0^{a_{\text{p}}} T_j(t,z) \begin{bmatrix} f_{\text{t}}\big(h_j(t,z)\big) \\ f_{\text{r}}\big(h_j(t,z)\big) \end{bmatrix} g_j(t,z)\mathrm{d}z, \tag{6.50}$$

where the transformation matrix is written as

$$T_j(t,z) = \begin{bmatrix} \cos\varphi_j(t,z) & \sin\varphi_j(t,z) \\ -\sin\varphi_j(t,z) & \cos\varphi_j(t,z) \end{bmatrix}. \tag{6.51}$$

Inserting the regenerative forcing model into the governing equation, then assuming small perturbation $\eta(t)$ about the periodic motion $q_{\text{p}}(t)$ of the stationary cutting, i.e., $q(t) = q_{\text{p}}(t) + \eta(t)$, the equation of the variational system omitting the periodic term is written as

$$\ddot{\eta}(t) + [2\zeta_l\omega_{\text{n},l}]\dot{\eta}(t) + [\omega_{\text{n},l}^2]\eta(t) = U^{\top}G(t)U\big(\eta(t) - \eta(t-\tau)\big), \tag{6.52}$$

where the directional matrix $G(t) = G(t+\tau)$ is introduced as

$$\begin{aligned} G(t) &= \frac{\partial F}{\partial r(t)}\big(t, r_{\text{p}}(t), r_{\text{p}}(t-\tau)\big) = \\ &= -\sum_{j=1}^{Z} \int_0^{a_{\text{p}}} T_j(t,z) \begin{bmatrix} K_{\text{t,c}} \\ K_{\text{r,c}} \end{bmatrix} \begin{pmatrix} \sin\varphi_j(t,z) \\ \cos\varphi_j(t,z) \end{pmatrix}^{\top} g_j(t,z)\mathrm{d}z, \end{aligned} \tag{6.53}$$

where the dependency on $g_j(t,z)$ for $j = 1,\ldots,Z$ make $G(t)$ discontinuous but piecewise smooth, see [30]. The TPDDE (6.52) can be rewritten into a first-order form

$$\begin{bmatrix} \dot{\eta}(t) \\ \ddot{\eta}(t) \end{bmatrix} = \begin{bmatrix} 0_d & I_d \\ -[\omega_{\text{n},l}^2] + U^{\top}G(t)U & -[2\zeta_l\omega_{\text{n},l}] \end{bmatrix} \begin{bmatrix} \eta(t) \\ \dot{\eta}(t) \end{bmatrix} +$$

$$\begin{bmatrix} 0_d & 0_d \\ -U^\top G(t) U & 0_d \end{bmatrix} \begin{bmatrix} \eta(t-\tau) \\ \dot{\eta}(t-\tau) \end{bmatrix}, \tag{6.54}$$

where I_d is the $d \times d$ identity matrix and 0_d is the $d \times d$ zero matrix. Given the discontinuity of G, we investigate the (robust) stability of (6.54) adopting the discretization of the domain $[-\tau, +T]$ as described in Section 6.5.

6.6.2 Case study and experiment

Experimentally determined stability limits are often different from the ones predicted based on a dynamical model. It is known that natural frequencies and damping ratios measured on the rotating spindle differ from the ones measured on the idle tool, and this effect can be responsible for variations in the stability lobe diagrams. However, these characteristics can be measured prior to the experiments or predicted based on preliminary chatter tests. In order to define values of the modes and of the modal parameters, two different approaches can be used: in the first one, we can compute the dominant modes and the modal parameters for the machine running in idle conditions, and assume these quantities as independent from the spindle speed; in the second one, some preliminary chatter tests can be performed and a dependency between the modes and the spindle speed can be introduced. In our work, the robust stability analysis is performed on the second model, but we will see that the first approach is instrumental to the second.

In what follows, we now consider an NCT EmR-610Ms milling machine defined by the machining parameters in Table 6.1. For the first approach, we

Table 6.1: Machining parameters

Tool	Workpiece Al2024-T351	Process
$Z = 2$	$K_{\mathrm{t,e}} = 16$ N/mm	50% down-milling
$D = 16$ mm	$K_{\mathrm{t,c}} = 1095$ MPa	$\varphi_{\mathrm{en}} = 90°$
$\beta = 30°$	$K_{\mathrm{r,e}} = 34$ N/mm	$\varphi_{\mathrm{ex}} = 180°$
	$K_{\mathrm{r,c}} = 176$ MPa	$f_Z = 0.1$ mm/tooth

performed an experimental modal analysis (EMA) on the real cutting tool during idle conditions, by measuring the responses and the excitations in directions x and y at the tool tip. The identified *spindle-speed independent* dominant modes and modal parameters for the system (6.54) are given in Table 6.2, where upper index zero in $\omega_{\mathrm{n},l}^{(0)}$ now refers to the reference value for the l-th natural frequency measured in idle state.

For the second approach, the cutter is replaced by a cylindrical dummy tool and a thorough operational modal analysis (OMA) was performed from 0 rpm

Table 6.2: Modal parameters measured at the tool tip

l	$\omega_{\mathrm{n},l}^{(0)}$ (Hz)	$\zeta_l^{(0)}$ (%)	$U_l \cdot 10^3$ ($\mathrm{kg}^{-1/2}$)
1	752.8	1.86	2.14 $[0\ 1]^\top$
2	782.7	1.84	1.92 $[1\ 0]^\top$
3	2063.5	3.24	3.59 $[0\ 1]^\top$
4	2351.4	2.51	3.37 $[1\ 0]^\top$

to 13000 rpm. In order to simulate the conditions of the cutting process (e.g. the interaction between the tool and the workpiece), during the OMA the tool was hit by a small bullet and vibrations were measured by a high-precision laser sensor. Then natural frequencies and damping ratios corresponding to the vibration modes of the real tool were identified, and the difference was scaled proportionally to match the modal parameters of the real cutter. The fitted data in the range 5000 – 13000 rpm can be seen in Fig. 6.8, where black dots denote the experimental data, while the dashed curves are second-order polynomials fitting the data. The *spindle-speed dependent* modes and modal parameters for the system (6.54) are computed by means of these polynomial, whose coefficients are reported in Table 6.3. Note that variation in the modeshapes U_l are difficult to measure and are often neglected (see [103]); in this study we then assume that the modeshapes do not change with the spindle speed, and we therefore still consider the values in Table 6.2.

Table 6.3: Change of modal parameters with the spindle speed ($\rho_k(\Omega) = a_{0,k} + a_{1,k}\Omega + a_{2,k}\Omega^2$, $\Omega \in [5000, 13000]$) and their uncertainty ($\Delta_k = \text{conts.}$)

ρ_k	$a_{0,k}$	$a_{1,k} \cdot 10^3$	$a_{2,k} \cdot 10^6$	Δ_k
$\omega_{\mathrm{n},1}$ (Hz)	751.43	1.6050	-0.269	7.89
$\omega_{\mathrm{n},2}$ (Hz)	779.74	0.7423	-0.239	9.09
$\omega_{\mathrm{n},3}$ (Hz)	2072.7	2.4369	-0.225	8.13
$\omega_{\mathrm{n},4}$ (Hz)	2354.6	1.4227	-0.176	8.49
ζ_1 (%)	2.042	-0.046	0.0212	0.81
ζ_2 (%)	1.940	-0.040	0.0180	0.42
ζ_3 (%)	3.236	-0.112	0.0122	0.42
ζ_4 (%)	2.711	-0.079	0.0083	0.27
$K_{\mathrm{t,c}}$ (MPa)	1095	-	-	109.5
$K_{\mathrm{r,c}}$ (MPa)	176	-	-	17.6

In Figure 6.9 we represent two stability boundaries for the system (6.54) assuming the process parameters in Table 6.1. One boundary (dashed black

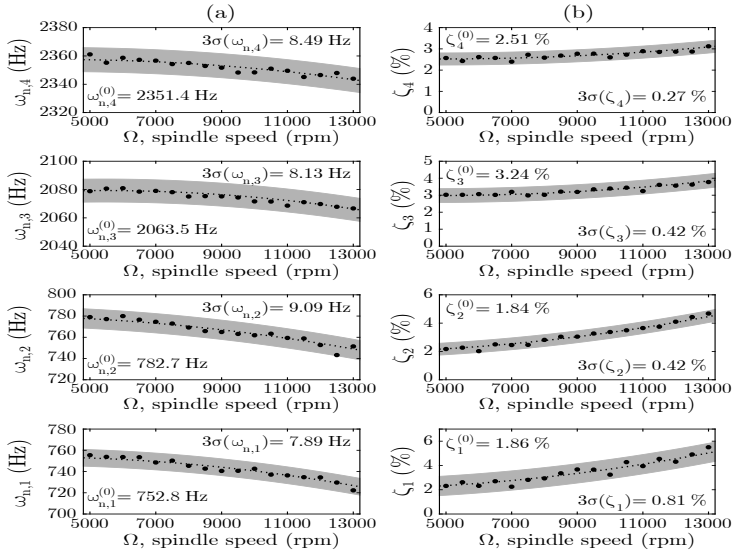

Figure 6.8: Change of modal parameters along the spindle speed. (a) Natural frequencies (b) Damping ratios. Black dots denote the fitted modal parameters, dashed curves are the fitting polynomials and gray region is the constant $\pm 3\sigma$ uncertainty region around the fitted mean.

line) corresponds to the *spindle-speed independent* model, while the other (solid blue line) corresponds to the *spindle-speed dependent* model. In the same figure, we report the results for *additional* experimental real chatter tests that were carried out with fine resolution from spindle speed 5000 rpm to 13000 rpm. Accelerometers were mounted onto the workpiece and spindle housing, moreover a microphone was also placed close to the machining area. Chatter was identified based on the spectra of the signals measured during cutting. Each measured point was marked by a circle if the operation was stable, by a cross if it was unstable, and by a triangle if chatter was not clearly identifiable. It is easy to see that the spindle-speed dependent approach allows to better describe the experimental chatter tests: for this reason, the robust stability analysis is performed on this model.

The uncertainty bound is determined by calculating the standard deviation (σ) around the mean of the fitted data shown in Figure 6.8. The uncertainty is then set equal to $\pm 3\sigma$, and it is represented with a gray region in Figure 6.8; therefore, the uncertainty is assumed to be constant. This deviation gives $\Delta_k \in \mathbb{R}$, $k = 1, ..., 8$, scalar parametric uncertainties on the speed-dependent modal parameters, which are included in Table 6.3. The cutting force characteristics were identified from preliminary cutting tests, where the tangential and radial

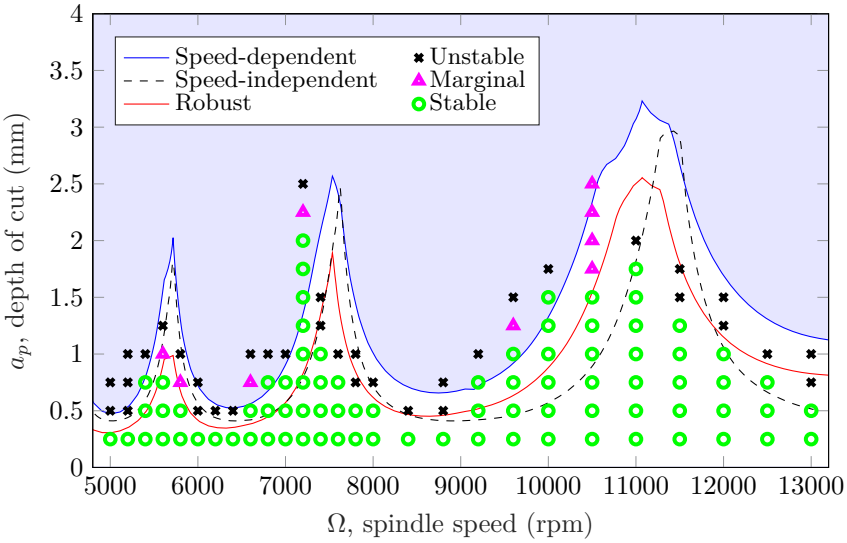

Figure 6.9: Experimental chatter tests are plotted against different stability diagrams: dashed black – speed-independent modal parameters, solid blue – speed-dependent modal parameters, solid red – robust stable for speed-dependent modal parameters.

cutting coefficients $K_{\mathrm{t,c}}$ and $K_{\mathrm{r,c}}$ were both assumed to have 10% relative uncertainty, see the last row of Table 6.3.

Therefore, we assume that the ten uncertainties reported in Table 6.3 affect the system (6.54), where the modal parameters depend on the spindle speed as already illustrated. Since $\omega_{\mathrm{n},l}$ and ζ_l show up nonlinearly in the system (6.54), we rewrite it into a larger system of TPDDEs by introducing a slack variable $v(t) = [\omega_{\mathrm{n},l}]\eta(t)$; then, the linearity is established and the system reads as follows

$$\overbrace{\begin{bmatrix} 0_d & 0_d & 0_d \\ I_d & 0_d & 0_d \\ 0_d & I_d & 2\zeta_l \end{bmatrix}}^{:=E} \begin{bmatrix} \dot\eta(t) \\ \ddot\eta(t) \\ \dot v(t) \end{bmatrix} = \begin{bmatrix} [\omega_{\mathrm{n},l}] & 0_d & -I_d \\ 0_d & I_d & 0_d \\ U^\top G(t) U & 0_d & -[\omega_{\mathrm{n},l}] \end{bmatrix} \begin{bmatrix} \eta(t) \\ \dot\eta(t) \\ v(t) \end{bmatrix} + \begin{bmatrix} 0_d & 0_d & 0_d \\ 0_d & 0_d & 0_d \\ -U^\top G(t) U & 0_d & 0_d \end{bmatrix} \begin{bmatrix} \eta(t-\tau) \\ \dot\eta(t-\tau) \\ v(t-\tau) \end{bmatrix}. \tag{6.55}$$

Observe that the leading matrix E of the system is not the identity matrix anymore, and that it is perturbed by the uncertainty affecting ζ_l: however,

the reasoning illustrated in Section 6.2 can be trivially extended to account for uncertain leading matrices as well. Regarding the computation of Floquet multipliers as introduced in Section 6.3, it is easy to see that I_n in the definition of matrix $B_1^{(t)}$ must be replaced by E.

In Figure 6.9 we indicate with a red solid line the robust stability boundary for the system (6.55) affected by uncertainty: although small uncertainties were assumed initially in the model, the robust stable maximum depth of cuts at the lowest points decrease by nearly 30%. On the other hand by measuring the vertical differences, 0.15–1 mm wide uncertainty band can be observed, which is also significant.

While most of the points are captured by the robust domain, some points lie outside the safe region, which indicates that there are still modeling errors and uncertainties present. Possible reasons can be the linear force characteristics used during calculations or the dynamical model with proportional damping which are simplifications of the complicated reality.

6.7 Conclusions

In this chapter we presented, to the best of the authors' knowledge, the first Floquet multipliers-based method to assess the stability robustness of a system of TPDDEs: the method computes the largest Floquet multiplier arising within a class of real-valued structured perturbations on the coefficient matrices A_i, and it is not conservative as it is grounded on a necessary and sufficient condition for the stability robustness. The uncertainties can be considered as either constant or periodically-varying. The method is easily extended to TPDDEs with discontinuous periodic functions and to TPDDEs with periodically-varying delays, which are very common in engineering applications: examples and numerical simulations are presented for an inverted pendulum subject to an act-and-wait controller, for a turning operation with spindle speed variation. Simulations for the robustness stability of a milling operation are tested against experimental results showing a satisfactory matching.

Instrumental to the methodology for assessing robust stability, a novel solver for the computation of Floquet multipliers has also been introduced, based on the approximation of the solution of the system of equations with a piecewise polynomial obtained as a truncated series of Chebyshev polynomials. The proposed solver results in the solution of a generalized eigenvalue problem whose entries are linear w.r.t. samples of the original system matrices in the time interval $[0, T]$.

Chapter 7

Conclusions

The main goal of this dissertation has been the development of novel algorithms to compute popular measures that assess the robust stability of dynamical systems. We have especially focused on time-delay systems, as before this thesis work, methods to compute quantities like the distance to instability and the pseudospectral abscissa were only available for specific systems and/or classes of perturbations.

With the purpose of introducing tools that are well motivated by applications, we have tried to consider classes of *real-valued* perturbations which are *as broad as possible*. As a matter of fact, the methods introduced for dynamical systems of LTI DDEs account for *structured* perturbations on the coefficient matrices, as well as uncertainties on the delay terms. Similarly, for systems of TPDDEs the presented methodology can handle *time-periodic, structured, real-valued* perturbations affecting the nominal matrices. In addition, the considered robust measures are not conservative, in the sense that they exploit an eigenvalue-based necessary and sufficient condition for the robust stability.

The practical use of the proposed algorithms is highlighted through the description of several applications: examples concern the design of robust feedback controllers for uncertain systems, and of decentralised controllers for interconnected time-delay systems with a network structure. Regarding systems of TPDDEs, the robust analysis can be employed to improve the performance of material removal processes which are widely used in engineering applications, such as the milling or the turning operation.

In this section, we will give a chapter by chapter overview of the contributions of this thesis, while in the next one we will formulate some possible directions for the future research.

Chapter 2: We consider a general class of EPs including PEPs, DEPs as well as linear EPs (standard, generalized). A set of real-valued unstructured

uncertainties is assumed to perturb the nominal matrices of the EP, and either the spectral or the Frobenius norm are adopted to bound the magnitude of each uncertainty. For both norms, it is demonstrated that the pseudospectral abscissa is generated by a set of *optimal* perturbations with maximal norm; another notable property of these perturbations is that they all have low-rank, which enables us to define a projected-gradient method over a search space of smaller dimensions. Besides the extension of the method from linear to nonlinear EPs, a significant contribution is the development of an algorithm which *indistinctly* converges to a real or complex globally rightmost point of the pseudospectrum. In addition, the low rank property is exploited to adapt the algorithm also to large-scale sparse nonlinear EPs (e.g., related to the (discretizations of) distributed parameter systems).

Chapter 3: This chapter analyses the case of a DEP associated with a system of DDAEs of retarded type, where *structured* uncertainties are defined on the nominal matrices, and the delay terms are assumed uncertain as well. Moreover, the possible interdependency among the matrix uncertainties is also considered. An algorithm to compute the pseudospectral abscissa is then presented, where the low-rank property of the optimal perturbations still holds. However, we demonstrate that *optimal structured* perturbations surprisingly might not have maximal norm, which results in a substantial modification of the algorithm presented in the previous chapter. The close connection between the notions of pseudospectral abscissa and distance to instability is then exploited, with the latter one being computed by means of a Newton-bisection method.

Chapter 4: It is easily proven that systems of DDAEs allow to systematically model interconnections of systems without the need for elimination of variables, including the interconnection between a plant model and a controller with fixed order or structure. The chapter exploits this property and proposes a novel method to design robust controllers for uncertain systems of DDAEs. The method grounds on the minimization of the pseudospectral abscissa, and uses a popular algorithm for non-smooth, non-convex optimization. In addition, we also present a methodology to design stabilizing fixed-order decentralised controllers for LTI large-scale interconnected time-delay systems with a network structure. The nodes of the network are assumed to host identical dynamic systems coupled with identical local controllers. The key ingredient is a decoupling transformation, which enables to reduce the information about the network topology to allowed values of a scalar eigenvalue parameter. By viewing this parameter as uncertainty, captured by the pseudospectral abscissa, we design decentralised controllers which achieve stability independently of the number of nodes of the network.

Chapter 5: In this chapter, we define another method to compute the distance to instability of time-delay systems of retarded type. The adopted strategy is based on the characterization of the distance to instability as the reciprocal of the global maximum of a structured singular value function. Compared to the method introduced in Chapter 3, the set of uncertainties is measured with a different norm, and it is also restricted to a more specific class of real-valued structured perturbations. On the other hand, the algorithm presented here globally converges, and the exhibited rate of convergence is quadratic. The method exploits the fact that the intersections of a constant function with a singular value function can be characterized as the imaginary axis eigenvalues of an Hamiltonian DEP with positive and negative delays. Instrumental to this method, we also propose a novel numerical solver to compute these imaginary characteristic roots, which combines a spectral discretization approximating the DEP with a linear EP, an automatic procedure to determine the number of discretization points, and a block-Newton correction to eliminate the approximation error.

Chapter 6: In this chapter, we aim at extending the proposed methods and algorithms for the robust stability from DDEs to TPDDEs. In order to still rely on an eigenvalue-based approach, we propose a novel solver for the computation of Floquet multipliers: these are computed as the roots of a GEP which is linear w.r.t. the entries of the nominal matrix functions of the system of TPDDEs. Thanks to this property, the Floquet pseudospectral radius of a system of TPDDEs affected by real-valued, structured and potentially time-periodic uncertainties is approximated by the largest eigenvalue in the pseudospectrum appropriately defined for the GEP. We still use a projected-gradient method to compute the Floquet pseudospectral radius, where the objective function of the maximization is now the modulus of the largest eigenvalue of the perturbed GEP. Several common problems in engineering applications have been investigated with the proposed methodology, such as the stabilization of linear systems by means of act-and-wait controllers, the turning and the milling operations. In particular, the numerical simulations for the latter have been tested against the experimental results, showing a satisfactory matching within the limits imposed by the modeling of a very complex problem.

7.1 Future research

We discuss a few possible directions for the future research:

- An extended version of the algorithm presented in Chapter 3 is currently being developed. This update allows to compute the pseudospectral abscissa of a DEP affected by both complex- and real-valued structured

uncertainties on the nominal matrices, in addition to disturbances on the delay values. There are several benefits of such an algorithm. First, given its close connection with the concept of distance to instability, it allows to compute the *robust* $\mathcal{H}_\infty$ norm of an uncertain time-delay system. Second, considering structured complex-valued uncertainties only, it allows to define fixed-order decentralised controllers for LTI large-scale interconnected time-delay systems as in Chapter 4, but this time network structures whose associated adjacency matrices admit complex-valued eigenvalues fall into the scope.

- In this dissertation, we have considered systems of DDAEs of retarded type because, as demonstrated in [89], the spectral abscissa of DEPs of neutral type may be sensitive to infinitesimal delay perturbations. In addition, the spectrum of DEPs of neutral type is characterized by chains of eigenvalues whose imaginary parts go to infinity while the real parts remain finite: this implies that a stability loss may also occur when the eigenvalues cross the imaginary axis at infinite frequencies. In order to extend the method to DDAEs of neutral type, a similar approach to [54] should be adopted: first, we must consider the worst-case asymptotic behaviour, i.e. for infinite frequencies; then, using the technique seen in this dissertation, we analyse the worst-case scenario for finite frequencies only, and finally we set the pseudospectral abscissa equal to the maximum of the two values. The well-posedness of DDAEs of neutral type also relies on Assumption 3.2, as this guarantees the principle of causality and prevents the system from having impulsive solutions. As already seen in Chapter 3, the class of perturbations must be defined in order to preserve the validity of Assumption 3.2 for any possible uncertainty.

- For LTI delay systems, the worst-case setting for uncertain delay values was easy to handle because the derivative of the rightmost eigenvalue w.r.t. the delay could be easily retrieved by the characteristic matrix. For TPDDEs, handling uncertainties on the delays (as well as on the period T) turns out to be more involved. Small variations of the delays and of the period may indeed induce a new discretization of the problem (i.e. a different number of subintervals Ω_j) and thus some non-smoothness in the approximation of the Floquet multipliers. This is an open problem and should be further investigated. However, there are some special cases where uncertainties on the delays and the period can be easily handled with the method introduced in Chapter 6: suppose for simplicity that we have a single delay τ, and that the relation $T = a\tau$ for $a \in \mathbb{R}$ always holds. Then, using the simple substitution $x(s) = x(t/\tau)$, our domain becomes $[-1, a]$ and the delay value τ can be included as an (uncertain) parameter multiplying the matrices of the system.

Appendix A

Eigenvalues and Eigenvectors

We consider a matrix $M \in \mathbb{C}^{n\times n}$,

$$M = \begin{bmatrix} m_{11} & \dots & m_{1n} \\ \vdots & \vdots & \vdots \\ m_{n1} & \dots & m_{nn} \end{bmatrix}$$

where $\mathbb{C}$ is the field of complex numbers. The *standard eigenvalue problem* associated with the matrix M is defined as follows

$$(\lambda I_n - M)y = 0, \tag{A.1}$$

where I_n is the *identity matrix* with dimension n, $\lambda \in \mathbb{C}$ is an *eigenvalue* of M and $y \in \mathbb{C}^n,\ y \neq 0$, is the *right eigenvector* associated with λ. The couple $(\lambda, y) \in \mathbb{C} \times \mathbb{C}^n$ is defined as an eigenpair of the standard eigenvalue problem. In addition to the right eigenvector y, there also always exists a *left eigenvector* $x \in \mathbb{C}^n,\ x \neq 0$, associated with λ, such that

$$x^*(\lambda I_n - M) = 0,$$

where x^* indicates the conjugate vector of x. The matrix $(\lambda I_n - M)$ is the *characteristic matrix* of the eigenvalue problem; the eigenvalues of M can be computed as solutions of the characteristic equation of problem (A.1), which can always be written in a polynomial form

$$0 = \det(\lambda I_n - M) = (\lambda - \lambda_1)(\lambda - \lambda_2)\cdots(\lambda - \lambda_n), \tag{A.2}$$

from which is clear that a standard eigenvalue problem of dimension n admits at the most n different eigenvalues $\lambda_1, \dots, \lambda_n$. The set of the eigenvalues of a matrix M form its *spectrum* $\Lambda(M)$.

- The algebraic multiplicity $\mu_M(\lambda_i)$ of an eigenvalue λ_i is the largest integer such that $(\lambda - \lambda_i)^{\mu_M(\lambda_i)}$ divides evenly the polynomial on the right-hand side of (A.2). If $\mu_M(\lambda_i) = 1$ then λ_i is a *simple* eigenvalue, otherwise it is a *multiple* eigenvalue;
- The geometric multiplicity $\gamma_M(\lambda_i)$ of an eigenvalue λ_i is the dimension of the kernel (or nullspace) of the matrix $(\lambda_i I_n - M)$, i.e. of the space

$$K_i = \{y : (\lambda_i I_n - M)y = 0\}.$$

  It can be proved that $\gamma_M(\lambda_i) \leq \mu_M(\lambda_i)$: if λ_i is a multiple eigenvalue such that $\mu_M(\lambda_i)$=$\gamma_M(\lambda_i)$, then λ_i is called a *semi-simple* eigenvalue.

In this dissertation we will largely exploit the notion of *rank* of a matrix, which is formally defined as the dimension of the vector space spanned by its columns (or rows). A simple property relating the rank of a square matrix M to its eigenvalues states that the rank of M is equal to the number of nonzero eigenvalues of M (considered with their algebraic multiplicity). Therefore, if $\text{rank}(M) = n$ then M is full-rank and thus *invertible*. On the other hand, if there is at least one eigenvalue equal to 0, the matrix M is *singular*.

Singular Value Decomposition

Given a matrix $M \in \mathbb{C}^{m \times n}$, its *singular value decomposition* (SVD) is defined as follows

$$M = U\Sigma V^*, \tag{A.3}$$

where

- $\Sigma \in \mathbb{R}^{m \times n}$ is a diagonal matrix with non-negative real entries on the diagonal: these values are the *singular values* of M and they are usually indicated as $\sigma_i = \Sigma_{ii}$ for $i = 1, \ldots, \min\{m, n\}$; by convention we order them in order to have $\sigma_1 \geq \sigma_2 \geq \cdots \geq \sigma_{\min\{m,n\}} \geq 0$;
- $U \in \mathbb{R}^{m \times m}$ is a unitary matrix, i.e. such that $U^*U = UU^* = I_m$, with U^* the conjugate of U;
- $V \in \mathbb{R}^{n \times n}$ is also a unitary matrix.

The i-th column u_i of matrix U and the i-th column v_i of matrix V are the *left* and *right singular vector* for σ_i respectively, and the following relations hold

$$Mv_i = \sigma_i u_i, \qquad M^* u_i = \sigma v_i.$$

It can be proved that the non-zero singular values of M are the square roots of the non-zero eigenvalues of both M^*M and MM^*.

If the matrix M has rank $r < \min\{m, n\}$, then the *compact singular value decomposition* can be introduced

$$M = U_r \Sigma_r V_r^*,$$

where now $U_r \in \mathbb{R}^{m\times r},\ \Sigma_r \in \mathbb{R}^{r\times r},\ V_r \in \mathbb{R}^{n\times r}$, the diagonal entries of Σ_r are the r non-zero singular values of M, and the columns of $U_r,\ V_r$ are the left and right singular vectors associated with $\sigma_1, \ldots, \sigma_r$.

The SVD decomposition of a matrix can also be used to compute two popular matricial norms:

- The spectral norm

$$\|M\|_2 := \max_{y\in\mathbb{C}^n} \frac{\|My\|}{\|y\|} = \max_{\substack{y\in\mathbb{C}^n \\ \|y\|=1}} \|My\| = \sigma_1(M); \tag{A.4}$$

- The Frobenius norm

$$\|M\|_F := \sqrt{\sum_{i,j=1}^{n} m_{ij}^2} = \sqrt{\sigma_1^2(M) + \cdots + \sigma_{\min\{m,n\}}^2(M)}. \tag{A.5}$$

Given the SVD of a matrix M with rank n, M can always be written as a sum

$$M = \sum_{i=1}^{n} \sigma_i u_i v_i^*. \tag{A.6}$$

Given this expression, it is very easy to see that for any square invertible $M \in \mathbb{C}^{n\times n}$, the matrix $M - \sigma_n u_n v_n^*$ is singular, and thus that

$$\sigma_{\min}(M) = \sigma_n(M) = \min_{\|\Delta\|_2} \{\Delta \in \mathbb{C}^{n\times n} : M + \Delta \textit{ is a singular matrix}\}. \tag{A.7}$$

Before we conclude, we demonstrate another important property of the largest singular value of a matrix M: let us consider a square matrix $M \in \mathbb{C}^{n\times n}$ with rank n and its SVD (A.3), and suppose we want to find the following quantity

$$\inf_{\Delta\in\mathbb{C}^{n\times n}} \{\|\Delta\|_2 : \det(I - M\Delta) = 0\}.$$

Let us adopt the decomposition $\Delta = V\widetilde{\Delta}U^*$, then

$$\det(I - M\Delta) = \det(I - U\Sigma V^* V\widetilde{\Delta}U^*) = \det(I - U\Sigma\widetilde{\Delta}U^*) = \det(I - \Sigma\widetilde{\Delta}),$$

where the last equality is possible because of the well-known property $\det(I - AB) = \det(I - BA)$. Now, in order to make $I - \Sigma\widetilde{\Delta}$ singular, the matrix $\Sigma\widetilde{\Delta}$

must have one eigenvalue equal to one. Then, with the aim of minimizing $\left\|\widetilde{\Delta}\right\|_2$, it suffices to choose

$$\widetilde{\Delta} = \left(\begin{array}{c|c} (\sigma_1(M))^{-1} & 0\cdots 0 \\ \hline 0 & \\ \vdots & [\widetilde{\Delta}]_{11} \\ 0 & \end{array}\right),$$

where the submatrix $[\widehat{\Delta}]_{11}$ obtained by eliminating the first row and the first column can be arbitrarily chosen, provided that it satisfies $\left\|[\widehat{\Delta}]_{11}\right\|_2 \leq (\sigma_1(M))^{-1}$. Therefore, the following holds

$$\frac{1}{\sigma_1(M)} = \inf_{\Delta\in\mathbb{C}^{n\times n}} \{\|\Delta\|_2 : \det(I - M\Delta) = 0\}.$$

Bibliography

[1] Altintas, Y. *Manufacturing Automation: Metal Cutting Mechanics, Machine Tool Vibrations, and CNC Design*. Cambridge University Press, Cambridge, 2012.

[2] Amiraslani, A., Corless, R. M., and Lancaster, P. Linearization of matrix polynomials expressed in polynomial bases. *IMA J. Numer. Anal. 29* (2009), 141–157.

[3] Arnoldi, W. The principle of minimized iterations in the solution of the matrix eigenvalue problem. *Q. Appl. Math. 9* (1951), 17–29.

[4] Bernhardsson, B., Rantzer, A., and Qiu, L. Real perturbation values and real quadratic forms in a complex vector space. *Linear Algebra Appl. 270* (1998), 131–154.

[5] Betcke, T., Higham, N. J., Mehrmann, V., Schröder, C., and Tisseur, F. Nlevp: A collection of nonlinear eigenvalue problems. *ACM Trans. Math. Softw. 39* (2013), 7:1–7:28.

[6] Borgioli, F., Hajdu, D., Insperger, T., Stépán, G., and Michiels, W. Pseudospectral method for assessing stability robustness for linear time-periodic delayed dynamical systems. *Int. J. Numer. Meth. Eng.* (2019). Submitted for publication, preprint available as Internal Report TW690, Department of Computer Science, KU Leuven, Belgium. URL: http: //www.cs.kuleuven.be/publicaties/rapporten/tw/TW690.abs.html.

[7] Borgioli, F., and Michiels, W. Computing the distance to instability for delay systems with uncertainties in the system matrices and in the delay terms. In *Proc. of the 2018 European Control Conference (ECC), Limassol, Cyprus*, pp. 1201–1207.

[8] Borgioli, F., and Michiels, W. Robust stabilisation of linear time-delay systems with uncertainties in the system matrices and in the delay terms. In *Proc. of the 14th IFAC Workshop on Time Delay Systems, Budapest, Hungary, 2018*, pp. 312–317.

[9] Borgioli, F., and Michiels, W. A design approach for structured controllers for uncertain delay systems grounded in the real structured pseudospectra framework. In *Stability, Control and Application of Time-Delay Systems*. Elsevier, 2019, pp. 185–207.

[10] Borgioli, F., and Michiels, W. A novel method to compute the structured distance to instability for combined uncertainties on delays and system matrices. *IEEE T. Automat. Contr.* (2019). DOI: 10.1109/TAC.2019.2934182.

[11] Borgioli, F., Michiels, W., and Guglielmi, N. Characterizing and computing real pseudospectral abscissa for nonlinear eigenvalue problems. Preprint available as Internal Report TW668, Department of Computer Science, KU Leuven, Belgium. URL: http://www.cs.kuleuven.be/publicaties/rapporten/tw/TW668.abs.html.

[12] Borgioli, F., Michiels, W., Lu, D., and Vandereycken, B. A globally convergent method to compute the real stability radius for time-delay systems. *Syst. Control Lett. 127* (2019), 44–51.

[13] Boyd, S., and Balakrishnan, V. A regularity result for the singular values of a transfer matrix and a quadratically convergent algorithm for computing its $\mathcal{L}_\infty$-norm. *Syst. Control. Lett. 15* (1990), 1–7.

[14] Breda, D., Maset, S., and Vermiglio, R. TRACE-DDE: A tool for robust analysis and characteristic equations for delay differential equations. In *Topics in Time Delay Systems: Analysis, Algorithm and Control*. Springer-Verlag Berling Heidelberg, 2009, pp. 145–155.

[15] Breda, D., Maset, S., and Vermiglio, R. Pseudospectral methods for stability analysis of delayed dynamical systems. *Int. J. Dynam. Control 2* (2014), 143–153.

[16] Breda, D., Maset, S., and Vermiglio, R. *Stability of Linear Delay Differential Equations: a Numerical Approach with MATLAB*. Springer-Verlag, New-York, 2015.

[17] Burke, J. V., Lewis, A. S., and Overton, M. L. Robust stability and a criss-cross algorithm for pseudospectra. *IMA J. Numer. Anal. 23* (2003), 359–375.

[18] Butcher, E. A., Ma, H., Bueler, E., Averina, V., and Szabo, Z. Stability of linear time-periodic delay-differential equations via chebyshev polynomials. *Int. J. Numer. Meth. Eng. 59* (2004), 895–922.

[19] Byers, R. A bisection method for measuring the distance of a stable matrix to the unstable matrices. *SIAM J. Sci. Stat. Comput. 9* (1988), 875–881.

[20] Chen, J., Gu, G., and Nett, C. A. A new method for computing delay margins for stability of linear delay systems. *Syst. Control Lett. 26* (1995), 107–117.

[21] De Souza, C. E., and Coutinho, D. F. Stability of linear discrete-time periodic systems with time-delay. Proc. 4th IFAC Workshop on Periodic Control Systems, August 26–28, 2010, Antalya, Turkey, pp. 51–56.

[22] De Souza, C. E., and Coutinho, D. F. Robust stability and control of uncertain linear discrete-time periodic systems with time-delay. *Automatica 50* (2013), 431–441.

[23] Demmel, J. *Applied Numerical Linear Algebra.* SIAM, Philadelphia, 1997.

[24] Deshmukh, V., Ma, H., and Butcher, E. A. Optimal control of parametrically excited linear delay differential systems via chebyshev polynomials. *Optim. Control Appl. Meth. 27* (2006), 123–136.

[25] Dieci, L., and Eirola, T. On smooth decompositions of matrices. *SIAM J. Matrix Anal. Appl. 20* (1999), 800–819.

[26] Diekmann, O., Van Gils, S. A., Verduyn Lunel, S. M., and Walther, H. O. *Delay equations: Functional, Complex and Nonlinear Analysis.* Springer-Verlag, New-York, 1995.

[27] Dileep, D., Borgioli, F., Hetel, L., Richard, J. P., and Michiels, W. A scalable design method for stabilising decentralised controllers for networks of delay-coupled systems. In *Proc. of the 5th IFAC Conference on Analysis and Control of Chaotic Systems, Eindhoven, The Nederlands, 2018*, pp. 68–73.

[28] Dileep, D., Van Parys, R., Pipeleers, G., Hetel, L., Richard, J. P., and Michiels, W. Design of robust decentralised controllers for mimo plants with delays through network structure exploitation. *Int. J. Control.* (2019). DOI: 10.1080/00207179.2018.1554268f.

[29] Ding, L., and Vandereycken, B. Criss-cross type algorithm for computing the real pseudospectral abscissa. *SIAM J. Matrix Anal. Appl. 38* (2017), 891–923.

[30] Dombovari, Z., Iglesias, A., Zatarain, M., and Insperger, T. Prediction of multiple dominant chatter frequencies in milling processes. *In. J. Mach. Tool. Manu. 51* (2011), 457 – 464.

[31] Dombovari, Z., and Stépán, G. The effect of helix angle variation on milling stability. *J Manuf. Sci. E-T ASME 134* (2012), 051015–1–6.

[32] Engelborghs, K., Dambrine, M., and Roose, D. Limitations of a class of stabilization methods for delay equations. *IEEE T Automat. Contr. 46* (2001), 336–339.

[33] Engelborghs, K., Luzyanina, T., and Samaey, G. DDE-BIFTOOL v. 2.00: a Matlab package for bifurcation analysis of delay differential equations. Tw report, Department of Computer Science, Katholieke Universiteit Leuven, Belgium, October 2001.

[34] Farkas, M. *Periodic Motions*. Springer-Verlag, New York, 1994.

[35] Francis, J. G. F. The QR transformation a unitary analogue transformation to the lr transformation - part 1. *Comput. J. 4* (1961), 265–271.

[36] Francis, J. G. F. The QR transformation - part 2. *Comput. J. 4* (1962), 332–345.

[37] Freitag, M. A., and Spence, A. A Newton-based method for the calculation of the distanceto instability. *Linear Algebra Appl. 435* (2011), 3189–3205.

[38] Fridman, E. Stability of linear descriptor systems with delay: a Lyapunov-based approach. *J. Math. Anal. Appl. 273* (2002), 24–44.

[39] Fridman, E. *Introduction to Time-Delay Systems: Analysis and Control*. Birkhäuser, Basel, 2014.

[40] Fridman, E. Tutorial on Lyapunov-based methods for time-delay systems. *Eur. J. Control 20* (2014), 271 – 283.

[41] Fridman, E., and Shaked, U. H_∞-control of linear state-delay descriptor systems: an LMI approach. *Linear Algebra Appl. 351-352* (2002), 271–302.

[42] Fridman, E., and Shaked, U. An improved stabilization method for linear time-delay systems. *IEEE T Automat. Contr. 47* (2002), 1931–37.

[43] Gahinet, P., and Apkarian, P. A linear matrix inequality approach to H_∞ control. *Int. J. Robust Nonlinear Control 4* (1994), 421–448.

[44] Genin, Y., Stefan, R., and Van Dooren, P. Real and complex stability radii of polynomial matrices. *Linear Algebra Appl. 351* (2002), 381–410.

[45] Gohberg, I., Lancaster, P., and Rodman, L. *Matrix Polynomials*. Academic Press, New York, 1982.

[46] Gomez, M. A., and Michiels, W. Characterization and optimization of the smoothed spectral abscissa for time-delay systems. *Int. J. Robust Nonlinear Control 29* (2019), 4402–4418.

[47] Green, K., and Wagenknecht, T. Pseudospectra and delay differential equations. *J. Comput. Appl. Math. 196* (2006), 567–578.

[48] Gu, K., Kharitonov, V. L., and Chen, J. *Stability of Time-Delay Systems*. Birkhäuser, Basel, 2003.

[49] Gu, K., Niculescu, S. I., and Chen, J. On stability of crossing curves for general systems with two delays. *J. Math. Anal. Appl. 311* (2005), 231–253.

[50] Guglielmi, N., and Lubich, C. Differential equations for roaming pseudospectra: paths to extremal points and boundary tracking. *SIAM J. Numer. Anal. 49* (2012), 1194–1209.

[51] Guglielmi, N., and Lubich, C. Low-rank dynamics for computing extremal points of real pseudospectra. *SIAM J. Matrix Anal. Appl. 34* (2013), 40–66.

[52] Guglielmi, N., and Overton, M. L. Fast algorithms for the approximation of the pseudospectral abscissa and pseudospectral radius of a matrix. *SIAM J. Matrix Anal. Appl. 32* (2011), 1166–1192.

[53] Gumussoy, S., and Michiels, W. A predictor-corrector type algorithm for the pseudospectral abscissa computation of time-delay systems. *Automatica 46* (2010), 657–664.

[54] Gumussoy, S., and Michiels, W. Fixed-order strong H-infinity control for interconnected systems using delay differential algebraic equations. *SIAM J. Control Optim. 49* (2011), 2212 – 2238.

[55] Hagan, M. T., Demuth, H. B., Beale, M. H., and De Jesus, O. *Neural Network Design*. 2014. 2nd Edition.

[56] Hajdu, D., Borgioli, F., Michiels, W., Takacs, D., Stépán, G., and Insperger, T. Robust stability of milling operations based on pseudospectral approach. *Int. J. Mach. Tool. Manu.* (2019). DOI: 10.1016/j.ijmachtools.2019.103516.

[57] Hale, J. K. *Theory of Functional Differential Equations*. Springer, New-York, 1977.

[58] Hammarling, S., Munro, C. J., and Tisseur, F. An algorithm for the complete solution of quadratic eigenvalue problems. *ACM Trans. Math. Software 39* (2013), 18:1–18:19.

[59] Hinrichsen, D., and Pritchard, A. J. Stability radius of structured perturbations and the algebraic Riccati equation. *Syst. Control Lett. 8* (1986), 105 – 113.

[60] Hochbruck, M., and Ostermann, A. Exponential integrators. *Acta Numer 19* (2010), 209–286.

[61] Hu, G., and Davison, E. J. Real stability radii of linear time-invariant time-delay systems. *Syst. Control Lett. 50* (2003), 209 – 219.

[62] Insperger, T., Kovacs, L. L., Galambos, P., and Stépán, G. Increasing the accuracy of digital force control process using the act-and-wait concept. *IEEE/ASME T Mech 15* (2010), 291–298.

[63] Insperger, T., Mann, B. P., Stépán, G., and Bayly, P. V. Stability of up-milling and down-milling, part 1: alternative analytical methods. *Int J Mach Tool Manu 43* (2003), 25–34.

[64] Insperger, T., and Stépán, G. Stability of the milling process. *Period. Polytech. Mech. Eng. 44* (2000), 47–57.

[65] Insperger, T., and Stépán, G. Semi-discretization method for delayed systems. *Int. J. Numer. Meth. Eng. 55* (2002), 503–518.

[66] Insperger, T., and Stépán, G. Stability chart for the delayed mathieu equation. In *Proc. of the Royal Society A* (2002), vol. 458, pp. 1989–1998.

[67] Insperger, T., and Stépán, G. On the dimension reduction of systems with feedback delay by act-and-wait control. *IMA J Math Control Inform 27*, 4 (2010), 457–473.

[68] Insperger, T., and Stépán, G. *Semi-Discretization for Time-Delay Systems*. Springer–Verlag, New-York, 2011.

[69] Jarlebring, E., Meerbergen, K., and Michiels, W. A Krylov method for the delay eigenvalue problem. *SIAM J. Sci. Comput. 32* (2010), 3278–3300.

[70] Jarlebring, E., Michiels, W., and Meerbergen, K. A linear eigenvalue algorithm for the nonlinear eigenvalue problem. *Num. Math. 122* (2012), 169–195.

[71] Jarlebring, E. *The spectrum of delay-differential equations: numerical methods, stability and perturbation.* PhD thesis, TU Braunschweig, Institut Computational Mathematics, 2008.

[72] Khasawneh, F. A., and Mann, B. P. A spectral element approach for the stability analysis of time-periodic delay equations with multiple delays. *Commun. Nonlinear. Sci. Numer. Simulat. 18* (2013), 2129–2141.

[73] Koch, O., and Lubich, C. Dynamical low rank approximation. *SIAM J. Matrix Anal. Appl. 29* (2007), 434–454.

[74] Kressner, D. A block Newton method for nonlinear eigenvalue problems. *Numer. Math. 114* (2009), 355–372.

[75] Kressner, D., and Vandereycken, B. Subspace methods for computing the pseudospectral abscissa and the stability radius. *SIAM J. Matrix Anal. Appl. 35* (2014), 292–313.

[76] Krstic, M. *Delay Compensation for Nonlinear, Adaptive and PDE systems.* Birkhäuser, Basel, 2009.

[77] Kublanovskaya, V. N. On some algorithms for the solution of the complete eigenvalue problem. *USSR Comput. Math. Math. Phys. 1* (1962), 637–657.

[78] Lawrence, C. T., Tits, A., and Van Dooren, P. A fast algorithm for the computation of an upper bound on the μ-norm. *Automatica 36* (2000), 449 – 456.

[79] Lehotzky, D., Insperger, T., Khasawneh, F. A., and Stépán, G. Spectral element method for stability analysis of milling processes with discontinuous time-periodicity. *Int. J. Adv. Manuf. Technol. 89* (2017), 2503–2514.

[80] Letyagina, O. N., and Zhabko, A. P. Robust stability analysis of linear periodic systems with delay. *Int. J. Mod. Phys. A 24* (2009), 893–907.

[81] Lewis, A., and Overton, M. L. Nonsmooth optimization via BFGS. Available from `http://cs.nyu.edu/overton/papers.html`.

[82] Lunze, J. *Feedback Control of Large Scale Systems.* Prentice-Hall International, 1992.

[83] Mackey, D. S., Mackey, N., Mehl, C., and Mehrmann, V. Vector spaces of linearizations for matrix polynomials. *SIAM J. Matrix Anal. Appl. 28* (2006), 971–1004.

[84] McMillan, G. K. *Industrial Applications of PID Control.* Springer London, London, 2012, pp. 415–461.

[85] Meerbergen, K., Michiels, W., Van Beeumen, R., and Mengi, E. Computation of pseudospectral abscissa for large-scale nonlinear eigenvalue problems. *IMA J. Numer. Anal. 37* (2017), 1831–1863.

[86] Mehrmann, V., and Voss, H. Nonlinear eigenvalue problems: a challenge for modern eigenvalue methods. *GAMM Mitteilungen 27* (2004), 121 – 152.

[87] Mengi, E. A support function based algorithm for optimization with eigenvalue constraints. *SIAM J. Optimiz. 27* (2017), 246–268.

[88] Mengi, E., Yildrim, E. A., and Kilic, M. Numerical optimization of eigenvalues of hermitian matrix functions. *SIAM J. Matrix Anal. Appl. 35* (2014), 699–724.

[89] Michiels, W. Spectrum based stability analysis and stabilization of systems described by delay differential algebraic equations. *IET Control Theory A. 5* (2011), 1829–1842.

[90] Michiels, W., Engelborghs, K., Roose, D., and Dochain, D. Sensitivity to infinitesimal delays in neutral equations. *SIAM J. Control Optim. 40* (2002), 1134–1158.

[91] Michiels, W., Engelborghs, K., Vansevenant, P., and Roose, D. The continuous pole placement method for delay equations. *Automatica 38* (2002), 747–761.

[92] Michiels, W., Fridman, E., and Niculescu, S. I. Robustness assessment via stability radii in delay parameters. *Int. J. Robust. Nonlin. 19* (2009), 1405–1426.

[93] Michiels, W., Green, K., Wagenknecht, T., and Niculescu, S. I. Pseudospectra and stability radii for analytic matrix functions with applications to time-delay systems. *Linear Algebra Appl. 418* (2006), 315–335.

[94] Michiels, W., and Guglielmi, N. An iterative method for computing the pseudospectral abscissa for a class of nonlinear eigenvalue problems. *SIAM J. Sci. Comput. 34* (2012), A2366–A2393.

[95] Michiels, W., and Niculescu, S. I. On the delay sensitivity of Smith predictors. *Int. J. Syst. Sci. 34* (2003), 543–52.

[96] Michiels, W., and Niculescu, S. I. *Stability, Control, and Computation for Time-Delay Systems*. SIAM, Philadelphia, 2014. 2nd edition.

[97] Michiels, W., and Nijmeijer, H. Synchronization of delay-coupled nonlinear oscillators: an approach based on the stability analysis of synchronized equilibria. *Chaos: An interdisciplinary journal of nonlinear science 19* (2009), 033110 1–15.

[98] Michiels, W., and Verriest, E. A systems theoretic framework of fast varying and state dependent delays. In *Proc. of the 50th IEEE Conference on Decision and Control and European Control Conference* (2011), pp. 6313–6318.

[99] Michiels, W., Vyhlídal, T., Ziték, P., Nijmeijer, H., and Henrion, D. Strong stability of neutral equations with an arbitrary delay dependency structure. *SIAM J. Control Optim. 48* (2009), 763–786.

[100] Milton, J., Cabrera, J. L., Ohira, T., Tajima, S., Tonosaki, Y., Eurich, C. W., and Campbell, S. A. The time-delayed inverted pendulum: implications for human balance control. *Chaos* (2009). doi: 10.1063/1.3141429.

[101] Niculescu, S. I. *Delay Effects on Stability. A Robust Control Approach*. Springer-Verlag, London, 2001.

[102] Overton, M. L. HANSO: a hybrid algorithm for nonsmooth optimization. Available from `http://cs.nyu.edu/overton/software/hanso/`, 2009.

[103] Özşahin, O., Budak, E., and Özgüven, H. N. In-process tool point FRF identification under operational conditions using inverse stability solution. *Int. J. Mach. Tool. Manu. 89* (2015), 64–73.

[104] Palmor, Z. J. Time-delay compensation - Smith predictor and its modifications. In *The Control Handbook*. CRC Press, New York, 1996, pp. 224–237.

[105] Pappas, G., and Hinrichsen, D. Robust stability of linear systems described by higher-order dynamic equations. *IEEE T Automat. Contr. 38* (1993), 1430–1435.

[106] Pepe, P., Karafyllis, I., and Jiang, Z. P. On the Liapunov-Krasovskii methodology for the ISS of systems described by coupled delay differential and difference equations. *Automatica 44* (2008), 2266–2273.

[107] Qiu, L., Bernhardsson, B., Rantzer, A., Davison, E., Young, P., and Doyle, J. A formula for computation of the real stability radius. *Automatica 31* (1995), 879–890.

[108] Rostami, M. W. New algorithms for computing the real structured pseudospectral abscissa and the real stability radius of large and sparse matrices. *SIAM J. Sci. Comput. 37* (2015), S447–S471.

[109] Schreiber, K. *Nonlinear eigenvalue problems: Newton-type methods and nonlinear Rayleigh functionals*. PhD thesis, TU Berlin, 2008.

[110] Seuret, A., and Johansson, K. H. Stabilization of time-delay systems through linear differential equations using a descriptor representation. In *Proc. of the 2009 European Control Conference (ECC), Budapest, Hungary*, pp. 4727–4732.

[111] Siljak, D. *Decentralized Control of Complex Systems*. Academic Press, London, 1991.

[112] Sinha, S. C., and Butcher, E. A. Symbolic computation of fundamental solution matrices for linear time-periodic dynamical systems. *J Sound Vib 206* (1998), 61–85.

[113] Sipahi, R., and Olgac, N. Complete stability robustness of third-order LTI multiple time-delay systems. *Automatica 41* (2005), 1413–1422.

[114] Sreedhar, J., Van Dooren, P., and Tits, A. L. A fast algorithm to compute the real structured stability radius. In *Stability Theory - Hurwitz Centenary Conference*. Birkhäuser, Basel, 1996, pp. 219–230.

[115] Stein, E. M., and Shakarchi, R. *Real Analysis*. Springer Series in Operations Research. Princeton University Press, Princeton, New Jersey, 2005.

[116] Stépán, G. *Retarded Dynamical Systems: Stability and Characteristic Functions*. Longman, Harlow, UK, 1989.

[117] Tisseur, F., and Higham, N. J. Structured pseudospectra for polynomial eigenvalue problems, with applications. *SIAM J. Matrix Anal. Appl. 23* (2001), 187–208.

[118] Tisseur, F., and Meerbergen, K. The quadratic eigenvalue problem. *SIAM Review 43* (2001), 235–286.

[119] Tlusty, J., and Spacek, L. *Self-Excited Vibrations on Machine Tools*. Czech Naklad, Prague, 1954.

[120] Tobias, S. A. *Machine-tool Vibration.* Blackie, London, 1965.

[121] Totis, G., Insperger, T., Sortino, M., and Stépán, G. Symmetry breaking in milling dynamics. *Int J Mach Tool Manu 139* (2019), 37–56.

[122] Trefethen, L. N., and Bau, D. *Numerical Linear Algebra.* SIAM, Philadelphia, 1997.

[123] Trefethen, N. *Spectral Methods in MATLAB.* SIAM, Philadelphia, 2000.

[124] Vanbiervliet, J., Verheyden, K., Michiels, W., and Vandewalle, S. A nonsmooth optimization approach for the stabilization of linear time-delay systems. *ESAIM: Control, Optimisation and Calcalus of Variations 14* (2008), 478–493.

[125] Verhees, D., Van Beeumen, R., Meerbergen, K., Guglielmi, N., and Michiels, W. Fast algorithms for computing the distance to instability of nonlinear eigenvalue problems, with application to time-delay systems. *Int. J. Dyn. Control 2* (2014), 133–142.

[126] Voss, H. An Arnoldi for nonlinear eigenvalue problems. *BIT Numer. Math. 44* (2004), 387 – 401.

[127] Voss, H. A new justification of the Jacobi-Davidson method for large eigenproblems. *Linear Algebra Appl. 424* (2007), 448–455.

[128] Vyhlídal, T., and Zítek, P. Mapping based algorithm for large-scale computation of quasi-polynomial zeros. *IEEE T Automat. Contr. 54* (2009), 171–177.

[129] Vyhlídal, T., and Zítek, P. QPmR- quasi-polynomial root-finder: Algorithm update and examples. In *Delay Systems. From Theory to Numerics and Applications.* Springer, Cham, 2014, pp. 299–312.

[130] Vyhlídal, T. *Analysis and synthesis of time delay system spectrum.* PhD thesis, Department of Mechanical Engineering, Chech Technical University at Prague, 2003.

[131] Wagenknecht, T., Michiels, W., and Green, K. Structured pseudospectra for nonlinear eigenvalue problems. *J. Comput. Appl. Math. 212* (2006), 245–259.

[132] Wu, Z., and Michiels, W. Reliably computing all characteristic roots of delay differential equations in a given right half plane. *J. Comput. Appl. Math. 236* (2012), 2499–2514.

Curriculum Vitae

General

Name:	Francesco Borgioli
Date of birth:	1 October 1990
Place of birth:	Florence, Italy
E-mail:	francesco.borgioli@cs.kuleuven.be

Experience

- **PhD Student** 2016-2020
  Department of Computer Science, KU Leuven, Belgium

- **Teaching Assistant** 2016-2020
  Department of Computer Science, KU Leuven, Belgium

Education

- **Master in Mathematics** 2013-2015
  University of Trento, Italy

- **Bachelor in Mathematics** 2009-2013
  University of Florence, Italy

List of publications

International journal papers

Borgioli, F., Michiels, W., Lu, D., Vandereycken, B. A globally convergent method to compute the real stability radius for time-delay systems. *Syst. Control Lett.*, 127 (2019), 44-51.

Borgioli, F., Michiels, W. A novel method to compute the structured distance to instability for combined uncertainties on delays and system matrices. *IEEE T. Automat. Control*, 2019, DOI: 10.1109/TAC.2019.2934182.

Borgioli, F., Hajdu, D., Insperger, T., Stépán, G., Michiels, W. Pseudospectral method for assessing stability robustness for linear time-periodic delayed dynamical systems. Submitted for publication to *Int. J. Numer. Meth. Eng.*, 2019.

Hajdu, D., Borgioli, F., Michiels, W., Takacs, D., Stépán, G., Insperger, T. Robust stability of milling operations based on pseudospectral approach. *Int. J. Mach. Tool. Manu.*, 2019, DOI: 10.1016/j.ijmachtools.2019.103516.

International conferences proceedings - full papers

Borgioli, F., Michiels, W. Computing the distance to instability for delay systems with uncertainties in the system matrices and in the delay terms. *Proc. of the 2018 European Control Conference (ECC)*, Limassol, Cyprus 2018, pp. 1201-1207.

Borgioli, F., Michiels, W. Robust stabilisation of linear time-delay systems with uncertainties in the system matrices and in the delay terms. *Proc. of the 14th IFAC Workshop on Time-Delay Systems*, Budapest, Hungary 2018, vol. 51, pp. 312-317.

Dileep, D., Borgioli, F., Hetel, L., Richard, J.P., Michiels, W. A scalable design method for stabilising decentralised controllers for networks of delay-

coupled systems. *Proc. of the 5th IFAC Conference on Analysis and Control of Chaotic Systems*, Eindhoven, Nederlands 2018, vol. 51, pp. 68-73.

International conferences proceedings - abstracts

Borgioli, F., Michiels, W. An iterative algorithm to compute the pseudospectral abscissa for structured real perturbations of a nonlinear eigenvalue problem. *European Conference on Computational Optimization*, Leuven, Belgium, September 2016.

Borgioli, F., Michiels, W. An iterative algorithm to compute the pseudospectral abscissa for real perturbations of a nonlinear eigenvalue problem. *Conference of the International Linear Algebra Society*, Ames, Iowa, USA, July 2017.

Book chapters

Borgioli, F., Michiels, W. A design approach for structured controllers for uncertain delay systems grounded in the real structured pseudospectra framework. *Stability, Control and Application of Time-Delay Systems*. Editors: Gao, Q., Karimi, H.R., Butterworth-Heinemann, 2019, pp. 185-207.



FACULTY OF ENGINEERING SCIENCE
DEPARTMENT OF COMPUTER SCIENCE
NUMA
Celestijnenlaan 200A box 2402
B-3001 Leuven
francesco.borgioli@cs.kuleuven.be
http://www.XXXXX.cs.kuleuven.be